Multi-Technology Offshore Wind Power Systems: Control and Dynamic Performance Assessment

Kamila Nieradzinska

A thesis presented in fulfilment of the requirements for the degree of Doctor of Philosophy

Industrial Control Centre
Department of Electronic and Electrical Engineering
University of Strathclyde
Glasgow G1 1XW

March 2017

The thesis, dissertation, design or report shall include, on the page immediately subsequent to the title-page, the following declarations of authenticity and author's rights:

‘This thesis is the result of the author’s original research. It has been composed by the author and has not been previously submitted for examination which has led to the award of a degree.’

Signed:

Date:

Ze specjalną dedykacją dla mojego Taty

Acknowledgements:

First and foremost I would like to thank my supervisor Dr Olimpo Anaya-Lara, for giving me the opportunity to undertake this work and for providing me with guidance, knowledge, advice and support when I need it the most.

Secondly I would like to thank my second supervisor Prof Bill Leithead for his help and support throughout the research part of this Ph.D. I would also like to thank Dr David Campos-Gaona for the numerous advices, the lengthy skype discussions and his patience during all those years.

I would like to thank to Det Norske Veritas (DNV) for co-funding my PhD and providing me with the opportunity to undertake this research. Furthermore, I would also like to thank all my colleagues at DNV for their support, feedback and advices throughout the PhD. Finally, I would also like to express my gratitude to Energy Technology Partnership (ETP), for co-funding this research and inviting me at their annual conferences.

I would also like to thank my internal and external examiners, Prof Stephen Finney and Dr Timothy Littler for their valuable suggestions and advice which further helped enhance my thesis.

I am also grateful for my friends for their support and believing I could achieve this much. Thank you to Dr Xavier Bellekens, Dimitrios Vozikis, Dr Jakub Konka, Gabrysia Baryla, and the many individuals who have contributed in one way or another to the completion of this PhD.

Chciałam przede wszystkim podziekować moim rodzicom oraz siostrze Asi za wsparcie podczas pisania tego dotoratu. Mojej Mamie za miłość i cierpliwość bez ktorych ta podróż nie byłaby możliwa, mojemu Tacie za to że zawsze we mnie wierzył, moje umiejetności i zachęcał do podjęcia tej jak i każdej innej przygody w moim życiu.

Abstract

This thesis presents a comprehensive study on the operation, principles and theory of wind farms consisting of doubly-fed induction (DFIG) and fully-rated converter (FRC) wind generators working together in a hybrid arrangement. The main objective of this study is to develop control strategies for the hybrid arrangement of wind turbines in order to improve the grid code compliance of the overall wind farm by exploiting the unique characteristics of both technologies to support each other in case of a fault happening. As a result, this thesis presents a novel control strategy for fully rated converter wind generators to improve the fault ride through capabilities of DFIG wind turbines during an AC voltage sag. The developed controller enables the creation of an environment where the FRC and DFIG technologies coexist for the purpose of compliance of grid code requirements. This type of environment can be created in both new wind farm developments and in already deployed DFIG-based wind farms where the addition of FRCs results in the overall improvement of the grid code compliance of the wind farm.

The novel controller developed in this thesis uses the FRC to supply reactive power to the hybrid wind farm network during faults with the objective of reducing the magnitude of the voltage dip. This has positive effects in DFIG rotor speed and DC voltage variables during and after the fault period. These variables, as explained in the thesis, play a crucial role in stabilising the dynamic fault ride through capabilities of the turbine. Additionally, the novel controller developed in this thesis does not compromise the integrity of the FRC system.

This thesis also contributes to the investigation of hybrid wind farms connected to the main grid using voltage source converter high-voltage direct current (VSC-HVDC) as a mean to increase renewable energy penetration and transmission capacity without affecting voltage stability or power quality of the specific case of the Great Britain's (GB) network. One main control approach was investigated on the sending-end converter to integrate offshore wind power from hybrid network where all generated power is injected to the point-to-point DC link with a stiff AC bus at the wind farm network. Additionally, two possible connection topologies of future VSC-HVDC were investigated for steady state and transient conditions. The operation of a multi terminal DC network (MTDC) for hybrid offshore wind farms is analysed with power flow studies of a 5-terminal MTDC model regulated by droop control.

Finally, this thesis investigates three VSC-HVDC connections schemes designed to transfer 2.4GW of power from two separate Dogger Bank wind farms to the GB grid, in terms of the

investment costs, controllability and reliability against expected scenarios. The benefits and drawbacks of all three scenarios are highlighted. These include the benefits of auxiliary cables on AC and DC site of the multi-terminal connections.

List of Contents

Abbreviations

AAMMC	Alternative Arm Modular Multilevel Converter
AC	Alternating Current
Cp	Power Coefficient
CSC	Current Source Converter
CSC-HVDC	Current Source Converter High Voltage Direct Current
DC	Direct Current
DCCB	Direct Current Circuit Breakers
DFIG	Doubly-Fed Induction Generator
DVR	Dynamic Voltage Restore
EWEA	European Wind Energy Association
FACTS	Flexible AC Transmission Systems
FRC	Fully Rated Converter
FRC-PMSG	Full Rated Converter Permanent-Magnet Synchronous Generator
FRT	Fault Ride-Through
FRT	Low Voltage Ride-Through
FSIG	Fixed Speed Induction Generator
GB	Great Britain
GSC	Grid Side Converter
GTO	Gate-Turn-Off Thyristor
HB-MMC	H-Bridge Modular Multilevel Converter
HVAC	High voltage alternating current
IG	Induction Generator
IGBT's	insulated-gate bipolar transistors
IGCT	Integrated Gate-Commutated Thyristor
LCC-HVDC	Line Commutated Converters High Voltage Direct Current
LVRT	Low Voltage Ride-Through
MMC	Modular Multilevel Converter
MPPT	Maximum Power Point Tracking
MTDC	Multi Terminal DC
MTTF	Mean Time to Fail
NPC	Neutral Point Clamped
NPV	Net Present Value
NSN	North Sea Network Link
O&M	Operations & Maintenance
OVPs	Overvoltage Protection
P	Active Power
PCC	Point of Common Coupling
PLL	Phase Locked Loop
PMSG	Permanent Magnet Synchronous Generator
PU	Per Unit
PWM	Pulse Width Modulation
Q	Reactive Power

RSC	Rotor Side Converter
RTTR	Required Time to Repair
SCIG	Squirrel Cage Induction Generator
SCR	Short Circuit Ratio
SCR	Silicon-Controlled Rectifier
STATCOM	Static Synchronous Compensator
TSO	Transmission System Operator
VAR	Volt-Ampere Reactive
VCO	Voltage Controlled Oscillator
VSC-HVDC	Voltage Source Converter High-Voltage Direct Current
WF	Wind Farm
XLPE	Cross-linked Polyethylene

List of Figures

List of Tables

Chapter 1:

Introduction

The electrical power grid is one of the most important engineering achievements of the 20th century. The complex design of modern large-scale power systems around the world, mainly based on alternating-current (AC) technology, can generate, transmit and distribute power to any accessible household.

In recent years due to rapid increase in electricity demand, it is now essential to increase power reliability, security and the ability to exchange power between widely distributed areas. The integration of large scale offshore wind energy projects, which encompass a number of different technologies, and which have to be Grid Code-compliant, becomes essential. There is an urgent need to introduce new connection and control approaches to multi-technology offshore wind power systems which are investigated in this thesis.

This chapter provides background research on high-voltage alternating current (HVAC) and high-voltage direct current (HVDC) power networks, giving a brief description on difficulties for power system transmission and operation of onshore and offshore wind energy developments. It also describes the challenges and motivations for this research. Lastly, it defines the focus of the thesis, the objectives and the contributions.

1.1 Introduction

The increasing demand for wind power production and reducing the visual impact is driving the development of offshore wind farms. The UK Government has issued plans to install more than 40 GW of renewable power generation by 2020, with most of the energy being delivered from both onshore and offshore wind energy sector around the coast of Great Britain [1-3]. However, there are some technical, and environmental issues, such as marine life, birds, etc., on offshore developments which will make very hard to meet 2020 energy target. The offshore wind created new technological demand in terms of grid connectivity,

transport installation and operation [4]. The Dogger Bank Round 3 offshore site in the North Sea is expected to be the largest site, with an initial planned output of 7.2GW [5].

Due to higher wind speeds and rich open areas, offshore wind farms are a promising option for large-scale power generation. The proposed expansion of wind energy sector brings many challenges needing to be addressed to enable energy security, power quality and reliability of supply, especially in this harsh offshore environment and at significant distances from the shore. Among these challenges there is a need for delivering reliable power from offshore wind farms to onshore grids. These challenges can cross a maximum economic distance for the HVAC transmission systems to be cost effective, hence emerging HVDC technologies need to be studied in more detail as future transmission system for offshore power plants.

1.2 Development of modern wind energy sector

The first machine generating energy from wind was built by Professor James Blyth of the Anderson's College in his holiday cottage in Scotland in 1887 [6]. From that time, wind power was steadily developing , and in 1980s gained more attention due to emerging needs of sustainable energy, as the energy production contributes to over a quarter of greenhouses gas emission. The necessity and research led to wind turbines and wind farms increasing in size over the years. In early 1990s, the average capacity of a wind turbine was 500kW, whereas modern wind turbine power output reaches 7.5MW Enercon [7] and 8MW Vestas wind turbines [8, 9]. Furthermore, the size of the overall installed capacity of individual wind farms has increased in accordance with the overall capacity of wind energy. The global installed capacity of wind power has grown exponentially over the last two decades and raised from 7.6GW in 1997 to 486GW in 2016, as shown in Figure 1-1.

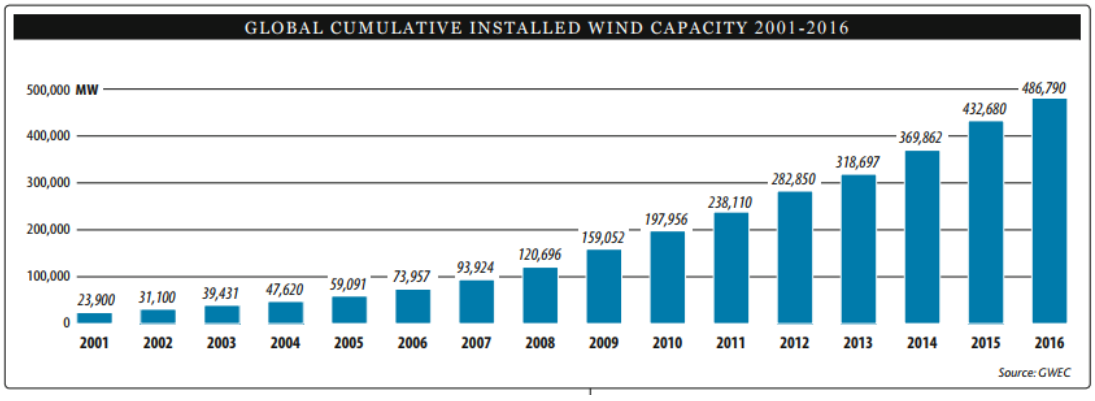

Figure 1-1 Global cumulative installed wind capacity 2000-2016 [10]

The vast majority of the installed capacity comes from onshore wind farms development around Europe, North America and Asia. At the end of 2016, the biggest contribution to the

global installed wind power capacity was represented by China and USA, with 34.7% and 16.9% respectively. The UK represents 3.0% of global installed wind power [10]. European countries such as the UK and Ireland have been dominating the growth of offshore energy generation, as they are surrounded by the North Sea, the Baltic Sea, the Irish Sea and the English Channel [10]. This provides numerous opportunities for offshore wind power developments. The offshore wind energy sector has not developed at the same scale as the onshore sector due to costs and many technical challenges. By way of example, regarding offshore transmission, HVAC is still the strongest, well established and proven to be very good for onshore wind farm connection, power transmission and distribution [11-13]. However, for offshore transmission it still has numerous disadvantages as described below [14-16]:

- The control of the two HVAC interconnected synchronous systems is done by individual unit control of the tie line power and frequency signals, which can be problematic due to the presence of large power oscillations which may inherently cause frequent tripping, decrease the stability and increase the fault level.
- Special arrangement is needed to keep the voltage at desired levels (i.e. shunt and series compensation).
- It can only be connected to synchronised grids.
- The transmission distance of the cables for offshore wind farms is limited due to the high capacitance of AC submarine cables.

All the above points suggest that other technology than HVAC should be used to deliver power from offshore resources located far from shore to European countries. Currently, as of 26 July 2016, the offshore wind energy sector connects 11.50GW in European waters, in which 5.05GW is the total installed capacity in the UK [17]. The European Wind Energy Association evaluated three scenarios where offshore wind capacity in Europe could reach from 19.5GW to 28 GW by 2020 [18].

Looking into the future there are many wind farm developments across the North Sea as shown in Figure 1-2 and located at significant distance from the shore, including most of the Crown Estate Round 3 sites with a potential of 9 GW (although Forewind agreed with The Crown Estate to 7.2GW of development potential [19]).

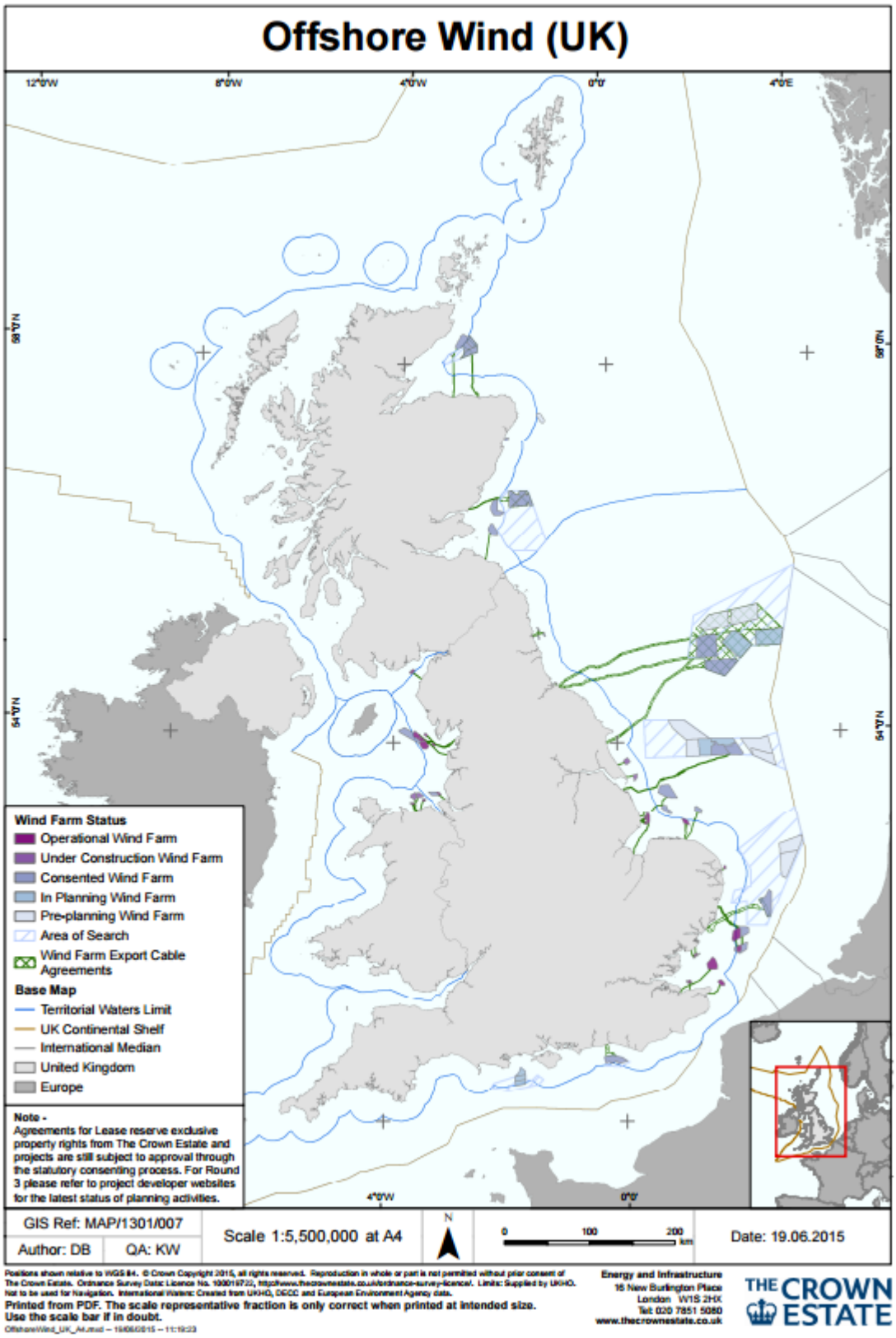

Figure 1-2 UK offshore wind farm map [20]

1.3 Research challenges and motivation

The increased penetration of wind in recent years into the AC networks in the UK and Europe has also introduced technical and operational challenges.

Some of these challenges are related to power stability, voltage quality and power transmission over long distances. Other challenges are associated with connecting large amounts of renewable energy via HVAC lines. These are narrowed by the economical limitation, system stability and increasing loses over the distance, which is showed in Figure 1-3 [21, 22]. The maximum economical distance for HVAC depends from the installed power, as shown in Figure 1-3, on average the maximum economical distance for an HVAC system is 75km [21, 22] The HVDC does not have the maximum economical distance as there is no restrictions in charging currents due to capacitive or inductive elements of the lines. The longest HVDC transmission nowadays is the 2,385km Madeira HDVC link in Brazil.

Offshore and onshore wind farms need to comply with current Grid Code requirements, i.e. fault ride-through capabilities, and contribute to the network support and operation in the same way as synchronous generators [23, 24].

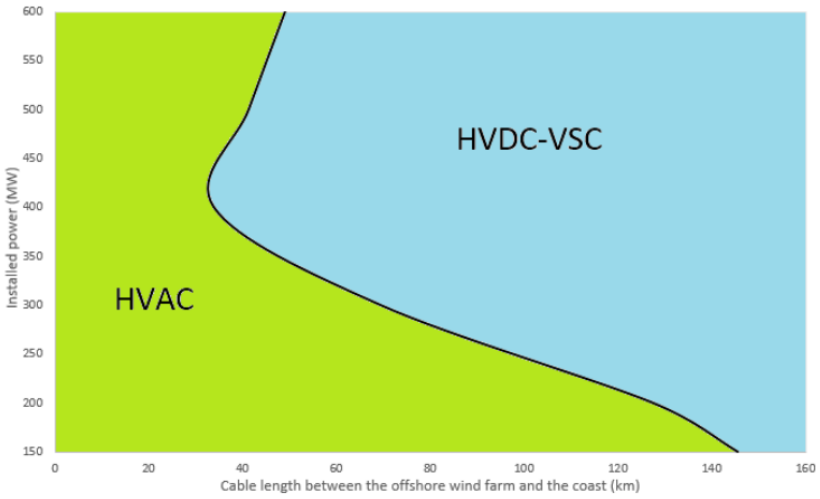

Figure 1-3 Power transfer vs distance for HVAC and HVDC [21]

HVDC technology has developed rapidly over the last couple of decades; hence, research has been focusing on VSC-HVDC transmission systems, as this technology can be used to overcome a number of challenges associated with transmission of large amount of power over long distances, as well as connecting offshore and onshore networks and provide additional services to both grids [25, 26]. VSC-HVDC technology decouples the onshore grid from the offshore wind farm, which makes wind farm dynamically separated from the onshore grid and vice versa. This also means that no disturbances are transferred to the

connected network. Additionally, VSC-HVDC can increase black-start capabilities of the offshore wind farm, and provide voltage support [27].

Other challenges are associated with government policies towards renewable energy, targets and potential connection of onshore and offshore bulk power. The European Commission set up a target of 20% of all consumed energy has to be produced by renewable energy sources by 2020 [28]. The UK target is set up to provide 15% of all consumed energy from renewables by 2020 [29].

The biggest wind farm development sites are located in the North Sea, the offshore winds are typically stronger and more stable than onshore which makes offshore power more attractive. This thesis focuses on investigating connections for large amount of power from the North Sea to the shore in order to meet the 2020 target set up by the EU and focuses on renewable energy, the reliability of such connections, the provision of additional services on the wind turbine level and on the grid level, and additionally investigates power exchange between countries.

1.4 Objectives and methodology

The main focus of this thesis is to investigate the use of hybrid wind farms connected to AC transmission system with VSC-HVDC with combination of different technologies engaged in power production and transfer. Furthermore, this research aims to design enhanced control strategies for future multi-technology offshore wind power systems to facilitate Grid Code(s) compliance (fault-ride through capability, power quality, provision of dynamic voltage and frequency support to the onshore power network, etc.). The potential connection of 2.4GW of power via VSC-HVDC transmission system, from two separate Dogger Bank wind farms to the UK grid has been investigated. Each option is described in terms of investment cost, controllability and reliability against expected fault scenarios. It also produces recommendations that can be used by the wind energy sector in the design of control approaches of offshore wind power systems. In order to achieve the research goals the following objectives were defined:

- To design and implement a model of a doubly-fed induction generator wind turbine (DFIG) for control design purposes and to assess behaviour during faults with particular emphasis of reactive power capabilities.
- To model a Full Converter wind turbine based on permanent-magnet synchronous generator (FRC-PMSG) and design controls to facilitate a multi-technology connection. Enhanced fault performance and reactive power provision are key control objectives.

- To design and implement a hybrid network model to assess performance and reactive power provision in induction-machine based wind farms.
- To implement VSC-HVDC models to integrate multi-technology offshore wind power systems to the onshore grid including controllers that allow an enhanced connection with provision of system services.
- To design and develop control strategies of multi-terminal HVDC systems to enable power flow between terminals.
- To established recommendations on control aspects for connecting offshore wind power more efficiently to onshore networks.

Throughout this thesis the Simulink/Matlab Software was used to conduct all studies. Based on mathematical calculations the systems were designed and simulated.

1.5 Contributions

The main contribution of this thesis is the provision of research tools to enable the safe operation of multi-technology wind farms along with multi-terminal VSC-HVDC systems in the context of transient and long-term disturbances in the AC grid. These tools comprise:

- A novel approach to enhance fault ride-through capabilities of DFIG wind turbines, the novel controller developed in this thesis uses the FRC to supplying reactive power to the hybrid wind farm network during faults with the objective of reducing the magnitude of the voltage dip.
- Investigation of offshore Renewable Energy Sources Penetration at grid level using VSC-HVDC to increase transmission capacity without affecting voltage stability or power quality of the specific case of the Great Britain network
- Investigation of 3 VSC-HVDC connections to transfer 2.4GW from two separate Dogger Bank offshore wind farms to GB grid.

1.6 Thesis structure

This thesis includes seven chapters and is organised as follow:

Chapter one provides an introduction to the current challenges for connecting large amount of power to the grid. It highlights the objectives of the research and contributions.

Chapter two gives an overview of multi-technology offshore wind power systems. Highlights wind turbine technologies used for offshore applications and analyses the selection of collection network and transmission system available depending on the distance.

Chapter three concentrates on two main types of wind power generations; DFIG and FRC-PMSG wind turbines. The chapter also develops mathematical models for both technologies. Based on these models a control system was designed for connecting different wind power generators with the AC grid. A novel control technique to improve fault ride-through capabilities and reactive power compensation of DFIGs via FRC-PMSGs is presented.

Chapter four presents dynamic models of the VSC-HVDC. Multi-task controls are designed to connect DFIG and FRC-PMSG wind turbines with point-to-point connection VSC-HVDC in order to ensure safe operation. The simulations are conducted during wind changes and three-phase faults.

Chapter five shows a multi-technology VSC-HVDC approach for connecting large amount of offshore power with both DFIG and FRC-PMSG wind turbine technologies and modified suitable controllers to meet Grid Code requirements.

Chapter six focuses on the case studies for connecting 2.4 GW from two separate wind farms from Dogger Bank to the UK electrical network. Each option is investigated in detail in terms of investment costs, and controllability and reliability against expected fault scenarios. These studies demonstrate the potential of 3 connections scenarios for Dogger Bank: with the use of VSC-HVDC point-to-point connection, VSC-HVDC with auxiliary services, and multi-terminal VSC-HVDC.

Chapter seven presents the conclusions of the thesis, gives recommendation for future offshore grid connections, and highlights perspectives for future work.

1.7 List of publications

The following publications have been obtained as a direct result of work related to this thesis: C.MacIverS.GillG.A.AgnewO.Anaya-LaraK.R.W.Bell

1.7.1 Journal Papers

K. Nieradzinska, C. MacIver, S. Gill, G.A. Agnew, O. Anaya-Lara, K.R.W. Bell, “Optioneering Analysis for Connecting Dogger Bank Offshore Wind Farms to the UK Electricity Network”, Elsevier, Renewable Energy, Vol. 91, pp. 120-129, DOI: org/10.1016/j.renene.2016.01.043, June 2016.

Nambo-Martinez, J. C., **Nieradzinska, K.,** Anaya-Lara, O.: “Dynamic series compensation for the reinforcement of network connections with high wind penetration,” Energy Procedia Journal, Vol. 53, pp. 86-94, DOI: 10.1016/j.egypro.2014.07.217, August 2014.

Kamila Nieradzinska, Juan-Carlos Nambo, Grain Philip Adam, Rafael Peña-Gallardo, Olimpo Anaya-Lara and William Leithead "North Sea Offshore Modelling Schemes with VSC-HVDC Technology: Control and Dynamic Performance Assessment", *Energy Procedia*, vol. 35, pp. 91-101, // 2013.

1.7.2 Conference proceeding

O. Anaya-Lara, G. Kalcon, G. P Adam, **K. Nieradzińska**, J. Tande, Kjetil Uhlen, Tore Undeland, "North Sea Offshore Networks Basic Connection Schemes Dynamics Performance Assessment" , EPE Joint Wind Energy and T&D Chapters Seminar, The Norwegian University of Science and Technology, Norway

Kamila Nieradzinska, Grain P. Adam, Olimpo Anaya-Lara, "Generalised Droop Control for Power Management in a Multi-Terminal HVDC System", EWEA, Copenhagen 2012

Kamila Nieradzinska, Juan-Carlos Nambo, Grain Philip Adam, Rafael Peña-Gallardo, Olimpo Anaya-Lara and William Leithead "North Sea Offshore Modelling Schemes with VSC-HVDC Technology: Control and Dynamic Performance Assessment", Trondheim Norway Deep Offshore 2013 conference.

Juan Carlos Nambo-Martinez, **Kamila Nieradzinska**, Olimpo Anaya-Lara, „Dynamic Series Compensation for the Reinforcement of Network Connections with High Wind Penetration" Trondheim Norway Deep Offshore 2014 conference.

1.7.3 Posters

Kamila Nieradzinska, Grain P. Adam, Roberts Proskovics, Olimpo Anaya-Lara "Voltage Droop Control for Power Management in a Multi-Terminal HVDC Offshore Network in the North Sea" Norway Deep Offshore 2012 conference

Kamila Nieradzinska, Olimpo Anaya-Lara, W. E. Leithead, "Multi-Terminal Offshore Wind Power Systems: Control and Dynamic Performance Assessment", Energy Technologies Partnership Event ETP, University of Strathclyde

Kamila Nieradzinska, Olimpo Anaya-Lara, Grain P. Adam, "Voltage control method for parallel inverters in multi-terminal network", Faculty Research Presentation Day 2012, University of Strathclyde

Kamila Nieradzinska, Olimpo Anaya-Lara, William Leithead "Optioneering Analysis for Connecting Dogger Bank Offshore Wind Farms to the UK Electricity Network", Faculty Research Presentation Day 2013, University of Strathclyde

Kamila Nieradzinska, Olimpo Anaya-Lara, W. E. Leithead, ”Multi-Terminal Offshore Wind Power Systems: Control and Dynamic Performance Assessment”, Energy Technologies Partnership Event ETP, University of Edinburgh

1.8 References

[1] EWEA, "The European Wind Initiative (2013) Wind power research and development to 2020," January 2013.

[2] European Environment Agency, "Europe's onshore and offshore wind energy potential," 2009.

[3] D. N. Fichaux and J. Wilkes, "Oceans of Opportunity. Harnessing Europe’s largest domestic energy resource," European Wind Energy Association 2009.

[4] M. Bilgili, A. Yasar, and E. Simsek, "Offshore wind power development in Europe and its comparison with onshore counterpart," *Renewable and Sustainable Energy Reviews*, vol. 15, pp. 905-915, 2011/02/01/ 2011.

[5] National Grid, "Offshore Electricity Transmission: Possible Options for the Future " 2011.

[6] T. J. Price, "James Blyth – Britain’s first modern wind power pioneer," *Wind Eng*, vol. vol. 29, no. 3, pp. 191–200, May 2005.

[7] Enercon. (2014). *E-126*. Available: http://www.enercon.de/en/products/ep-8/e-126/

[8] N. Fichaux, J. Beurskens, and P. Jensen, "Upwind: Design limits and solutions for very large wind turbines," *Sixth Framew*, Program., 2011.

[9] Vestas. (2015). *V164-8.0 MW® breaks world record for wind energy production*. Available: http://www.mhivestasoffshore.com/v164-8-0-mw-breaks-world-record-for-wind-energy-production/

[10] Global Wind Energy Council, "Global Wind Energy Report: Annual Market Update 2016," ed, 2017.

[11] K. Meah and S. Ula, "Comparative Evaluation of HVDC and HVAC Transmission Systems," in *Power Engineering Society General Meeting, 2007. IEEE*, 2007, pp. 1-5.

[12] F. Delea and J. Casazza, "The Technology of the Electric Transmission System," in *Understanding Electric Power Systems:An Overview of the Technology, the Marketplace, and Government Regulation*, ed: Wiley-IEEE Press, 2010, pp. 97-113.

[13] Prabha Kundur, Neal J. Balu, and M. G. Lauby, *Power System Stability and Control*. New York, USA, 1994.

[14] R. Sharma, T. W. Rasmussen, K. H. Jensen, and V. Akamatov, "Modular VSC converter based HVDC power transmission from offshore wind power plant: Compared to the conventional HVAC system," in *Electric Power and Energy Conference (EPEC), 2010 IEEE*, 2010, pp. 1-6.

[15] K. R. Padiyar, *HVDC power transmission systems : technology and system interactions*, New Academic Science Ltd; 2 edition (29 Aug. 2011).

[16] I. Z. D. M. Larruskain , A. J. Mazón , O. Abarrategui , J. Monasterio, "Transmission and distribution networks: Ac versus dc," *9th Spanish-Portuguese Congress on Electrical Engineering*.

[17] Wind Europa. (12.12.2016). *The European offshore wind industry. Key trends and statistics 1st half 2016*. Available: https://windeurope.org/wp-

content/uploads/files/about-wind/statistics/WindEurope-mid-year-offshore-statistics-2016.pdf
[18] J. Moccia, "Wind energy scenarios for 2020," ed, June 2014.
[19] Forewind. (2014, 01.12.2016). *Forewind revises Dogger Bank Zone capacity*. Available: http://www.forewind.co.uk/index.php?mact=News,cntnt01,detail,0&cntnt01articleid=101&cntnt01returnid=54
[20] The Crown Estate. (2014). *Offshore Wind (UK).* . Available: http://www.thecrownestate.co.uk/media/5674/ei-offshore-wind-uk.pdf
[21] J. Machado, M. Ventim Neves, and P. J. Santos, "Economic limitations of the HVAC transmission system when applied to offshore wind farms," in *Compatibility and Power Electronics (CPE), 2015 9th International Conference on*, 2015, pp. 69-75.
[22] W. L. Kling, R. L. Hendriks, and J. H. den Boon, "Advanced transmission solutions for offshore wind farms," in *Power and Energy Society General Meeting - Conversion and Delivery of Electrical Energy in the 21st Century, 2008 IEEE*, 2008, pp. 1-6.
[23] National Grid, "The Grid Code," 26 August 2015.
[24] M. Tsili and S. Papathanassiou, "A review of grid code technical requirements for wind farms," *Renewable Power Generation, IET*, vol. 3, pp. 308-332, 2009.
[25] G. K. O.Anaya-Lara1, G. P Adam, K. Nieradzinska, J. Tande, Kjetil Uhlen, Tore Undeland, "North Sea Offshore Networks Basic Connection Schemes Dynamics Performance Assessment," Trondheim 2012.
[26] L. Hongzhi and C. Zhe, "Contribution of VSC-HVDC to Frequency Regulation of Power Systems With Offshore Wind Generation," *Energy Conversion, IEEE Transactions on*, vol. 30, pp. 918-926, 2015.
[27] Z. Mingxia, L. Sheng, Z. Jianhua, L. Zongqi, and L. Yinhui, "A study on the black start capability of VSC-HVDC using soft-starting mode," in *Power Electronics and Motion Control Conference, 2009. IPEMC '09. IEEE 6th International*, 2009, pp. 910-914.
[28] "REPORT FROM THE COMMISSION TO THE EUROPEAN PARLIAMENT, THE COUNCIL, THE EUROPEAN ECONOMIC AND SOCIAL COMMITTEE AND THE COMMITTEE OF THE REGIONS ", BrusselBrussels 2015.
[29] "UK Renewable Energy Roadmap," DepartmentofEnergy&CimanteChange, Ed., ed, July 2011.

Chapter 2:

Multi-technology offshore wind power systems

Multi-technolgy offshore wind power systems will be the future of upcoming wind technology and transmission systems, combining different technologies within the wind farms and transmission system.

This chapter reviews the multi-technology onshore and offshore for wind power systems available on the market as well as different types of wind turbines and transmission systems that have been developed over last three decades. Moreover, it describes the architecture of different wind farm arrays, traditional HVAC connection, line commutated converters high voltage direct current (LCC-HVDC) and voltage source converter high voltage direct current (VSC-HVDC) connections. This chapter will also provide an introduction to different technologies combined together in order to demonstrate multi-technology transmission systems. Figure 2-1 shows an example of artificial scenarios to illustrate the various subsystems and technologies that may appear in a large onshore and offshore wind project. These schemes can be used in the future for power transmission from offshore wind located around Europe as well as for international power exchange links.

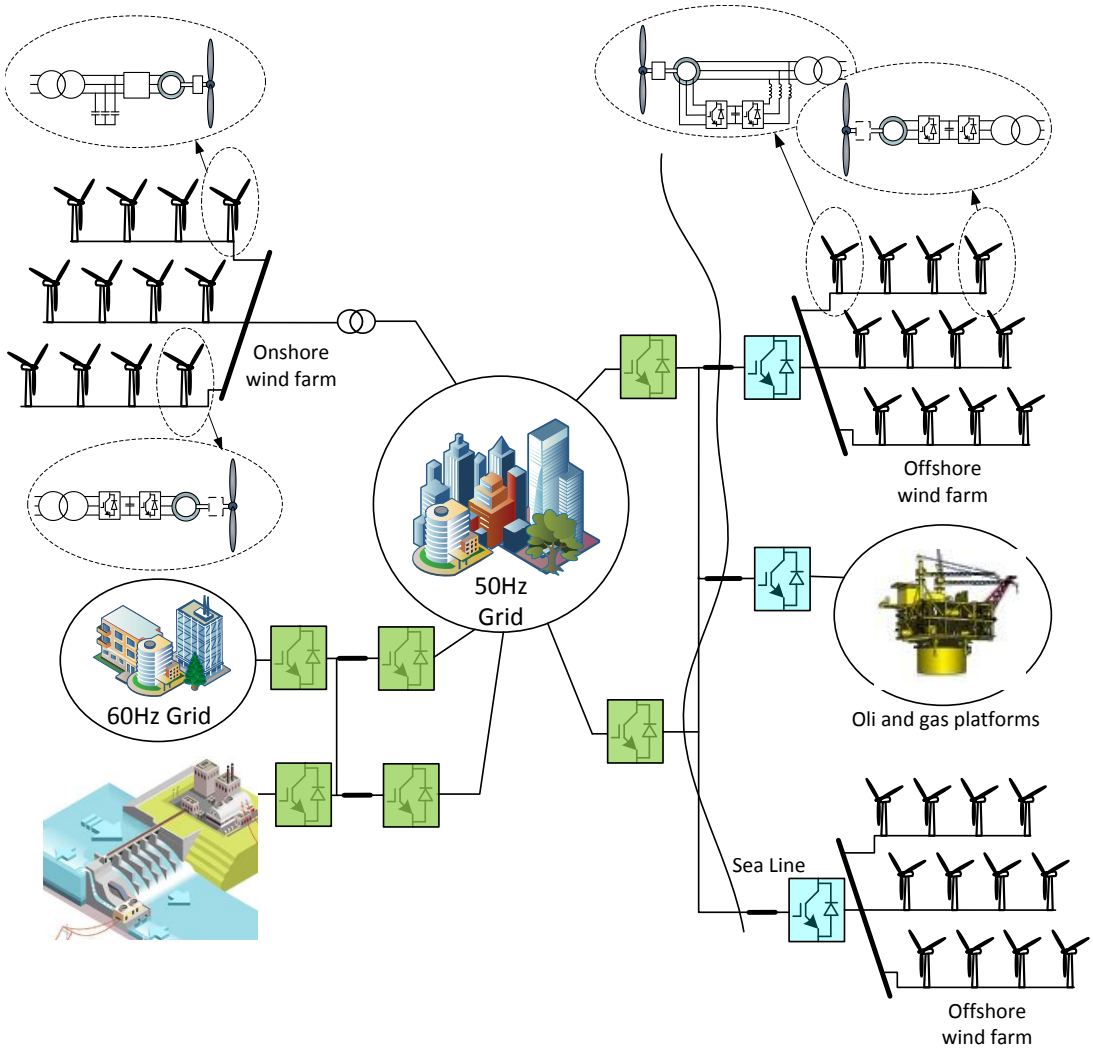

Figure 2-1 An artificial scenario to illustrate the future potential of multi-technology grid.

2.1 Wind power technology

Wind turbine technology has gained increased attention in the last few decades. This is due to intensive interest of environmental organisations and national governments in tackling climate change through reduction of greenhouse gas and CO_2 emissions. Despite the benefits to the environment, renewable energy units bring new challenges to power system planning and operation.

The current trend is to build more offshore wind farms and to increase the power output from a single wind turbine, which reflects the physical size. The modern typical wind turbine for commercial use is a 3-bladed upwind machine with a rated power ranging from 0.75MW to 8MW. Figure 2-2 shows how wind turbines have increased in size over the years. The increase of wind turbines in size brought some concerns for power system operators due to the lack of primary frequency support and inertia response capabilities. Several studies have

been undertaken to investigate the integration of wind turbines on the power system including control issue to support the grid [1-4].

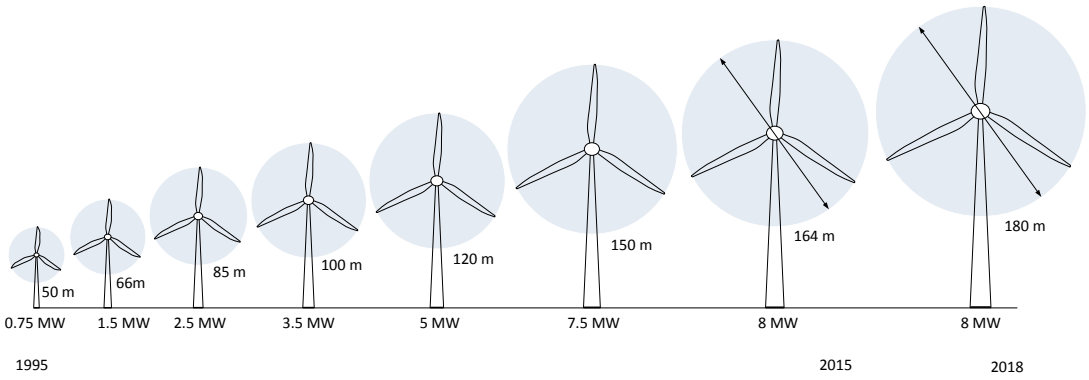

Figure 2-2 Wind turbine sizes over time

At present, wind turbines technology uses four main generators, with some not being used in current, large wind turbines. The first wind turbines were fixed speed induction generator (FSIG) wind turbines with squirrel cage induction generator (SCIG), and they were directly connected to the electrical network. This means their rotational speed almost fixed to the power grid frequency. This particular generator is no longer used for large scale wind farms because they have the maximum power extraction in one particular point of the power-curve characteristic of the wind turbine and depend on the size of the turbine. It also means that, most of the time, they are not operating at maximum efficiency. Additionally, they consume reactive power [5]. Over time, variable-speed wind turbines have been developed and have become the most widely used types of generators in wind turbines. Variable-speed wind turbines can employ one of the following configurations: Opti-Slip induction generator, doubly-fed induction generator (DFIG) or full-converter wind generators based on synchronous generators or squirrel-cage induction generators. The last two configurations have maximum power point tracking (MPPT) capability, which makes them much more efficient.

To avoid instability in power systems during fault, the transmission system operator (TSO) requires wind farms to act as a conventional synchronous generation plant and comply with current Grid Codes. Some of the requirements involve Fault Ride-through (FRT) capabilities from the wind turbine or wind farm. Additionally, wind turbines are required to support grid voltage during a fault and inject reactive power. Different techniques and control strategies for FRT capabilities and voltage support will be discussed further in this section.

Currently, most wind turbine generators produce power output from a single unit at a voltage ranging from 690V to 3.3kV. However, the current trend in large-scale offshore wind farms

is to use medium voltage wind generators at 3.3kV or higher [6, 7]. Transformers are used to step up the voltage to 33 kV used for the collection system within the wind farm.

The next section describes wind turbine concepts, basic configurations and characteristics, and highlights some research challenges addressed in this thesis.

2.1.1 Fixed speed wind turbine (stall regulated)

The first models of commercial wind turbines were fixed speed; this means that the rotor speed is constant for all wind speeds and operating slip variation is very small, around 1% [8]. Fixed speed wind turbine uses a squirrel cage induction generator (SCIG). They are directly connected to the grid; this means that their rotational speed is very close to that of the the frequency of the network. FSIG uses soft start and capacitor bank (30% of the wind turbine capacity) for reducing reactive power compensation demand from the grid. They are connected to the grid via a step–up transformer; which allows to increase the voltage and connect to the distribution network. From an electrical point of view, they are simple machines consisting of an aerodynamic rotor, a low speed shaft, a gearbox, a high-speed shaft and a SCIG connected to the power system through the transformer. Figure 2-3 shows a typical configuration of fixed speed induction generator wind turbine.

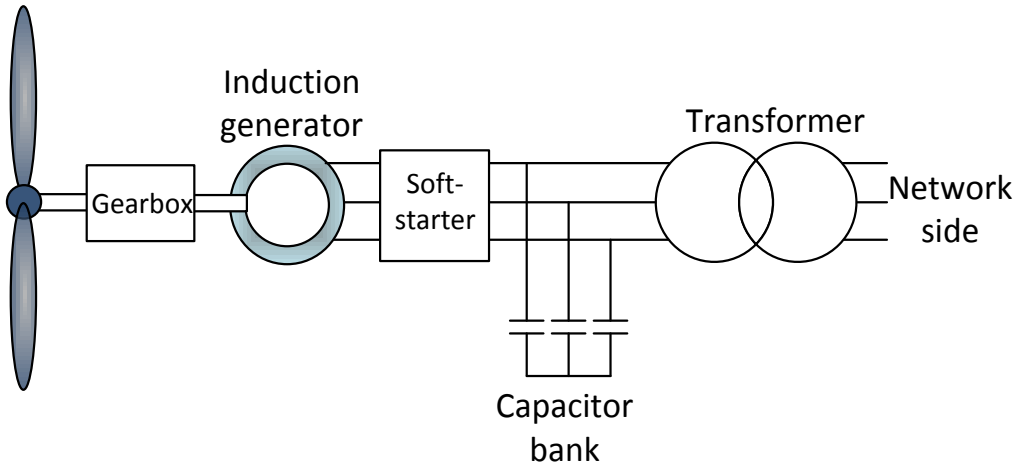

Figure 2-3 Basic configuration of FSIG wind turbine

The wind turbine has its optimum power efficiency at one particular wind speed. Early FSIG wind turbines used stall control. The control technique is to limit the power captured at high wind speeds, after the rated power of the wind turbine is achieved. The use of stall control to limit power output is fairly simple and highly reliable; however, it has some disadvantages like lower efficiency, large dynamic loads on the blades, nacelle and wind turbine tower. Other major issue is that fixed speed wind turbines require a fixed number of reactive power compensation devices to improve operation and to help regulate the voltage in the cluster.

The regulation of the voltage in the cluster could be addressed by adding some additional fully rated converter wind turbines to the cluster to create a hybrid wind farm, which will be investigated in Chapter 3.

2.1.2 Doubly fed induction generator wind turbines

The doubly fed induction generator (DFIG) wind turbines are the most widely used variable speed wind turbines. They maximise the energy captured from the wind by maintaining optimum tip-speed ratio (λ) through varying the rotational speed of the turbine.

To achieve variable-speed operation, for below rated power, a few methods can be used. One way of varying the rotational speed is to vary the resistance in the rotor; this can increase the generator slip up to 10%. Another method to achieve variable speed operation is to use a frequency converter.

DFIGs are typically wound rotor induction machines with stator windings directly connected to the grid and rotor windings connected to the grid via frequency converters. In modern wind turbines, the frequency converter is a self-commutated Pulse Width Modulation (PWM) back-to-back variable frequency, voltage source partial converter; only around 30% of power is fed thought the rotor the grid. Figure 2-4 shows a doubly-fed induction generator wind turbine with power converters.

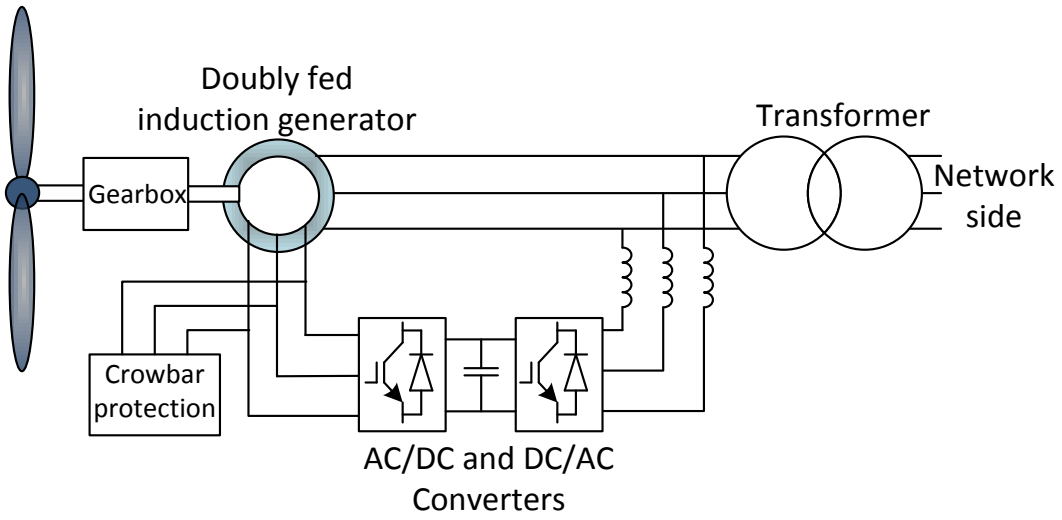

Figure 2-4 Simplified schematic of Doubly-fed induction generator wind turbine

The use of frequency converter introduces losses to the electrical system in the DFIG wind turbine; however it allows improved control over the rotational speed of the machine and reduces stress on the mechanical drive train and also allows the control of power output of the turbine. Nevertheless, due to the sensitivity of power converters, DFIGs need special

attention during faults in the grid. In the case of a fault, there is a high increase in current flowing through the converters, which may damage its internal devices. To avoid the risk of damage, the power converters the DFIG make use of a crowbar protection system which disconnects the converters. This type of protection system turns the DFIG generator into a fixed speer induction machine [9, 10] and introduces a major problem as control over the wind turbine is lost during fault with excessive reactive power consumption from the grid, which results in further grid instability. To extend the connection to the grid of the DFIG during a voltage sag. Additional fully rated converter wind turbines can improve low voltage fault ride-through capabilities.

2.1.3 Fully rated converter wind turbines

Recently, there has been an increasing interest in fully rated converter (FRC) wind turbines due to their high reliability for offshore wind applications. This type of wind turbines can employ synchronous or asynchronous generator. Depending on the generator, the drive train of the machine can contain a gearbox or not. Gearless FRC are also known as "direct drive" systems. If a gearbox is used, the rotational speed of turbine rotor is stepped up form 8-25rpm to 1500rpm -1800rpm, which is suitable for standard generators. In direct drive wind turbines low speed shaft is directly connected to the generator, as shown in Figure 2-5. This is achieved by modifying the generators to operate at low speeds.

In FRC wind turbines, the stator windings are connected to the grid through fully rated back-to-back converter.

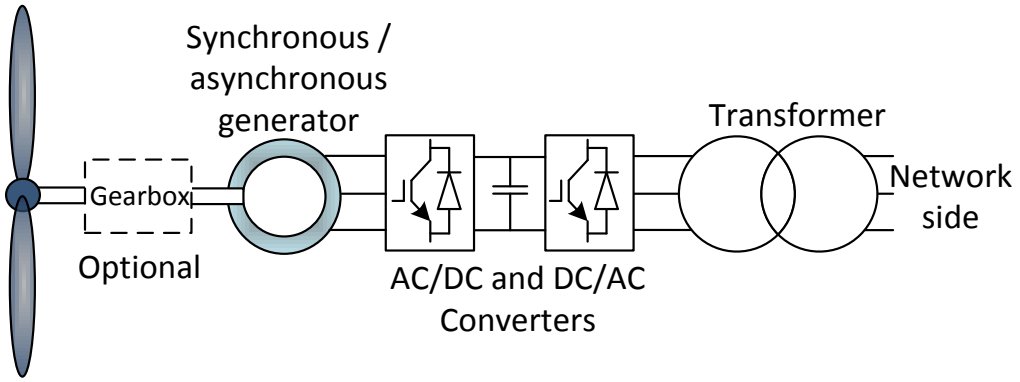

Figure 2-5 Simplified schematic of fully rated converter wind turbine

Decoupled operation of FRC enables the variable speed operation; the mechanical rotor speed is independent from the grid frequency.

The next sections describe selected controllers for improving the performance of the wind turbines.

2.1.4 Wind farm primary frequency control

As wind energy generation increases worldwide, wind turbine control systems are becoming more complex. Traditionally, the primary objective of a wind turbine controller was to maximise the power output from an individual turbine. However, there has been an increasing demand for wind turbines to actively control power output to participate in grid frequency regulation.

In [11] authors studied electrical grids with high wind penetration in the grid and the dynamic security response of the system after disturbances. The study investigates the impact on the system frequency during winter peak because of a higher wind penetration. With the increased amount of wind the primary frequency control capability of the power grid decreases. This is problematic for the system operator and for the system's security. The authors propose the turbines to operate with a pitch angle below rated speed, so as to create a reserve of energy available.

Frequency control of the power grid for different types of wind turbine generators has been studied in [1]. The research concluded that FSIG wind turbines can contribute to the frequency support, whereas DFIG does not provide any frequency support and would require an additional control loop to provide inertia response.

The work conducted in [12] focuses on DFIG wind turbine control for synthetic inertia response. The authors propose "changing the torque set point of the DFIG for changes in grid frequency." The idea behind this is to increase maximum power (Pmax) beyond rated power by 20% to release kinetic energy. However, this comes at the cost of negatively impacting the rotors speed after the synthetic inertia provision.

Further research was undertaken in [13] to improve the primary frequency control and to meet Grid Codes requirements for large-MW wind turbine in order to provide grid support just as a conventional synchronous power plant. In this study, the authors introduced a pitch angle controller which limits the rotor speed to provide 10% primary power reserve.

The above studies contribute to the primary frequency support to the AC grid via appropriate control techniques on the turbine level. Another novel approach for providing ancillary services to the grid is the use of Energy Storage Systems. Energy Storage Systems (ESS) can play a vital role for frequency control and voltage support in AC grids. They are flexible devices (batteries in particular) that can easily charge and discharge to support ancillary services, and help with load balancing for the grid. There are various types of ESS according

to the energy conversion process. Authors in [14] revised all available ESS technologies, including the capabilities of each to provide wind farm support.

2.1.5 Fault Ride-through Capability

Another Grid Code requirement is that wind turbines need to comply with Fault Ride-through (FRT) capability, also known as Low Voltage Ride-through (LVRT). The FRT objective is for wind turbines to stay connected to the grid during low grid-voltage periods. The FRT requirements of wind farms is important from the TSO point of view, since the wind farms are getting bigger in size, and loss of large amount of wind power would create power imbalance in the AC networks. As an example, the maximum loss of load limits for the Great Britain (GB) are: "Infeed Loss Risk is 1320MW, and Infrequent Infeed Loss Risk is 1800MW", specified in the National Electricity Transmission System Security and Quality of Supply Standards (NETS SQSS) in GSR015 [15]. The period that the wind turbine should withstand low voltage, remain in operation and slowly recover varies from country to country. The summary of FRT is presented in Figure 2-6 and Table 2-1. Figure 2-6 shows the FRT requirements curve, it illustrates a voltage level at the grid side against time, and points from A to H indicate the voltage levels specified in Table 2-1. Lets take the GB Grid Code as an example and look at Figure 2-6 and Table 2-1. Here if the specified voltage level BC is equal to 0% it means that wind farm have to stay connected for a time specified by BD which is 0.14 milliseconds, anything over that time period is allowed to trip. Furthermore the primary services should support the grid for time noted as AF which is 1.2 seconds. During that time and the voltage should be restored up to 80% of the pre fault condition. Further the voltage needs to be restored in 2.5s noted as AH to 15% of is original value which is specified as GH.

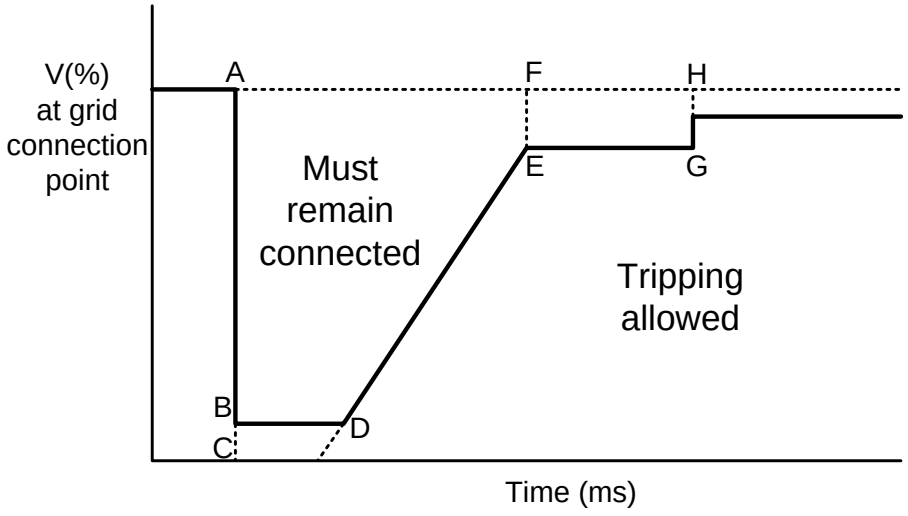

Figure 2-6 Example Curve of Fault Ride through Requirements

Table 2-1 shows a summary of wind turbine FRT requirements in different countries, the percentage of a voltage drops and times for how long wind plant must remain connected to the grid [16-18]. From the examples, the most stringent Grid Code requirements are in Great Britain and Germany where wind plants need to withstand voltages as low as 0% for as long as 140 and 150 milliseconds, respectively. These requirements from Grid Codes regulations has brought challenges to the turbine manufacturers pushing them to design complex control strategies to comply with the Grid Code regulations.

Table 2-1 Wind farm FRT requirements by country

Grid Code	BC	BD	AF	FE	AH	GH
Denmark	25%	0.1s	0.75s	25%	10s	n/a
Germany	0%	0.15s	0.15s	30%	0.7s	10%
Great Britain	0%	0.14s	1.2s	20%	2.5s	15%
Ireland	15%	0.625s	3s	10%	n/a	n/a
Italy	20%	0.5s	0.8s	25%	2s	10%
Spain	20%	0.5s	1s	20%	15s	5%
Poland	15%	0.6s	3s	20%	n/a	n/a
USA	15%	0.625s	3s	10%	n/a	n/a

In the last few years, several studies have been undertaken regarding Grid Code compliance of wind turbines with FRT capability. In general, modern wind turbines with appropriate control techniques and sometimes external devices (i.e. VAR, STATCOM) are able to comply with FRT. Flexible AC Transmission System (FACTS) devices have been used and investigated in [19-22].

Authors in [23, 24] implemented an electronic interface resistor which is connected in the DFIG between the rotor and the rotor side converter. The set of resistors connected this way is also known as a crowbar protection. This type of protection uses the resistors to restrain the induced current on the rotors windings. This method not only fulfils the FRT Grid Codes requirements but also protects the DC link capacitor and RSC against overcurrent and overvoltage during a fault. The proposed crowbar circuit is shown in Figure 2-7.

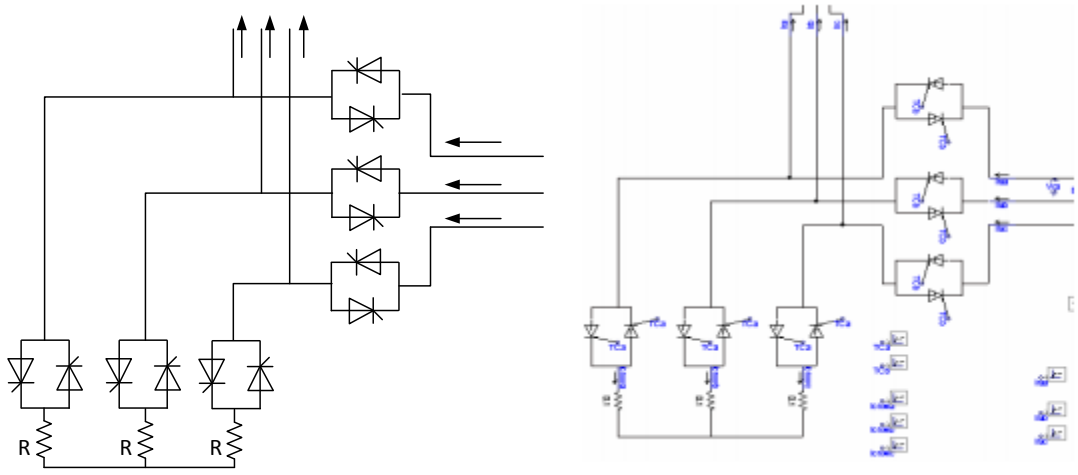

Figure 2-7 DFIG crowbar circuit based on [23].

The operation of the proposed circuit is activated when currents exceed pre-defined values or the grid voltage falls below a pre-defined level, which depends on the control technique used in the model in the Figure 2-7.

New operation strategies were investigated in [25] to enhance the FRT capability of PMSG in small wind farms. The operation of PMSG wind turbine is fully decoupled from the grid via back-to-back converters. As a result of the decoupled operation, the generator is not sensitive to any changes happening on the grid side. However, the grid side converter (GSC) will detect the fault and will switch from normal operation to FRT operation mode to support the grid. At that point, the reactive current is injected allowing the turbine to comply with Grid Codes requirements. However, the GSC cannot supply or absorb active power which may results in damaging the DC capacitors. To avoid over- or under-voltage of the DC capacitors, the author used over-voltage protection scheme (OVPs) as shown in Figure 2-8.

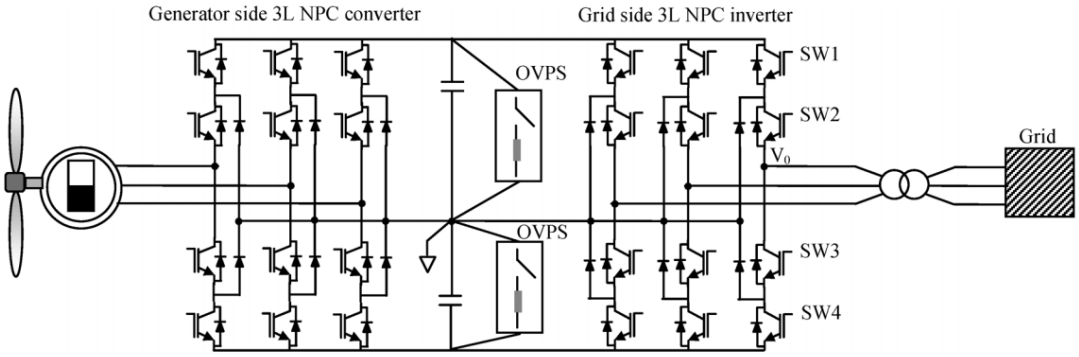

Figure 2-8 Electrical scheme of VSWT-PMSG from [25].

This arrangement is regarded as being very effective for FRT as the wind turbine stays connected to the grid and injects reactive power during fault and after the fault.

As described before, FRT is extremely important for the grid since the power system dynamics can become a big issue if there is large amount of wind power disconnected from the grid creating load/ generation imbalance. Work conducted in [26] proposes a solution to existing wind turbines to improve non-FRT wind turbines operation by introducing external devices - Dynamic Voltage Restore (DVR). During a fault DVR decuples wind turbine from the grid, by restoring AC voltage at the wind turbine terminal.

2.2 Technology choice for offshore wind turbines

The offshore environment creates additional challenges on wind turbines when compared to an onshore wind turbine. An offshore turbine is far less accessible for Operations & Maintenance (O&M) compared to onshore turbine. Even bottom-fixed, near-shore turbines can be inaccessible for weeks at a time due to changing climate and sea conditions. This can increase the time frame between a fault occurring and the repairs being made which significantly increases in overall downtime. Additionally, the profit margins are generally higher for offshore projects, making the overall economic losses relating to downtime greater.

The O&M for offshore wind turbines is also associated with much higher cost, however the average size of the wind turbine can be much bigger than onshore which can make per MW O&M lower overall [27]. This advantage of harvesting more power from the offshore environment comes at cost of turbine loads from sea currents and waves, which can have negative impact on life time of turbine structures [28]. Experience with bottom-fixed turbines has led manufacturers to introduce a number of improvements to turbine designs that will help them to survive the offshore climate [29, 30].

In order to ensure that the turbine is operational for as high a percentage of the time as possible, it is necessary to shift to a policy of more preventive maintenance, as well as selecting technologies that are as reliable and low maintenance as possible [31]. A review of wind turbine condition monitoring, provisional maintenance, available strategies for O&M can be found in [32].

All in all, there is a room for improvement for offshore wind turbine design to lower the machine downtime and extend lifetime in offshore environment.

2.2.1 Collection system for offshore wind farm.

There are various arrangements for offshore wind park electric collector systems. The reliability of the collector system has a strong impact on the reliability of the wind farm. There are several types of electrical collector structure such as:

- Radial
- Single side ring design
- Single return with single hub design
- Double-side ring design
- Star design
- Single return with multi hub design

The most popular design for a collector system is the radial design shown in Figure 2-9 a. Each wind turbine is connected to the same feeder in a string; this configuration has big influence on the system reliability. Fault in the collector circuit will result in disconnection of all wind turbines. The maximum number of wind turbines on one cable is determined by two factors: capacity of the generator(s) and rating of the subsea cables [33]. Figure 2-9 b shows single side ring design, which allows auxiliary path for enhanced power security in the case of the fault in radial design.

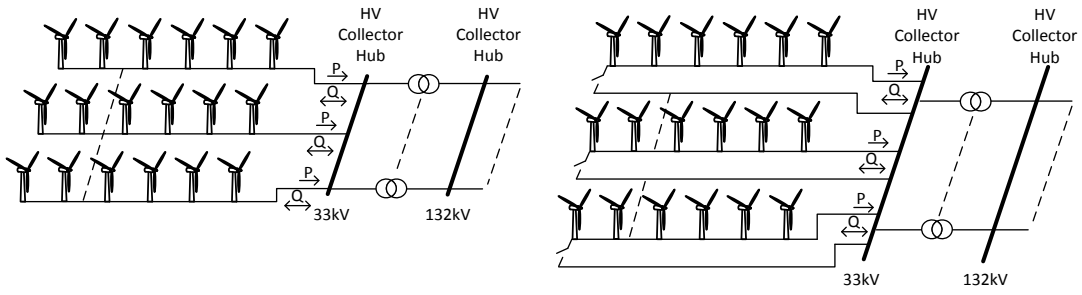

a) radial design **b) single side with return design**

Figure 2-9 Radial and single side ring design of a collector network.

The single-sided ring design shown in Figure 2-10a is based on radial design with additional cable connected to the end of each turbine. The additional cable must be of similar current rating as the single string, which results in lower installation costs compared to single side ring design [34]. In Figure 2-10b the double-sided ring design, also known as ring design, is shown. This type of design has even number of cables. The last wind turbine on one cable is interconnected to an adjacent cable. The size of each cable should be doubled to handle extra loading in case of the one string fault next to the hub. This may increase the capital cost of the wind farm [35].

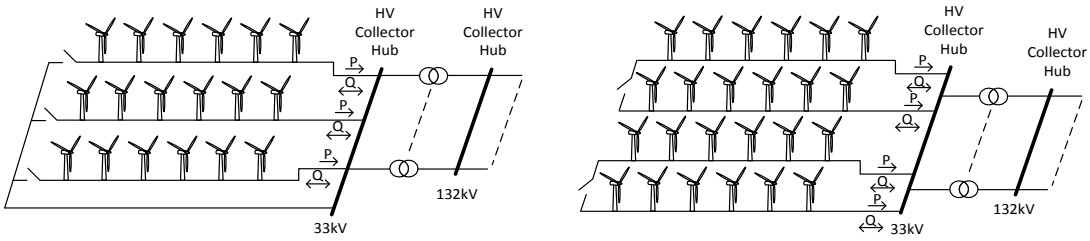

a) Single return design **b) single hub design**

Figure 2-10 Single return with single hub design and double-side ring design.

The star design shown in Figure 2-11a has the advantage of cable length savings. However, more complex switchgear is required in the central wind turbine. The star design offers a better voltage regulation as well as lower power losses between wind turbines link cables [35].

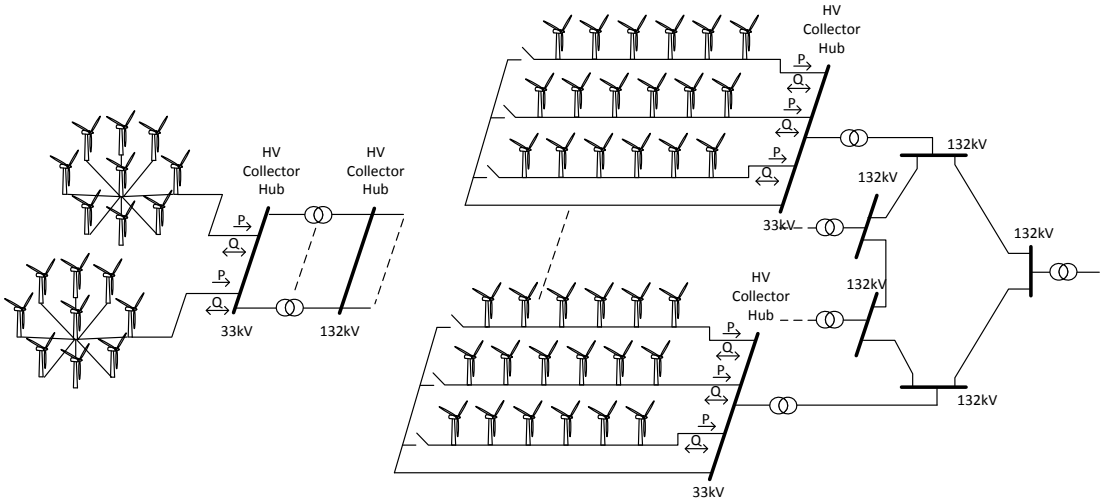

a) Star design **b) single return with multi-hub design**

Figure 2-11 Star design and single return with multi-hub design.

The most complex design is the single return with multi-hub seen in Figure 2-11b. This design offers of high level of security for offshore wind plants, which is an important asset. Due to many redundancy paths, power can be generated and delivered even if one hub is lost [35].

2.2.2 Hybrid collection network

Each collection system can employ one type of wind turbine or create a hybrid system and combine different wind turbine generation technologies. One of the advantages of hybrid network is the potential support for induction generator based wind farms. Hybrid wind farms combined from FSIG and FRC wind turbines are capable of reactive power compensation during a wind variation [36]. In [37], a novel current source converter (CSC) based wind turbine controller was investigated to improve operating performance of FSIG

wind turbine in a hybrid collection network. The investigation of reactive power compensation of DFIG will be studied in Chapter 3.

2.3 Transmission technologies for offshore wind power

Transmission systems have progressed significantly over last few decades. There are three solutions available on the market for transmitting power from the offshore wind farms: high-voltage alternating current (HVAC), Line commutated converters LCC-HVDC and voltage source converters VSC-HVDC. In this section an overview of the key three technologies is provided.

2.3.1 HVAC technologies

The majority of offshore wind farms are connected to the onshore grid via conventional AC connections. Currently the London Array is the biggest operating offshore wind farm, consisting of 175 turbines with total capacity of 630MW. It is located 20km from shore and connected to shore by 150 kV AC cables [38, 39]. The AC transmission system has been proved as an effective way to transfer and distribute power from close located offshore wind farms, however there are some performance limitations which makes this technology not suitable for distant applications [40].

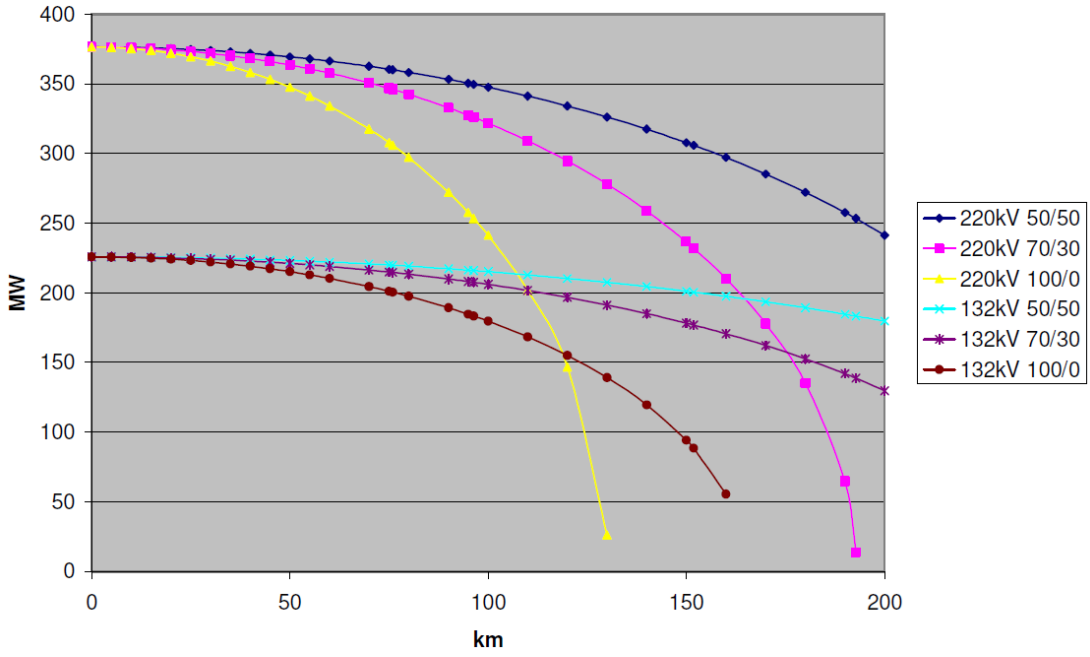

Figure 2-12 Maximum active power transfer in HVAC cables for reactive compensation split between onshore and offshore substation [41].

One of the main disadvantages limiting the active power transfer in AC system is that AC cables are subjected to capacitive effect. For short distances and wind farms located close to

shore this is minor disadvantage, but with distance increment this becomes a major issue. To prevent this problem, reactive power compensation units are used, located at either end of the cable route. However, for a long distances it is necessary to place a reactive power compensation unit mid-way [42]. In offshore applications, this practice may become prohibitive because of the associated cost. This is because in offshore wind farm there may be the case of building another separate platform or space on converter platform. **Error! Reference source not found.** shows limitation of active power transfer in HVAC cables for long distances applied to offshore wind farms.

2.3.2 LCC-HVDC Technology

The alternative solution for HVAC transmission is HVDC transmission. The majority of HVDC transmission systems in operation are thyristor-based current source converter type. This is a well-established technology and has been in use for over five decades. HVDC requires a converter station at each end of the line to transform AC power to DC power and vice versa. It is well suited for a transmission of large amounts of power over long distances. Moreover, it can provide decoupled operation and connect grids which are not synchronised [43] . The HVDC transmission system is more expensive compared to HVAC, however it uses direct current for energy transmission; this implies cables to not subjected to the same changing currents as it is in the AC cables. This translates in transmission losses much lower compared to the same power transferred capacity. The choice between HVAC or HVDC transmission system is made based on economical and technical aspects, such transmission distance, type of cables, control, and type of protection [44]. The debate between HVAC and HVDC for offshore wind farms has been addressed is several studies [40, 45, 46] and all concluded that there is a breakeven distance after which HVDC system become more cost effective. Figure 2-13 shows the economical choice between AC and DC transmission system.

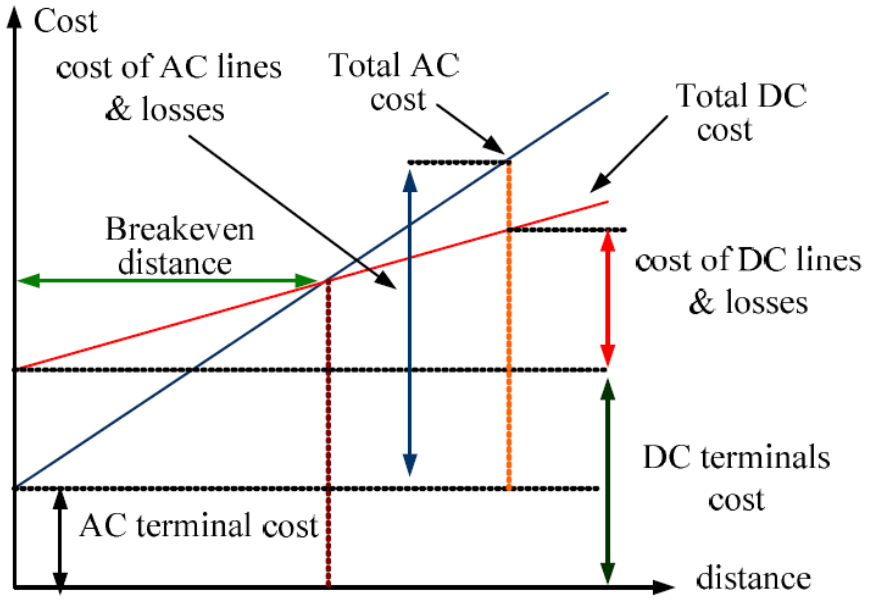

Figure 2-13 Costs comparison for HVAC vs HVDC transmission system vs distance [47].

The first HVDC transmission system, the Gotland link in Sweden, was installed in 1954. It used line commutated current source converters (LCC) with mercury-ark valves, which in 1970 were replaced by mercury-ark thyristor valves [48]. LCC-HVDC transmission technology use thyristor (semiconductors) bridge converters and can be used at very high power levels. The semiconductor components allows current to be passed only in one direction and power flow can be reversed by changing DC voltage polarity. It can operate as rectifier or inverter depending on the firing angle. The typical converter consists of a six-pulse thyristor bridge or a 12-pulse thyristor bridge shown in Figure 2-14

Figure 2-14 Typical six-pulse and twelve-pulse LCC HVDC converter configuration

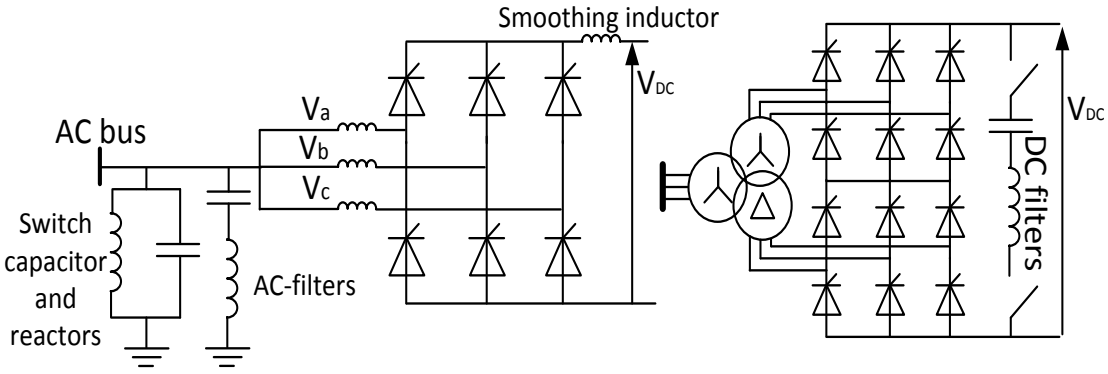

Figure 2-14 Typical six-pulse and twelve-pulse LCC HVDC converter configuration

The operation of HVDC transmission system is mainly affected by the network strength. The strength of the network can be defined by short circuit ratio (SCR) or equivalent impedance at the busbar. It can be described by equations:

$$SCR = \frac{S}{P_{dc}} \tag{1.1}$$

$$ESRC = \frac{S - Q_C}{P_{dc}} \tag{1.2}$$

where S is the apparent power (MVA) at converter terminals (AC bus), $P_{dc}$is rated DC power (MW), Q_C is the reactive power (MVAr).

To ensure commutation and avoid voltage instability, LCC-HVDC needs to be connected to relatively strong AC network with a short circuit ration of 2 [49]. This is a limitation to connect relatively weak offshore wind farm to the AC grid using LCC-HVDC. Another limitation for the use of LCC-HVDC in offshore application is the large station footprint due to reactive power supply and filtering equipment. Large platform could be more expensive in offshore environment. As mentioned before, the power flow reversal in HVDC can be achieved by polarity reversal, which means the control of a multi-terminal system is difficult [50]. However there are a couple of three terminal CSC-HVDC systems in operation to date, the HVDC Italy-Corsica-Sardinia and Radisson - Nicolet - Des Cantons circuit between Canada and the USA [51].

2.3.3 VSC-HVDC technology

A decade after the CSC-HVDC arrived the appearance of semiconductor switches, such as insulated-gate bipolar transistors (IGBT's) and integrated gate-commutated thyristors (IGCT's), have revolutionised the industry and enabled the voltage source converter (VSC) technology. VSC-HVDC transmission system has become an area of growing interest due to its benefits over the classical HVDC and conventional HVAC transmission system. First manufactured and tested by ABB also known as HVDC-light [52] and by Siemens known as HVDC-plus, further this concept has also been used by Alstom who called it HVDC MaxSine. This technology uses IGBTs devices and can switch ON and OFF current [53, 54]. This allows the pulse width modulation (PWM) to be applied as well as multi-level conversion. The general layout of a VSC-HVDC is shown in Figure 2-15.

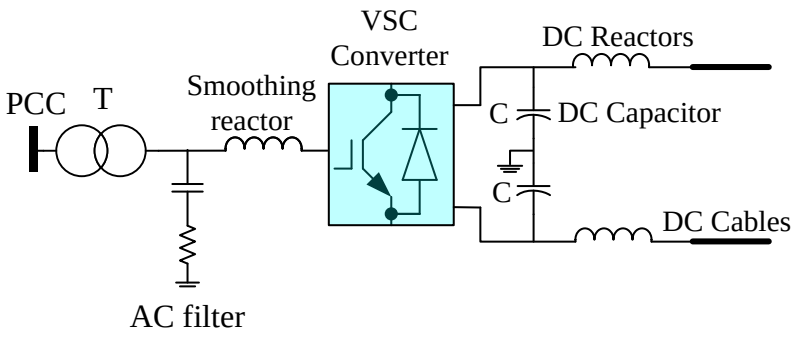

Figure 2-15 Schematic of a typical VSC-HVDC system

Table 2-2 summarises recent and planned projects using VSC-HVDC technology.

Table 2-2 Example of existing and future VSC-HVDC transmission systems.

Project	Rating (MW)	DC Voltage (kV)	Distance (km)	Commissioning year
NSN Link	1400	515	730	2020
Nemo Link	1000	400	140	2019
SydVästlänken	2x720	±300	260	2016
HelWin2	690	±320	130	2015
AL-link	100	±80	158	2015
DolWin1	800	±320	165	2015
North Sea Network	1400	515	730	2012
HVDC Troll	80	60	70	2004

VSC-HVDC technology has big advantages over the LCC-HVDC such as independent control over the active and reactive power, bi-directionality (no need for polarity reversal as in conventional HVDC). It can be connected to the weak AC network which makes it ideal for connecting offshore wind farms and it also has black-start capability [4]. In [55, 56] it is shown that a point-to-point VSC-HVDC connection improves voltage quality in the grid compared with an AC connection, where wind variation may cause propagation of voltage fluctuations. This work also highlights the advantages of decoupled operation of the transmission system and investigates different potential control strategies.

Furthermore the VSC-HVDC allows multi-terminal operation, offshore wind integration, and provide auxiliary services to the grid [57-60]. Multi-terminal VSC-HVDC is studied in [61, 62] in terms of flexible control capabilities and as a future option for connecting a large amount of power from offshore wind farms. These studies suggest that this is a very attractive option for interconnection between countries and of offshore oil and gas platforms.

However, the drawback of the converter technology is that they generate harmonics and bring the need for filtering equipment which adds another component to the multi-technology nature of the systems. Power converters also have problems during faults and making difficult to comply with grid codes during fault scenarios, therefore this research is working on advanced controls that will enable this power converter-based system to be grid-code compliant. Examples of possible applications of VSC-HVDC are shown in Figure 2-16.

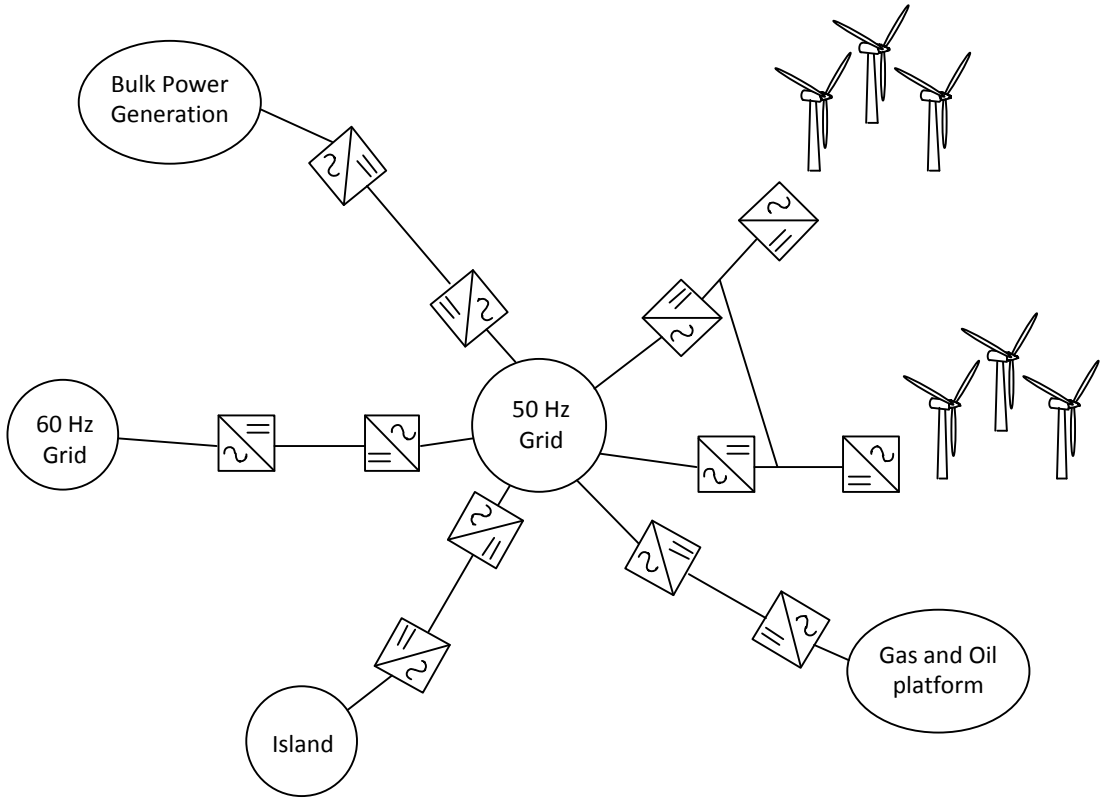

Figure 2-16 Examples of VSC-HVDC applications adapted from [63].

According to [64] the VSC-HVDC converter topologies can be divided into two main categories:

Monolithic topologies like:

- Two-level topology
- Three level neutral point clamped topology
- Diode clamped multi-level topology
- Floating capacitor multi-level topology

These topologies cannot be expanded, and usually need a large number of devices connected in series.

And modular topologies like:

- Modular multilevel converter (MMC)
- Hybrid converters (e.g: AAC)

The two-level converter topology is the most established technology, it employs PWM to achieve the desired AC waveform. This arrangement has two devices on each phase to switch on and off the voltage between two level ±Vdc. The switching frequency can be as high as 2kHz to achieve AC sinusoidal waveform which then is smoothen and filtered. The harmonic component is lower compared to LCC-HVDC which improves footprint as the converter platform can be reduced up to 50% [65]. However the main drawback of high switching frequency of two level converters is high losses, up to 1.75% [66]. Additionally, the transformer is exposed to high voltage stress which results in much larger converter transformers thus making the system less cost effective.

The design of three-level neutral point clamped (NPC) allows to use lower switching frequencies which results in lower switching losses compared to two-level converters.

Monolithic multilevel converters topology is appropriate for HV application. The principal operation is similar to two and three-level converters, however has larger number (n-number) of series connected switching devices. Numerous types of multilevel converters have been proposed based on different structures. Authors in [67, 68] focused theirs studies on NPC, in [69, 70] the aspect of flying capacitors was investigated.

Modular multilevel converter topologies made a breakthrough and become very attractive option for VSC-HVDC systems, it is relatively new concept and first installation was in San Francisco in 2010 developed by Siemens [71]. It has cascaded connection of half-bridge IGBT, which makes high-quality AC waveform using numerous discrete voltage steps.

MMC have many advantages over two-level or a three-level converter, first of all the waveform is higher quality which means smaller filtering equipment is required. Moreover losses per converter are smaller (around 0.9%) and they can be compared to CSC system this is due to switching frequency is lower per IGBT.

There are many proposed design of MMC as this concept is very attractive in both industrial applications and academic research. Another option of MMC is H-bridge modular multilevel converter (HB-MMC) [72]. It has double of IGBT devices which significantly increases the cost of converter and on state losses compare to half bridge MMC. Authors in [72] shows how this design improves an important feature of reserved current blocking capabilities

during DC fault. The alternate arm modular multilevel converter (AAMMC) is one of the hybrid convert topologies concept. This option can block DC fault currents while it has increased efficiency compare to FB-MMC.[73]. Other various topologies of VSC have been under investigation of industry and academia to deliver most likely converter design for offshore wind farm systems which will be not only reliable, with low losses but also cost effective.

2.4 Scenarios for the North Sea Offshore Network grid topologies.

There are several connection scenarios for connecting North Sea offshore wind farms to the onshore grid via VSC-HVDC transmission system. These options range from a simple radial design of a single wind farm, to a fully meshed system to connect offshore wind [74-77]. Each topology varies in terms of functionality, reliability and investment cost. Different scenarios will be discussed in this section, the main focus is the North Sea development area as it has vast wind energy potential shown in Figure 2-17.

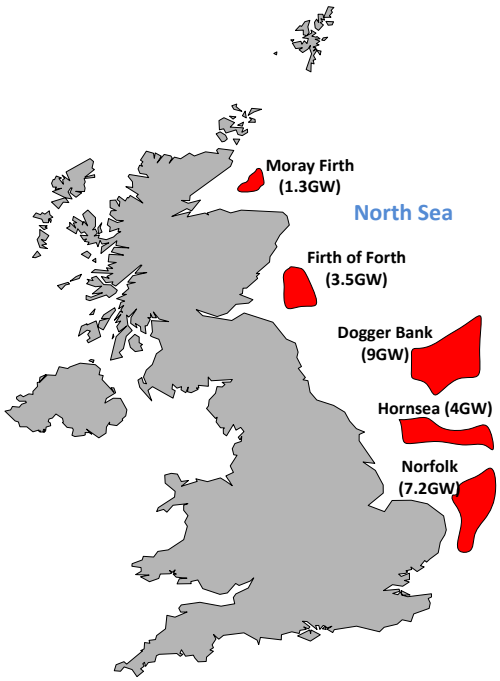

Figure 2-17 North Sea offshore wind farm zone with potential generating capacities

2.4.1 Point to point connection to shore

Most of the existing offshore wind farm projects have been realised as single point-to-point connection or multiple single confections, as presented in Figure 2-18.

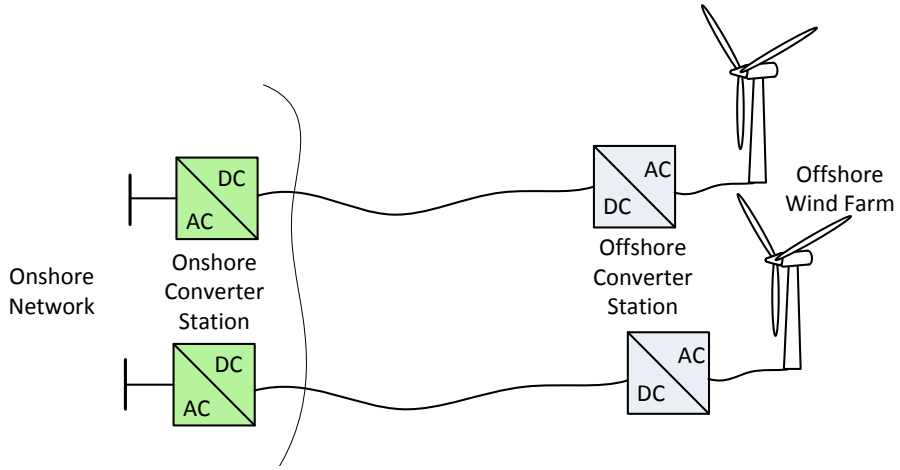

Figure 2-18 Point-to-point connection of offshore wind farms to shore

VSC-HVDC transmission system is one of the ideal solutions of connecting the offshore wind farm to the grid. This is the simplest method and has the proof of concept in multiple existing and planned projects across the world.

Most of the North Sea development zones are located far from shore, because of this, the VSC-HVDC connection is required. The VSC-HVDC system requires two converter stations on the offshore site and onshore site along with suitable landing and appropriate grid connection. There are several options which can be used for radial connection. One of the options is hybrid HVDC system with MMC based VSC and LCC system, which improves overall converter losses [78]. Another example of hybrid transmission studies are presented in [79] where authors connects a diode series connected rectifier and VSC connected inverter to deliver power from the wind farm. A new studies shows that in theory it would be possible to remove offshore converter station if connection would entirely DC from wind turbines to the onshore connection point [80].

The idea of use point-to-point connection for offshore wind farms has been reduced with the increasing number of offshore wind development. Recent proposed projects have highlighted the difficulties to obtain permission for developing major onshore grid infrastructure [81]. Also recent studies show that the overall cost of radial connection for new planned wind farms is uneconomical [76]. It is becoming economically difficult to use independent point-to-point connections for offshore wind farms to meet current targets and to minimise the associated costs. Moreover, the AC regional system will lose the wind power during loss of one of the converter station which is inappropriate as the scale of individual project comes up to 1GW from single wind farm.

2.4.2 Offshore wind farm hub connection

The concept of hub connection, also known as a cluster connection, can help solve some of the issues related to point-to-point connection. The multiple cluster connection would connect n-number of wind farms with close approximation distance between them to one common connection point and they would share one transmission path.

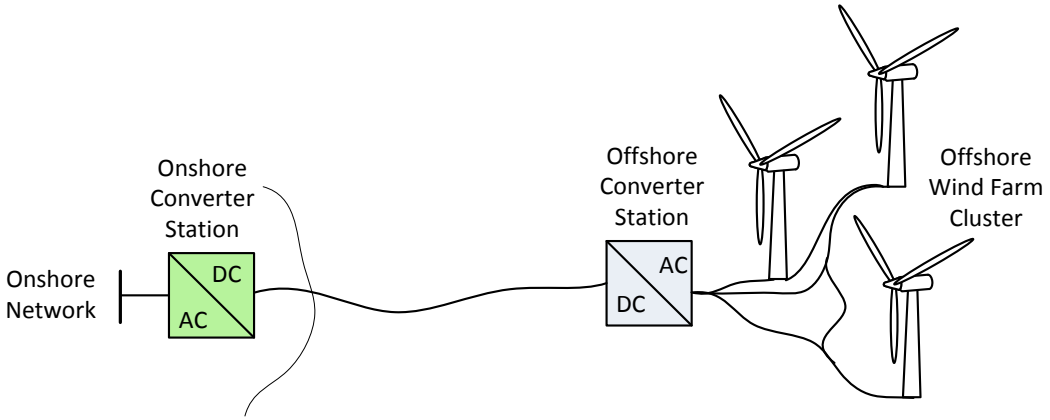

Figure 2-19 Offshore wind farm hub

The offshore wind farm hub is shown in Figure 2-19 this solution is proposed in UK Round 3 development zone [82].

The studies conducted in [76] presents that wind farm cluster connection can be more cost effective compare to connection of individual wind farms by radial connection. The main drawback of offshore wind far hub connection is technology, the size of the converter stations has to be sized for the total capacity of the whole cluster of wind farms and additionally it is limited by the capacity of the transmission cables.

In cluster connection additional auxiliary paths between wind farms can be provided so, in the event of failure, power still can be delivered to the shore. However, radial design and hub design are still subjected to single point of failure in the converter station or cables which will lead to loss of wind resources.

2.4.3 Multi terminal (three-terminal) connection options

The multi-terminal DC system is further option for connecting offshore wind, it has priority over previous described connections in term of capacity, reliability, controllability and cost [83].

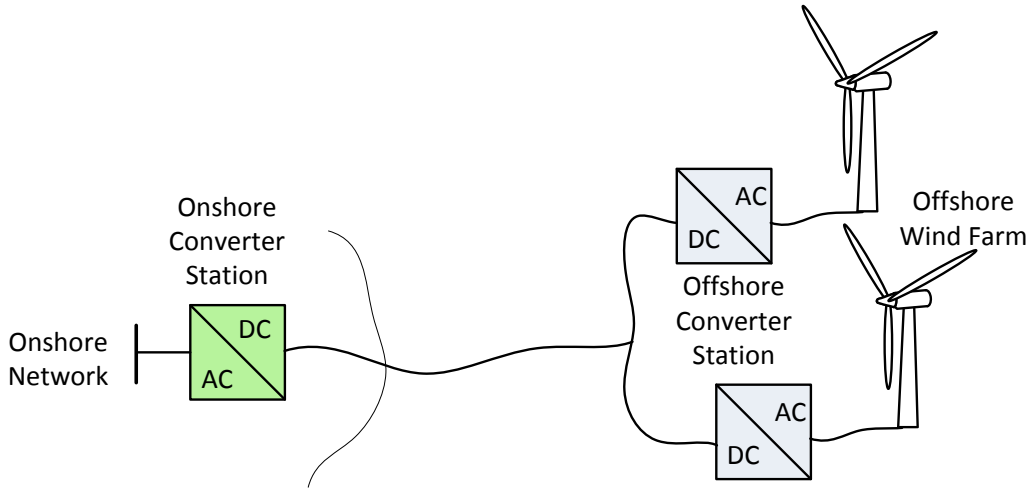

Figure 2-20 Three-terminal VSC-HVDC system, double input single output.

As we know wind farms across the North Sea are geographically dispersed over wide areas, there are several solutions for multi-terminal DC connection; the three terminals are shown in Figure 2-20 with double input and single output. This solution requires less investment cost and less land space requirements, system can address the issue of scarcity of land for right-of-way. It increases the power flow flexibility and improves system reliability and stability during the outage of VSC converter, or loss of the DC link cable [84].

Figure 2-21 shows another arrangement for connecting offshore wind power via three terminal system with two routes for power transmission to two separate AC main lands. It can improve trading power between countries yet introducing regulatory complications. The example is the Cobra project where authors in investigation potential connection of German wind farm to planned development between Denmark and Netherlands. This options shows that three different countries have a stake in such system which can be financially beneficial but introducing the need of new regulatory framework.

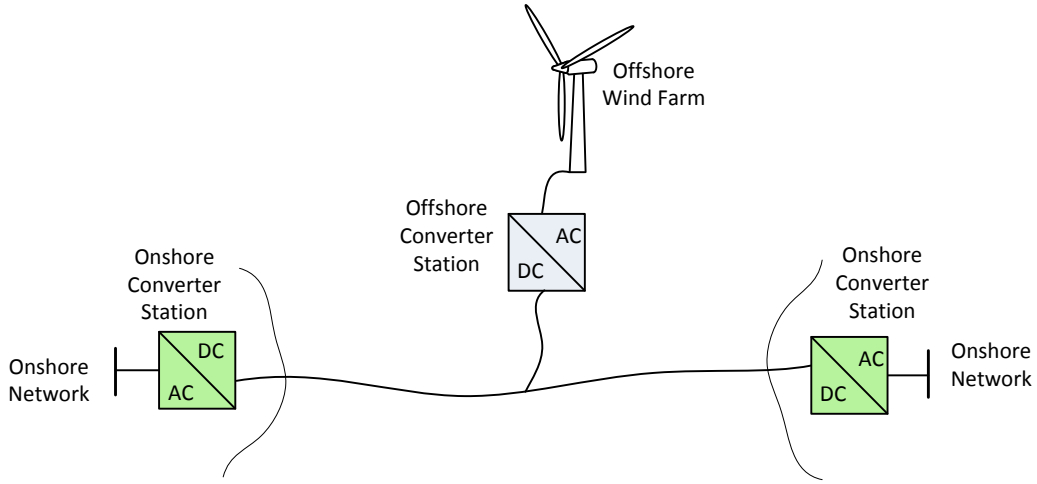

Figure 2-21 Three terminal one input double output.

2.4.4 Multi-terminal (four terminal) option

Two point-to-point connections to shore can be connected on the DC site to form the multi-terminal DG grid shown in Figure 2-22. An additional DC link could be added to existing two point-to-point connection and add benefits of security of power supply by providing alternative transmission path.

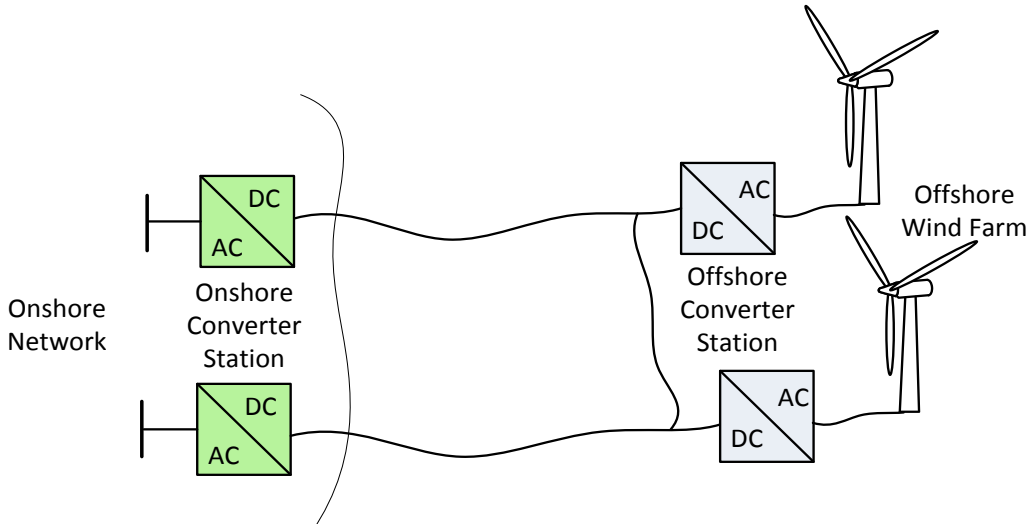

Figure 2-22 Multi-terminal connection, two input two output

2.4.5 Ring DC Network

Another option to facilitate integration of offshore wind farms in addition to power trading between regional AC networks is ring DC network design, as shown in Figure 2-23. This design provides many advantages, such as storage for power levelling between regions, additionally it can allow the use of underground or/and submarine cables as a transmission medium, supply of isolated Islands and combine different renewable technologies. However,

by adding additional power plants in to the DC ring one might exceed a total transmission capacity. This could lead to reduction of the total capacity available for transferring power between the regional links; it also could lead to curtail wind power from offshore resources. Ring DC network can help in trading power between countries but, as described before in section 2.4.3, may lead to issues involving distribution of capital costs and with some parties benefit from the project more than others.

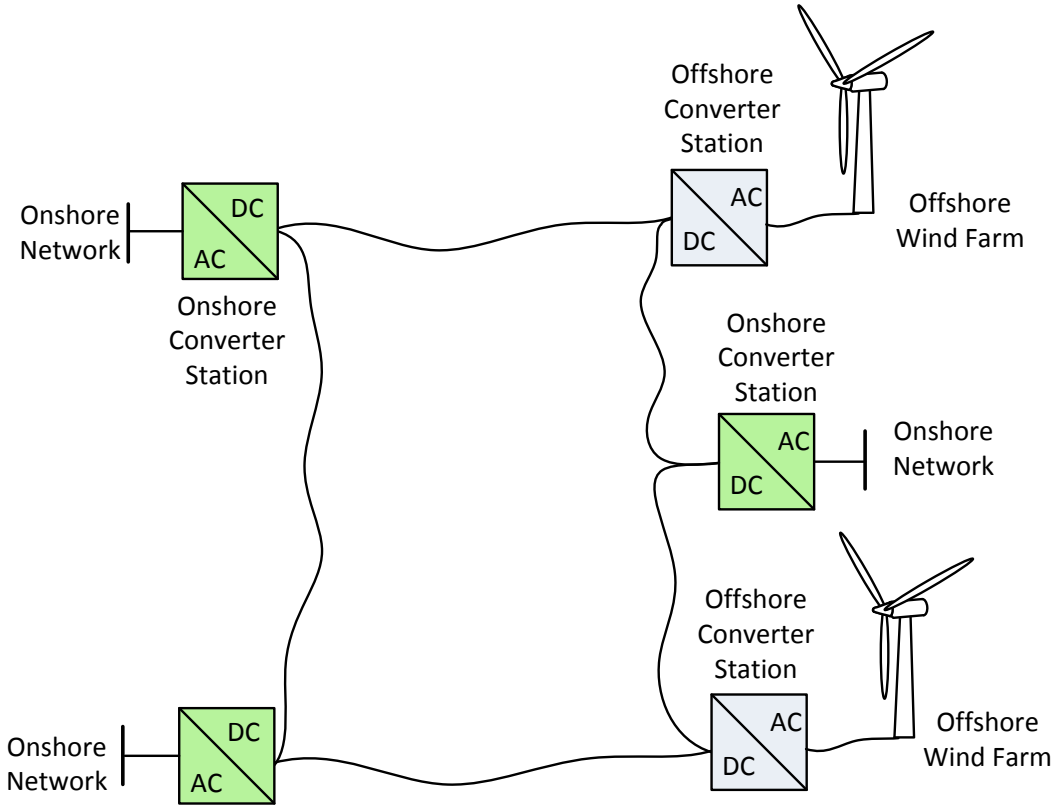

Figure 2-23 Multi-terminal DC ring design

2.4.6 Meshed design

To increase the reliability of the ring DC network system and ensure stable operation, meshed DC system can be used. The key aspect of this design is that it provides multiple transmission paths to shore and for AC regional interconnection systems. During emergency conditions, such a maintenance or loss of a DC cable, additional paths are available to push the power through [61].

The multi-terminal ring DC network or meshed system grids with VSC-HVDC systems are still vulnerable to faults occurring in the DC link and it has this limits its practical application. In this type of systems, were many cables can be connected in parallel to the one

converter station, lack of limiting impedance can occur and the fault currents can become very large very quickly and could damage VSC converters [66]. The technology gap in isolating mechanism of the DC fault and absence of reliable DC breakers is a big problem for VSC-HVDC systems.

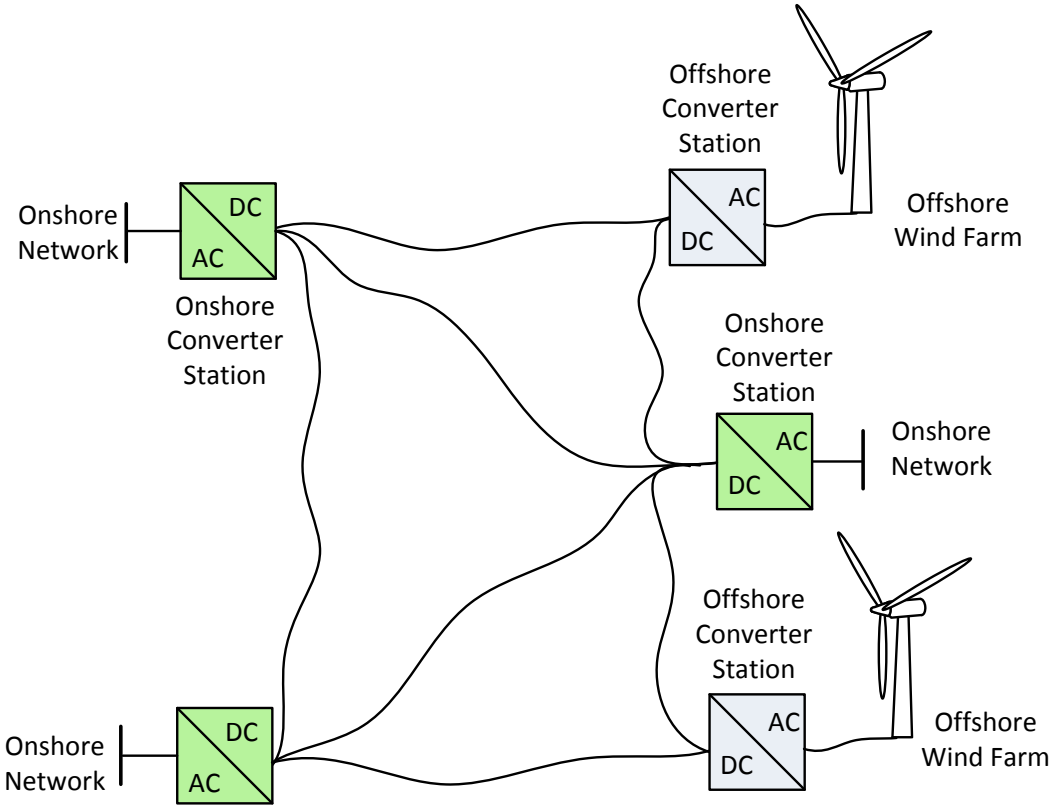

Figure 2-24 Meshed DC network based on VSC-HVDC

New technologies to solve problem of DC breakers has been introduced by industry and academia, at least in concept, however it can take number of years before the proof of concept. Furthermore the final cost of breakers is unknown and might reach up to 30% of the converter station [85].

2.5 Summary

In this chapter a present state of the art for offshore technologies has been conducted. The importance of technology choice for future wind farms is key factor for a successful system development; hence this chapter discussed the technology choice for offshore wind turbine to different transmission technologies.

A general consensus can be been made after the studies made in this chapter with the conclusion that for offshore wind farms, the choice of the low maintenance wind generator technology (such as FRC) should be used, also as there is no visual impact and it would be

beneficial to install 5MW wind turbines and larger to lower the costs of installation and maximize generated power. However there is still need for existing wind turbines to comply with FRT capabilities which will be investigated in this thesis.

Regarding the power transmission system it is clear that for the Dogger Bank located in the North Sea, the VSC-HVDC is the ideal choice. It has finical benefits in coordinated three-terminal or multi-terminal VSC-HVDC transmission system over the point-to-point connection.

2.6 References

[1] G. Lalor, A. Mullane, and M. O'Malley, "Frequency control and wind turbine technologies," *Power Systems, IEEE Transactions on,* vol. 20, pp. 1905-1913, 2005.

[2] R. Doherty, A. Mullane, G. Nolan, D. J. Burke, A. Bryson, and M. O'Malley, "An Assessment of the Impact of Wind Generation on System Frequency Control," *Power Systems, IEEE Transactions on,* vol. 25, pp. 452-460, 2010.

[3] M. Kayikci, Milanovic, x, and J. V., "Dynamic Contribution of DFIG-Based Wind Plants to System Frequency Disturbances," *Power Systems, IEEE Transactions on,* vol. 24, pp. 859-867, 2009.

[4] M. P. Palsson, T. Toftevaag, K. Uhlen, and J. O. G. Tande, "Large-scale wind power integration and voltage stability limits in regional networks," in *Power Engineering Society Summer Meeting, 2002 IEEE,* 2002, pp. 762-769 vol.2.

[5] S. S. Murthy, B. Singh, P. K. Goel, and S. K. Tiwari, "A Comparative Study of Fixed Speed and Variable Speed Wind Energy Conversion Systems Feeding the Grid," in *Power Electronics and Drive Systems, 2007. PEDS '07. 7th International Conference on*, 2007, pp. 736-743.

[6] ABB. (2012). *PCS 6000 for large wind turbines Medium voltage, full power converters up to 9 MVA*. Available: https://library.e.abb.com/public/c4de28147e528b0cc1257a8b00595934/PCS6000Wind_3BHS351272_E01_RevA.pdf

[7] S. Mohan and R. Naik, "Design approach for high power, medium voltage power conversion systems for wind turbines," in *Power Electronics and Applications (EPE'14-ECCE Europe), 2014 16th European Conference on*, 2014, pp. 1-9.

[8] O. Anaya-Lara, N. Jenkins, J. Ekanayake, P. Cartwright, and M. Hughes, *Wind Energy Generation: Modelling and Control*: Wiley, 2009.

[9] F. Sulla, "Fault Behavior of Wind Turbines ", Department of Measurement Technology and Industrial Electrical Engineering, Lund University 2012.

[10] W. Feng, D. M. Vilathgamuwa, and S. Choi San, "Design of mode switching scheme for low-voltage ride-through of doubly fed induction generators," *Renewable Power Generation, IET,* vol. 9, pp. 109-119, 2015.

[11] G. Lalor, J. Ritchie, S. Rourke, D. Flynn, and M. J. O'Malley, "Dynamic frequency control with increasing wind generation," in *Power Engineering Society General Meeting, 2004. IEEE,* 2004, pp. 1715-1720 Vol.2.

[12] D. Gautam, L. Goel, R. Ayyanar, V. Vittal, and T. Harbour, "Control Strategy to Mitigate the Impact of Reduced Inertia Due to Doubly Fed Induction Generators on Large Power Systems," *Power Systems, IEEE Transactions on,* vol. 26, pp. 214-224, 2011.

[13] D. Raoofsheibani, E. Abbasi, and K. Pfeiffer, "Provision of primary control reserve by DFIG-based wind farms in compliance with ENTSO-E frequency grid codes," in *Innovative Smart Grid Technologies Conference Europe (ISGT-Europe), 2014 IEEE PES*, 2014, pp. 1-6.

[14] M. Świerczyński, R. Teodorescu, C. N. Rasmussen, P. Rodriguez, and H. Vikelgaard, "Overview of the energy storage systems for wind power integration enhancement," in *2010 IEEE International Symposium on Industrial Electronics*, 2010, pp. 3749-3756.

[15] ofgem. (2014). *Security and Quality of Supply Standard (SQSS) GSR015: Normal Infeed Loss Risk*. Available: https://www.ofgem.gov.uk/ofgem-publications/52793/gsr007-decision-letter-final.pdf

[16] A. D. H. Florin Iov, Poul Sørensen, and N. A. Cutululis, "Mapping of grid faults and grid codes " July 2007.

[17] National Grid, "The Grid Code," 26 August 2015.

[18] European Network of Transmission System Operators for Electricity, "Network Code for Requirements for Grid connection Applicable to all Generators. Requiremenrs in the Context of Present Practices. ," 2012.

[19] N. W. Rolf Grünbaum, "FACTS to facilitate AC grid integration of large scale wind integration " *ABB White Paper*, 2010.

[20] A. Adamczyk, R. Teodorescu, R. N. Mukerjee, and P. Rodriguez, "Overview of FACTS devices for wind power plants directly connected to the transmission network," in *Industrial Electronics (ISIE), 2010 IEEE International Symposium on*, 2010, pp. 3742-3748.

[21] M. Fischer and M. Schellschmidt, "Fault ride through performance of wind energy converters with FACTS capabilities in response to up-to-date German grid connection requirements," in *Power Systems Conference and Exposition (PSCE), 2011 IEEE/PES*, 2011, pp. 1-6.

[22] M. Molinas, J. A. Suul, and T. Undeland, "Low Voltage Ride Through of Wind Farms With Cage Generators: STATCOM Versus SVC," *Power Electronics, IEEE Transactions on,* vol. 23, pp. 1104-1117, 2008.

[23] O. Anaya-Lara, L. Zifa, G. Quinonez-Varela, and J. R. McDonald, "Optimal DFIG crowbar resistor design under different controllers during grid faults," in *Electric Utility Deregulation and Restructuring and Power Technologies, 2008. DRPT 2008. Third International Conference on*, 2008, pp. 2580-2585.

[24] A. H. Kasem, E. F. El-Saadany, H. H. El-Tamaly, and M. A. A. Wahab, "An improved fault ride-through strategy for doubly fed induction generator-based wind turbines," *Renewable Power Generation, IET,* vol. 2, pp. 201-214, 2008.

[25] S. M. Muyeen, R. Takahashi, T. Murata, and J. Tamura, "A Variable Speed Wind Turbine Control Strategy to Meet Wind Farm Grid Code Requirements," *Power Systems, IEEE Transactions on,* vol. 25, pp. 331-340, 2010.

[26] N. Amutha and B. Kalyan Kumar, "Improving fault ride-through capability of wind generation system using DVR," *International Journal of Electrical Power & Energy Systems*, vol. 46, pp. 326-333, 3// 2013.
[27] The Crown Estate, "A Guide to UK Offshore Wind Operations and Maintenance," ed, 2013.
[28] P. Agarwal and L. Manuel, "Simulation of offshore wind turbine response for long-term extreme load prediction," *Engineering Structures*, vol. 31, pp. 2236-2246, 10// 2009.
[29] Masahide Umaya, Toshihide Noguchi, Michiya Uchida, Masaaki Shibata, Yasuhiro Kawai, and Ryosuke Notomi, "Wind Power Generation. Development status of Offshore Wind Turbines," 2013.
[30] S. Bala, P. Jiuping, D. Das, O. Apeldoorn, and S. Ebner, "Lowering failure rates and improving serviceability in offshore wind conversion-collection systems," in *Power Electronics and Machines in Wind Applications (PEMWA), 2012 IEEE*, 2012, pp. 1-7.
[31] H. Stiesdal; and P. H. Madsen, "Design for Reliability," presented at the Copenhagen Offshore Wind 2005, Cpoenhagen, 2005.
[32] P. Tchakoua, R. Wamkeue, M. Ouhrouche, F. Slaoui-Hasnaoui, T. A. Tameghe, and G. Ekemb, "Wind Turbine Condition Monitoring: State-of-the-Art Review, New Trends, and Future Challenges," *Energies*, vol. 7, 2014.
[33] S. Dutta and T. J. Overbye, "A clustering based wind farm collector system cable layout design," in *Power and Energy Conference at Illinois (PECI), 2011 IEEE*, 2011, pp. 1-6.
[34] ABB;, "National Offshore Wind Energy Grid Interconnection Study Executive Summary," 2014.
[35] S. J. Shao and V. G. Agelidis, "Review of DC System Technologies for Large Scale Integration of Wind Energy Systems with Electricity Grids," *Energies*, vol. 3, p. 1303, 2010.
[36] A. E. Leon, J. M. Mauricio, A. Gomez-Exposito, and J. A. Solsona, "An Improved Control Strategy for Hybrid Wind Farms," *Sustainable Energy, IEEE Transactions on*, vol. 1, pp. 131-141, 2010.
[37] W. Zheng, Y. Bo, and C. Ming, "Improvement of operating performance for the wind farm with a novel CSC type wind turbine-SMES hybrid system," in *Industrial Electronics (ISIE), 2012 IEEE International Symposium on*, 2012, pp. 1017-1022.
[38] londonarray. (2015). *London Array. The world's largest offshore wind farm*. Available: https://www.londonarray.com/wp-content/uploads/London-Array-Brochure.pdf
[39] S. Rodrigues, C. Restrepo, E. Kontos, R. Teixeira Pinto, and P. Bauer, "Trends of offshore wind projects," *Renewable and Sustainable Energy Reviews*, vol. 49, pp. 1114-1135, 9// 2015.
[40] J. Machado, M. Ventim Neves, and P. J. Santos, "Economic limitations of the HVAC transmission system when applied to offshore wind farms," in *Compatibility and Power Electronics (CPE), 2015 9th International Conference on*, 2015, pp. 69-75.
[41] National Grid, "Electricity Ten Year Statement Appendix E – Technology Sheets " 2013.

[42] G. Guidi and O. B. Fosso, "Investment cost of HVAC cable reactive power compensation off-shore," in *2012 IEEE International Energy Conference and Exhibition (ENERGYCON)*, 2012, pp. 299-304.
[43] C. Nguyen-Mau, K. Rudion, and Z. A. Styczynski, "HVDC application for enhancing power system stability," in *Science and Technology, 2011 EPU-CRIS International Conference on*, 2011, pp. 1-6.
[44] D.M. Larruskain, I. Zamora, A.J. Mazón, O. Abarrategui, and J. Monasterio, "Transmission and Distribution Networks: AC versus DC," *IEEE Power Engineering Society General Meeting,*, 24-28 June 2007.
[45] W. Li and T. Mi Sa Nguyen, "Comparative Stability Analysis of Offshore Wind and Marine-Current Farms Feeding Into a Power Grid Using HVDC Links and HVAC Line," *Power Delivery, IEEE Transactions on*, vol. 28, pp. 2162-2171, 2013.
[46] D. Elliott, K. R. W. Bell, S. J. Finney, R. Adapa, C. Brozio, J. Yu, *et al.*, "A comparison of AC and HVDC options for the connection of offshore wind generation in Great Britain," *Power Delivery, IEEE Transactions on*, vol. PP, pp. 1-1, 2015.
[47] G. P. Adam, K. H. Ahmed, S. J. Finney, K. Bell, and B. W. Williams, "New Breed of Network Fault-Tolerant Voltage-Source-Converter HVDC Transmission System," *IEEE Transactions on Power Systems*, vol. 28, pp. 335-346, 2013.
[48] ABB, "Special Report 60 years of HVDC," 2014.
[49] National Grid, "Electricity Ten Year Statement 2015, Appendix E," 2015.
[50] ENTSO-E;, "Offshore Transmission Technology," 2011.
[51] D. Van Hertem and M. Ghandhari, "Multi-terminal VSC HVDC for the European supergrid: Obstacles," *Renewable and Sustainable Energy Reviews*, vol. 14, pp. 3156-3163, 12// 2010.
[52] K. Eriksson;, "HVDC Light™ and development of Voltage Source Converters," *ABB Utilities;*, 2003.
[53] M. D. M. Davies, J. Dorn, J. Lang, D. Retzmann, D. Soerangr, "HVDC PLUS – Basics and Principle of Operation," 2008.
[54] N. Kirby, "Alstom Grid HVDC Tres Amigas and VSC Technology," 2011.
[55] D. Huang and Y. Mao, "The Study of Control Strategy for VSC-HVDC Applied in Offshore Wind Farm and Grid Connection," in *Power and Energy Engineering Conference (APPEEC), 2011 Asia-Pacific*, 2011, pp. 1-4.
[56] X. Lie, Y. Liangzhong, and C. Sasse, "Grid Integration of Large DFIG-Based Wind Farms Using VSC Transmission," *Power Systems, IEEE Transactions on*, vol. 22, pp. 976-984, 2007.
[57] L. Jun, J. Tianjun, O. Gomis-Bellmunt, J. Ekanayake, and N. Jenkins, "Operation and Control of Multiterminal HVDC Transmission for Offshore Wind Farms," *Power Delivery, IEEE Transactions on*, vol. 26, pp. 2596-2604, 2011.
[58] C. Meyer, M. Hoing, A. Peterson, and R. W. De Doncker, "Control and Design of DC Grids for Offshore Wind Farms," *Industry Applications, IEEE Transactions on*, vol. 43, pp. 1475-1482, 2007.
[59] K. Nieradzinska, J.C. Nambo, G.P. Adama, G. Kalconb, R. Peña-Gallardoc, O. Anaya-Lara, *et al.*, "North Sea Offshore Modelling Schemes with VSC-

HVDC Technology: Control and Dynamic Performance Assessment," *Elsevier*, 2013.

[60] J. Beerten, S. Cole, and R. Belmans, "Modeling of Multi-Terminal VSC HVDC Systems With Distributed DC Voltage Control," *Power Systems, IEEE Transactions on*, vol. 29, pp. 34-42, 2014.

[61] Twenties. (2013). *Deliverable: D5.4: DC grids: motivation, feasibility and outstanding issues*. Available: http://www.twenties-project.eu/system/files/D5%204_FINAL.pdf

[62] N. Uddin Ahmad Chowdhury and A. Yanushkevich, "Power flow analysis of meshed AC-DC super grid," in *PowerTech, 2015 IEEE Eindhoven*, 2015, pp. 1-6.

[63] V. K. S. Gil-Soo Jang Seong-Joo Lim Seok-Jin Lee Chan-Ki Kim, *HVDC Transmission: Power Conversion Applications in Power Systems,*, April 2009.

[64] A. Nami, L. Jiaqi, F. Dijkhuizen, and G. D. Demetriades, "Modular Multilevel Converters for HVDC Applications: Review on Converter Cells and Functionalities," *Power Electronics, IEEE Transactions on*, vol. 30, pp. 18-36, 2015.

[65] M. Barnes and A. Beddard, "Voltage Source Converter HVDC Links – The State of the Art and Issues Going Forward," *Deep Sea Offshore Wind R&D Conference, Trondheim, Norway, 19-20 January 2012*, 2012.

[66] Cigré Working Group B4-52, "HVDC Grid Feasibility Study," 2013.

[67] A. Nabae, I. Takahashi, and H. Akagi, "A New Neutral-Point-Clamped PWM Inverter," *Industry Applications, IEEE Transactions on*, vol. IA-17, pp. 518-523, 1981.

[68] T. Bingyong, G. Congzhe, L. Xiangdong, and L. Jingliang, "A voltage balancing controller with fuzzy logic strategy for neutral point clamped multilevel converter," in *Electrical Machines and Systems (ICEMS), 2014 17th International Conference on*, 2014, pp. 2490-2494.

[69] G. P. Adam, B. Alajmi, K. H. Ahmed, S. J. Finney, and B. W. Williams, "New flying capacitor multilevel converter," in *Industrial Electronics (ISIE), 2011 IEEE International Symposium on*, 2011, pp. 335-339.

[70] M. Khazraei, H. Sepahvand, K. Corzine, and M. Ferdowsi, "A generalized capacitor voltage balancing scheme for flying capacitor multilevel converters," in *Applied Power Electronics Conference and Exposition (APEC), 2010 Twenty-Fifth Annual IEEE*, 2010, pp. 58-62.

[71] H. G. J. DORN, J. STRAUSS, and J. A. T. WESTERWELLER, "Trans Bay Cable – A Breakthrough of VSC Multilevel Converters in HVDC Transmission " *Cigre*, 2012.

[72] G. P. Adam, S. J. Finney, K. Bell, and B. W. Williams, "Transient capability assessments of HVDC voltage source converters," in *Power and Energy Conference at Illinois (PECI), 2012 IEEE*, 2012, pp. 1-8.

[73] M. M. C. Merlin, T. C. Green, P. D. Mitcheson, D. R. Trainer, R. Critchley, W. Crookes, *et al.*, "The Alternate Arm Converter: A New Hybrid Multilevel Converter With DC-Fault Blocking Capability," *Power Delivery, IEEE Transactions on*, vol. 29, pp. 310-317, 2014.

[74] National Grid, "Offshore Electricity Transmission: Possible Options for the Future " 2011.

[75] National Grid, "Round 3 Offshore Wind Farm Connection Study," 2011.
[76] P. K. Jan De Decker, "OffshoreGrid: Offshore Electricity Grid Infrastructure in Europe," 2011.
[77] O. Anaya-Lara, G. Kalcon, G. Adam, K. Nieradzinska, G. Tande John Olav, K. Uhlen, *et al.*, "North Sea Offshore Networks Basic Connection Schemes Dynamics Performance Assessment," presented at the EPE Joint Wind Energy and T&D Chapters Seminar, 2011.
[78] R. Zeng, L. Xu, L. Yao, S. J. Finney, and Y. Wang, "Hybrid HVDC for Integrating Wind Farms with Special Consideration on Commutation Failure," *Power Delivery, IEEE Transactions on*, vol. PP, pp. 1-1, 2015.
[79] N. Thanh Hai, L. Dong-Choon, and K. Chan-Ki, "A Series-Connected Topology of a Diode Rectifier and a Voltage-Source Converter for an HVDC Transmission System," *Power Electronics, IEEE Transactions on*, vol. 29, pp. 1579-1584, 2014.
[80] D. Elliott, "A Study of the Feasibility of Connecting Large Offshore Wind Turbines in Electrical Clusters," Department of Electronic and Electrical Engineering University of Strathclyde, 2014.
[81] S. Government;, "Environmental Statement - Proposed Beauly to Denny 400kV Overhead Transmission Line," ed.
[82] T. C. E. National Grid, "Offshore Transmission Network Feasibility Study," 2011.
[83] G. P. Adam, O. Anaya-Lara, and G. Burt, "Multi-terminal DC transmission system based on modular multilevel converter," in *Universities Power Engineering Conference (UPEC), 2009 Proceedings of the 44th International*, 2009, pp. 1-5.
[84] M. M. Temesgen M. Haileselassie, Tore Undeland, "Multi-Terminal VSC-HVDC System for Integration of Offshore Wind Farms and Green Electrification of Platforms in the North Sea," *Nordic Workshop*, 2008.
[85] D. Jovcic, D. Van Hertem, K. Linden, J. P. Taisne, and W. Grieshaber, "Feasibility of DC transmission networks," in *Innovative Smart Grid Technologies (ISGT Europe), 2011 2nd IEEE PES International Conference and Exhibition on*, 2011, pp. 1-8.

Chapter 3:

Wind Turbine modelling and enhanced control

The usual control task of a wind turbines seeks to maximise the energy generation from the incoming wind and also to operate the wind generator in a fashion that meets the requirements of operation stated in the Grid Codes specified in section CC.6. The penetration of wind power in the power grid has made necessary the creation of new grid codes for wind turbines in order to guarantee stability and reliability of power system. Specifically, since more wind turbines are being connected to the grid and the wind farms are getting larger in size, there is an unavoidable need to operate and control the wind power systems in an enhanced, more robust manner. Additionally, the new requirements for wind power plants also demand the capacity to provide auxiliary services to the grid. Since DFIG wind turbines is one of the most used technologies for wind power plants,[1] [2, 3] there has been extensive research effort focused in making the DFIG technology compatible with the new grid code requirements [4-8]. Nevertheless, it is foreseen that the dominant technology of the near future wind farms will shift towards the fully-rated converter technology. This shift, however, will be gradual and for a long period of time the two technologies will work together, sometimes within the same wind farm, to generate power from the wind. Because of this, any analysis and improvement of grid code compatibility of wind power plants should include the interaction of the two main commercial technologies of wind farms.

In the event of the fault or voltage sag the wind turbines are required to remain connected to the grid for duration of time specified by National Grid in Grid Code specified in section CC.6.3.15.1 [9]. The Low Voltage Ride-Through (LVRT) requirements for wind turbines in GB are shown in Figure 3-1.

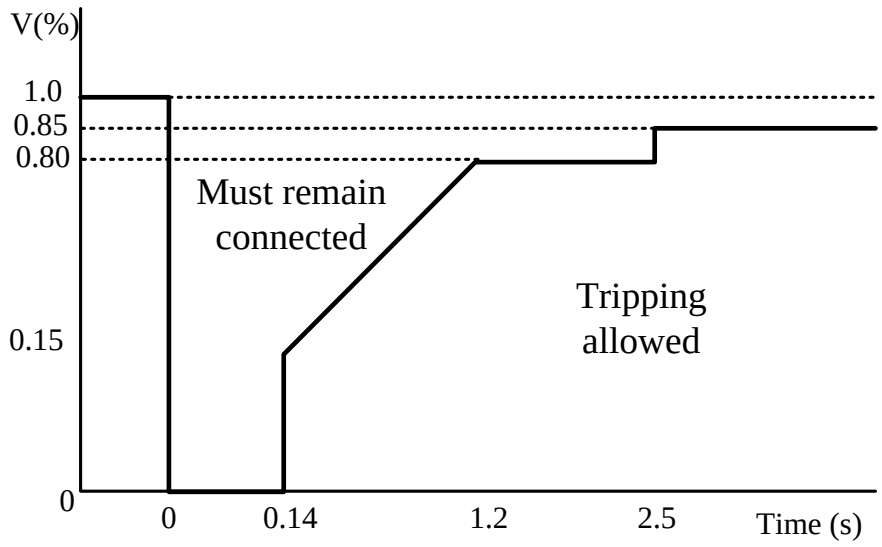

Figure 3-1 Under Voltage Ride-Through requirements for GB grid

This chapter provides operation principles and theory of operation on doubly-fed induction machine and fully-rated converter wind turbine generators working together in the same wind farm. Furthermore, this chapter explores novel control to improve AC voltage during voltage sag in a hybrid wind farm, consisting of DFIG and FRC wind turbines, with the aim of improving the hybrid system compatibility with grid codes.

3.1 Double-Fed Induction Generator (DFIG) wind turbine

Double Fed Induction Generators are widely used in variable speed wind power plants. Most of the current onshore and offshore wind farms are composed of DFIG wind turbines [10]; however the trend is going towards FRC wind turbines for offshore sector due to higher reliability [11, 12]. Figure 3-2 shows a typical diagram of DFIG wind turbine showing the directions of power flow in the stator and in the rotor, as well as the control variables of the system. A DFIG is a wound-rotor induction machine which can feed power to the network from the stator, and through the rotor via a bi-directional power converter. The stator is directly connected to the network and the rotor is connected to the AC network through a back-to-back converter. DFIGs are variable-speed wind turbines that use slip rings to control the current on the rotor windings to maximize power extraction as wind speed varies. This is achieved by injecting a controllable voltage into the rotor circuit.

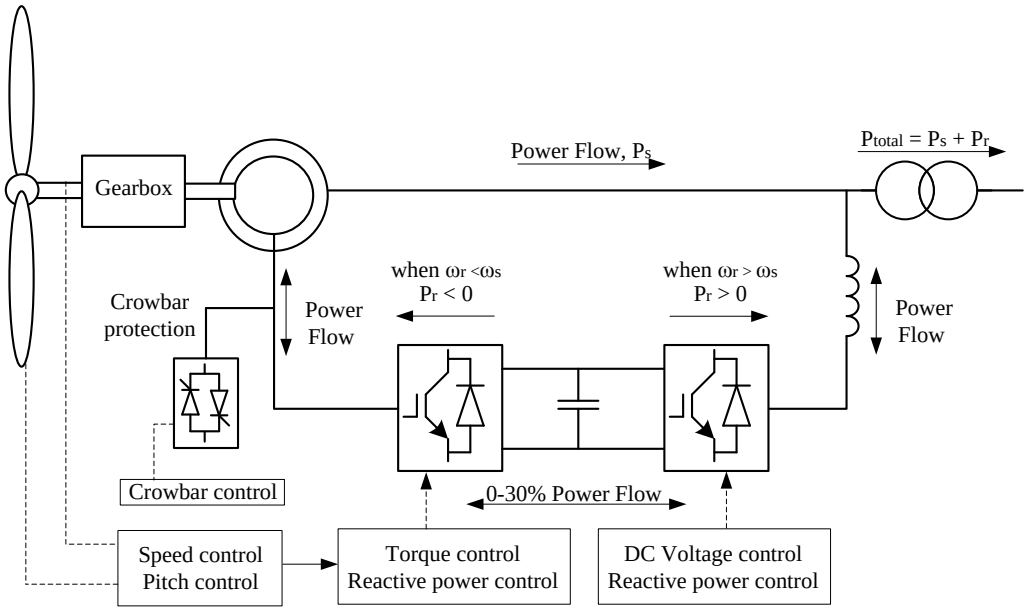

Figure 3-2 diagram of DFIG-Based Wind Turbine Induction Machine

There are several advantages of using variable-speed DFIG wind turbines, such as reduced mechanical stress on the rotor and structure of the turbine and low acoustic noise [13]. Variable-speed wind turbines, which are using power converters, have controllability of active and reactive power. They also enable a reduction in the fluctuation in output power and voltage (flicker) due to wind variations, which helps to meet Grid Code requirements specified in section CC.5, for connection of large wind farms at a reduced cost. In addition, they allow maximum power extraction over a wide range of wind speed (unlike FSIGs) [14]. Usually, to protect the power electronics converters of the DFIG during an AC network fault, a crowbar protection is connected to the rotor windings and actives when rotor currents exceed around 1.5pu of the nominal current. A crowbar protection is an electrical circuit used to protect the back-to-back's rotor converter from over-currents in the rotor circuit or over-voltage in the DC link during grid voltage dips. The crowbar protection is composed of a bank of resistors that are connected to the rotor windings instead of the rotor-side converter when a fault happens. The crowbar resistance is big enough to reduce transient currents for short period of time. To comply with Grid Code Fault Right-Through requirements CC.6.3.15.1, a good number of DFIG have been fitter with the crowbar protection [15]. Without crowbar protection, DFIG wind turbines cannot remain connected to the ac system during a fault, since large transient currents would damage its back to back converter. When the crowbar is activated, the DFIG behaves identically to an FSIG and absorbs reactive power from the grid. This is a major problem as it causes the grid voltage to drop further and interrupts normal grid operation as explained in next section.

3.2 DFIG wind turbines under fault conditions

DFIG wind turbines, just as any induction machine, require reactive power to induce a magnetic field in the stator and rotor windings. However in the case of DFIG the provision of this reactive power comes from the interaction of currents created by the power electronics connected to its rotor circuit, meaning this, that no reactive power from grid is needed for the proper operation of a DFIG [16]. Nevertheless, a major problem with DFIGs is that, during a fault, the device becomes a large consumer of reactive power due to loss of the reactive power provision from the power electronics (because of the crowbar protection action). This is a major problem for wind farms based in the DFIG technology, especially in cases with large-scaled wind farms [17]. The reactive power consumed by a DFIG wind farm subjected to a fault might cause voltage instabilities; hence the need of reactive power compensation units during the fault period is unavoidable.

During a fault, the DFIG transient currents exceed the nominal currents by several degrees of magnitude [18]. The magnitude of these transient currents depends on the severity of the fault, the operating slip value, and the incoming wind. To analyse the case of the fault currents of a DFIG machine, next section presents an analysis of the DFIG technology and the equations involved in the magnitude of the currents and electrical torque of a DFIG in both steady state and transient conditions.

3.2.1 Mathematical model of induction machine in *abc* reference frame for steady state and transient current calculation.

Figure 3-3 Conventional single-phase equivalent circuit of an induction machine

shows conventional per-phase equivalent circuit of induction generator [19]. The model consists of stator winding and rotor winding with slip ring. In this figure v_s and v_r are the stator and rotor voltages, R_s, R_r are the stator and rotor resistances resistance and L_s, L_r are the stator and rotor inductances.

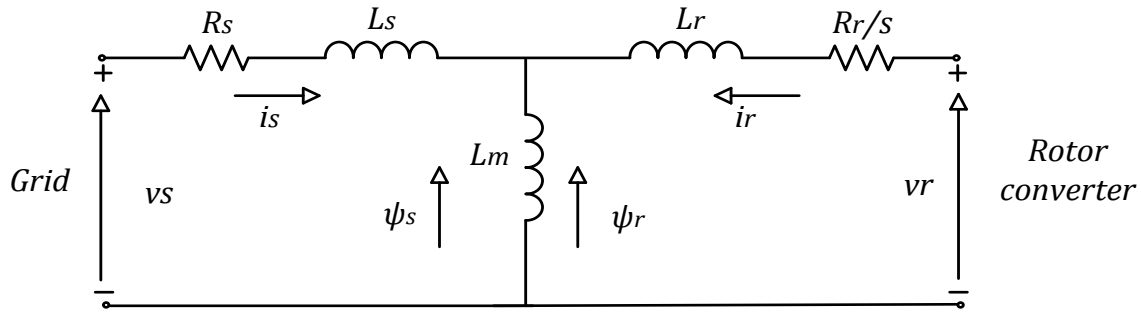

Figure 3-3 Conventional single-phase equivalent circuit of an induction machine

Voltage equations for induction machine stator can be written as:

$$v_{as} = R_s i_{as} + \frac{d\psi_{as}}{dt} \tag{3.1}$$

$$v_{bs} = R_s i_{bs} + \frac{d\psi_{bs}}{dt} \tag{3.2}$$

$$v_{cs} = R_s i_{cs} + \frac{d\psi_{cs}}{dt} \tag{3.3}$$

And analogically for the rotor:

$$v_{ar} = R_r i_{ar} + \frac{d\psi_{ar}}{dt} \tag{3.4}$$

$$v_{br} = R_r i_{br} + \frac{d\psi_{br}}{dt} \tag{3.5}$$

$$v_{cr} = R_r i_{cr} + \frac{d\psi_{cr}}{dt} \tag{3.6}$$

Where $v_{abcs}, v_{abcr}, i_{abcs}, i_{abcr}$ are the stator and rotor voltages and currents, and ψ_{abcs}, ψ_{abcr} are the stator and rotor flux linkages.

The fluxes of the machine are defined by:

$$\psi_{as} = L_s i_{as} + L_m i_{ar} \tag{3.7}$$

$$\psi_{bs} = L_s i_{bs} + L_m i_{br} \tag{3.8}$$

$$\psi_{cs} = L_s i_{cs} + L_m i_{cr} \tag{3.9}$$

$$\psi_{ar} = L_r i_{ar} + L_m i_{as} \tag{3.10}$$

$$\psi_{ar} = L_r i_{ar} + L_m i_{as} \tag{3.11}$$

$$\psi_{br} = L_r i_{br} + L_m i_{bs} \tag{3.12}$$

$$\psi_{cr} = L_r i_{vr} + L_m i_{cs} \tag{3.13}$$

Where L_m is the mutual inductance between stator and rotor windings. The IG speed rotor is defined as:

$$\frac{d\omega_r}{dt} = \frac{1}{J_g}(T_m - T_e) \tag{3.14}$$

Where J is the moment of inertia, T_m is mechanical torque and T_e is electrical torque.

3.2.2 Current and torque behaviour during DFIG faults.

A DFIG machine running at synchronous speed with no load would produce a steady state stator current "*a*" of magnitude (neglecting R_s and assuming $i_{ar} = 0$ and following equations (3.4), (3.7) [20]:

$$i_{as}e^{j\omega_s t} = \frac{v_{as}e^{j\omega_s t}}{j\omega_s L_s} \tag{3.15}$$

Where ω_s is the synchronous frequency. However, during a symmetrical voltage dip, the stator flux becomes non-stationary, and the stator transient current can be expressed as [20, 21]:

$$\begin{aligned} i_{as,0} = \frac{v_{as}(1-u)e^{j\omega_s t}}{j\omega_s L_s} + \frac{uv_{as}}{j\omega_s L_s}e^{-\frac{t}{T_s}} \\ -(k_r)\ x\left[k_s\frac{[v_{as}(1-u)e^{j\omega_s t} + uv_{as}e^{-\frac{t}{T_s}}}{j\omega_s L_s}\right. \\ \left. + \frac{v'_{ar}}{s_\omega}e^{j\omega_s t}\right] \end{aligned} \tag{3.16}$$

Where $i_{as,0}$ is phase *a* current at t=0, *u* is the magnitude of the voltage dip, k_s, k_r are the stator and rotor coupling factors defined as $k_s = \frac{L_m}{L_s}, k_r = \frac{L_m}{L_r}$, $e^{-\frac{t}{T_s}}$ is a time constant changing with a duration of the fault, v'_{ar} is the rotor a-phase voltage, s_ω is the slip of the DIFG.

The above equation shows that during the voltage sag the machine transient currents are mostly inductive and strongly depend on the magnitude of the voltage sag, with a magnitude defined by *u* and the value of L_s. This is shown in the first term of the right-hand side of (3.16), the second term on the right-hand side shows that the stator transient currents also provides a DC current with a decay time constant $e^{-\frac{t}{T_s}}$. The last part of (3.16) equation demonstrates that rotor flux will add some DC and AC current to the stator current.

Also, during a fault, the behaviour of the electromagnetic torque of the generator (T_e) during voltage sag is severely affected. To illustrate this equation (3.17) shows the behaviour of electromagnetic torque T_e in steady state:

$$T_e = \frac{3}{\omega_s}\frac{R_r'}{s_\omega}\left[\frac{|v^2|}{\left(r_s' + \frac{r_r'}{\omega_s}\right)^2 + (X_s + X_r')^2}\right] \tag{3.17}$$

Where X_s, X_r' are stator reactance and rotor reactance respectively. The equation (3.17) shows that the generated T_e of the machine depends on the magnitude of the voltage (more specifically, it is proportional to the square of the supplied voltage). This means that a decrement of the voltage will cause T_e to decreases in a quadratic manner. During a steady state operation T_e and T_{mech} are equal. Thus, any difference between T_e and T_{mech} reflects in the machine speed, either slowing down or speeding up. Therefore, during a voltage sag and a reduction of T_e the rotor speed ω_r increases according to the equation of motion of the induction machine:

$$J\frac{d}{dt}\omega_r = T_{mech} - T_e - B_m\omega_r$$

Where J is the moment of inertia of the IG and B_m is the damping factor. If ω_r increases excessively the machine reaches a point where synchronism is lost and T_e permanently collapses, leading to a further increase in the speed of the machine. This scenario may lead to a failure of mechanical components.

3.2.3 Mathematical model of DFIG wind turbine in arbitrary dq reference frame.

The model of asynchronous machine in this case is a fourth-order state-space model; Figure 3-4 shows the equivalent circuit on the induction machine in arbitrarily rotating frame and is expressed in terms of two axis *d* and *q*. To simplify the design of the control and analysis of the machine dynamics, for stator and rotor of the DFIG wind turbine, the three-phase equations (abc) are expressed in the dq0 reference frame, the voltage equations for the stator can be shown [22]:

$$v_{ds} = R_s i_{ds} + \frac{d\psi_{ds}}{dt} - \omega_s\psi_{qs} \tag{3.19}$$

$$v_{qs} = R_s i_{qs} + \frac{d\psi_{qs}}{dt} + \omega_s\psi_{ds} \tag{3.20}$$

Where v_{ds}, v_{qs} are the dq components of the stator voltage, i_{ds} , i_{qs} are the dq0 components of the stator currents, ψ_{ds} , ψ_{qs} are the dq component of the stator flux, and ω_s is angular frequency and is the same used in the dq0 reference frame.

The flux-linkage equations for the stator are expressed as:

$$\psi_{ds} = L_{ls} i_{ds} + L_m (i_{ds} + i_{dr}) \tag{3.21}$$

$$\psi_{qs} = L_{ls} i_{qs} + L_m (i_{qs} + i_{qr}) \tag{3.22}$$

The voltage equations for the rotor are stated as:

$$v_{dr} = R_r i_{dr} + \frac{d\psi_{dr}}{dt} - (\omega_s - \omega_r)\psi_{qr} \tag{3.23}$$

$$v_{qr} = R_r i_{qr} + \frac{d\psi_{qr}}{dt} + (\omega_s - \omega_r)\psi_{qr} \tag{3.24}$$

Where v_{dr}, v_{qr} are the dq0 components of the rotor voltage, i_{dr} , i_{qr} are the dq0 components of the rotor currents, ψ_{dr} , ψ_{qr} are the dq0 component of the rotor flux, and ω_s ω_r are angular frequencies.

The flux-linkage equations for the rotor are expressed as:

$$\psi_{dr} = L_{lr} i_{dr} + L_m (i_{ds} + i_{dr}) \tag{3.25}$$

$$\psi_{qr} = L_{lr} i_{qr} + L_m (i_{qs} + i_{qr}) \tag{3.26}$$

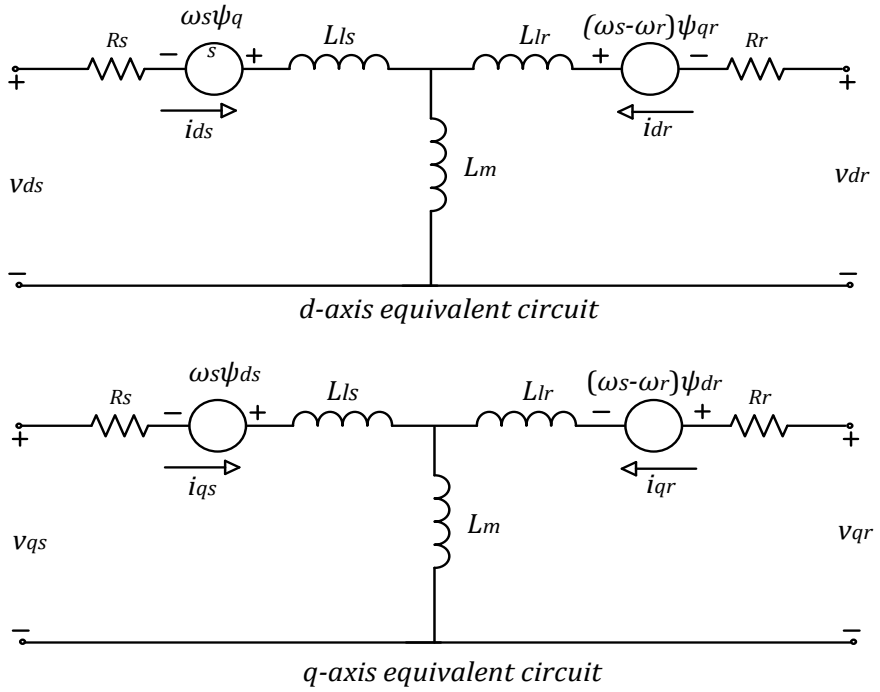

Figure 3-4 Dynamic or d,q equivalent circuit of an induction machine.

The electromechanical torque T_e of the machine is expressed as:

$$T_e = \left(\frac{3}{2}\right)\left(\frac{P}{2}\right)(i_{dr}\psi_{qr} - i_{qr}\psi_{dr}) \tag{3.27}$$

Where *P* is the number of pole pairs of the induction machine.

The majority of the induction machine has delta or 'Y' connection with no neutral, hence the zero sequence variables are zero, and not included in the calculations.

3.2.4 Control of DFIG wind turbine

The control of a DFIG wind turbine consists of four main controllers and they are achieved via back-to-back converters control. In a DFIG, the variables to control are: rotor speed (ω_r), DFIG reactive power (*Qs*), DC voltage of the back-to-back converter (v_{dc}) and reactive power of the grid side converter (GSC). In order to control the DFIG, the controller controls the currents circulating between RSC and rotor windings (i_{dr} i_{qr}) and also currents circulating between the grid side converter (GSC) and the grid ($i_{d\,gsc}$ $i_{q\,gsc}$). These currents are controlled by rotor side converter (RSC) voltages (v_{dr} v_{qr}) and GSC voltages ($v_{d\,gsc}$ $v_{q\,gsc}$).

Figure 3-5 Simplified diagram of a DFIG control loops

Figure 3-5 illustrates a simplified diagram of a DFIG wind turbine control loops.

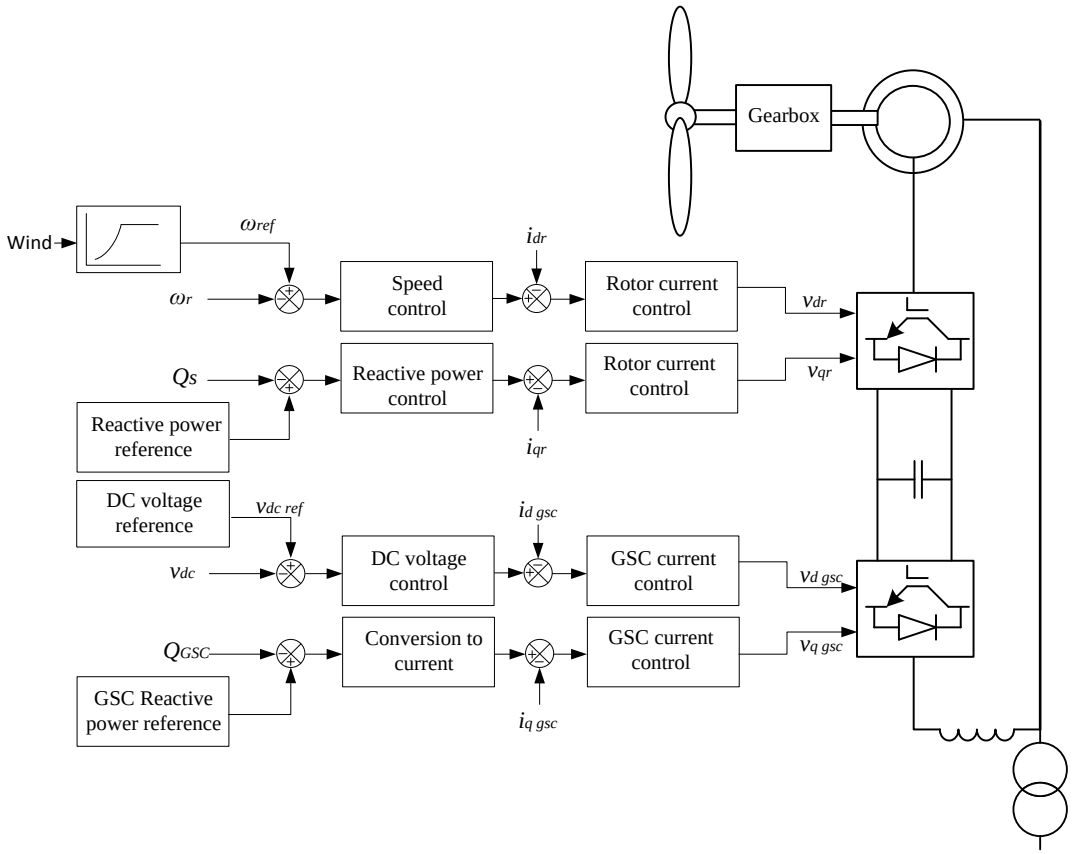

Figure 3-5 Simplified diagram of a DFIG control loops

3.2.5 Control of the rotor site converter

The rotor side control loop is shown in Figure 3-6. The rotor speed control (ω_r) is compared to a reference value, then, the error is reduced to 0 by the PI controller by modifying the electrical torque *Te_ref*. The relationship between i_{dr} current and electrical torque T_e can be derived from equations (1.15) (1.17) and (1.19) assuming $\psi_{ds} = 0$ and $\psi_{qs} = const$, this is:

$$T_e = \left(\frac{3}{2}\right)\left(\frac{P}{2}\right)\left(\frac{-L_m \psi_{qs}}{L_{ls} + L_m}\right) i'_{dr} \tag{3.28}$$

Having found the relationship between i_{dr} and T_e, the PI controller for the rotor speed can be derived as follows:

The transfer function of the mechanical system of a DFIG, $P_\omega(s)$, is given by (considering the mechanical torque as a disturbance);

$$P_\omega(s) = \frac{\omega_r(s)}{T_e(s)} - \frac{1}{Js + B_m} \tag{3.29}$$

Where B_m is the friction coefficient. Equation (3.29) shows that the open loop mechanical system of the DFIG has a stable pole at $-B_m/J$. This pole can be canceled with the zero provided by a PI controller with proportional constant $K_{p\omega}$ and an integral constant $K_{i\omega}$.

Choosing $K_{i\omega}/K_{p\omega} = B_m/J$ and $K_{p\omega}/J = 1/t_\omega$ where t_ω is the time constant of the closed loop system then dynamics of the closed control loop are defined by:

$$\frac{1}{t_\omega s + 1} \tag{3.30}$$

Which is a first order transfer function with unity gain. The selection of t_ω defines the closed loop bandwidth of the system.

Once the $i^*_{dr\_ref}$ is obtained, it is compared with i_{dr} to reduce error between the currents to zero. This is carried out by manipulating v_{dr}.

The reactive power controller Q_s is compared with reference value Q_{s_ref}, reducing the error to zero by the PI controller, the transfer function for the reactive power is

$$K_Q(s) = \frac{3}{2}\frac{Ki_Q}{s}\left[\frac{v_{ds}(\psi_{qs} - L_m)}{L_{ls} + L_m}\right] \tag{3.31}$$

Where v_{ds} is the stator voltage, ψ_{qs} is the stator flux, $L_{ls}\ and\ L_m$ are stator inductance and mutual inductance respectively, Ki_Q is the integral gain of the controller, where selecting $Ki_Q = 1/t_\omega$ and t_ω is the time constant of the closed loop system, then dynamics of the closed control loop are defined by:

$$G_Q(s) = \frac{Q_{s\_ref}}{Q_s} = \frac{1}{t_Q s + 1} \tag{3.32}$$

The equation 3.32 means that the closed loop transfer function from the set point to the variable is governed by first-order dynamics. The term t_Q determinates the speed of the controller and can be chosen accordingly to a desired closed loop response.

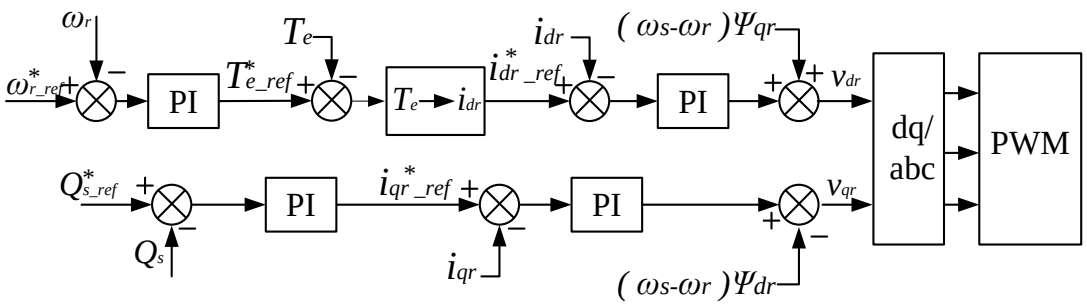

Figure 3-6 Simplified schematic of the RSC controllers

3.2.6 DFIG Simulation Results

(b) Reactive power control

Figure 3-7 shows the performance of the DFIG wind turbine speed control and reactive power control during a wind speed increment and reactive power reference change.

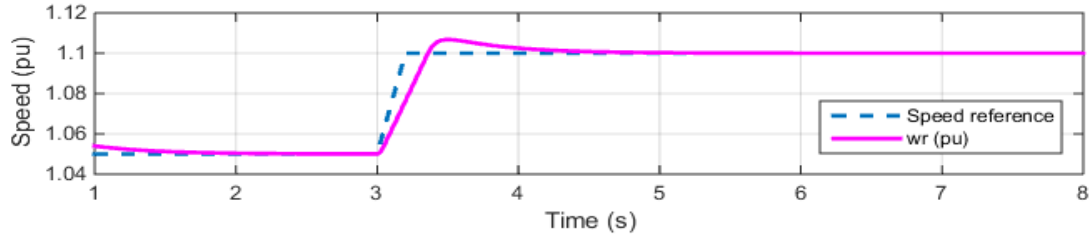

(a) Speed control

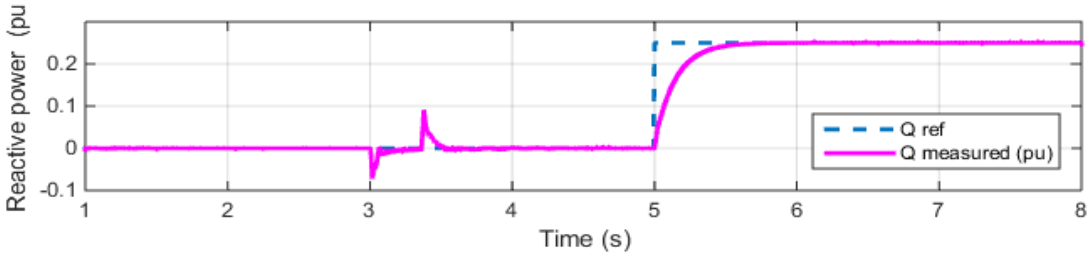

(b) Reactive power control

Figure 3-7 DFIG RSC controller performance, speed control and reactive power control.

Initially the system operates at wind speed 10m/s. At t=3 the wind speed changes to 10.5 m/s and, at the same time, the controller reacts and the rotor speed (ω_r) increases following the maximum power tracking speed reference shown in Figure 3-7 (a). The Figure 3-7(b) shows the reactive power control, at t=3 there is influence of the speed controller due to the coupling terms and corrected directly by the control action of the reactive power controller. At t=5 the reactive power reference is increased to 0.25pu and reactive power follows the reference speed. This demonstrates the robust of the speed and the reactive power controllers under the step changes.

In the case of the DFIG speed control, assessing exactly how fast the measured signal follows the reference depends firstly on the inertia of the machine and secondly on the k_p and k_i gains, in the case of this study the inertia of the machine is H=2.5 and speed of the PI controllers.

3.2.7 Control of the Grid Side Converter

The grid side converter control loop is show in the Figure 3-8. This controller is responsible for maintaining DC voltage between the RSC and GSC converters and for reactive power. In the DC controller, the PI controller is reducing the error between the V_{dc} and $v^*_{dc\_ref}$, to get current reference $i^*_{dr\_ref}$ which can be compared with current value i_{dr} to again reduce the error between the set point and the measured variable. That can be achieved by poles-zero cancellation method. To model the system and derive transfer function for the DC controller, to the original control loop the additional control loop is added to make the system more robust. This additional loop takes under consideration power provided or consumed by the RSC as a disturbances and improves the natural response of the system [21] [23], and is represented by following equation:

$$\frac{v^2_{dc}(s)}{i_{d\_gsc}} = -\frac{P_{dc}(s)}{1 + P_{dc}(s)G_{dc}} = -\frac{3v_d}{C_s + 3v_d G_{dc}} \tag{3.33}$$

That process will obtain the controllable voltage V_{d_gsc}. The reactive power controller provides inner control loop with the current reference value $i^*_{qr_gsc_ref}$to compare with measured current i_{qr}then the error is reduced to 0 by the PI controller, the V_{q_gsc} value is a consequence of the PI control actions.

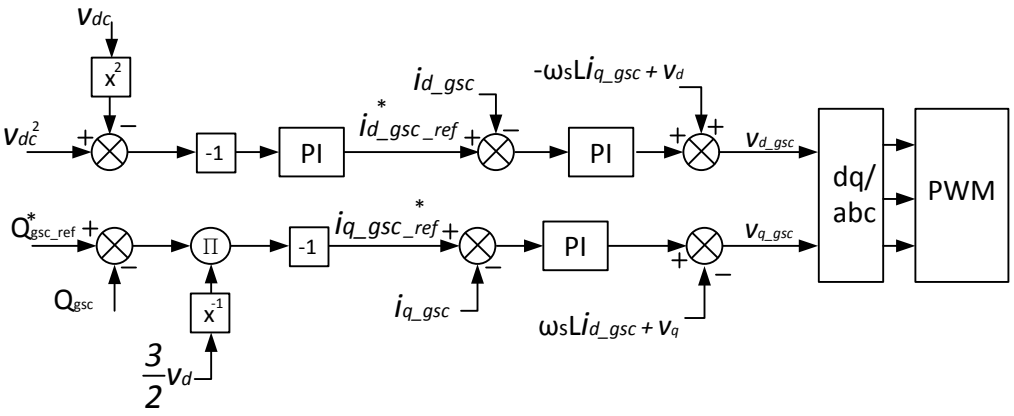

Figure 3-8 Simplified schematic of the GSC controllers

Simulation Results

Figure 3-9 shows the performance of the DC voltage controller and reactive power controller. The Figure 3-9 (a) shows that DC voltage is kept constant while the reactive power in Figure 3-9 (b) at t=5 is increased from 0 pu to 0.25 pu.

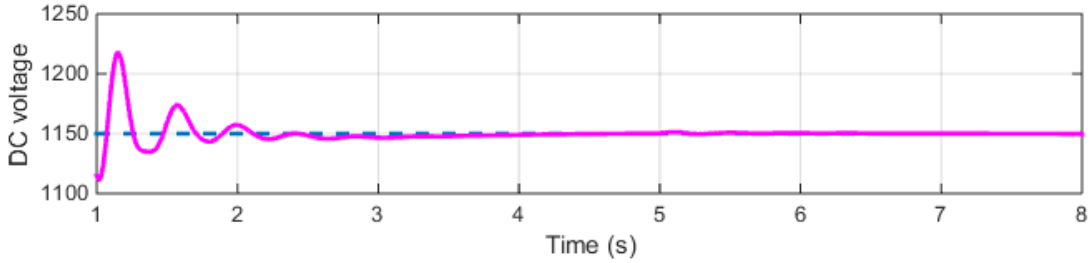

(a) DC voltage control

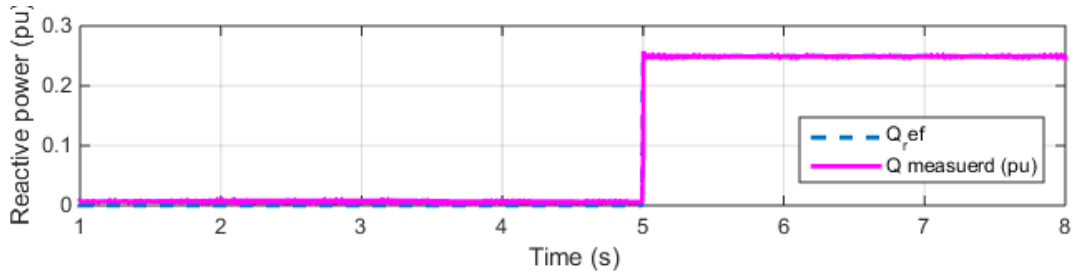

(a) Reactive power control

Figure 3-9 DFIG GSC controller performance, DC voltage control and reactive power control.

3.3 FRC Permanent magnet wind turbine generator

The block diagram of the PMSG FRC wind turbine is shown in Figure 3-10. The system consists of the following components; wind turbine, direct drive permanent magnet synchronous generator, back-to-back-converter, transformer, and control and protection system. The DC-chopper is a protection measure for the wind turbine and contains the breaking resistor connected in parallel with the capacitor in the DC link of the back-to-back converter. The resistor in the circuit dissipates the energy coming from the wind turbine during a fault or unbalanced conditions and helps maintain the balance in the DC link.

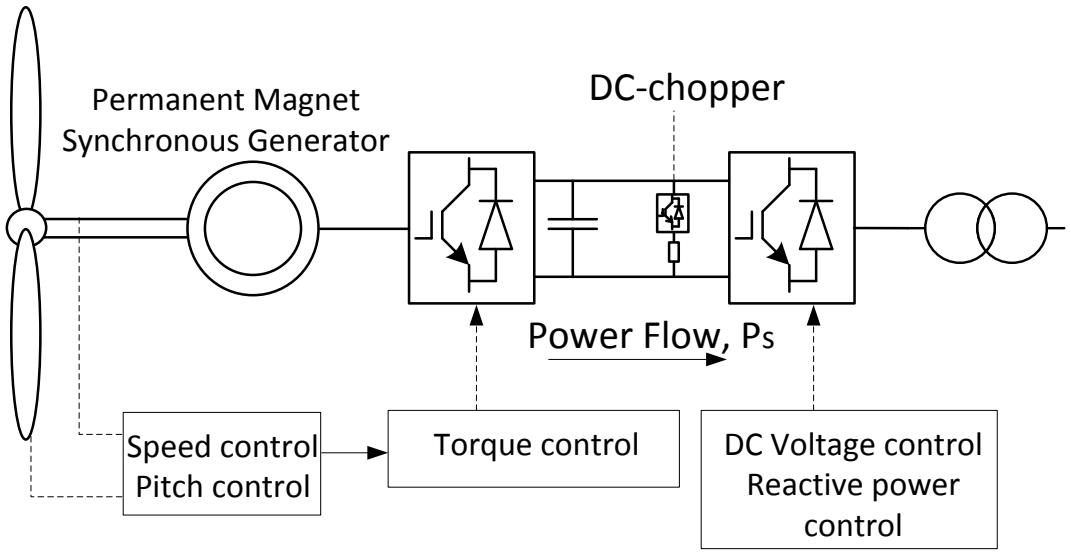

Figure 3-10 Schematic diagram of FRC PMGS wind turbine

The majority of wind turbines contain a gearbox as the turbine speed is much lower than generator speed, however due to high failure rate of the gearbox the trend for offshore wind turbine is going towards direct drive generators. Direct-driven generators have several advantages over the ones with gearbox, i.e. the structure is simpler, there is lower maintenance cost especially offshore, there is a reduction in losses in the drive train and also the noise reduction [24]. Furthermore, direct-driven generators are employed in FRC wind turbines, their decoupled control performance is much less sensitive to generator variations. This is highly required, as the Grid Code requirements Section CC.6.3 for wind plant becoming more and more restricted and need to comply as traditional power plants.

3.3.1 Mathematical model of PMSG in the *abc* reference frame

The mathematical model of PMSG is presented in this section. The machine consists of a rotor which is a permanent magnet and stator which is the stationary armature connected to the grid.

The terminal voltages for PMS machine stator can be written as [25]:

$$v_{as} = R_s i_{as} + \frac{d\psi_{as}}{dt} \tag{3.34}$$

$$v_{bs} = R_s i_{bs} + \frac{d\psi_{bs}}{dt} \tag{3.35}$$

$$v_{cs} = R_s i_{cs} + \frac{d\psi_{bs}}{dt} \tag{3.36}$$

The balance phase currents in the PMSG can be expresses as:

$$i_{as} = I_m \cos(\omega_s t) \tag{3.37}$$

$$i_{bs} = I_m \cos(\omega_s t - 120) \tag{3.38}$$

$$i_{cs} = I_m \cos(\omega_s t + 120) \tag{3.39}$$

Where $\omega_s = 2\pi f$ is the angular frequency of stator currents, I_m is the maximum value of sinusoidal varying current.

3.3.2 Mathematical model of PMSG in dq0 reference frame

The mathematical model of the PMSM represented in the dq0 synchronous rotating reference frame can be found in [26, 27] and is given by equations:

$$\frac{di_{sd}}{dt} = \frac{1}{L_{sd}}(-R_s i_{sd} + \omega_e L_{sq} i_{sq} + v_{sd}) \tag{3.40}$$

$$\frac{di_{sq}}{dt} = \frac{1}{L_{sq}}(-R_s i_{sq} - \omega_e (L_{sd} i_{sd} + \lambda p) + v_{sq}) \tag{3.41}$$

Where L_d and L_q are the inductances of the generator, R_s is the stator resistance, ω_e represents the rotor speed, i_{sd}, i_{sq} and v_{sd}, v_{sq} are currents and voltages respectively. λ represents the flux induced by rotors PM in the stator phases.

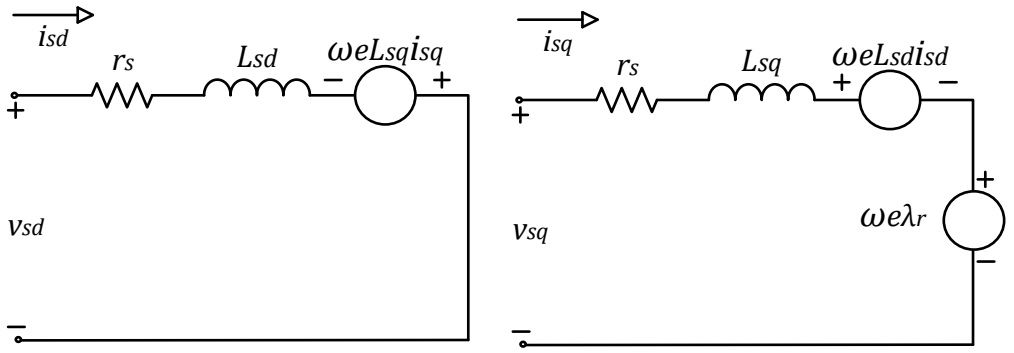

Figure 3-11 The dq- frame equivalent circuit of PMSG.

The electrical torque can be expressed as:

$$T_e = 1.5p(\psi_f i_{sq} + (L_{sd} - L_{sq}) i_{sd} i_{sq}) \tag{3.42}$$

In this study of the system the d-axes and q-axis inductances are equal $(L_{sd} - L_{sq}) = 0$ therefore the torque expression can be written as:

$$T_e = 1.5p\psi_f i_{sq} \tag{3.43}$$

3.3.3 Control of the PMSG wind turbine

The control of the PMSG wind turbines focuses strictly on four variables; the converter on the machine site controls the optimal generated power at different wind speeds (ω_e) and the control of the reactive power on the machine side converter (Q_{msc}), the grid side converter controls the reactive power injected to the grid and maintains the DC voltage between the converters.

Figure 3-12 shows a simplified control of a direct driven PMSG with a similar control principles as DFIG wind turbine, however here the i_{sq} current controls active power, and the i_{sd} current controls reactive power of the machine.

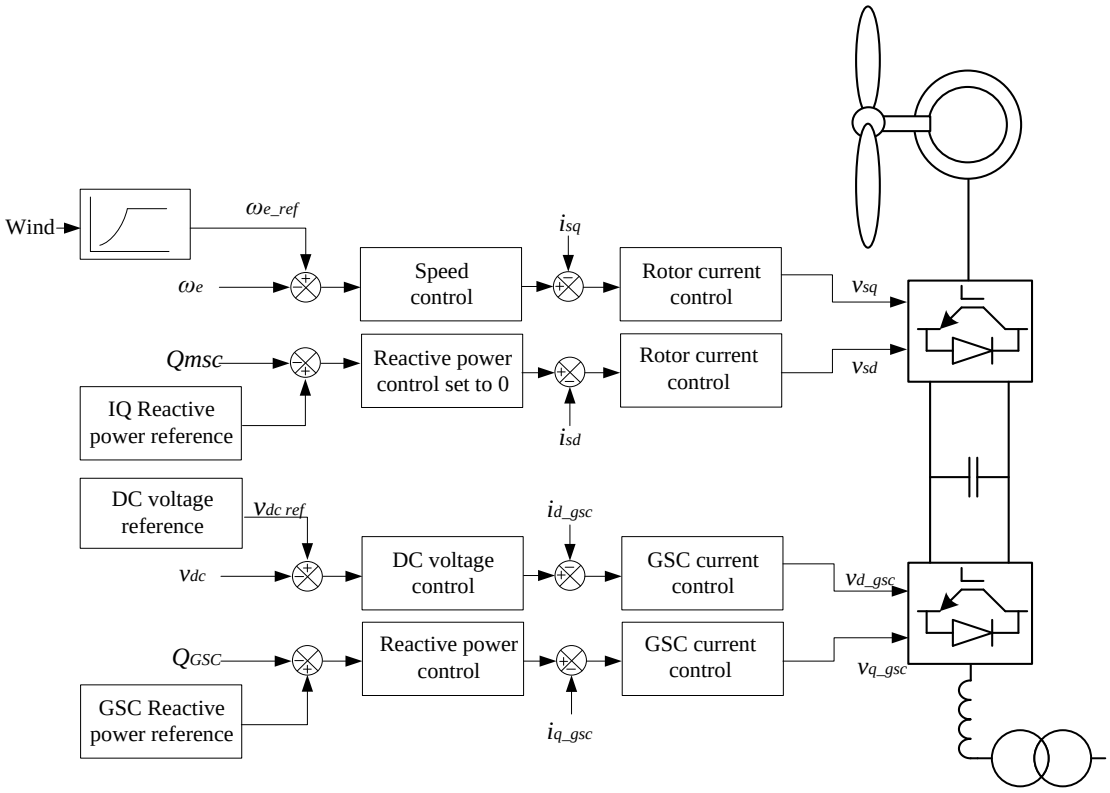

Figure 3-12 Simplified diagram of a PMSG-FRC control loops.

3.3.4 Control of the rotor site converter for PMSG

The RSC controls speed of the machine by controlling i_{sq}current, and i_{sd} to control reactive power opposite to the DFIG where the speed control determined by the i_{rd} currents. As the reactive power can be controlled by GSC $i_d$can be set up to 0. Based on ideal PMSG model, the stator voltages to control the machine can be expressed as:

$$v_{sd} = r_s i_{sd} + L_{sd}\frac{di_{sd}}{dt} - \omega_e L_{sq} i_{sq} \tag{3.44}$$

$$v_{sq} = r_s i_{sq} + L_{sq}\frac{di_{sq}}{dt} + \omega_e L_{sd} i_{sd} + \omega_e \psi_{pm} \tag{3.45}$$

Where v_{sd} and $v_{sq}$are stator voltages, r_s is stator resistance, i_{sd} and $i_{sq}$are stator currents, L_{sd} and L_{sq} are the stator inductances,ψ_{pm} is the permanent magnet flux, and $\omega_e$is the rotating speed and is given by:

$$\omega_e = p\omega_g \tag{3.46}$$

Where p is number of pole pairs of the generator and ω_g is the rotor speed.

The relationship between i_{qr} current and electrical torque T_e can be expressed as and implemented in the controller:

$$\frac{i_q}{T_e} = \frac{1}{1.5p\psi_f} \tag{3.47}$$

The PI controller for the rotor current can be derived from the plant's equation (1.23) as follows:

$$v_{sq} = r_s i_{sq} + L_{sq}\frac{di_{sq}}{dt} \tag{3.48}$$

Considering the cross-coupling terms ($\omega_e L_{sd} i_{sd} + \omega_e \psi_{pm}$) as a constant disturbance not present during the calculation of the control rules but later compensated in the control action, as shown in a schematic diagram of the speed control for PMSG in Figure 3-13, then the transfer function from the (v_{sq}) to (i_{sq}) is reduced to:

$$\frac{i_{sq}}{v_{sq}} = \frac{1}{sL_{sq} + Rs} \tag{3.49}$$

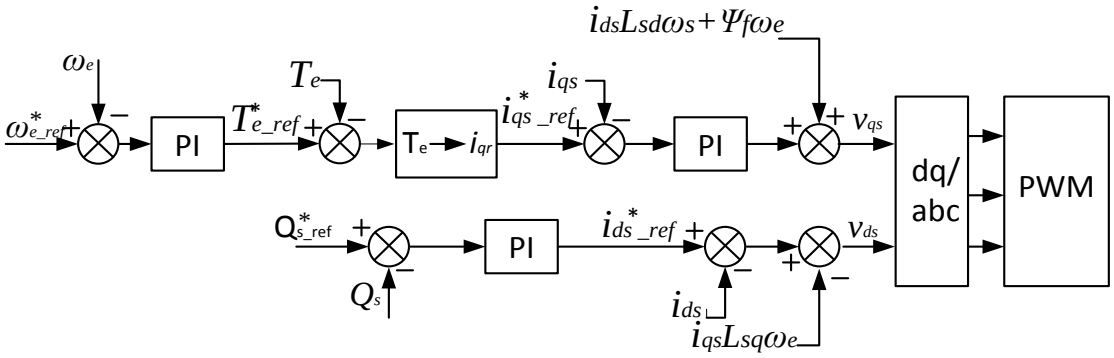

Figure 3-13 Machine side control for a PMSG wind turbine

Simulation Results

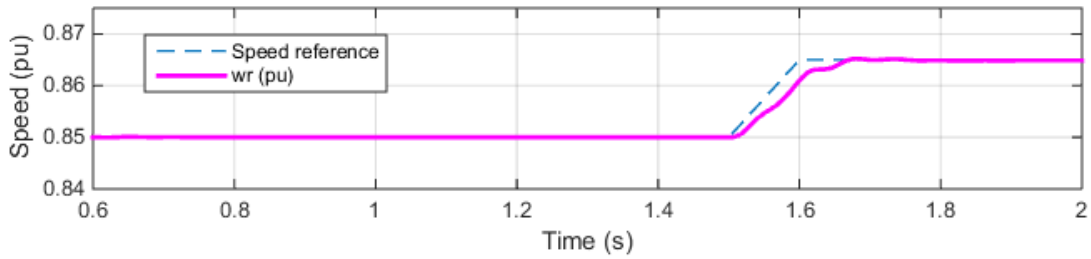

Figure 3-14 PMSG MSC speed control performance.

Initialy the system operates at wind speed 9m/s and at time t=1.5 wind speed increases to 9.5m/s shown in Figure 3-14. The speed reference value is increasing accordingly to the wind speed, the rotor speed (ω_r) controller of the wind turbine is designed to follow the speed reference value.

3.3.5 Control strategy for Grid-Side Converter PMSG

The grid side converter of the PMSG is designed to control reactive power and maintain DC voltage similar matter to the DFIG wind turbine. To simplify the control system the GSC control strategy is expressed in synchronous dq0 reference frame based on grid voltage oriented vector control. The equations for the RSC inverter and can be defined with following equations:

$$v_d = ri_{d\_gsc} + L\frac{di_{d\_gsc}}{dt} - \omega_g L i_{q\_gsc} + v_{d\_gsc} \tag{3.50}$$

$$v_q = ri_{q\_gsc} + L\frac{di_{q\_gsc}}{dt} + \omega_g L i_{d\_gsc} + v_{q\_gsc} \tag{3.51}$$

Where r and L are resistance and inductance of the grid side converter, v_{d_gsc}, v_{q_gsc} i_{d_gsc} and i_{q_gsc} are voltages and currents in dq frame generated by GSC.

The process of obtaining the transfer function for the grid side converter of FRC wind turbine is exactly the same as DFIG and is already show in 3.2.7 section. Figure 3-15 shows a simplified schematic controller for the FRC PMSG wind turbine.

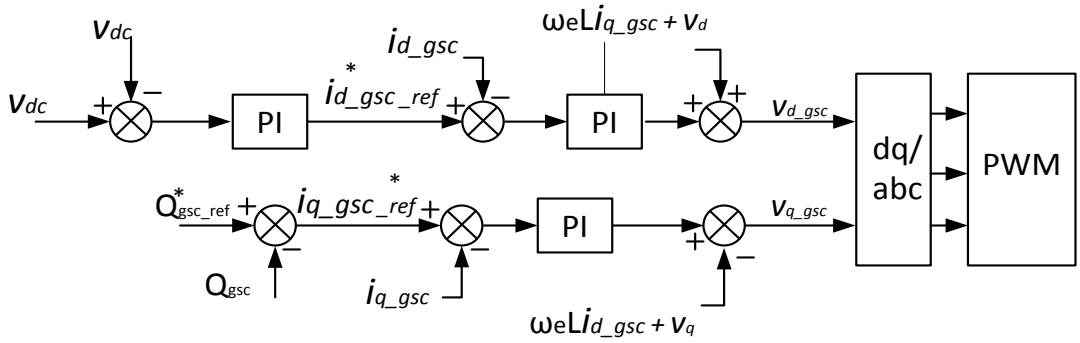

Figure 3-15 Schematic diagram of GSC control for PMSG

Simulation Results

Figure 3-16 shows the control perfomance of the reactive power and DC voltage controllers. The Figure 3-16 (a) shows the reactive power control (Q). inisialy starts with 0 reactive power provision and at t=1s is icreasing to 0.3pu. The Figure 3-16(b) shows the control actions to maintain DC voltage at all times.

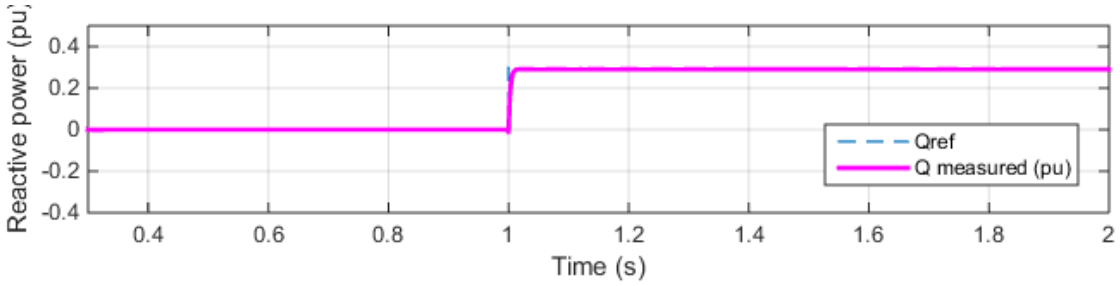

(a) Reactive power controller

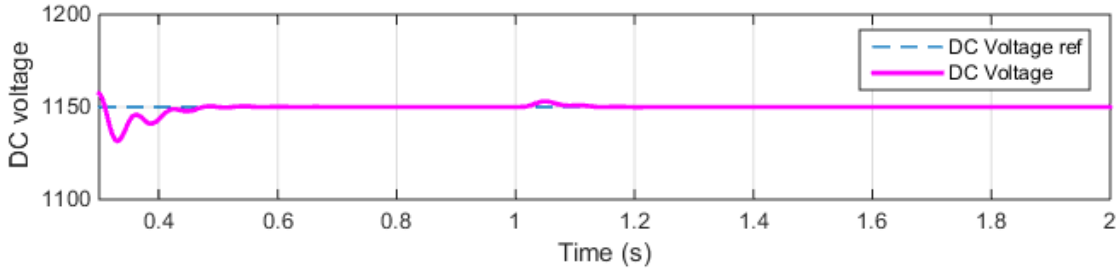

(b) DC voltage controller

Figure 3-16 FRC GSC controller performance, reactive power and DC voltage control.

3.3.6 Control Strategy for reactive power compensation of a PMSG

The steady-state analysis of voltage compensation using phasor algebra has been dealt with in detail in [28], [29]. For a circuit as shown in Figure 3-17, when line voltage drops are small in comparison with the source voltage, the PCC voltage magnitude can be expressed as

$$V_{pcc} = V_g \left(1 - \frac{Q_{DFIG} - Q_{PMSG}}{S_{sc}}\right) \tag{3.52}$$

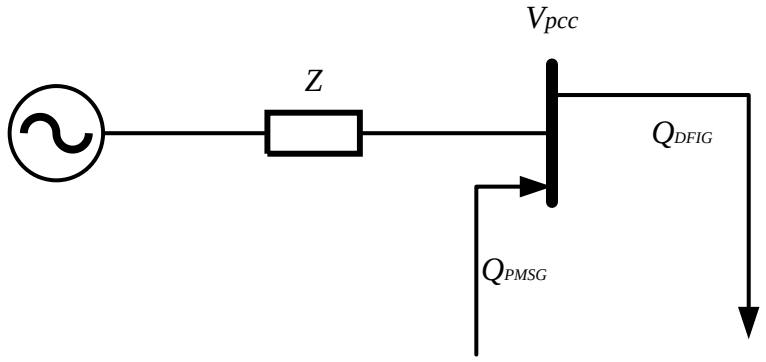

Figure 3-17 Single line diagram of System

Where V_{pcc} is the voltage at the point of common coupling, Q_{DFIG} is the reactive power consumed by the DFIG, Q_{PMSG} is the reactive power provided by the PMSG and S_{sc} is the short circuit level at point of common coupling.

Thus, under steady state conditions, a defined change in V_{pcc} is brought about by a magnitude of reactive power. Extending this concept, a control strategy to achieve compensation of voltage transients at V_{pcc} is presented next.

The new control strategy to improve reactive power compensation via FRC wind turbine is achieved in one stage. The management of reactive power injected to the grid is provided by voltage controller (q-component) of the grid side converter FRC wind turbine. This controller controls the voltage at the point of common coupling (PCC). Figure 3-18 shows the new voltage controller implemented in FRC wind turbine, which gives the capability to manage the reactive power injection accordingly to voltage dip on the PCC.

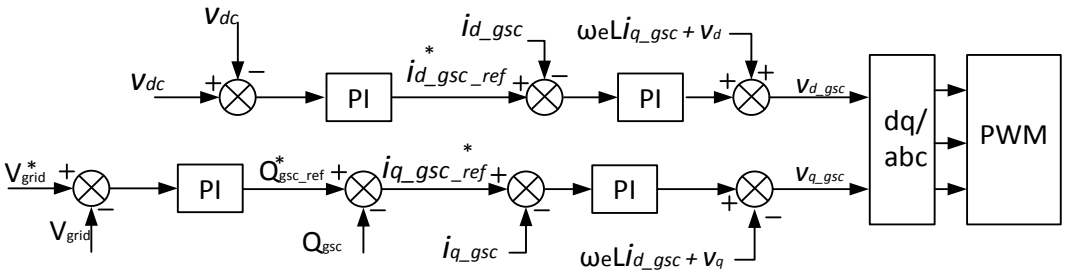

Figure 3-18 Proposed control for reactive power compensation

In the Q controller, the reference is provided by the AC grid voltage V_{pcc}. The measured voltage V_{pcc} is compared with the reference voltage V_{grid}^{*} to obtain the reactive power reference $Q_{gsc\_ref}^{*}$. The mathematical model of the controller is:

$$Q^{*} = k_{pgrid}\left(V_{pcc}^{*} - V_{pcc}\right) + k_{igrid}\int (V_{pcc}^{*} - V_{pcc})dt \tag{3.53}$$

Where k_{pgrid} and k_{igrid} are the proportional and integral gain of the voltage controller. The Figure 3-19 shows the schematic of the controller.

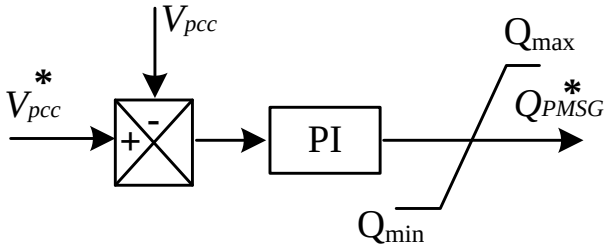

Figure 3-19 Voltage control to support DFIG reactive power compensation

Reactive power influences the voltage accordingly to the equation:

$$\mathrm{V} = \sqrt{QX} \tag{3.54}$$

Where X is a circuit reactance.

3.4 DFIG and FRC wind turbines in hybrid network

The big challenge for the wind turbine generators is to meet Grid Code requirements for fault ride-through compliance specified in CC.6.3.15.1 [7, 30]. Most of the current wind turbines are able to fulfil the requirements by using their control capabilities. However, some of the wind turbines can weaken the grid as they will lose control during a fault or a voltage sag as the crowbar protection is activated. Early wind turbines were connected directly to the electrical network. This means that their rotational speed was fixed by the electrical frequency, usually 50 Hz or 60 Hz. These types of the wind turbines are using an induction generator and are known as fixed speed wind turbines. These wind turbines have a peak efficiency (Cp) at one particular tip speed ratio, meaning that they do not operate at optimum operation point and do not extract as much power as modern wind turbines [31]. Present wind turbines are maximising energy captured by tracing optimum tip speed ratio and it's achieved by varying the rotational speed of the wind turbine. To achieve variable speed operation in earliest wind turbine generators involved switching the numbers of the generator's stator pole windings or by changing rotor resistance [32]. A latter method uses

frequency converters to decouple the rotational speed of the generator from the network frequency to achieve variable speed operation [33]. Frequency converters have been used in two ways: one configuration is known as DFIG concept that connects the rotor windings of induction generator to the AC grid via back-to-back converter, while the stator winding remains directly connected, and the second, known as full rated power converter wind turbine, decouples the stator windings from the network via a fully rated back to back converter. An FRC configuration is very attractive for hybrid configuration as the operation is of the generator is decoupled from the grid operation and can be used to supply reactive power to the grid. Its only limitations are the rating of the machine and the wind availability.

The hybrid network is becoming an interesting solution for cases such as:

- Improving existing IG wind farms, where they need to be uprated and comply with the FRT requirements. Currently the usual solutions for wind farms are adding reactive power compensation units or their decommissioning and selling to other less demanding countries.
- Improving operation of the DFIG based wind farms, where additional reactive power support during a fault or voltage sag improves the Low-Voltage Fault-Ride Through (LVFRT) capabilities and simply extends time for how long wind turbine can remain connected to the grid.

Figure 3-20 shows an example of a hybrid wind farm composed of DFIG and FRC wind turbines. The previous sections reviewed the operational principles and control of the DFIG and the FRC wind turbines

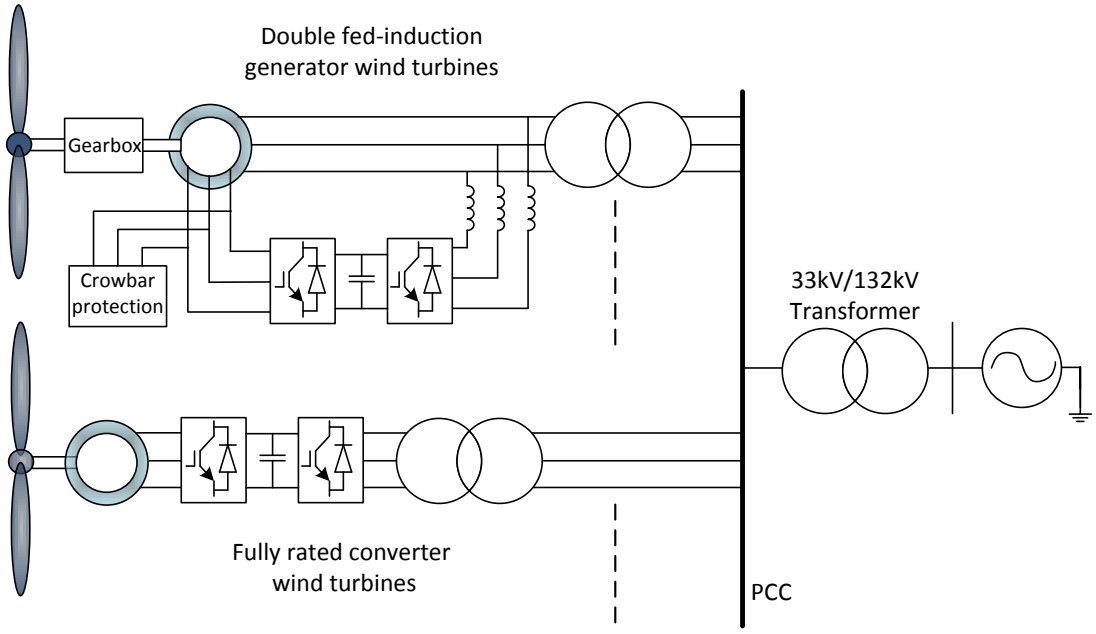

Figure 3-20 Wind farm hybrid collection network

The new approach of combining different type of wind turbine generators with FRC wind turbine in a hybrid wind farm network provides several advantages over one type wind farm. The FRC wind turbine can be combine with any IG-based turbine which requires reactive power support during voltage sag or AC fault. The main advantage of this arrangement is the provision of reactive power compensation to any IG-based wind turbines. This approach can be used in existing wind farm by adding FRC wind turbines instead of STATCOM or other reactive power equipment. Moreover, this approach can be used for a newly designed wind farm. It not only improves and fulfil the whole wind farm FRT capabilities but it might be more cost efficient in the long run as FRC wind turbine is in operation all the time and delivers active power during the time when STATCOM would not be in use.

3.5 Improved DFIG FRT capabilities in a hybrid network

The FRC wind turbine inclusion in the hybrid network is able to improve the DFIG wind turbine performance, or any other IG-based wind turbine, throughout the voltage sag and extent the connection period to the grid during the fault period. Figure 3-21 shows the full constant values of a hybrid arrangement of the DFIG wind turbine and FRC wind turbine. The DFIG wind turbine is a 1.5 MW, 690V machine with a gearbox. The PMSG-FRC is a 2MW, 690V direct driven wind turbine with chopper fitted to dissipate the excess power when required. Both wind turbines are equipped in a step-up transformer 690/11kV and fed

to one network and the transmission lines are 30km long. The performance of the hybrid network throughout the voltage sag is studied in this section.

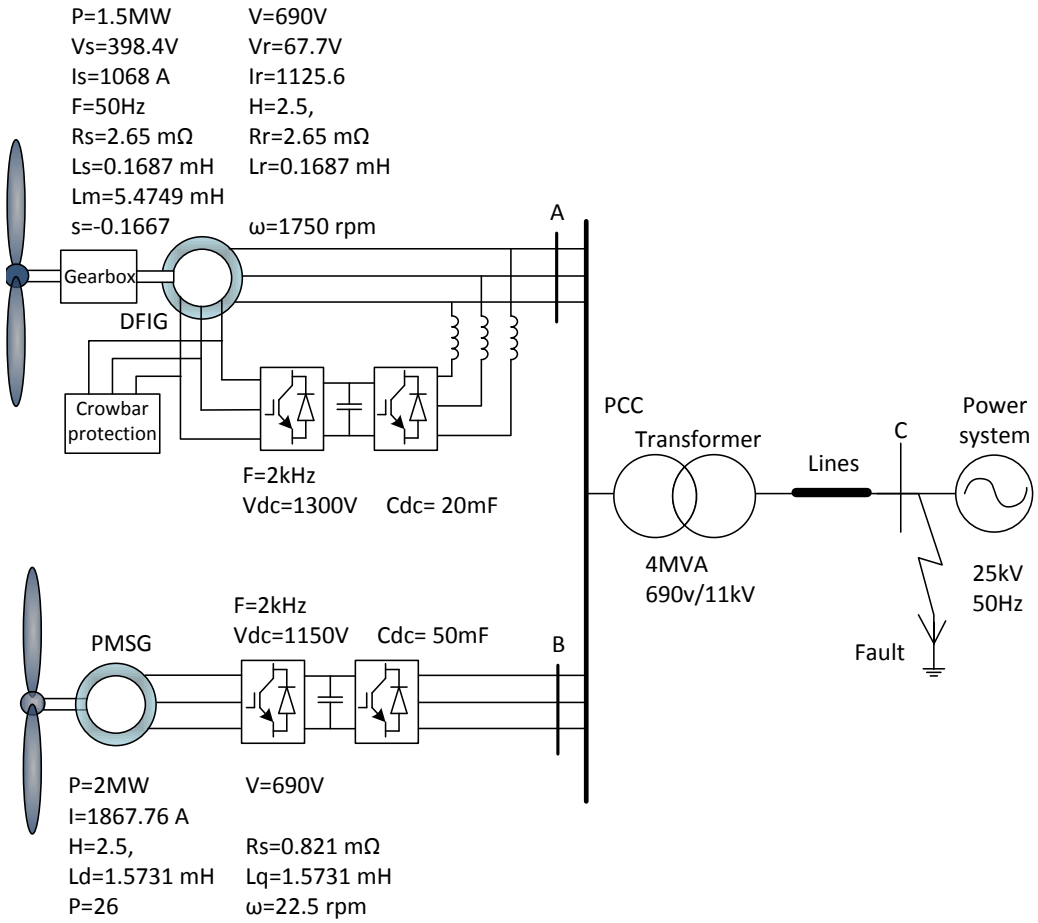

Figure 3-21 System configuration and parameters in hybrid network

The wind farm operates in a steady state with a constant wind speed of 9.5 m/s until the system is subjected, at t=15.8, to voltage dip is seen in Figure 3-21 lasting for 150 ms. The first simulation result, shown in Figure 3-22, shows the impact in the voltage at the point of common coupling when voltage support is provided against a case where no voltage support is provided by the FRC. As seen in, Figure 3-22, when voltage support is provided, the voltage dip is decreases by 0.1 PU (i.e. the voltage at the point of common coupling increases from 0.62 PU to 0.72 PU).

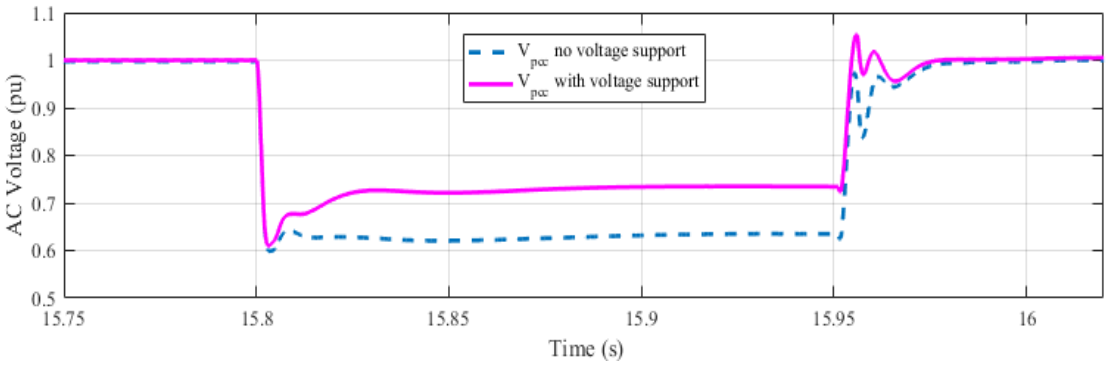

Figure 3-22 Voltage at point of common coupling with and without voltage support from the FRC

The decrease of voltage dip, when voltage support is provided, is because of the reactive power provision of the FRC, which changes from 0 PU to 1 PU shortly after the fault. To better illustrate this, Figure 3-23 shows the effects of the reactive power provision of the FRC when voltage support is provided against a case where no voltage support is provided by the FRC. As seen in Figure 3-23, the reactive power provision of the FRC changes from 0 PU to 1 PU in less than 20ms after the start of the fault. In the case where no voltage support is provided, the reactive power of the FRC remains in 0 PU, being only affected by the current transients at the start and end of the fault, as appreciated by the dotted line in Figure 3-23.

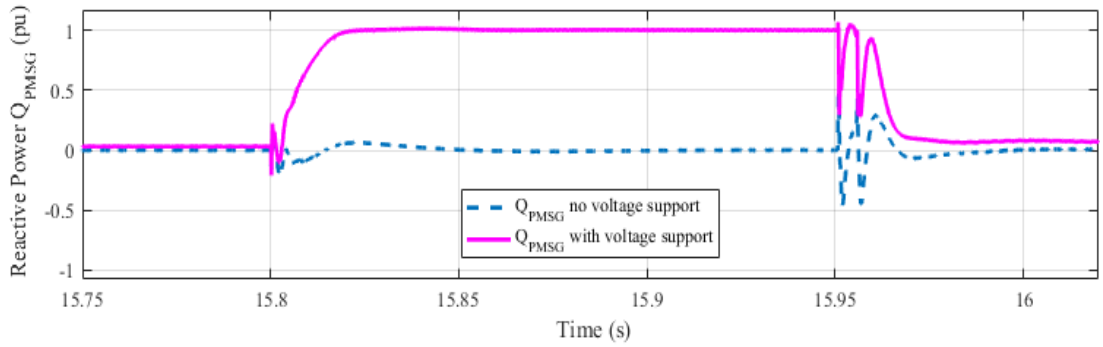

Figure 3-23 Reactive power provision of the FRC with and without voltage support from the FRC

The positive effects of the FRC voltage support provision on the DFIG variables is illustrated in Figure 3-24 and Figure 3-25. Figure 3-24 shows the behaviour of the DFIG back-to-back converter DC voltage when voltage support is provided against a case where no voltage support is provided by the FRC. As seen in Figure 3-24, the transient peaks of the DFIG DC voltage reduces in magnitude when voltage support is provided by the FRC. This is because the magnitude of the transient currents affecting the DFIG back-to-back converter during the start and the end of the fault reduce in magnitude thanks to the additional voltage provision.

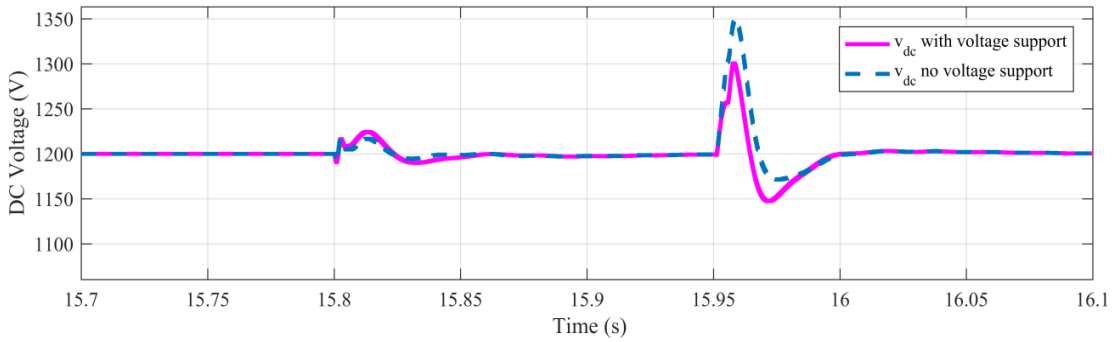

Figure 3-24 DFIG DC voltage with and without voltage support from the FRC

Figure 3-25 shows the behaviour of the DFIG rotor speed when voltage support is provided against a case where no voltage support is provided by the FRC. As seen in Figure 3-25, the rotor speed acceleration during the fault period is lesser when voltage support is provided, this is because the electrical torque of the DFIG wind turbine decreases in lesser degree when the voltage support is provided. Additionally, the post fault rotor speed also benefits from the voltage support provision, which is able to return to pre-fault levels before than the case without voltage provision. This is because the transient electrical torque of the DFIG after the voltage dip is less severe in when voltage support is provided. This means a lesser deviation of rotor speed from its set point reference.

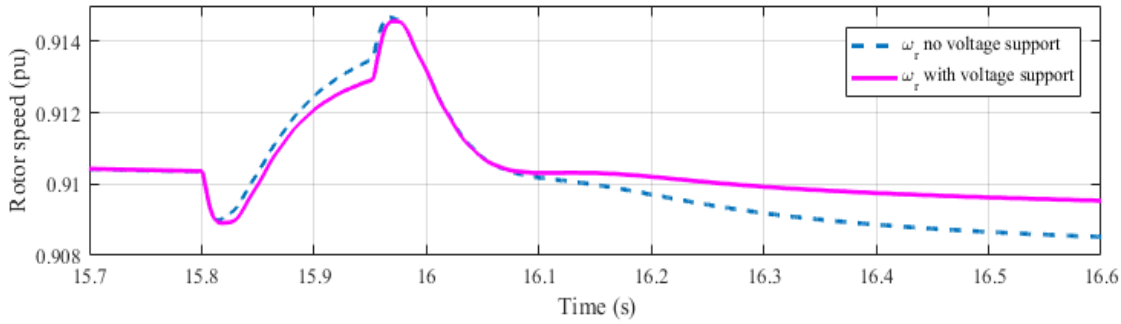

Figure 3-25 DFIG rotor speed with and without voltage support from the FRC

Evidently, using the FRC to provide voltage support also affects the variables in the FRC control system. In order to assess the impact of the FRC voltage support provision in the relevant variables of the FRC Figure 3-26 to Figure 3-29 show the behaviour of relevant FRC variables when the voltage support provision is enabled and compares them to a case where no voltage support is provided.

Figure 3-26 shows the apparent power usage of the FRC grid side converter when the voltage support is provided. As seen in Figure 3-26, prior the fault the apparent power usage of the grid side converter is around 0.5 PU which is primarily the active power coming from the generator. During the fault period the apparent power usage of the grid side converter

increases to 1.2 PU because of the sudden increase in the reactive power provision from the FRC. Now the apparent power usage of the grid side converter is a combination of active and reactive power, with a higher component of reactive power provision. A 1.2 PU power usage is overloading to some degree the operation of the converter. However, this transient overload is permitted only in for a short period of time and it is never allowed to increase beyond the maximum safety limit of 1.2 PU.

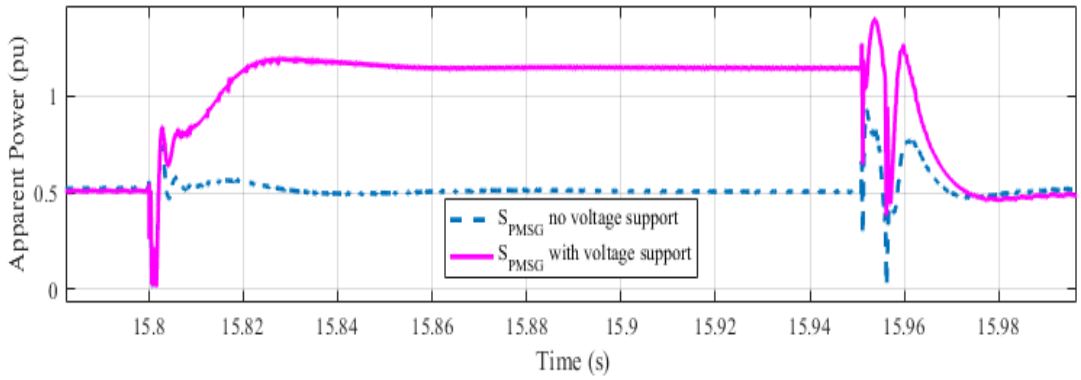

Figure 3-26 Apparent power usage of the FRC grid side converter with and without voltage support from the FRC

Figure 3-27 shows the behaviour of the DC voltage of the FRC when the voltage support provision is enable and compares it to a case where no voltage support is provided. As seen in Figure 3-27, the DC voltage transients increase when the FRC is providing voltage support. This is due to the extra provision of reactive power from the grid side converter. This causes DC voltage fluctuations higher in scale than in the case where no voltage support is provided, since the value of the dc voltage bus is directly linked to the balance of active power between the machine side converter and the grid side converter. However, even though the dc voltage transient peak at the beginning and end of the fault are higher (for the case of voltage support) the magnitude of these voltages is still within the limits considered safe for the operation of a back to back converter (i.e >= 1.2 PU in voltage level). As such, it is concluded that the impact of using voltage support from the FRC produces negative effects in the FRC function but not to a degree to discourage its use when a comparison of cost-benefit is made.

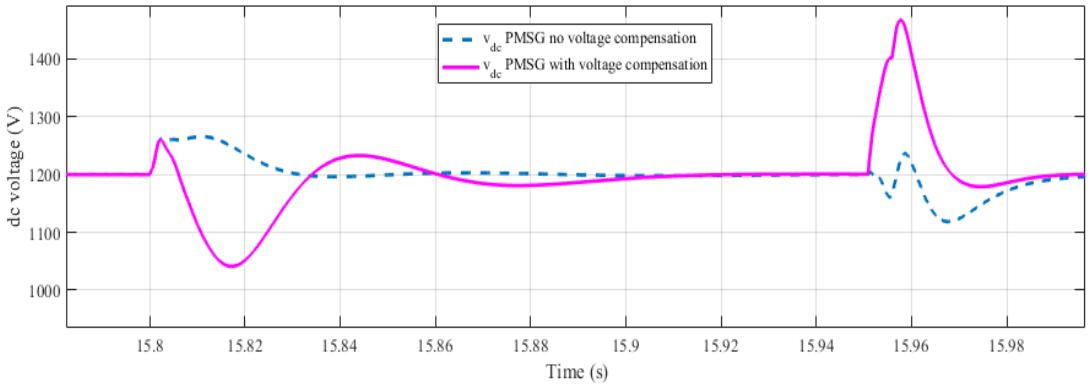

Figure 3-27 FRC DC voltage with and without voltage support from the FRC

Furthermore, if an active DC chopper or DC crowbar is fitted to the FRC, then excessive DC voltage peaks can be effectively reduced. To illustrate this, Figure 3-28 shows the dc voltage behaviour of a FRC when the voltage support provision is enable and a dc crowbar (triggered at 1250V) is fitted in the dc bus.

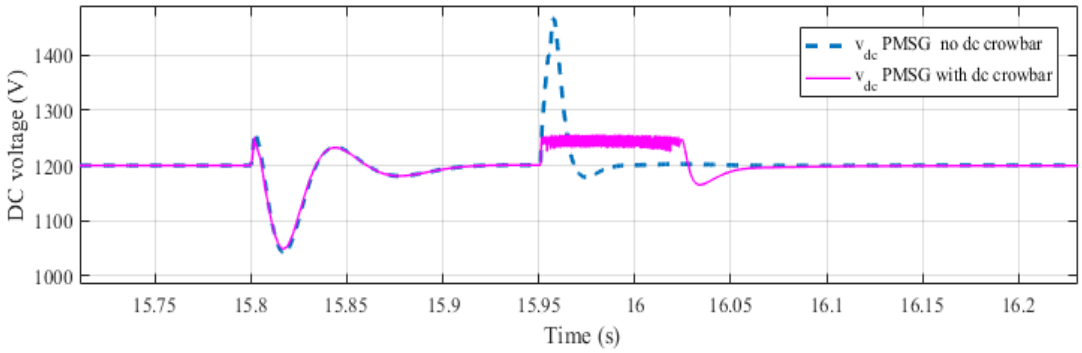

Figure 3-28 FRC DC voltage with and without dc crowbar when voltage support from the FRC is provided.

As seen in Figure 3-28 when the DC crowbar is fitted to the FRC the extra energy that produced the dc voltage peak is dissipated in the DC crowbar resistance and the dc voltage does not exceed from a value of 1250V

Finally, the voltage support provision from the FRC does not affect the functioning of the PMSG connected to the machine side converter, this is because the back-to-back converter effectively decouples the machine circuit from the faulted AC system. To illustrate this, Figure 3-29 shows the PMSG speed and torque when voltage support is provided and compares the case when no voltage support is provided. As seen in Figure 3-29 the variables suffer no change no matter if voltage support is provided or not.

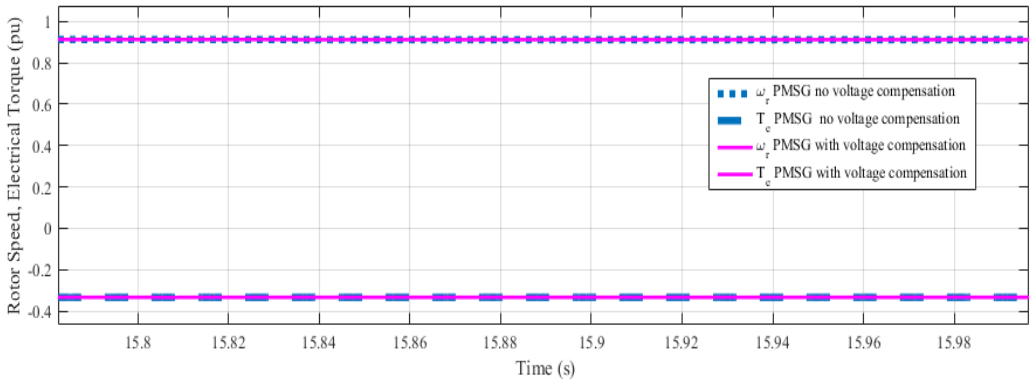

Figure 3-29 PMSG speed and torque values with and without voltage support from the FRC

3.6 Summary

The studies presented in this chapter have investigated the improvement of the wind farm plant with different wind turbines designs into hybrid wind plant.

It has been analysed that DFIG wind turbines may negatively affect the voltage stability of the power system when its crowbar protection is activated. Also it has also been analysed that a voltage dip at the DFIG terminals produces a great reduction of the machine mechanical torque, which in turn reflects into an over-speeding of the machine.

This chapter also focused on low voltage ride-through capabilities of the induction generator based wind turbines and its improvement. It has been found that by connecting FRC-based wind turbines, to the DFIG-based wind farm, the reactive power support can be provided during voltage sag. This reactive power support reduces the magnitude of the voltage dip during the fault and has positive effects in DFIG rotor speed and dc voltage during and after the fault period.

The analysis of simulation results in this chapter also evidenced that the converter of the FRC turbines can be overloaded and the dc voltage of the system presents larger transients if voltage support is provided. However, it has been concluded that this event can be contained within safe limits if digital control saturation and dc active crowbars are provided. The conclusion is that hybrid wind farm can improve low voltage fault-right through capabilities with potential of cost reduction as FRC acts as a STATCOM without compromising the integrity of the FRC system.

3.7 References

[1] A. Hansen and L. Hansen, "Wind turbine concept market penetration over 10 years (1995-2004)," *Wind Energy*, vol. 10, pp. 81-97, 2007.

[2] R. Rechsteiner, "Wind Power in Context – A clean Revolution in the Energy Sector," Energy Watch Group, Berlin Germany december 2008.

[3] F. Blaabjerg, "Power Electronics for Modern Wind Turbines ", First ed: Morgan & Claypool Publishers, 2006, p. 24.

[4] G. Pannell, D. J. Atkinson, and B. Zahawi, "Minimum-Threshold Crowbar for a Fault-Ride-Through Grid-Code-Compliant DFIG Wind Turbine," *Energy Conversion, IEEE Transactions on,* vol. 25, pp. 750-759, 2010.

[5] F. Iov, A. D. Hansen, P. Sørensen, and N. A. Cutululis, "Mapping of grid faults and grid codes," Risø National Laboratory, Roskilde, Denmark 2007.

[6] X. Bing, B. Fox, and D. Flynn, "Study of fault ride-through for DFIG based wind turbines," in *Electric Utility Deregulation, Restructuring and Power Technologies, 2004. (DRPT 2004). Proceedings of the 2004 IEEE International Conference on*, 2004, pp. 411-416 Vol.1.

[7] G. Mokryani, P. Siano, A. Piccolo, and Z. Chen, "Improving Fault Ride-Through Capability of Variable Speed Wind Turbines in Distribution Networks," *IEEE Systems Journal,* vol. 7, pp. 713-722, 2013.

[8] Y. Lihui, X. Zhao, J. Ostergaard, D. Zhao Yang, and W. Kit Po, "Advanced Control Strategy of DFIG Wind Turbines for Power System Fault Ride Through," *Power Systems, IEEE Transactions on,* vol. 27, pp. 713-722, 2012.

[9] "The Grid Code," NATIONAL GRID ELECTRICITY TRANSMISSION, London, United Kingdom 2010.

[10] Javier Serrano González and R. L. Arantegui, "Technological evolution of onshore wind turbines—a market-based analysis," *Wind Energy,* 2016.

[11] A. Tan. (2010). *A Direct Drive to Sustainable Wind Energy*.

[12] Edited by:Chong Ng and Li Ran, *Offshore Wind Farms: Technologies, Design and Operation* Elsevier Ltd, 2016.

[13] Y. Xing-jia, L. Shu, X.-D. Wang, C.-c. Guo, X. Zuo-xia, and J. Hong-Liang, "Doubly-fed induction generator control for variable-speed wind power generation system," in *Mechatronics and Automation, 2009. ICMA 2009. International Conference on*, 2009, pp. 855-859.

[14] L. Shuhui, T. A. Haskew, and J. Jackson, "Power generation characteristic study of integrated DFIG and its frequency converter," in *Power and Energy Society General Meeting - Conversion and Delivery of Electrical Energy in the 21st Century, 2008 IEEE*, 2008, pp. 1-9.

[15] K. E. Okedu, S. M. Muyeen, R. Takahashi, and J. Tamura, "Wind Farms Fault Ride Through Using DFIG With New Protection Scheme," *Sustainable Energy, IEEE Transactions on,* vol. 3, pp. 242-254, 2012.

[16] J. Kretschmann, H. Wrede, S. Mueller-Engelhardt, and I. Erlich, "Enhanced Reduced Order Model of Wind Turbines with DFIG for Power System Stability Studies," in *Power and Energy Conference, 2006. PECon '06. IEEE International*, 2006, pp. 303-311.

[17] D. Campos-Gaona, E. L. Moreno-Goytia, and O. Anaya-Lara, "Fault Ride-Through Improvement of DFIG-WT by Integrating a Two-Degrees-of-Freedom Internal Model Control," *Industrial Electronics, IEEE Transactions on,* vol. 60, pp. 1133-1145, 2013.

[18] I. Erlich, H. Wrede, and C. Feltes, "Dynamic Behavior of DFIG-Based Wind Turbines during Grid Faults," in *Power Conversion Conference - Nagoya, 2007. PCC '07*, 2007, pp. 1195-1200.

[19] I. Boldea, "2. Wound Rotor Induction Generators," in *Variable Speed Generators*, ed: CRC Press, 2006, pp. 2-24.

[20] J. Morren and S. W. H. d. Haan, "Short-Circuit Current of Wind Turbines With Doubly Fed Induction Generator," *Energy Conversion, IEEE Transactions on* vol. 22, pp. 174 - 180 March 2007.
[21] D. C.-G. Olimpo Anaya-Lara, Edgar Moreno-Goytia, Grain Adam, *Offshore Wind Energy Generation: Control, Protection, and Integration to Electrical Systems*, 2014.
[22] C.-M. Ong, "6.8 Simulation of an induction machine on the stationary reference frame," in *Dynamic Simulations of Electric Machinery: Using MATLAB/SIMULINK*, ed: Prentice Hall PTR 1998, p. 196.
[23] R. Ottersten, "On Control of Back-to-Back Converters and Sensorless Induction Machine Drives," Department of Electric Power Engineering Chalmers University of Technology, 2003.
[24] O. Anaya-Lara, N. Jenkins, J. Ekanayake, P. Cartwright, and M. Hughes, *Wind Energy Generation: Modelling and Control*: Wiley, 2009.
[25] C. K. A.E. Fitzgerald, JR., Stephen D. Umans, *Electric Machinery*, 2003.
[26] P. Kundur, *Power System Stability and Control*, 1994.
[27] F. M. Gonzalez-Longatt, P. Wall, and V. Terzija, "A simplified model for dynamic behavior of permanent magnet synchronous generator for direct drive wind turbines," in *PowerTech, 2011 IEEE Trondheim*, 2011, pp. 1-7.
[28] R. S. Weissbach, G. G. Karady, and R. G. Farmer, "Dynamic voltage compensation on distribution feeders using flywheel energy storage," *IEEE Transactions on Power Delivery*, vol. 14, pp. 465-471, 1999.
[29] T. J. E. Miller, *Reactive Power Control in Electric Systems*: Wiley, 1982.
[30] Cigré Working Group B4-52, "HVDC Grid Feasibility Study," 2013.
[31] T. Ackermann, *Wind Power in Power Systems*: Wiley, 2012.
[32] Tony Burton, David Sharpe, Nick Jenkins, and E. Bossanyi, *Wind Energy Handbook* vol. Vol 1, 2008.
[33] F. Iov and F. Blaabjerg, "Power electronics and control for wind power systems," in *Power Electronics and Machines in Wind Applications, 2009. PEMWA 2009. IEEE*, 2009, pp. 1-16.

Chapter 4:

Multi-technology Voltage Source Converters – High Voltage Direct Current (VSC-HVDC)

The multi-technology offshore wind power systems refers to the connections of more than one wind technology at the time in the offshore wind electrical system. The objective of such an arrangement is to maximise wind energy production and increase reliability. It was alluded in the previous chapter that hybrid cluster collection network could improve large-scale wind farms and provide reactive power support.

This chapter investigates the VSC-HVDC transmission system. The objective is the development of a dynamic mathematical model of the VSC-HVDC that is useful to design and tune the controllers for power transmission between the offshore and the onshore AC networks. The controllers designed in this chapter are used for transferring power from offshore hybrid wind farm which combines the DFIG-based wind turbine and FRC wind turbines. Additionally, this chapter also investigates the dynamic behaviour of the controllers during wind variation.

4.1 Introduction

The VSC-HVDC was developed to overcome challenges associated with CSC-HVDC[1]. The correct modelling and control techniques are important issues in future HVDC-VSC

applications and will bring significant changes to the AC power network. Furthermore, the control system has a pivotal role for the future power system stability [2].

VSC-HVDC converters use fully controllable switches, such as[1]:

- IGBT (Insulated-Gate Bipolar Transistor) which is a three-layer semiconductor device
- GTO (Gate-Turn-Off Thyristor) which is a four-layer semiconductor device
- IGCT (Integrated Gate-Commutated Thyristor) similar to the GTO devices.

These devices can be switched ON and OFF at any time during a cycle, which is not the case with silicon-Controlled Rectifier (SCR)-based drivers, which can be switched on but to switch off the current needs to fall below certain threshold. VSC-HVDC uses PWM technique (Pulse Width Modulation), to translate the digital control signals of the system into an analogue voltage output. In PWM, the modulating signal is compared with a triangular waveform, as shown in Figure 4-1, to generate a train pulse to turn on/off the IGBTs of the converter. In these converters, current can be leading or lagging AC voltage so converters can supply or consume reactive power to the connected network which also eliminates the need for expensive power compensation devices.

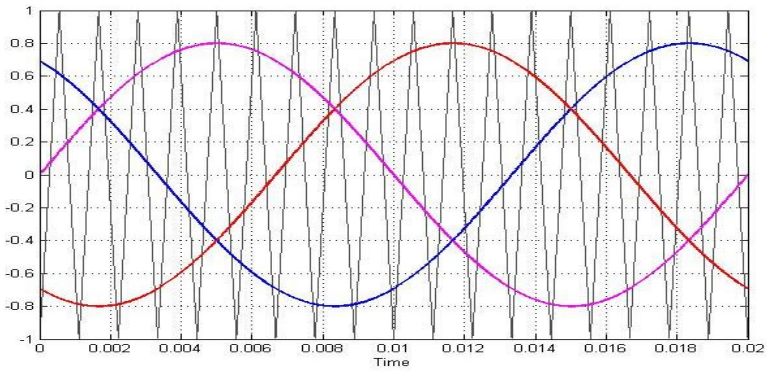

Figure 4-1 Three phase sinusoidal reference and triangular waveform.

Some other advantages of voltage source converters are [1, 3]:

- DC Power can be transferred over long distances with lower power losses compared to an AC transmission.
- Independent control over active and reactive power through pulse width modulation technique, which allows control of the magnitude and phase angle of the AC voltage.
- Voltage support is achieved by lagging or leading reactive power.
- Interconnected networks are decoupled, which in the case of a wind farm may improve its Fault Ride-Through capability.

- VSC-HVDC can operate as 'sleeping mode' (In the case where there is no need of power exchange between two regional links), which means there is no active power exchange, each converter station can act as a STATCOM to regulate AC voltage.
- Black start capability, where restoring power is done without the external transmission network.
- No need for start-up generator, which is more cost effective.

4.2 Design and operating principle of VSC-HVDC

The principle operation of the VSC-HVDC can be described by considering the VSC connected to the AC network via a phase reactor shown in Figure 4-2.

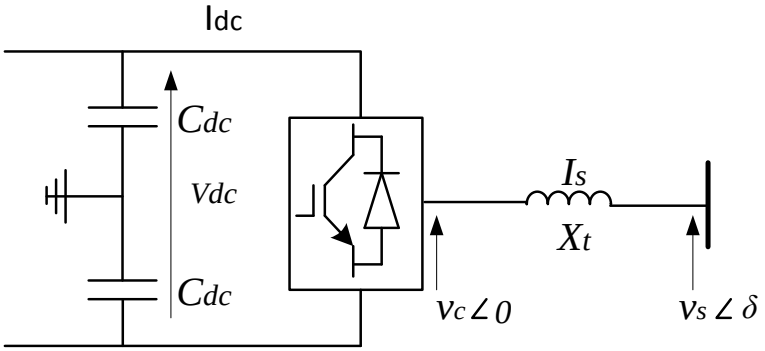

Figure 4-2 Simplified representation of VSC connected to AC grid.

The VSC can be expressed by equivalent AC and DC circuits, where the VSC is modelled as a controlled current source at the DC side and controlled as a voltage source at the AC side [4]. The sinusoidal output wave form from the DC converter can be described by following equation [5, 6]:

$$v_c = \frac{1}{2} v_{dc} M sin(\omega t + \delta) \quad (4.1)$$

Where M is the modulation index, v_{dc} is the DC voltage, ω is the system frequency and δ is the phase shift of the output voltage. The VSC controller can adjust the modulation index M and δ to obtain any combination of voltage amplitude and phase shift in relation to the fundamental frequency voltage, hence active and reactive power flow control.

The active power of the converter can be controlled by controlling the phase angle δ, whereas reactive power control is achieved by the relative difference in magnitude. The

active (P) and reactive (Q) power transferred from the generator to the VSC converter can be defined by simplified equations of power transfer between active sources [7]:

$$P = V_{dc} I_{dc} = \frac{v_c \, v_s}{X_t} \sin(\delta) \tag{4.2}$$

$$Q = \frac{v_c \, v_s cos(\delta)}{X_t} - \frac{v_c^2}{X_t} \tag{4.3}$$

The phasor diagram shown in Figure 4-3 illustrates the dependency of the active and reactive power from the phase angle δ and amplitude of the converter voltage v_c .

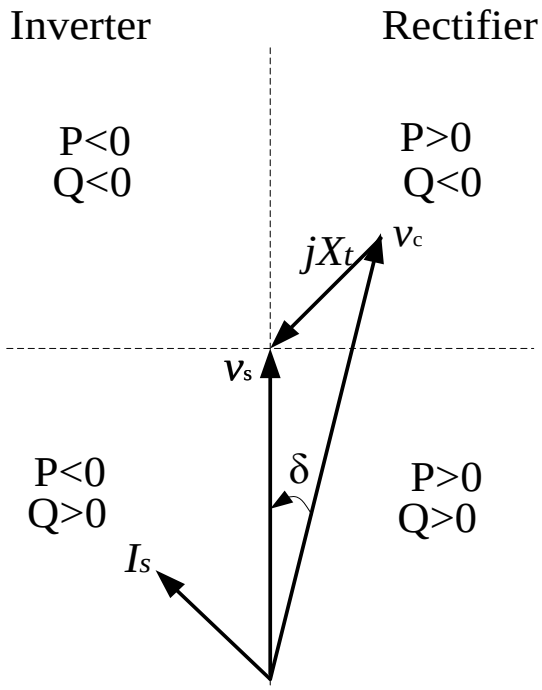

Figure 4-3 Phasor diagram of VSC and direction of the power flow

The active and reactive power capabilities of VSC can be observed in the P-Q characteristic in Figure 4-4 [8] and can operate in all four quadrants of the plane. With some restrictions due the maximum DC voltage, the maximum DC power and the maximum current. The VSC can act as a static reactive power compensator and control AC voltage by injecting or consuming reactive power, depending on requirements. The response of the VSC converter is instantaneous as it has no inertia [7].

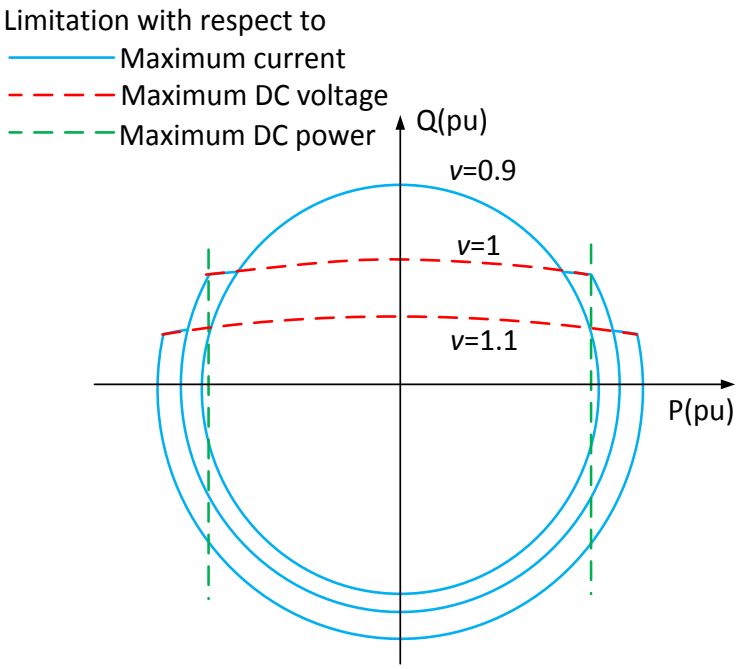

Figure 4-4 Capability curve of VSC-HVDC [9]

4.3 VSC-HVDC components

Components of VSC-HVDC system are shown in Figure 4-5, which are: transformer, AC harmonic filter, smoothing reactor, VSC Converter, DC capacitors and DC cables [10].

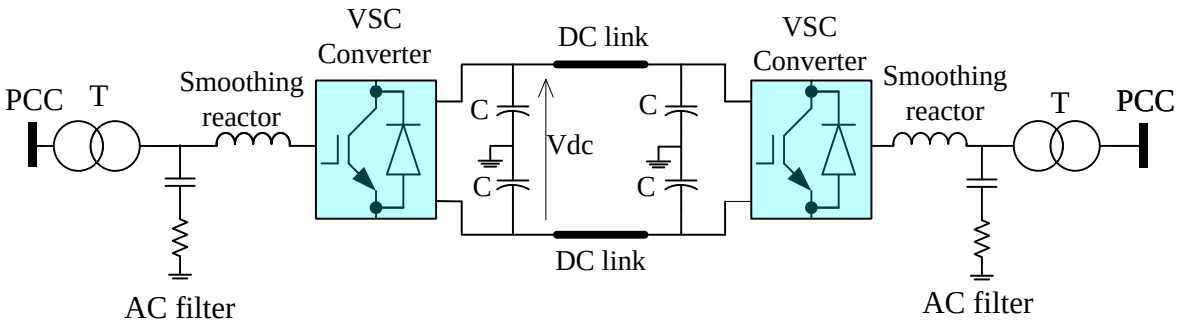

Figure 4-5 Schematic of VSC-HVDC

4.3.1 Voltage Source Converter Unit

VSC-HVDC use IGBT semiconductor devices with an anti-parallel freewheeling diode as a switching device; it is the most important element of the system as it has reversal blocking capacity [7, 11]. To accomplish the required rating of HVDC transmission, the single unit consists of a number of switches connected in series.

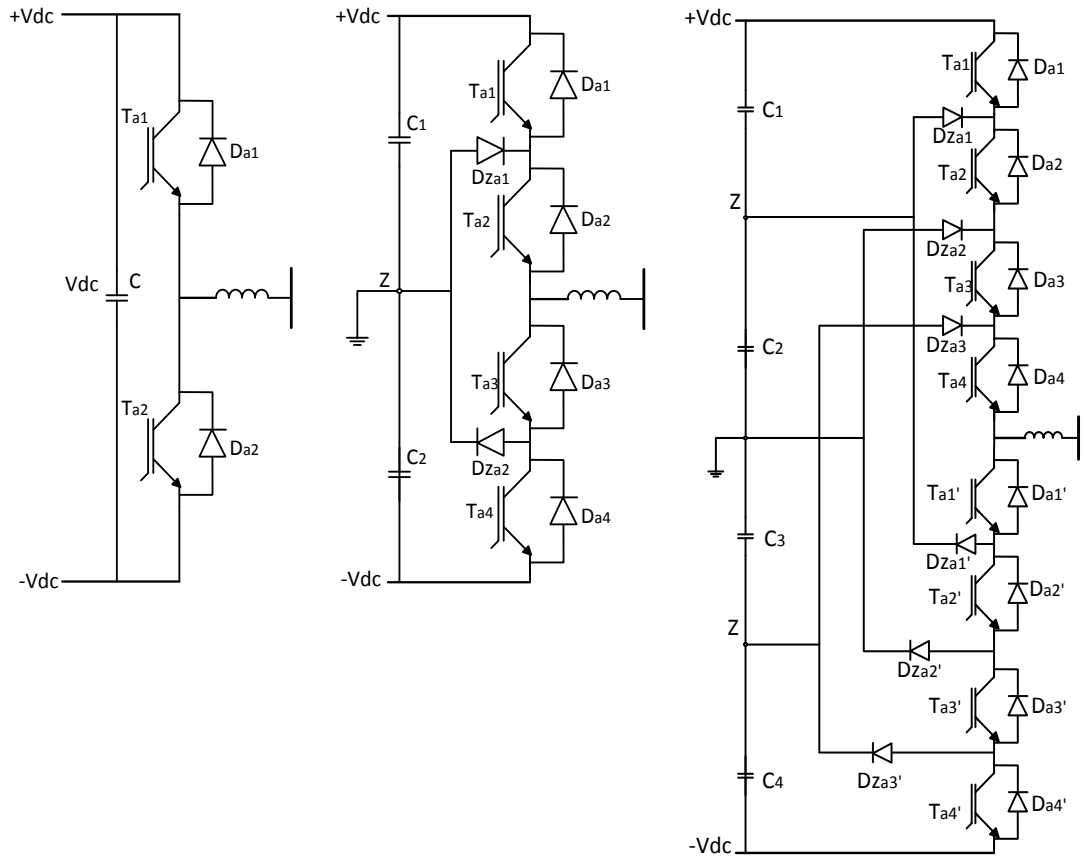

Figure 4-6 Two-level, three-level and multi-level converters

The VSC switching devices can be connected in different ways to build various types of converters topologies [12] described in chapter two of this thesis. The circuit configuration of two-level, three-level and multi-level converters are shown in Figure 4-6. In this thesis the two level converter topology will be used for simulation purposes.

4.3.2 Transformer

In VSC-HVDC systems, the transformers are used to increase the converter voltage to transmission levels. The design of the transformer depends of the power level of the converter. To increase voltage controllability, the transformers are equipped with tap changers devices which changes the ratio of the winding turns on the transformer [13].

4.3.3 AC harmonic filter

IGBT uses high-frequency PWM techniques which produce high-order harmonic components. Hence, passive filters are required in the system to eliminate these harmonics and to prevent the circulation of harmonic currents into the AC grid. Usually a second or third order high-pass filter is used in VSC-HVDC shown in the Figure 4-7, the characteristic frequency of which is selected is based on the switching use in the VSC system.

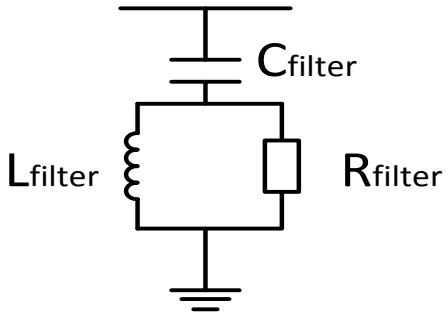

Figure 4-7 Second order high-pass filter

The capacitance (C_{filter}), inductance (L_{filter}) and the resistance (R_{filter}) of the filter can be calculated from following equations:

$$C_{filter} = \frac{(h^2 - 1)Q_{filter}}{h^2 \omega_s v_{LL}^2} \tag{4.4}$$

$$L_{filter} = \frac{1}{C_{filter} h^2 \omega_e^2} \tag{4.5}$$

$$R_{filter} = Q_{filter} \sqrt{\frac{L_{filter}}{C_{filter}}} \tag{4.6}$$

Where h is the harmonic to be filtered and Q_{filter} refers to the quality factor of the harmonic filter.

4.3.4 Smoothing reactor

The reactors between the VSC and the grid enable the power transfer between the converter and the AC grid. This reactor also functions as current filter. The inductance of the reactors is calculated in function of the desired current ripple and the maximum short circuit current between the VSC and the AC grid.

4.3.5 DC capacitor and configuration

The main functions of the DC capacitors are to keep the power balanced during transient conditions and for decreasing voltage ripple on the DC side of the converter.

Capacitor represents the relationship between charge stored on the capacitor and voltage across the capacitor, this linear relation is shown:

$$q = CV \tag{4.7}$$

The following equation is used to calculate the DC capacitor size:

$$\tau = \frac{0.5 \cdot C_{dc} \cdot V_{dc}^2}{S_n} \quad (4.8)$$

Where τ is a time constant, C_{dc} is the DC capacitor, V_{dc} is the dc voltage, and S_n is the apparent power of the converter [14].

4.3.6 DC cables

The VSC-HVDC system uses DC cables which are typically XLPE Cross-Linked polyethylene cables used in underground and under-water applications. XLPE cables are also low-weight, flexible and have a high mechanical strength [15-17].

Since offshore wind power is moving towards higher voltages HVDC cables are more efficient for long distances for offshore wind farms than HVAC cables, the graph that illustrates the costs comparison for HVAC vs HVDC transmission system vs distance is show in chapter 2 Figure 20. With DC cables, there is no need for reactive power compensation devices like for AC submarine cables and due the nature of the DC power transmission, losses are lower. [16, 17].

4.4 Dynamic model of VSC-HVDC

The typical structure of VSC-HVDC is shown in Figure 4-9. The three-phase AC source voltages are distributed 120° apart (v_{sa}, v_{sb}, v_{sc}) and make three ideal sinusoidal waveforms shown in Figure 4-8.

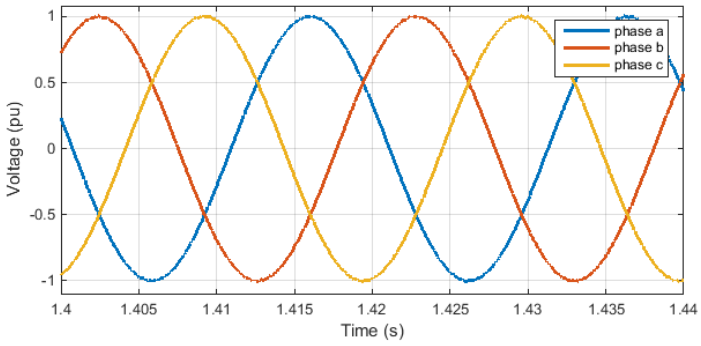

Figure 4-8 three-phase AC voltages

The three-phase current is represented as (i_{sa}, i_{sb}, i_{sc}) and flows form the AC source to the VSC converter or in the reverse direction. The VSC voltages and currents are represented as (v_{ca}, v_{cb}, v_{cc}) and (i_{ca}, i_{cb}, i_{cc}), R_F and L_F are the resistance and inductance of the coupling reactor, V_{dc} and I_{dc} are DC link voltage and current. The left side converter works as a rectifier and power from the AC side is transferred to the DC side. The right side of the model operates as an inverter and power is transferred from the DC side to the AC side.

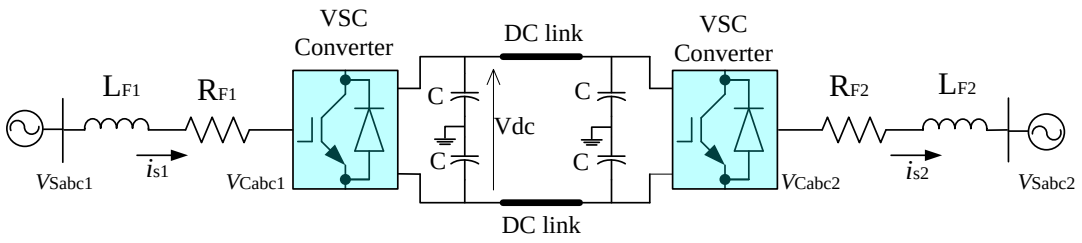

Figure 4-9 Model of VSC-HVDC

For the analysis of the system, the equations describing system behaviour are presented based on [18, 19]. Considering the converters connected to the grid the dynamic equations for the rectifier can be expressed as:

$$\mathrm{v_{sa1}} = \mathrm{v_{ca1}} + R_{F1}\mathrm{i_{sa1}} + \mathrm{L_{F1}}\frac{di_{sa1}}{dt} \tag{4.9}$$

$$\mathrm{v_{sb1}} = \mathrm{v_{cb1}} + R_{F1}\mathrm{i_{sb1}} + \mathrm{L_{F1}}\frac{di_{sb1}}{dt} \tag{4.10}$$

$$\mathrm{v_{sc1}} = \mathrm{v_{cc1}} + R_{F1}\mathrm{i_{sc1}} + \mathrm{L_{F1}}\frac{di_{sc1}}{dt} \tag{4.11}$$

And for inverter side:

$$\mathrm{v_{sa2}} = \mathrm{v_{ca2}} + R_{F2}\mathrm{i_{sa2}} + \mathrm{L_{F2}}\frac{di_{sa2}}{dt} \tag{4.12}$$

$$\mathrm{v_{sb2}} = \mathrm{v_{cb2}} + R_{F2}\mathrm{i_{sb2}} + \mathrm{L_{F2}}\frac{di_{sb2}}{dt} \tag{4.13}$$

$$\mathrm{v_{sc2}} = \mathrm{v_{cc2}} + R_{F2}\mathrm{i_{sc2}} + \mathrm{L_{F2}}\frac{di_{sc2}}{dt} \tag{4.14}$$

After rearranging the equations with respect to the rectifier side:

$$\frac{di_{sabc1}}{dt} = -\frac{R_{F1}}{\mathrm{L_{T1}}}\mathrm{i_{sabc1}} + \frac{1}{\mathrm{L_{F1}}}(\mathrm{v_{sabc1}} - \mathrm{v_{cabc1}}) \tag{4.15}$$

And for the inverter side:

$$\frac{di_{sabc2}}{dt} = -\frac{R_{F2}}{\mathrm{L_{F2}}}\mathrm{i_{sabc2}} + \frac{1}{\mathrm{L_{F2}}}(\mathrm{v_{sabc2}} - \mathrm{v_{cabc2}}) \tag{4.16}$$

The design of a three-phase control system needs to be expressed in dq0 rotational reference frame to simplify the analysis by using a Park Transformation [20]:

$$f_{dq0} = \mathrm{T} f_{abc} = \sqrt{\frac{2}{3}} \begin{bmatrix} \cos\emptyset & \cos(\emptyset - \frac{2\pi}{3}) & \cos(\emptyset + \frac{2\pi}{3}) \\ -\sin\emptyset & -\sin(\emptyset - \frac{2\pi}{3}) & -\sin(\emptyset + \frac{2\pi}{3}) \\ \frac{\sqrt{2}}{2} & \frac{\sqrt{2}}{2} & \frac{\sqrt{2}}{2} \end{bmatrix} \begin{bmatrix} f_a \\ f_b \\ f_c \end{bmatrix} \quad (4.17)$$

Applying equations to the Park's transformation the rectifier side dq0 reference frame is:

$$\frac{di_{sd1}}{dt} = -\mathrm{i_{sd}} \frac{R_{F1}}{\mathrm{L_{F1}}} + \omega i_{sq1} + \frac{1}{\mathrm{L_{F1}}} (\mathrm{v_{sd1}} - \mathrm{v_{cd1}}) \quad (4.18)$$

$$\frac{di_{sq1}}{dt} = -\mathrm{i_{sq}} \frac{R_{F1}}{\mathrm{L_{F1}}} - \omega i_{sd1} + \frac{1}{\mathrm{L_{F1}}} (\mathrm{v_{sq1}} - \mathrm{v_{cq1}}) \quad (4.19)$$

Where (i_{sd1}, $is_{q1,}$) are the d and q components of the currents, (v_{sd1}, $v_{sq1,}$) are the d-q components of the source voltages, (v_{cd1}, $v_{cq1,}$) are the d-q components of the converter voltages. And for an inverter:

$$\frac{di_{sd2}}{dt} = -\mathrm{i_{sd}} \frac{R_{F2}}{\mathrm{L_{F2}}} + \omega i_{sq2} + \frac{1}{\mathrm{L_{F2}}} (\mathrm{v_{sd2}} - \mathrm{v_{cd2}}) \quad (4.20)$$

$$\frac{di_{sq2}}{dt} = -\mathrm{i_{sq}} \frac{R_{F2}}{\mathrm{L_{F2}}} - \omega i_{sd2} + \frac{1}{\mathrm{L_{F2}}} (\mathrm{v_{sq2}} - \mathrm{v_{cq2}}) \quad (4.21)$$

In order to design the controller, equations are coupled as follow and analogically for the inverter:

$$\mathrm{V_{cd1}} = \mathrm{u_{d1}} - \omega L_{F1} i_{\mathrm{sq1}} + \mathrm{V_{sd1}} \quad (4.22)$$

$$\mathrm{V_{cq1}} = \mathrm{u_{q1}} + \omega L_{F1} i_{\mathrm{sd1}} + \mathrm{V_{sq1}} \quad (4.23)$$

Where $\mathrm{u_{cd1}}$ and $\mathrm{u_{cq1}}$ regulate the d-q-axis current for the rectifier and the inverter:

$$\mathrm{u_{cd1}} = R_{F1} i_{\mathrm{sd1}} + L_{F1} \frac{\mathrm{d}i_{\mathrm{sd1}}}{\mathrm{dt}} \quad (4.24)$$

$$\mathrm{u_{cq1}} = R_{F1} i_{\mathrm{q}} + L_{F1} \frac{\mathrm{d}i_{\mathrm{sq}}}{\mathrm{dt}} \quad (4.25)$$

Using state space representation and substituting equation (4.22) into equation (4.24) the current of the system can be written as:

$$\frac{d}{dt}\begin{bmatrix} i_{sd1} \\ i_{sq1} \end{bmatrix} = \begin{bmatrix} -\frac{R_{F1}}{L_{F1}} & 0 \\ 0 & -\frac{R_{F1}}{L_{F1}} \end{bmatrix}\begin{bmatrix} i_{sd1} \\ i_{sq1} \end{bmatrix} + \begin{bmatrix} \frac{1}{L_{F1}} & 0 \\ 0 & \frac{1}{L_{F1}} \end{bmatrix}\begin{bmatrix} u_{cd1} \\ u_{cq1} \end{bmatrix} \quad (4.26)$$

4.5 Control of VSC-HVDC

The control of the VSC-HVDC considers four main arrangements: control of active power flow, control of reactive power flow, AC voltage and DC voltage by using the pulse width modulation PWM [21]. The modulation index M and converter phase angle θ can be adjusted independently by the VSC controller and can give any combination of voltage and phase shift [22] . Therefore, it is possible to control active and reactive power using the VSC station at the wind farm side as a rectifier, and the VSC station working as inverter can maintain constant DC voltage in the HVDC link and regulate the AC voltage at the point of connection with the onshore grid. The vector control based in d-q transformation is used to modify M and phase angle θ to get the desired control function.

Vector control is the most popular technique used to adjust the modulation index and the converter phase angle. The first step in vector control, before calculating the modulation index and phase angle, is to transform three-phase rotating voltage and current from the abc-frame to the d-q reference frame, this transformation is synchronized with AC three phase voltages via a Phase Locked Loop (PLL), (angle θ).

To control variables (P, Q, Vdc or Vac) and generate desired values of *M*, specific set points are given to the controllers and the control variable is forced to follow the reference values by adjusting the magnitude and the angle of the voltage at the VSC terminals. A general controller of a VSC which is composed of an inner controller, an outer controller and a Phase Locked Loop (PLL) is shown in Figure 4-10.

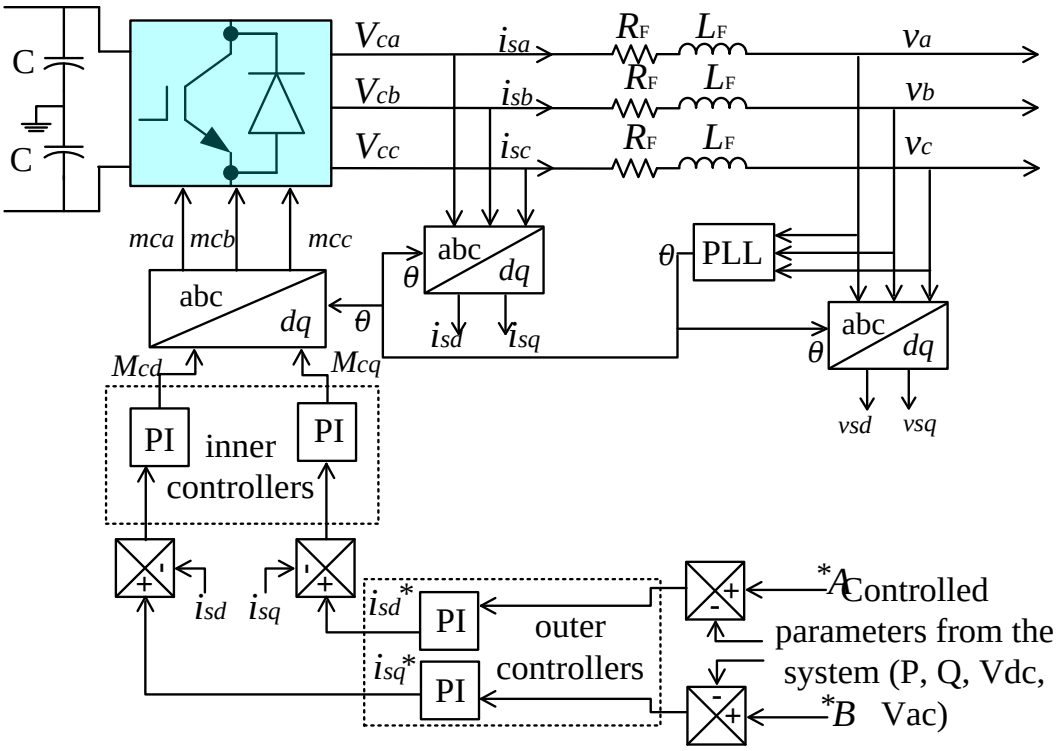

Figure 4-10 Control schematic of a VSC-HVDC

4.5.1 Phase Locked Loop

The mission of the Phase-locked loop (PLL) is the synchronization of the converter currents with their respective voltages. The main challenges in the design of a PLL for a grid-tie converter are:

- Tight synchronization is needed for power flow and the PLL should provide the adequate angle of the d-q-reference frame for the power converter.
- The grid voltages may contain harmonics, may be unbalanced and are subject to disturbances (in amplitude and frequency). Therefore, the PLL should be robust to these variations.

Hence, it can be stated that the PLL has a huge impact in the d-q-control of the three-phase converter. The overall system is shown in Figure 4-11.

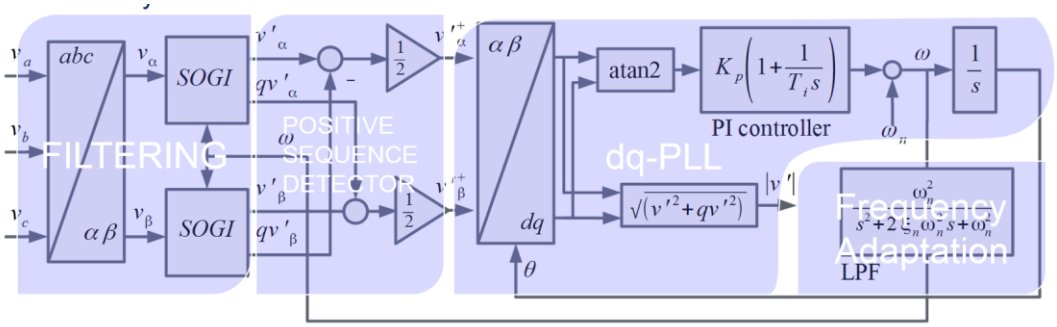

Figure 4-11 Overall PLL for the Grid-Tie Converter

The d-q-PLL, shown in Figure 4-11 is the core of the overall system. A useful analogy for the PLL behaviour consists of a servo motor that tries to catch a rotating mass. The angle provided by the PLL output is synchronized with the positive sequence of the filtered grid voltage. The PLL measures the alpha and beta components of the voltage and translates them to the d-q-reference frame. If the d-q-frame is fully aligned with the alpha component, the angle of the voltage vector should be ideally zero. If the d-q-frame is not fully aligned there is an error, and the angle of the voltage vector in the d-q-reference frame will not be zero. The closed loop control will try to increase/decrease the reference frame angular speed to make that angle null. For this aim, the PLL passes the angle error through a PI controller. The output of this PI controller is the angular speed (frequency) of the rotating d-q-reference frame. The phase of the d-q-reference frame is obtained by using an integrator (a Voltage Controlled Oscillator (VCO) in a traditional PLL) for the previous frequency.

4.5.2 Current inner control loop

The inner controller is responsible for controlling the VSC currents that enable the power flow between the VSC and the grid. Additionally, the current controllers protect the converter from overloading during system disturbances. The inner controller for the wind farm converters must follow the equations listed below and is shown in Figure 4-12. To design the controller cross-coupling terms should be decouple as shown:

$$V_{cd1} = u_{cd1} - \omega L_F i_{sq1} + V_{sd1} \tag{4.27}$$

$$V_{qd1} = u_{cq1} + \omega L_F i_{sd1} + V_{sq1} \tag{4.28}$$

Where u_{d1} and u_{q1} regulate the dq-axis current from equations (4.27, 4.28).

A control signal is then derived from the proportional-integral (*PI*) controller:

$$u_{cd1} = k_p(i^*_{sd1} - i_{sd1}) + k_i \int (i^*_{sd1} - i_{sd1})dt \quad (4.29)$$

$$u_{cq1} = k_p(i^*_{sq1} - i_{sq1}) + k_i \int (i^*_{sq1} - i_{sq1})dt \quad (4.30)$$

Where k_p and k_i are the proportional and integral gains of the controller.

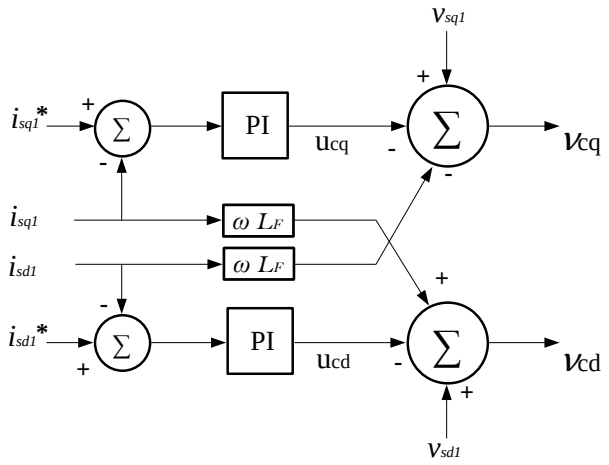

Figure 4-12 Current control loop for VSC-HVDC

The general block diagram shown in Figure 4-13 represents current control loop. The configuration of Figure 4-13 is repeated for the d and the q current controllers.

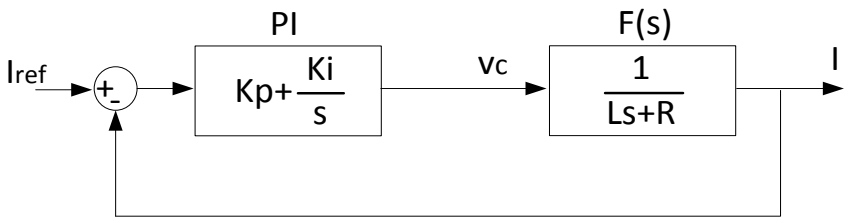

Figure 4-13 Block diagram of the current control loop

The current control system can be simplified to a single transfer function F(s) as shown below:

$$F(s) = \frac{i_{sd1}(s)}{v_{cd}(s)} = \frac{i_{sq1}(s)}{v_{cq}(s)} = \frac{1}{L_f s + R_f} \quad (4.31)$$

The open loop control system can be written as:

$$G(s) = \left(k_p + \frac{k_i}{s}\right)\left(\frac{1}{Ls + R}\right) = \frac{\frac{k_p}{L}(s + \frac{k_i}{k_p})}{s^2 + s\frac{R}{L}} \tag{4.32}$$

The closed loop control system H(s):

$$G(s) = \frac{\frac{k_p}{L}(s + \frac{k_i}{k_p})}{s^2 + s\left(\frac{R + k_p}{L}\right) + \frac{k_i}{L}} \tag{4.33}$$

The control parameters for the proportional and integral gains of the current controller are given as follow[6]:

$$k_p = 2\zeta\omega_n L_F - R_F \tag{4.34}$$

$$k_i = \omega_n^2 L_F \tag{4.35}$$

Where: ω_n is natural frequency of the system and ζ is a damping factor.

$$2\zeta\omega_n = (k_p + R_F)/L_F \tag{4.36}$$

$$\omega_n^2 = k_i/L_F \tag{4.37}$$

This is a second order system; to tune the controller different techniques can be applied to find temporary gains values of k_p and k_i.

4.5.3 Active and reactive power control

The apparent power of a 3 phase AC system, *S*, in terms of *dq* voltages and currents is defined as:

$$S = \frac{3}{2}(v_{sdq})(i_{sdq})^* = \frac{3}{2}(v_{sd} + jv_{sq})(i_{sd} + ji_{sq}) \tag{4.38}$$
$$= \frac{3}{2}(v_{sd}i_{sd} + v_{sq}i_{sq}) + j(v_{sq}i_{sd} - v_{sd}i_{sq}) = P + jQ$$

Where P is the active power and Q is the reactive power. If the *d* axis of the dq0 rotatory frame is assumed to be aligned with the AC space vector, then the voltage representation in d-q consist only of *d* components (i.e. $\omega_{dq} = \omega_s$, $v_d = v_s$ and $v_q = 0$) as seen in Figure 4-14. In this case, equation x can be simplified to

$$P = \frac{3}{2}v_{sd}i_{sd} \tag{4.39}$$

$$Q = -\frac{3}{2} v_{sd} i_{sq} \tag{4.40}$$

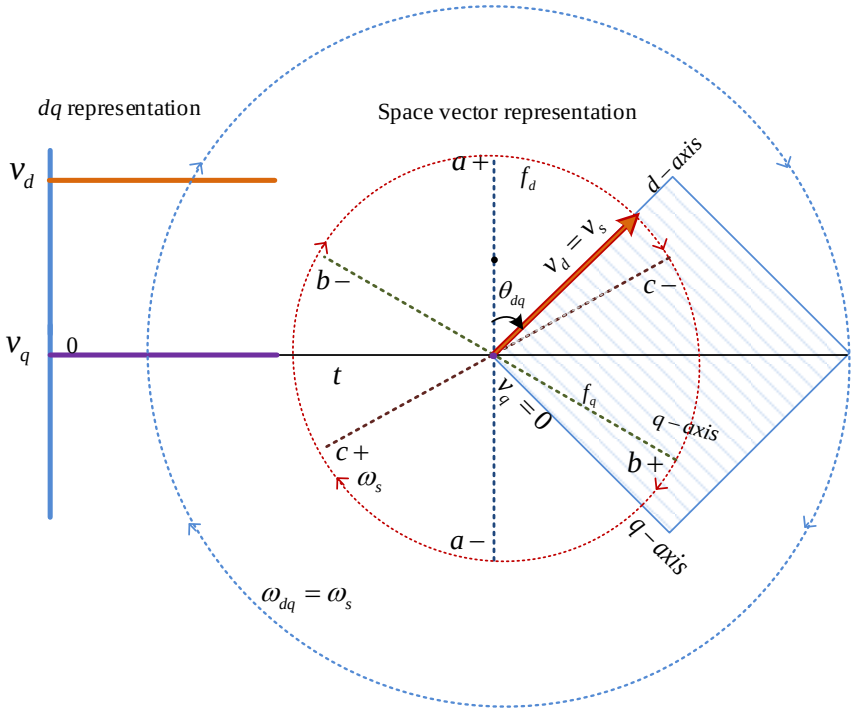

Figure 4-14 *dq0* Transformation of the Grid Voltages when the d Axis is aligned to the AC Space Vector

Active Power Control

According to equation (3.49) the relationship between the amount of d current and the inverter active power is directly proportional (assuming constant AC voltage). Because of this, a simple integral controller is enough to control the active power with first order dynamics and 0 steady state error. The transfer function, G_P, from the active power P to the i_d current is given by

$$G_P = \frac{i_{sd}}{P} = \frac{2}{3v_{sd}} \tag{4.41}$$

If an integral controller of the type $C_P(s) = Ki_P / s$, (where Ki_P is the integral constant of the active power controller and s is the Laplace variable) is added in cascade with G_P the following open loop expression is obtained:

$$A_P(s) = G_P * C_P(s) = \frac{2K_{iP}}{3v_{sd}s} \tag{4.42}$$

If Ki_P is selected to have a value of $Ki_P = 3v_d\alpha_P / 2$, where α_P can be regarded as the closed loop bandwidth of the controller, then the open loop expression $A_P(s)$ and the closed loop expression $E_P(s)$ from the active power reference P_{ref} to P are:

$$A_P(s) = \frac{2}{3v_{sd}s}\frac{3v_{sd}\alpha_P}{2} = \frac{\alpha_P}{s} \tag{4.43}$$

$$E_P(s) = \frac{P}{P_{ref}} = \frac{A_P(s)}{1 + A_P(s)} = \frac{\alpha_P}{s + \alpha_P} \tag{4.44}$$

As seen in equation (4.44) the closed loop dynamics of the active power control loop are first order with a closed loop bandwidth of α_P. The value of α_P can be selected for a given rise time of the control variable by following the formula that defines the relationship between bandwidth and rise time in first order systems. This formula is given by:

$$\alpha_P \approx \frac{0.35}{t_{r\_P}}\text{(Hz) or } \alpha_P \approx \frac{2.2}{t_{r\_P}}\text{(rad)} \tag{4.45}$$

Where t_{r_p} is the desired rise time of the closed loop system. Figure 4-15 shows the block diagram of the active power control loop

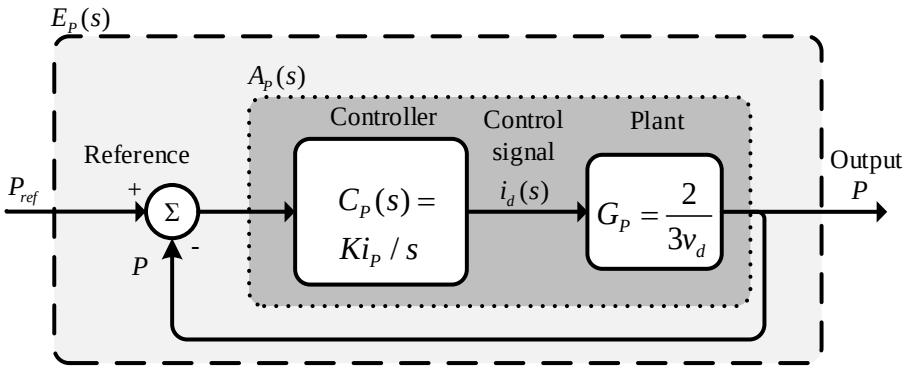

Figure 4-15 Schematic Diagram of the Active Power Control Loop

Figure 4-16 shows the step response and the bode plot of active power closed loop control system for a bandwidth of $\alpha_P = 220$ rad. ($t_{r\_P} = 0.01$ sec).

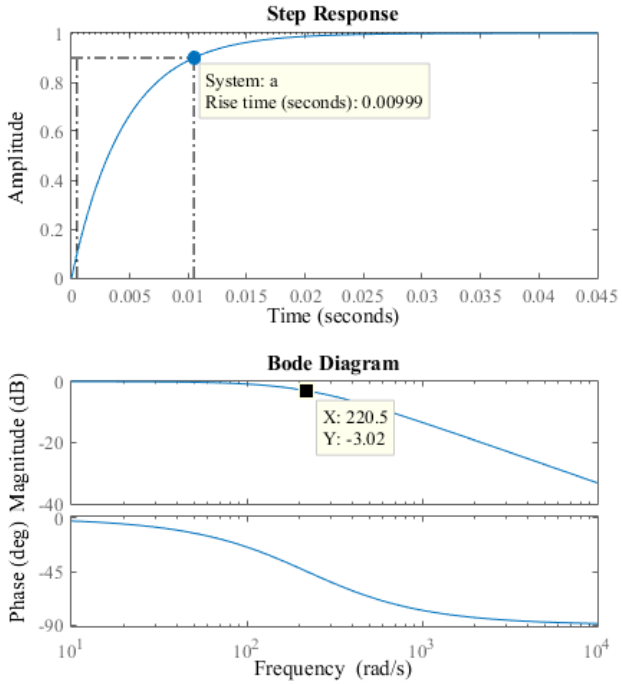

Figure 4-16 Step response and bode plot of the closed loop active power controller

4.5.4 Reactive Power Control

According to equation (4.40), the relationship between the amount of q current and the inverter reactive power is directly proportional if the AC voltage is assumed to be a constant value. Because of this, a simple integral controller is enough to control the reactive power with first order dynamics and 0 steady state error. The transfer function, G_Q, from the reactive power Q to the i_q current is given by

$$G_Q = \frac{i_q}{Q} = -\frac{2}{3v_{sd}} \tag{4.46}$$

If an integral controller of the type $C_Q(s) = Ki_Q / s$, (where Ki_Q is the integral constant of the reactive power controller) is added in cascade with G_Q the following open loop expression is obtained:

$$A_Q(s) = G_Q * C_Q(s) = -\frac{2K_{iQ}}{3v_{sd}s} \tag{4.47}$$

If Ki_Q is selected to have a value of $Ki_Q = -3v_d\alpha_Q / 2$, where α_Q can be regarded as the closed loop bandwidth of the controller, then the open loop expression $A_Q(s)$ and the closed loop expression $E_Q(s)$ from the reactive power reference Q_{ref} to Q are:

$$A_Q(s) = -\frac{2}{3v_{sd}s}\left(-\frac{3v_{sd}\alpha_Q}{2}\right) = \frac{\alpha_Q}{s} \tag{4.48}$$

$$E_Q(s) = \frac{Q}{Q_{ref}} = \frac{A_Q(s)}{1 + A_Q(s)} = \frac{\alpha_Q}{s + \alpha_Q} \tag{4.49}$$

As seen in equation (4.49) the closed loop dynamics of the active power control loop are first order with a closed loop bandwidth of α_Q. The value of α_Q can be selected for a given rise time of the control variable by following the formula that defines the relationship between bandwidth and rise time in first order systems. This formula is described in (4.45)

Figure 4-17 shows the block diagram of the reactive power control loop

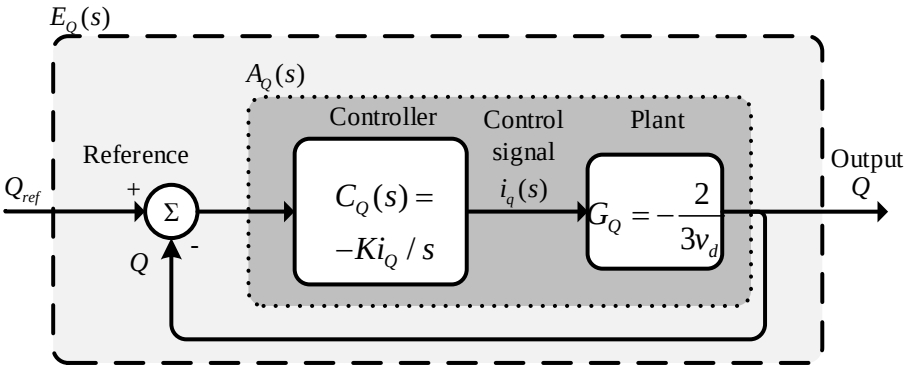

Figure 4-17 Schematic Diagram of the Reactive Power Control Loop

The step response and bode plots of the reactive power closed loop control system for a bandwidth of $\alpha_P = 220$ rad. ($t_{r\_P} = 0.01$ sec) is similar to the one presented in Figure 4-16.

4.5.5 DC and AC controllers

The DC and AC voltage controllers compare the measured voltages with the reference voltages V_{dc}^* or V_{ac}^* and then the error signal is fed to PI controllers to obtain a reference current as shown in Figure 4-12. The reference current signals i_{sd}^* and i_{sq}^* can be obtained from the PI controllers:

$$\mathrm{i_{sd}^*} = \mathrm{k_{pdc}}(\mathrm{V_{dc}^*} - \mathrm{V_{dc}}) + \mathrm{k_{idc}} \int (\mathrm{V_{dc}^*} - \mathrm{V_{dc}})\mathrm{dt} \tag{4.50}$$

$$\mathrm{i_{sq}^*} = \mathrm{k_{pac}}(\mathrm{V_{ac}^*} - \mathrm{V_{ac}}) + \mathrm{k_{iac}} \int (\mathrm{V_{ac}^*} - \mathrm{V_{ac}})\mathrm{dt} \tag{4.51}$$

Where k_{pdc}, k_{idc}, k_{pac}, k_{iac} are the proportional and integral gains of the DC and AC controllers respectively.

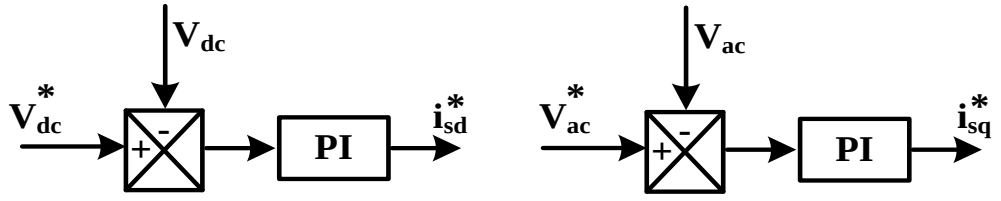

Figure 4-18 Block diagrams of the DC and AC voltage controllers.

4.6 Point-to-point connection of VSC-HVDC system between two AC networks.

In this section, the steady state and transient response of a VSC-HVDC station are investigated for point-to-point system as shown in Figure 4-19. To demonstrate the performance of the system controlled the simulations were carried out in MATLAB/Simulink [23].

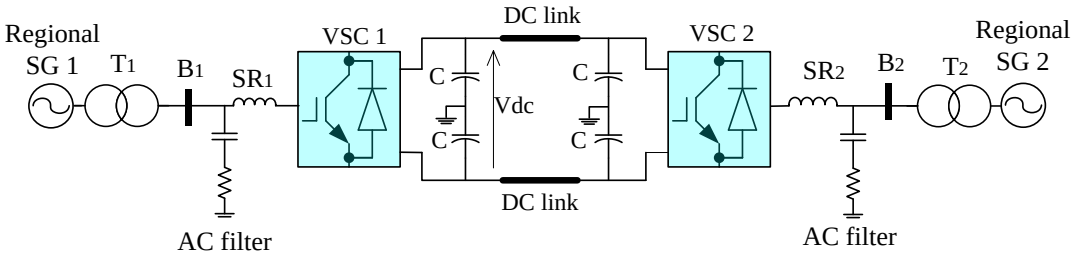

Figure 4-19 Three VSC-HVDC transmission system connected to AC network

Details of the model are shown in the Table 4-1, the parameters are taken from MATLAB/Simulink library and do not represents a real network.

Table 4-1 VSC-HVDC parameters for simulation

Generators SG_1 and SG_2	3000MVA, 13.8kV, 50Hz, Xd=1.69, Xd'=0.210, Xd" =0.17, Xq=1.615, Xq"=0.223 Xl=0.16, Rs=0.0025, H=4.25
Transformers $T_{1gen,}$ T1 and T2 T_{2gen}	T_{1gen}(13.8/275 kV, 1000MVA, R1=0.005pu, L1=0.2pu) T_1(275/132 kV, 1000MVA, R1=0.005pu, L1=0.2pu) T_{2gen}(275/18.8 kV, 1000MVA, R1=0.005pu, L1=0.2pu) T_2(132/275 kV, 1000MVA, R1=0.005pu, L1=0.2pu)
AC network cables on both sides	R=0.013Ω/km, L=0.934mH/km, 60km length
AC filters	F1= high pass filter (15MVAr, Quality factor=15) F2= high pass filter (65MVAr, Quality factor=15)
DC link	V_{dc}=300kV, C =1000μ F, cable (0.018Ω/km, 180km)

4.6.1 Control design of the point-to-point connection

The control of point-to-point VSC-HVDC can be set up to control active and reactive power from or DC and AC voltages. In this study, the system is chosen to control active power flow and maintain AC voltage at the bus B1 show in Figure 4-20. While the other converter is set up to control DC voltage and again maintain AC voltage at the bus B2 shown in Figure 4-21. In both converters, the controllers of the AC voltage can be changed to control reactive power with small modifications shown in 4.5

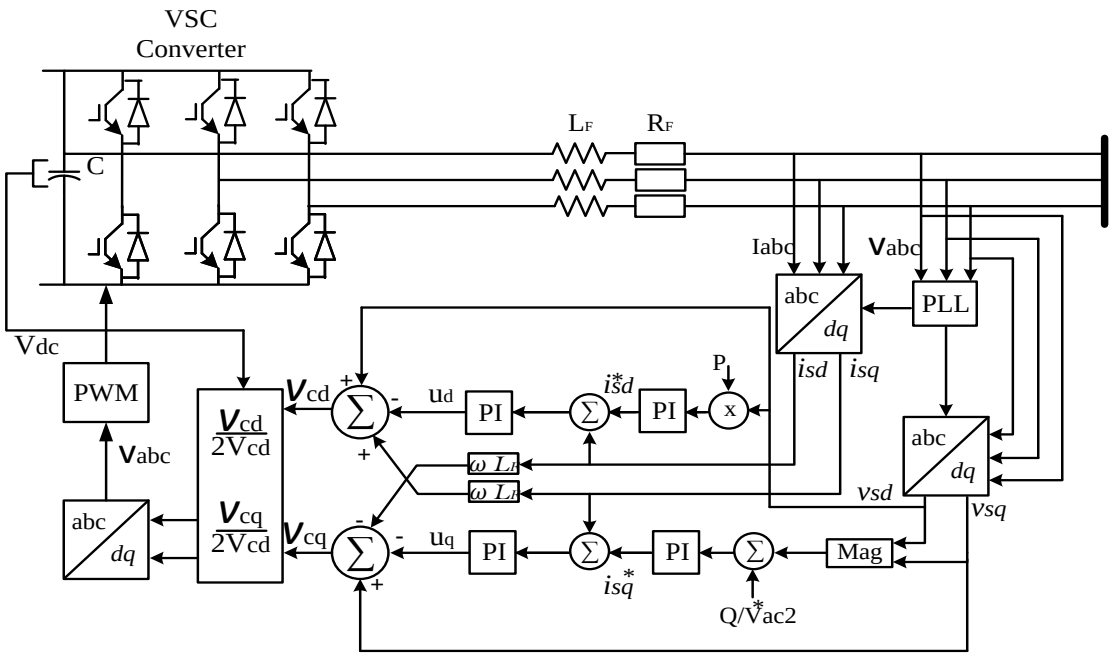

Figure 4-20 Simplified schematic of P and AC voltage control

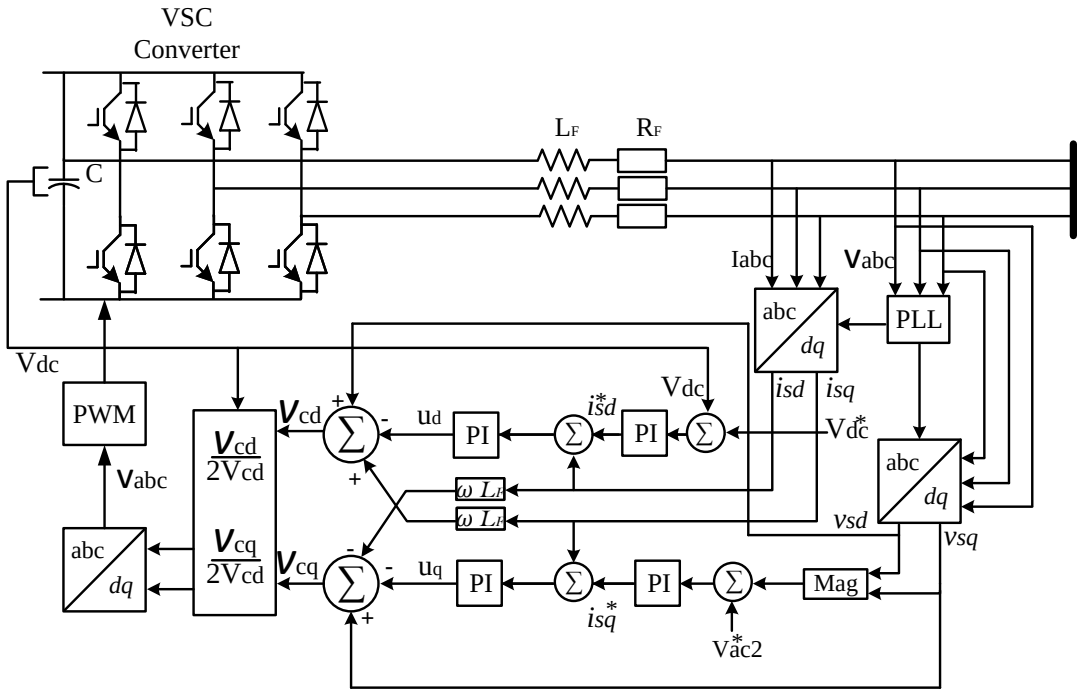

Figure 4-21 Simplified schematic of DC and AC voltage control

4.6.2 Dynamic behaviour of the system during power exchange

The dynamic response of the VSC-HVDC is shown in this section. The first simulation shows power reversal from +1pu to -1pu carried out gradually and not as step change.

The active power on the both sides of the converter stations are shown in Figure 4-22 and Figure 4-23. The power reversal starts at t=1 and continues to t=2.6s.

The changes in active power reflects with changes in the DC voltage on the sending end (VSC1) as seen in Figure 4-25. The Receiving end controller DC voltage controller maintains the voltage across its capacitors at 300kV. The difference of DC voltage between the sending and receiving stations forces the current to flow accordingly to the desired power set point change of the power controller.

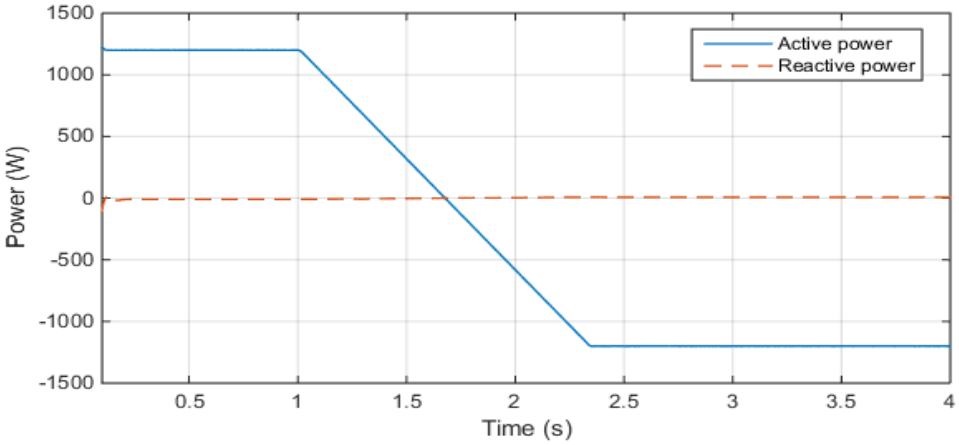

Figure 4-22 Active and reactive power at bus 1

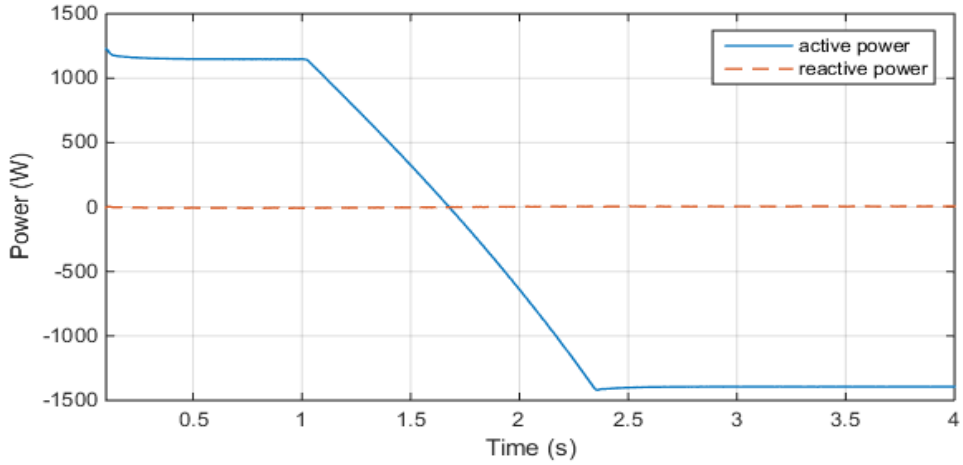

Figure 4-23 Active and reactive power at bus 2

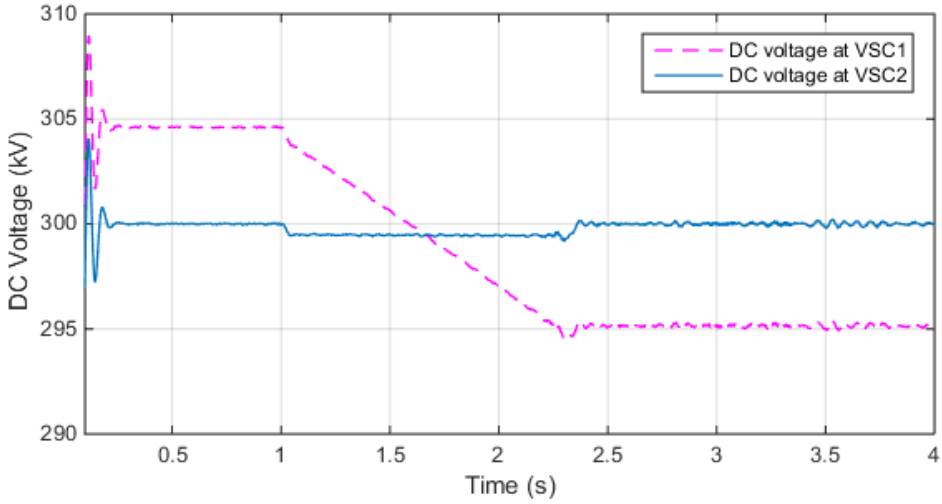

Figure 4-24 DC voltages at VSC1 and at VSC2

The AC voltage at the bus1 and bus2 are kept constant and only small variation is noticeable during the simulations shown in Figure 4-25. This is because the controllers in the converters are set up to keep a constant AC voltage regardless of the active power flow. Thus the VSC stations acts as a static reactive power device. The behaviour of the receiving end converter AC currents is shown in Figure 4-26.

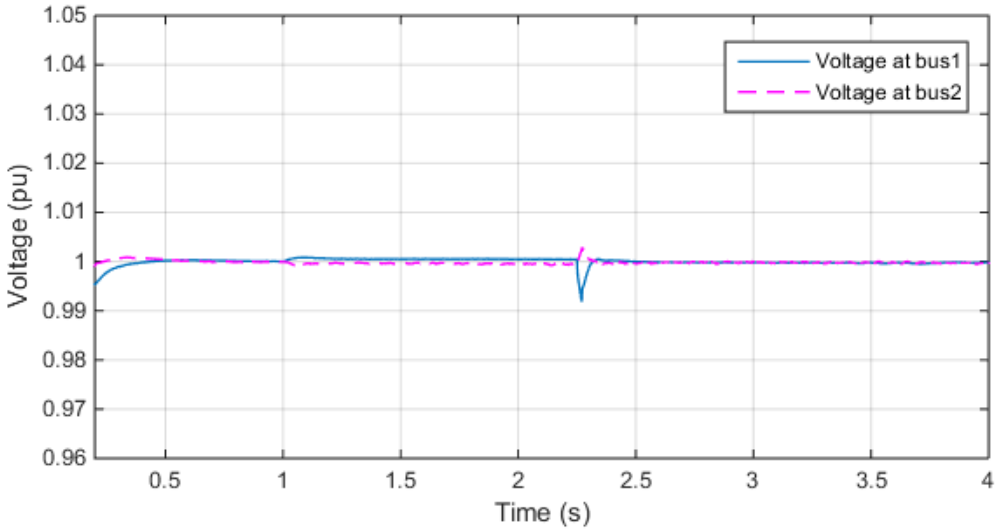

Figure 4-25 Voltages at bus1 and at bus2

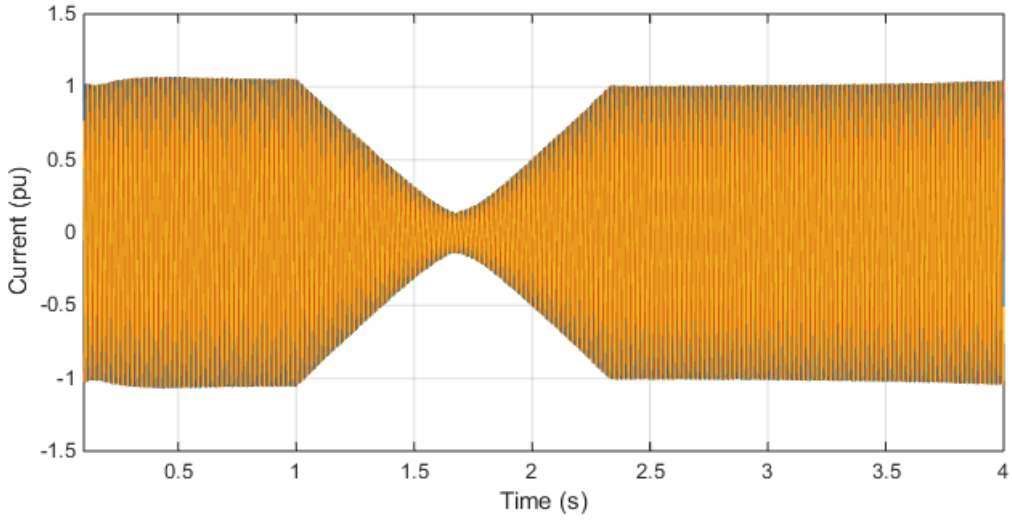

Figure 4-26 Phase current at bus 1

4.7 Offshore wind power integration

VSC-HVDC is one of the three options to connect offshore wind power to the onshore grid. As mentioned in chapter 2, VSC-HVDC transmission system can overcome shortcomings of traditional HVDC and HVAC systems due to the features explained at the beginning of this chapter [24].

4.7.1 High Voltage Alternating Current for offshore wind farm integration

Many offshore wind plants are connected via High Voltage AC transmission system. This technology is well-proven and cost effective solution for connecting close located offshore wind farm [25]. The main disadvantage of this connection type is distance limitation as cables are subjected to a capacitive changing effect that limits the active power transfer [26]. To overcome this limitation onshore, reactive power compensation units are used on each end of the cable route; in the offshore this requires the use of expensive platforms. Another major weakness of HVAC system connected to offshore wind farms is fault propagation: faults on the AC site will directly affects wind farms and faults in the wind farm sides have direct effects on the AC network. The basic configuration of an offshore HVAC system is show in Figure 4-27.

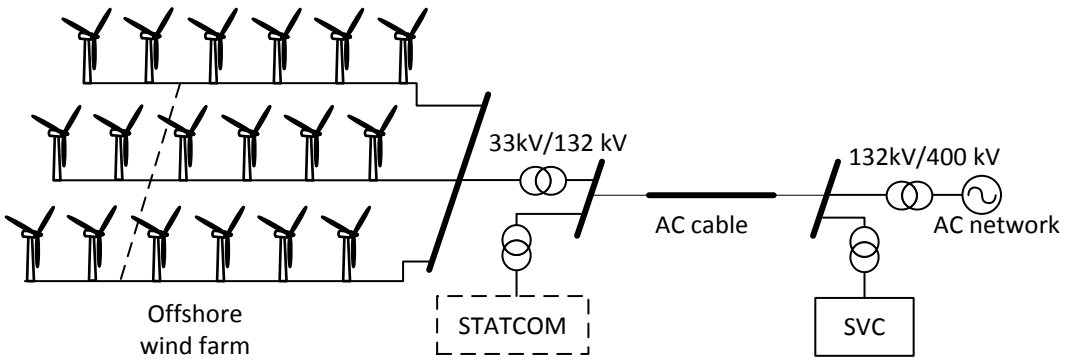

Figure 4-27 HVAC connection for wind farm integration

Middelgrunden was the first offshore wind farm off the Danish coast connected to the shore using HVAC. The project was commissioned in 2000 with a total capacity of 40MW. However, the first large-scale wind farm project Horns Rev1 with total capacity of 160MW was also located of Danish coast. The transmission levels for HVAC offshore wind farm varies from 132-220kV: Table 4-2 describes some of the most recent HVAC projects around Europe in terms of total capacity of the wind farm, AC voltages and distance from shore.

Table 4-2 HVAC offshore wind farms

Wind farm	Capacity (MW)	AC Voltage (kV)	Distance (Km)	Commissioning Date
Gwynt y Mor	160x3.6=576	132	18	2015
Westermost Rough	25x6=210	150	8	2015
West of Duddon Sands Wind Farm	108x3.6=398	155	14	2014
Anholt Offshore Wind Farm	111x3.6=400	220	21	2013
London Array	175x2.6=630	150	11	2012

4.7.2 Current source converter for offshore wind farm integration

CSC-HVDC transmission is a well-established technology and much older than VSC-HVDC. Since this technology is used in multiple projects for interconnection the AC networks, till today it has never used to connect offshore wind farm to the shore grid. There are several reasons why it was not used in offshore wind farms yet. The major reason is the need of special arrangements of filters to smooth the AC currents and allow operation during

wind variations such as STATCOM. Conventional HVDC also absorbs reactive power at both ends, the footprint is much higher compare to VSC-HVDC, and system cannot provide independent control over active and reactive power [27].

The typical LCC-HVDC layout for connecting the wind farm to the grid consist in s AC collection network, an offshore substation with converter and a start-up generator (or STATCOM), filters, DC cables, onshore substation, AC harmonic filter, as shown in Figure 4-28.

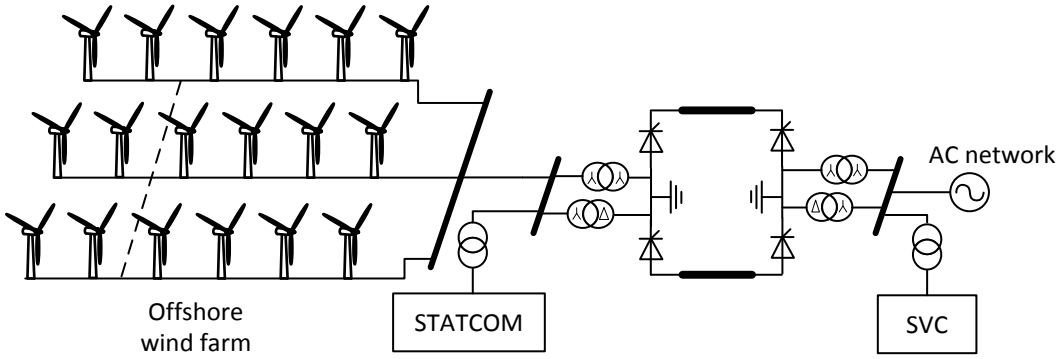

Figure 4-28 Configuration of LCC-HVDC for connecting offshore wind farm

4.7.3 Voltage source converter for offshore wind farm integration

VSC-HVDC provides an attractive alternative to HVAC and conventional HVDC power transmission. It also gives room to wind farms to meet Grid Code requirements. When comparing VSC-HVDC to HVAC, the former reduces transmission losses and permits asynchronous operations between the wind farm and AC onshore grid. Moreover, it does not require additional reactive power compensation units on the ends of the transmission lines [28-30]. VSC-HVDC also have lower footprint compare to traditional HVDC since it doesn't require reactive power compensation units, hence requires 30% less space on the offshore platform which translates into cost reduction.

4.7.4 VSC-HVDC point-to-point hybrid offshore wind farm integration

A VSC-HVDC connection of a large-scale offshore wind farm is presented in Figure 4-29. It is a hybrid wind farm and consist of two types of the wind turbine machines: double-fed induction generators wind turbines and permanent magnet synchronous generator machines with fully rated converter. The aggregated model of a wind farm was used for the purpose of the simulation, which is composed of one aggregated model of the DFIG wind turbines of the farm and one aggregated model of the FRC wind turbines. The hybrid wind plant comprises 120 x 5MW DFIG wind turbines and 120 x 5MW FRC wind turbines connected

to 33kV collection network. The DC cable length between the wind farm converter station and onshore converter station is 150km. The converter stations are rated at 1200MVA and currently are the biggest size available on the market.

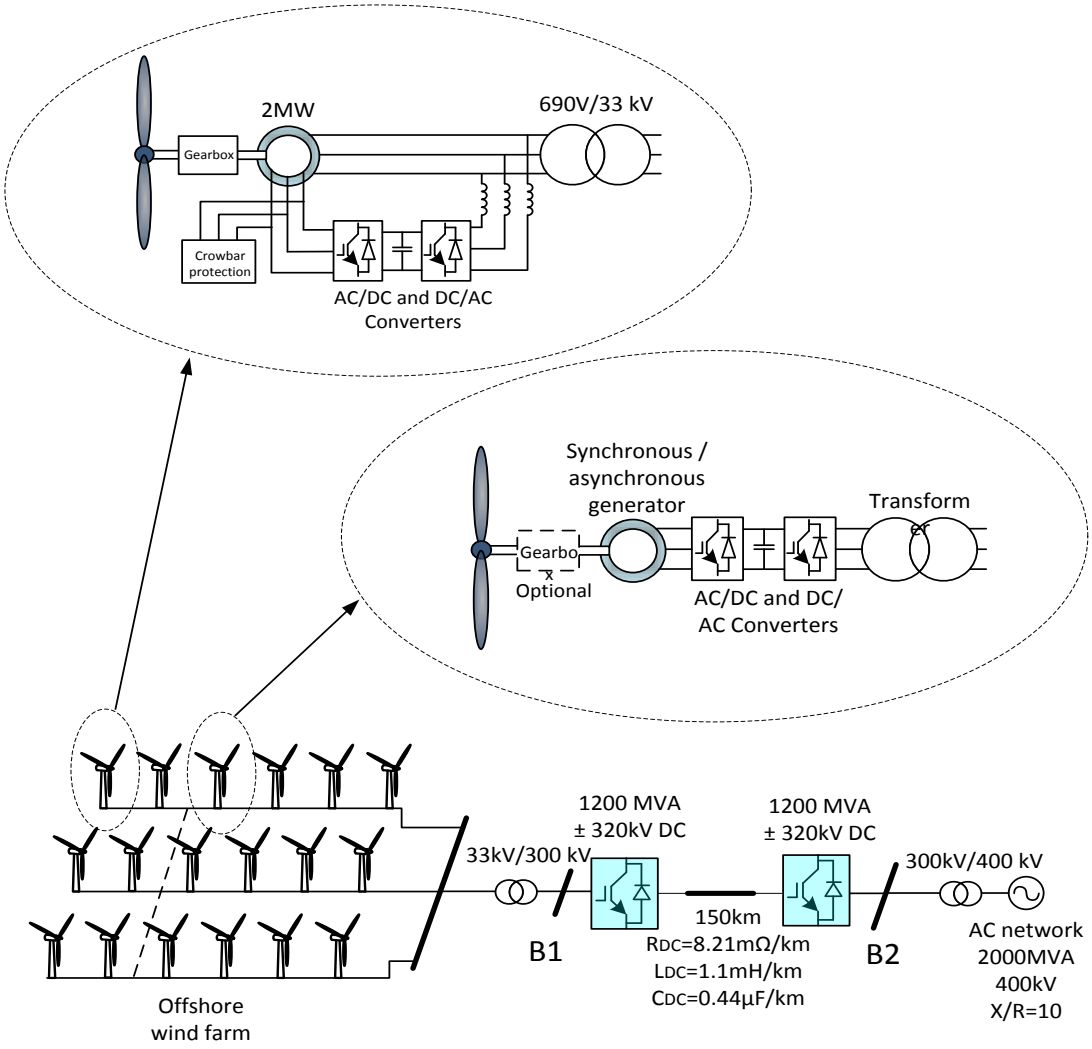

Figure 4-29 Point-to-point connection of a large-scale hybrid wind farm

The control systems for wind turbines are described in Chapter 3 of this thesis.

4.7.5 Control design for offshore wind power integration

The control of the wind farm side VSC-HVDC link is illustrated in Figure 4-20. The wind farm converter is designed to allow the generated wind power to be fully transferred to the DC side by just keeping an AC voltage of 1pu at the converter terminals. The current flowing from the turbines to the converter is rectified and transferred fully to the DC side.

The onshore converter control is shown in Figure 4-21. It is responsible for controlling DC link voltage and reactive power at bus bar B2. With additional control loops, wind turbine

coordinated control is possible to provide auxiliary services (reactive power support) to the onshore grid.

The grid side converter shown in the Figure 4-21 is responsible for maintaining DC link voltage and AC voltage at the PCC. The current references i_{dg}^{*} and i_{qg}^{*} are derived from DC and AC voltage controller which are set up at 1pu.

$$i_{dg}^{*} = k_{pdc}(V_{dc}^{*} - V_{dc}) + k_{idc}\int (V_{dc}^{*} - V_{dc})dt \quad (4.52)$$

$$i_{qg}^{*} = k_{pac}(V_{ac}^{*} - V_{ac}) + k_{iac}\int (V_{ac}^{*} - V_{ac})dt \quad (4.53)$$

4.7.6 VSC-HVDC behaviour of the system during power delivery from offshore wind farm

The performance of the whole system during power delivery from the offshore grid farm is investigated in this section. In order to investigate the system with realistic wind behaviour, the wind model was designed to simulate wind variations shown in Figure 4-30.

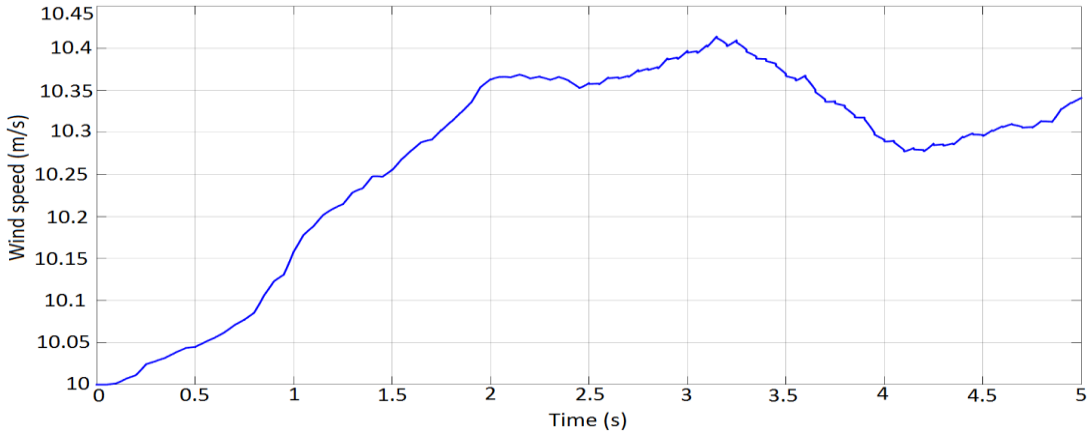

Figure 4-30 Wind variation

The active and reactive power flow is demonstrated in the Figure 4-31 and Figure 4-32. To demonstrate the auxiliary services provided by grid side converter at the t=2.5 the reactive power is switched to 300MVAr.

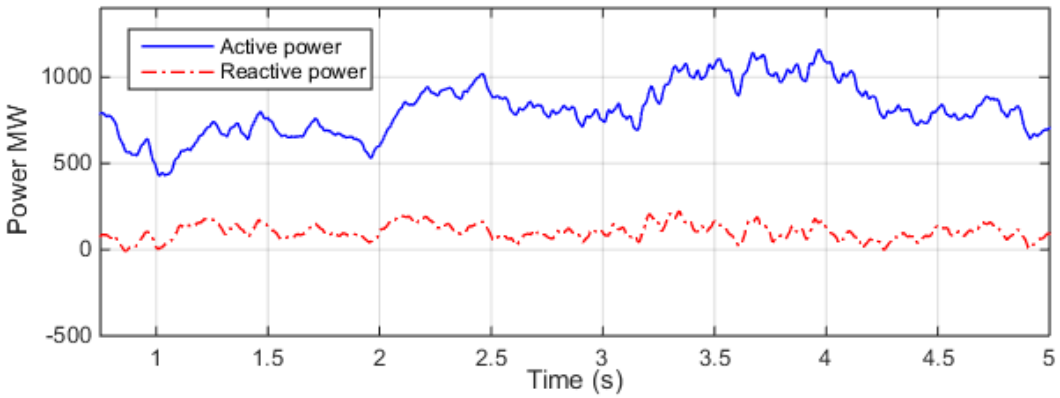

Figure 4-31 Active and reactive power at B1

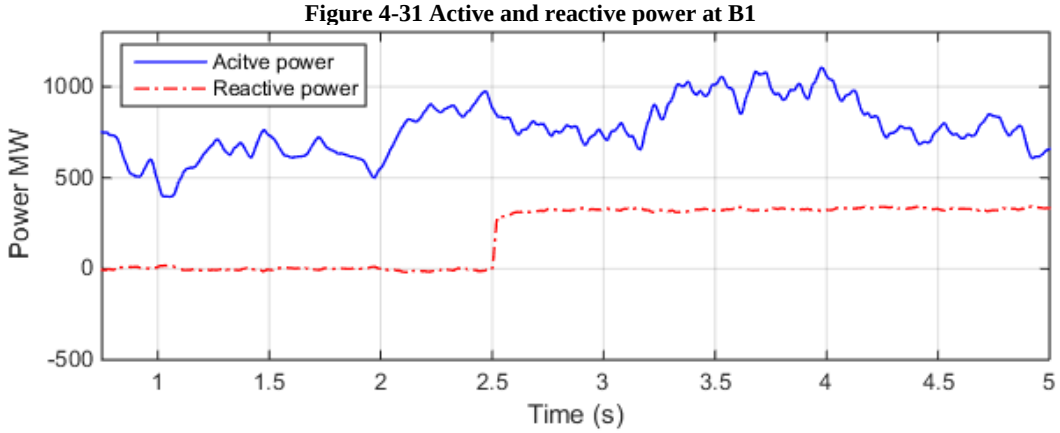

Figure 4-32 Active and reactive power at B2

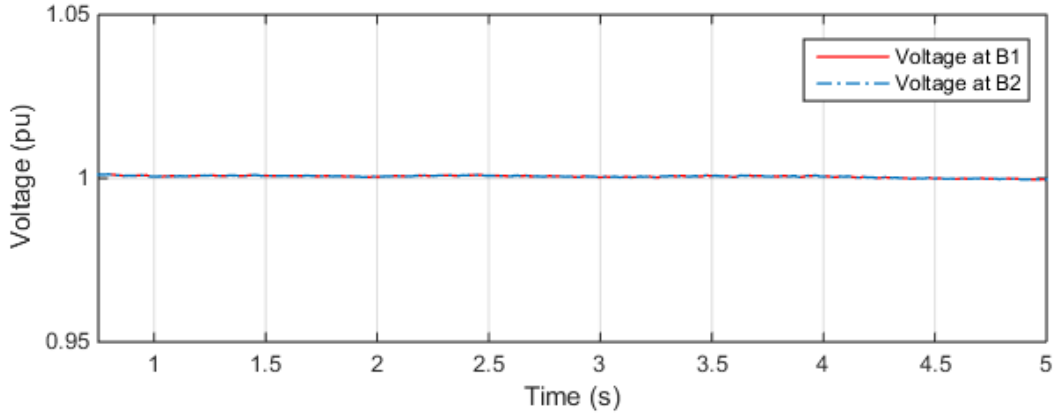

Figure 4-33 AC voltage at busbar B1 and B2

Figure 4-33 shows voltages at buses B1 and B2 are constant although the power and the currents are changing continuously. The phase currents at B1 are shown in Figure 4-35. The changes of active power at both ends cause the perturbations on the DC link voltage. However, the DC link controller at the VSC2 manages to keep the DC voltage at desired 300kV. Then the power flow is from VSC1 to VSC2 the DC link voltage is grater then 300kV; otherwise, the controller keeps it at 300kV shown in Figure 4-34.

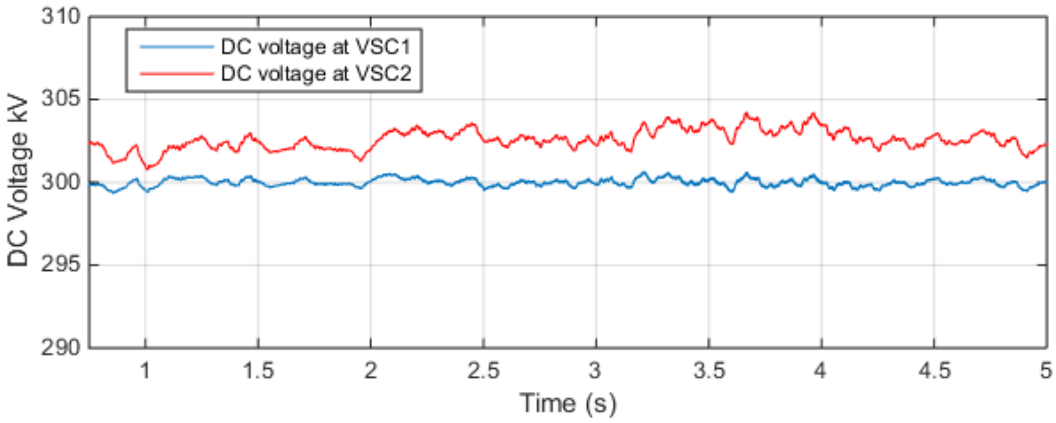

Figure 4-34 DC voltages at VSC 1 and VSC 2

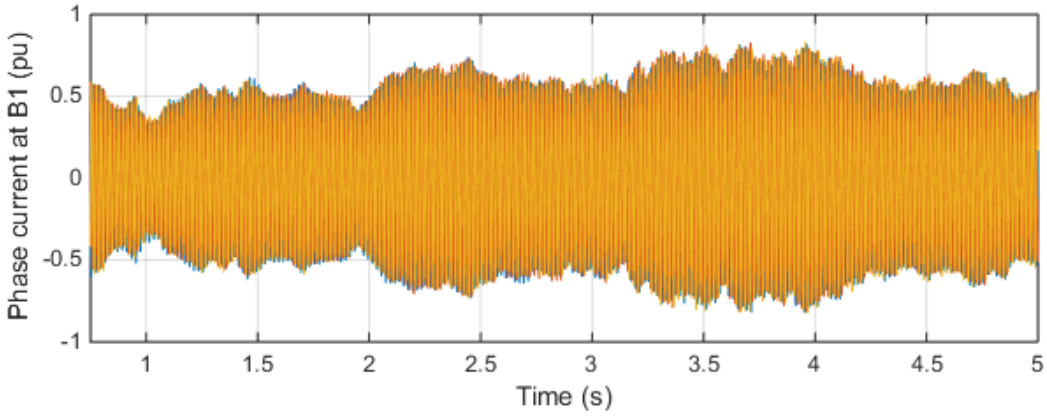

Figure 4-35 Phase current at busbar B1

4.7.7 System behaviour during three-phase AC fault

To demonstrate the transient behaviour of the VSC-HVDC system connected to hybrid windfarm and AC grid, the system is subjected to a three-face fault at t=2s with duration of 5 cycles for 50Hz which is 100ms.The VSC-HVDC improves the FRT capabilities of overall system, during a fault the AC network in the wind farm side of is not severely affected by the onshore AC three-face fault. Figure 4-36 illustrates the AC voltage magnitude during a fault, it can be seen that the voltage collapse at t=2 and get back to pre-fault conditions after the three-phase fault is cleared. The figure also shows that the voltage in the offshore terminal increases. This is due the fact that the HVDC link is no longer able to export the power from the wind turbines, meaning that this power is reflected as an overcharge in the voltage of the DC capacitors. However, once the onshore fault is cleared, the power flow is restored and the voltage level at the wind farm network returns to a 1 PU value.

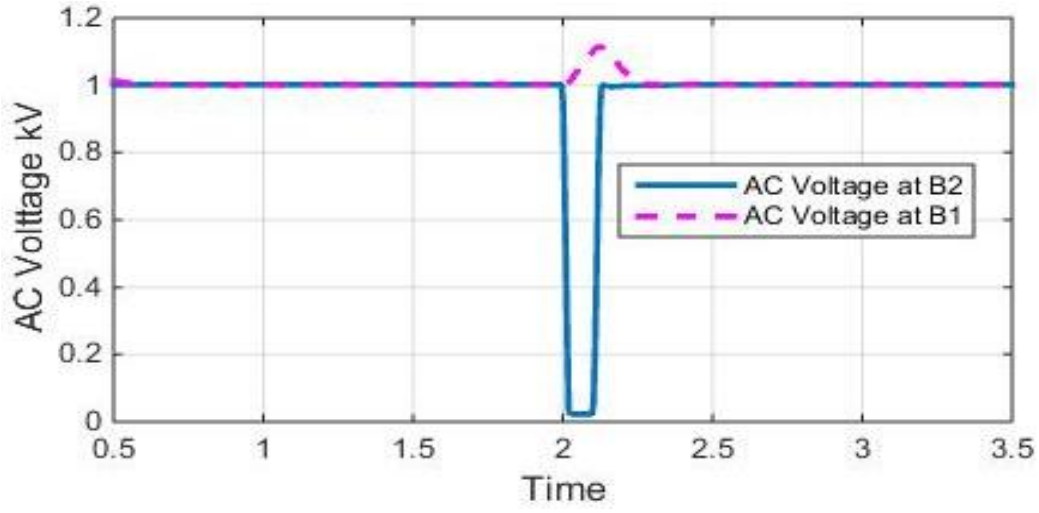

Figure 4-36 AC Voltage at busbar B1 and busbar B2

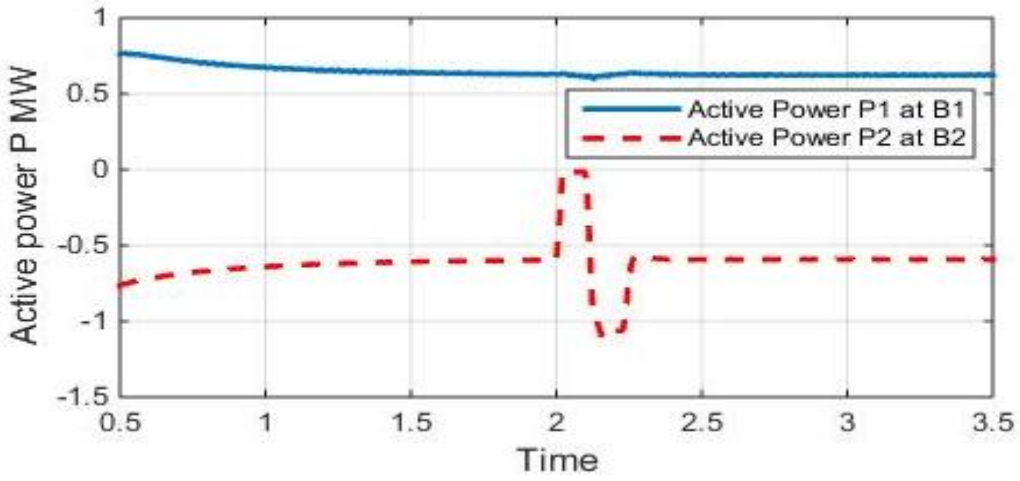

Figure 4-37 Active power at Busbar B1 and B2

Figure 4-37 show that the active power in the onshore decreases to zero during the fault. After the fault is cleared the extra active power stored in the DC link capacitors is released, creating a temporary increase in the active power provision from the converter, as seen in figure 4-37.

Figure 4-38 show the behaviour of the DC voltage of the HVDC link during the fault. As seen in Figuer 4-38. During the fault period, the interruption of the power flow produces an increase of the DC voltage of the link. However once the fault is cleared the excess of energy stored in the DC capacitors is released and the DC voltage returns to its set point value.

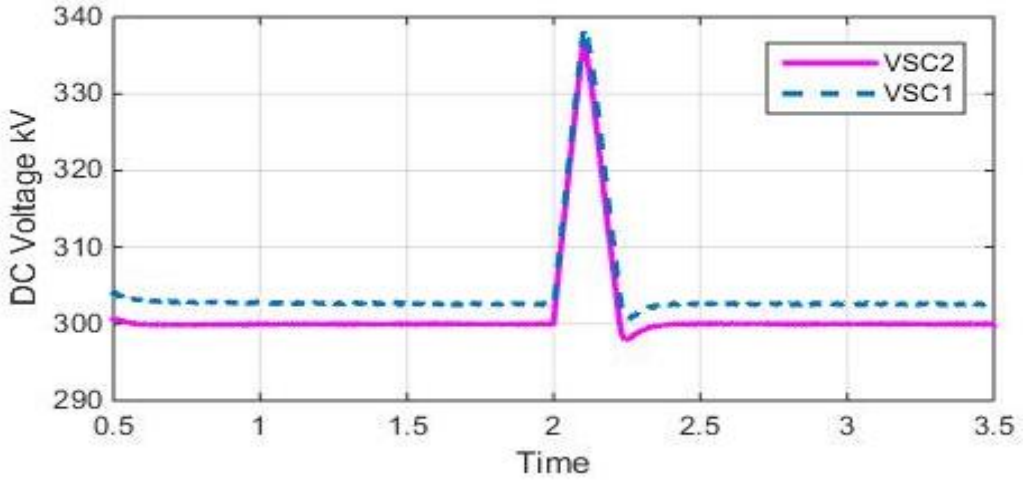

Figure 4-38 DC Voltage at VSC1 and VSC2

4.8 Summary

In this chapter, investigations of the control and operation of VSC-HVDCs have been conducted. The components and functions of the system, have been described and the advantages and disadvantages of the VSC-HVDC system are summarized. The description of HVAC and LCC-HVDC transmission systems is also presented.

The steady-state and dynamic model of the VSC-HVDC system has been studied. Moreover, the full control design of the rectifier and inverter were investigated. Additionally, the tuning method for the PI controllers was shown to ensure robust control of the system. The steady-state and dynamic performance of the VSC-HVDC connected to the offshore DFIG- based wind farm was examined. Studies done in this chapter shows that VSC-HVDC can fulfil the Grid Code requirements, it can provide grid support, can rapidly reverse power flow and retain AC voltage constant.

4.9 References

[1] N. Flourentzou, V. G. Agelidis, and G. D. Demetriades, "VSC-Based HVDC Power Transmission Systems: An Overview," *IEEE Transactions on Power Electronics*, vol. 24, pp. 592-602, 2009.

[2] C. Du, M. H. J. Bollen, E. Agneholm, and A. Sannino, "A New Control Strategy of a VSC–HVDC System for High-Quality Supply of Industrial Plants," *IEEE Transactions on Power Delivery*, vol. 22, pp. 2386-2394, 2007.

[3] C. Bajracharya, "Control of VSC-HVDC for wind power," Electrical Power Engineering, Norwegian University of Science and Technology, 2008.

[4] L. Xu, B. W. Williams, and L. Yao, "Multi-terminal DC transmission systems for connecting large offshore wind farms," in *Power and Energy Society*

General Meeting - Conversion and Delivery of Electrical Energy in the 21st Century, 2008 IEEE, 2008, pp. 1-7.

[5] B. R. Andersen, L. Xu, and K. T. G. Wong, "Topologies for VSC transmission," in *AC-DC Power Transmission, 2001. Seventh International Conference on (Conf. Publ. No. 485)*, 2001, pp. 298-304.

[6] T. A. L. D. Grahame Holmes, *Pulse Width Modulation for Power Converters: Principles and Practice*, 2003.

[7] Y. H. L. Jos Arrillaga, Neville R. Watson, *Flexible Power Transmission - The HVDC Options*, 2007.

[8] G. A. Stefan G Johansson, Erik Jansson, Roberto Rudervall "POWER SYSTEM STABILITY BENEFITS WITH VSC DC-TRANSMISSION SYSTEMS " *CIGRE* 2004.

[9] S. K. Chaudhary, R. Teodorescu, and P. Rodriguez, "Wind Farm Grid Integration Using VSC Based HVDC Transmission - An Overview," in *2008 IEEE Energy 2030 Conference*, 2008, pp. 1-7.

[10] S. Cole and R. Belmans, "Transmission of bulk power," *Industrial Electronics Magazine, IEEE*, vol. 3, pp. 19-24, 2009.

[11] M. Matteini, "Control techniques for matrix converter adjustabe speed drivers," Electrical Engineering, University of Bologna 2001.

[12] A. Nami, L. Jiaqi, F. Dijkhuizen, and G. D. Demetriades, "Modular Multilevel Converters for HVDC Applications: Review on Converter Cells and Functionalities," *Power Electronics, IEEE Transactions on*, vol. 30, pp. 18-36, 2015.

[13] G. Dawei, L. Qingchun, and L. Jishou, "A new scheme for on-load tap-changer of transformers," in *Power System Technology, 2002. Proceedings. PowerCon 2002. International Conference on*, 2002, pp. 1016-1020 vol.2.

[14] C. Du, M. H. J. Bollen, E. Agneholm, and A. Sannino, "A New Control Strategy of a VSC HVDC System for High-Quality Supply of Industrial Plants," *Power Delivery, IEEE Transactions on*, vol. 22, pp. 2386-2394, 2007.

[15] L. Weimers, "New markets need new technology," in *Power System Technology, 2000. Proceedings. PowerCon 2000. International Conference on*, 2000, pp. 873-877 vol.2.

[16] G. P. Adam, O. Anaya-Lara, and G. Burt, "Multi-terminal DC transmission system based on modular multilevel converter," in *Universities Power Engineering Conference (UPEC), 2009 Proceedings of the 44th International*, 2009, pp. 1-5.

[17] O. Anaya-Lara, G. Kalcon, G. Adam, K. Nieradzinska, G. Tande John Olav, K. Uhlen, *et al.*, "North Sea Offshore Networks Basic Connection Schemes Dynamics Performance Assessment," presented at the EPE Joint Wind Energy and T&D Chapters Seminar, 2011.

[18] Z. Xiaodong and L. Kang, "Control of VSC-HVDC for wind farm integration based on adaptive backstepping method," in *Intelligent Energy Systems (IWIES), 2013 IEEE International Workshop on*, 2013, pp. 64-69.

[19] D. Woodford, "Voltage-Sourced Converters in Power Systems [Book Reviews]," *Power and Energy Magazine, IEEE*, vol. 10, pp. 86-89, 2012.

[20] L. P. S. Chinnaraj Kamalakannan, Subhransu Sekhar Dash, Bijaya Ketan Panigrahi, *Power Electronics and Renewable Energy Systems: Proceedings of ICPERES 2014*, 2014.

[21] R. I. Amirnaser Yazdani, *Voltage-Sourced Converters in Power Systems. Modeling, Control and Applications*: Wiley & Sons, Inc., 2010.

[22] K. Nieradzinska, J. C. Nambo, G. P. Adam, G. Kalcon, R. Peña-Gallardo, O. Anaya-Lara, *et al.*, "North Sea Offshore Modelling Schemes with VSC-HVDC Technology: Control and Dynamic Performance Assessment," *Energy Procedia*, vol. 35, pp. 91-101, // 2013.

[23] MathWorks. (2016). *simulink*.

[24] G. F. Reed, H. A. A. Hassan, M. J. Korytowski, P. T. Lewis, and B. M. Grainger, "Comparison of HVAC and HVDC solutions for offshore wind farms with a procedure for system economic evaluation," in *Energytech, 2013 IEEE*, 2013, pp. 1-7.

[25] G. S. P. Mathew Sathyajith, *Advances in Wind Energy Conversion Technology*, 2011.

[26] J. Machado, M. Ventim Neves, and P. J. Santos, "Economic limitations of the HVAC transmission system when applied to offshore wind farms," in *Compatibility and Power Electronics (CPE), 2015 9th International Conference on*, 2015, pp. 69-75.

[27] M. Barnes and A. Beddard, "Voltage Source Converter HVDC Links – The State of the Art and Issues Going Forward," *Energy Procedia*, vol. 24, pp. 108-122, 2012/01/01 2012.

[28] G. P. Adam, K. H. Ahmed, S. J. Finney, K. Bell, and B. W. Williams, "New Breed of Network Fault-Tolerant Voltage-Source-Converter HVDC Transmission System," *IEEE Transactions on Power Systems*, vol. 28, pp. 335-346, 2013.

[29] L. Zhang, H. P. Nee, and L. Harnefors, "Analysis of Stability Limitations of a VSC-HVDC Link Using Power-Synchronization Control," *IEEE Transactions on Power Systems*, vol. 26, pp. 1326-1337, 2011.

[30] A. Korompili, Q. Wu, and H. Zhao, "Review of VSC HVDC connection for offshore wind power integration," *Renewable and Sustainable Energy Reviews*, vol. 59, pp. 1405-1414, 6// 2016.

Chapter 5:

Enhanced control to support power system operation in multi-terminal VSC-HVDC

The current approach to connecting the large offshore wind farms dispersed over wide areas is to use multi-terminal VSC-HVDC networks rather than point-to-point HVDC transmission systems. The aim behind the multi-terminal VSC-HVDC approach is to improve the security of supply and minimise the loss of generation during scheduled maintenance or unexpected disturbances in any part of the power network.

This chapter provides an overview of the operation of a multi-terminal HVDC network, connecting offshore wind farms to different mainland AC grids. The control system for 3 different network arrangements are designed to facilitate the study of steady-state power exchange, optimal power dispatch using droop control, transient stability and provision of ancillaries.

5.1 Introduction

HVDC transmission systems can be connected to the onshore grid via point-to-point or multi-terminal networks. Almost all existing HVDC connections are configured as point-to-point, however the VSC-HVDC multi-terminal can provide greater flexibility of supplied

power [1]. Furthermore, the European Wind Energy Association (EWEA) suggests that installed offshore capacity could reach 23.5GW by 2020, and that there is a growing desire for interconnection of European grids[2, 3] .

As many proposed projects will be located offshore, transmission grids are likely to be predominantly HVDC. The traditional LCC-HVDC transmission system in point-to-point and multi-terminal connection requires converter polarity changes to reverse power flow, as well as application of a different control mode [4]. As previously mentioned in Chapter 2, the control is complex and there are only two existing multi-terminal CSC-HVDC systems in operation:

- The HVDC Italy-Corsica-Sardinia connection. It transfers power between Italian mainland, Corsica and Sardinia. It was first built as a point-to-point connection of 200MW at 200kV and has been commissioned in 1968, expanded of third terminal in 1986 [5].
- Radisson - Nicolet - Des Cantons circuit. Phase 1 of this multi-terminal connection project operated as bipolar point to point connection between Des Cantons and Comerford in 1986. In the 1990, phase 2 of the project extended the third terminal to deliver 1800MW of power to Sandy Pond [6].

VSC-HVDC is the most suitable technology for multi-terminal configuration as it reverses DC current without the need to change the polarity of the voltage link [7]. The control of active power flow in the multi-terminal connection is achieved by the converters responsible for controlling active power and DC drop control in the converter, where DC voltage is controlled [8-10]. These control schemes may be different when the converter controlling the power is connected to the offshore wind farm where the main purpose is to obtain the maximum power generated by the wind turbines. In this instance, the converter controller should operate in such a way that avoids power imbalance between the AC and DC networks.

5.2 Multi-terminal configuration for offshore wind power in the North Sea.

The development of VSC-HVDC has opened a new way of looking at power distribution and sharing. The potential of multi-terminal HVDC technology has been envisioned as a key technology for harvesting energy from the vast growing offshore wind energy fair in the Dogger Bank. It is also an ideal solution for power trading power between countries without interfering in their Grid Code regulation.

5.2.1 Radial connection to the shore

There are different configurations for multi terminal systems described generally in Chapter 2 sections 2.4. Figure 5-1 – Figure 5-4 illustrate a proposed DC grid configuration for GB to harvest offshore wind power and exchange power with neighbouring countries like Norway. This can be an ideal solution for The North Sea Network Link (NSN) interconnection between the UK and Norway, shown as a Norway Hub in Figure 5-1. The radial connection is the simplest solution to connect a wind farm to the onshore grid. The remaining connections share the same infrastructure as the radial arrangement used to transmit power from the offshore wind farms to the onshore grid. In the following subsections, a range of potential connection scenarios with crucial protection strategies and power redundant paths are shown for Dogger Bank in the North Sea.

Various DC grid scenarios are formulated around five 1100MW offshore wind farms development in Dogger Bank, where all of the networks are assumed to be in a symmetrical monopole configuration with two cables operating at opposite polarity. The scenarios are based on GB round 3 [11] offshore developments with an additional connection of the 'Norway Hub' which interconnects UK and Norway.

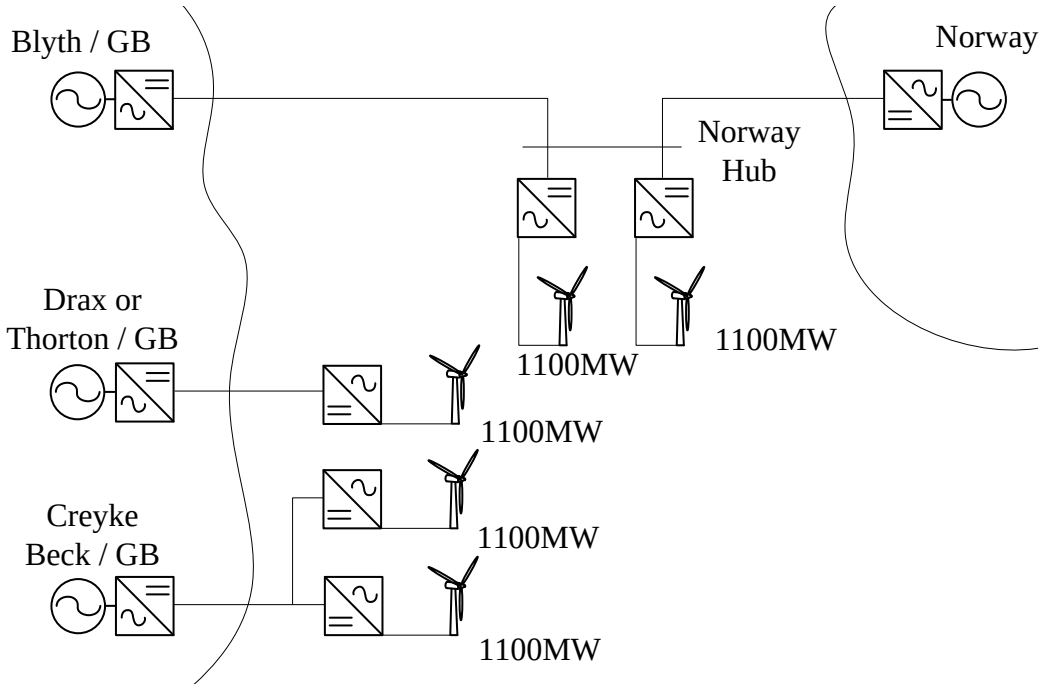

Figure 5-1 Grid configuration scenario

5.2.2 Multi-terminal connection with DC redundant paths

Figure 5-2 shows a DC multi-terminal network with redundancy paths on the DC site. This option has the minimum number of Direct Current Circuit Breakers (DCCBs), which are only located at the main transmission path from the wind farm to the onshore grid. It is

reliable solution as it has several routes to redirect power during fault or maintenance, however it also comes with extra costs due to number of additional DC cables [12].

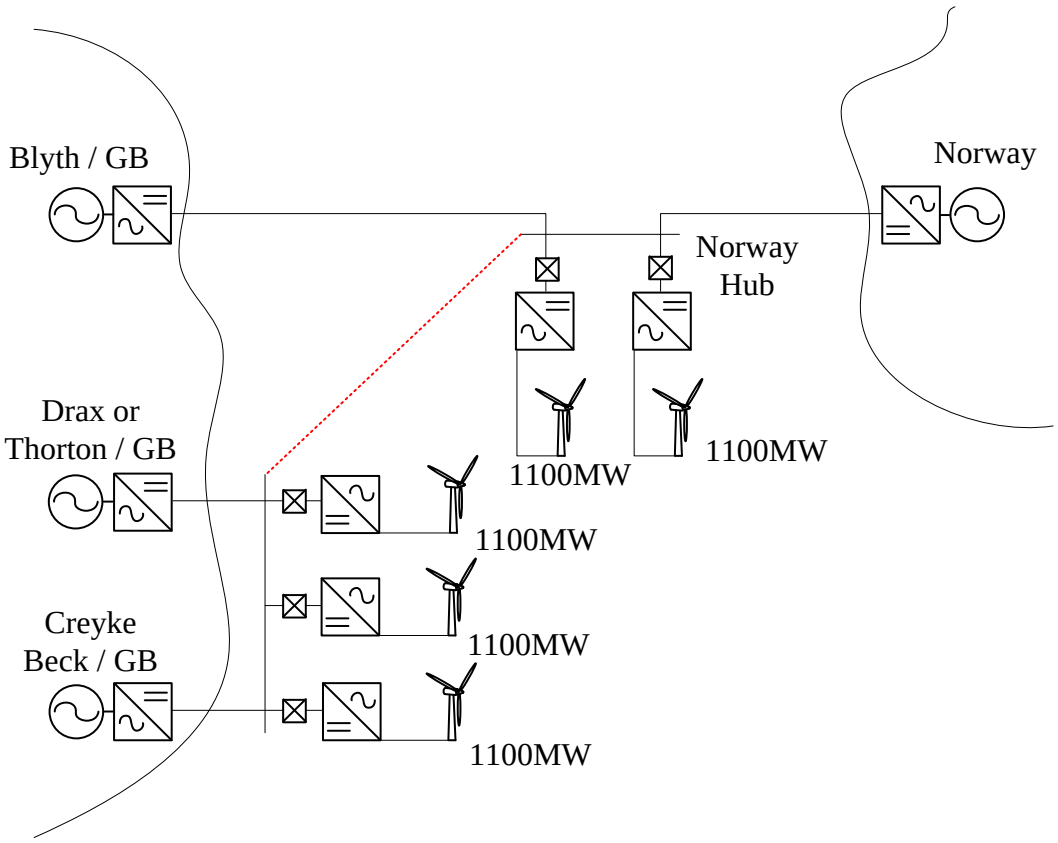

Figure 5-2 Multi-terminal connection with DC redundant paths (seen as red line)

5.2.3 Multi-terminal with redundant path on the AC side

Figure 5-3 shows a multi-terminal configuration that provides redundant transmission paths on the AC side of the wind farm. This option considers DC grid protection on the AC side, where the link between two stations is disconnected under abnormal operating condition, then connected when one of the offshore stations is not in operation. This solution provides the most reliable protection as it also can function when any of the converter stations is out of operation. The three main limitations of this arrangement are: the limit in oversizing the system, the AC auxiliary cables due to reactive charging currents and the need for compensation have limited distances [13, 14].

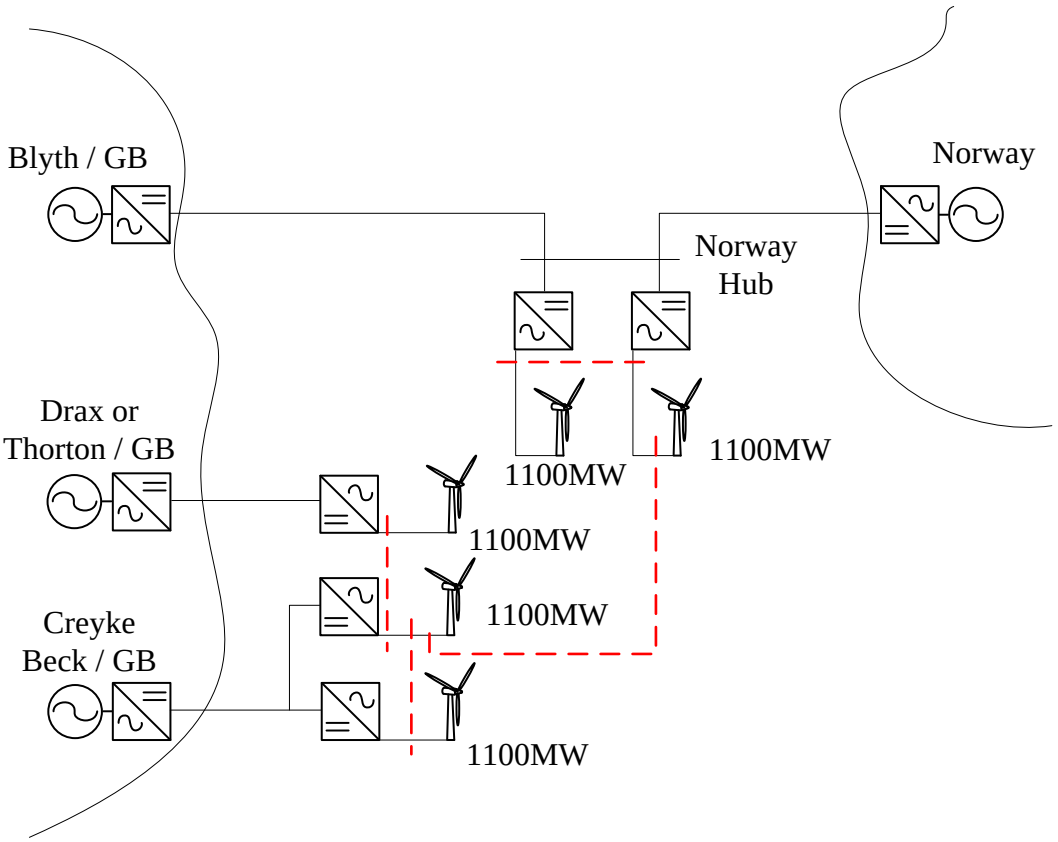

Figure 5-3 Redundant path on the AC site (seen as red line)

5.2.4 Multi-terminal with DC circuit breakers

The Multi-terminal configuration with the highest number of DCCBs is shown in Figure 5-4. In this configuration, the grid can be divided into zones, and transmit power with any route. This option is the most reliable, however also the least cost effective due to the number of DCCBs. Research demonstrated in [15] discusses potential development of DCCBs with appropriate power levels within the coming years. There is still uncertainty over how much DCCB will cost, however the estimated price is expected to be up to 30% of the VSC station cost. Hence it would be the most expensive solution to implement across the whole system [16].

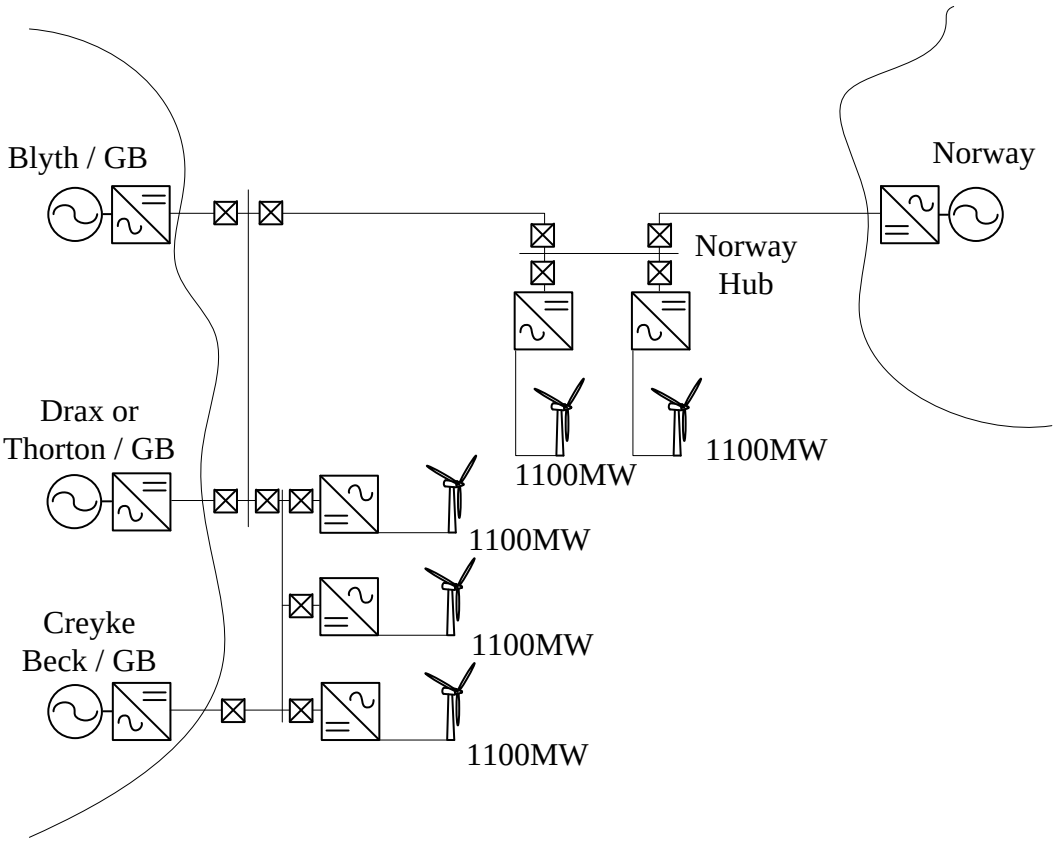

Figure 5-4 Multi-terminal with DC circuit breakers

5.3 Power management in multi-terminal HVDC system

In a multi-terminal VSC-HVDC connection, the power management system plays a key role in maintaining power balance in the network, and has the ability to exchange power between the grids. To dispatch power in the multi-terminal system, several techniques can be applied at the receiving end converter working as an inverter from the sending end converter working as a rectifier [7]. There are three main power management schemes [17]:

- Equal power distribution. The inverter converters will share power equally and, only during a loss of one of the converters, power will be send through auxiliary cables. In the case of equal power sharing, the DC voltage is kept constant.
- Proportional power distribution. The inverter does not share power equally under this scheme, and appropriate control techniques such as constant voltage control, voltage margin control and voltage droop control enable the power share as required. The voltages in the DC cables at the terminals of the converters are not equal.
- Priority power distribution. In this scheme, one of the inverter converters has priority over the others. In this case the required power is sent to the prioritised converter, while excess power is send to other receiving-end converters. The appropriate control techniques are also required to supply obligatory power [10].

5.4 Multi-terminal HVDC system with droop control

As discussed in previous sections, there are many different configurations for multi-terminal HVDC systems. To demonstrate the viability of using a multi-technology network to accommodate large amounts of power from offshore wind farms, the five-terminal VSC-HVDC has been designed and investigated based on examples from Figure 5-1-Figure 5-4. The system configuration is as shown in Figure 5-5.

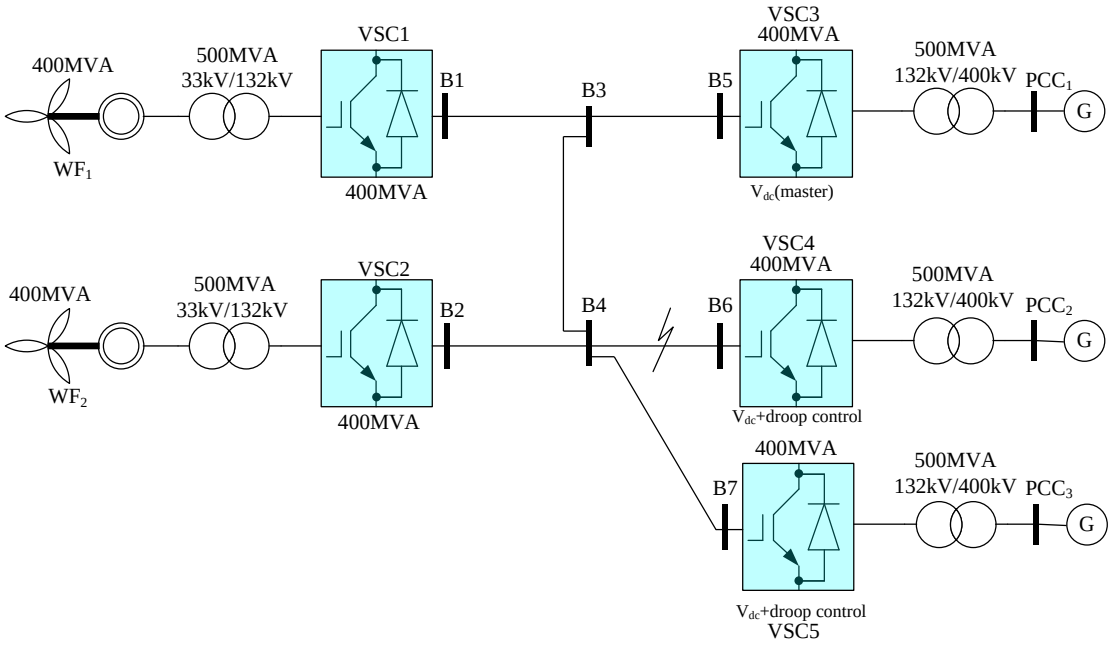

Figure 5-5 Five-terminal VSC-HVDC system schematic

The five wind farms have been clustered into two aggregated models in the Dogger Bank offshore development site. For the purpose of this simulation, each cluster is a 400 MW wind farm and connected to three different onshore grids, e.g. Blyth - GB, Drax – GB and Norway.

The DC voltage droop control has been implemented to facilitate the power dispatch (sharing) from the wind farms to the onshore networks, also investigated in [18, 19]. The droop control presented exploits the current split concept to enable power dispatch at the onshore grid-side converters according to arbitrary current ratios $N_1:N_2:N_3:\ldots N_n=I_1:I_2:I_3\ldots I_n$, where n is the number of onshore grid-side converter terminals; N_1 to N_n are the ratios at which the total power transmitted from the offshore wind farm is shared between the onshore grid-side terminals; and I_1 to I_n are the DC currents corresponding to each converter terminal, as shown in Figure 5-6.

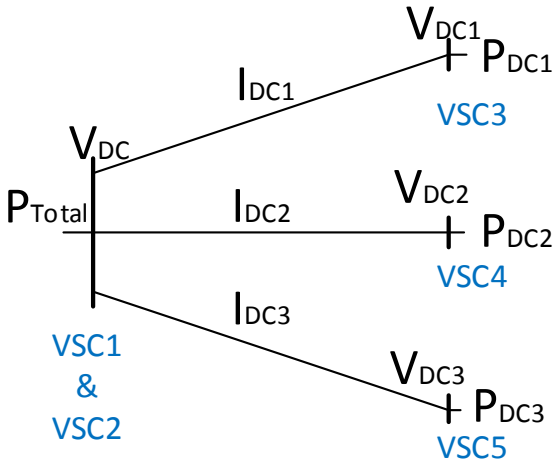

Figure 5-6 Simplified concept of droop control principles

In Figure 5-5, VSC3, VSC4 and VSC5 are controlling DC and AC voltages. VSC4 and VSC5 are additionally equipped with droop control in order to facilitate the power sharing between onshore grid-side converters. The proposed DC voltage droop controls the amount of power according to the needs of the onshore AC grids. When the DC droop control is activated and the voltages in the DC link of VSC 4 and VSC5 are increased above the set point, current will flow towardsVSC3, which results in increased power flow to that converter. If the process is reversed and the DC link voltage decreases at the VSC4 and VSC5 converters, the current flow will increase in these two converters. The active power DC droop characteristic is illustrated in Figure 5-8.

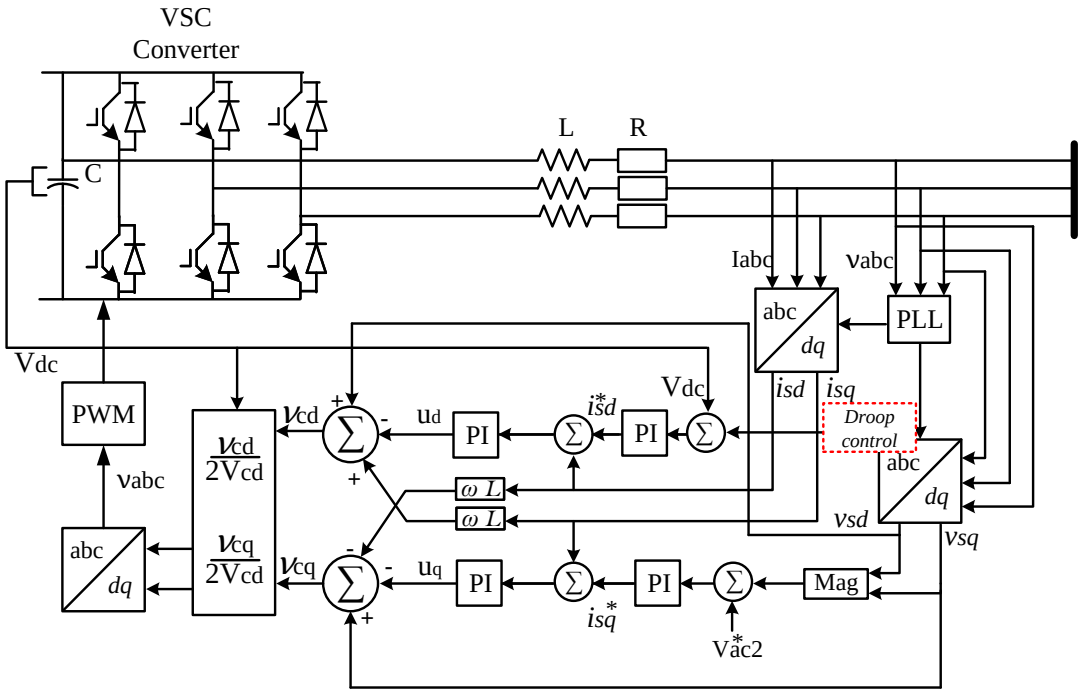

Figure 5-7 Proposed droop control applied in VSC4 and VSC5 converters

Figure 5-7 shows that the proposed droop control that provides a reference voltage to the DC voltage controller *'i'* taking into account the voltage at the support node, *'j'*, and is delivered as following:

$$V_{DC} - V_{DC1} = I_{DC1}\mathrm{R} \Rightarrow P_{DC1} = V_{DC1}\frac{(V_{DC} - V_{DC1})}{R} \tag{5.1}$$

$$V_{DC} - V_{DC2} = I_{DC2}\mathrm{R} \Rightarrow P_{DC2} = V_{DC2}\frac{(V_{DC} - V_{DC2})}{R} \tag{5.2}$$

$$V_{DC} - V_{DC3} = I_{DC3}\mathrm{R} \Rightarrow P_{DC3} = V_{DC3}\frac{(V_{DC} - V_{DC3})}{R} \tag{5.3}$$

Where P_{DCj} is the power active power of the *j* converter. After rearranging Eq. 1.1-1.3 the droop control is defined as:

$$V_{DCi} = \frac{1}{2}V_{DCj} + \frac{1}{2}\sqrt{V_{DCj}^2 - 4R_{ji}P_i} \tag{5.4}$$

Where *P* is active power between converters, *Rji* is the resistance between the DC nodes *j* and *i*, *i=1* to *N-1*, where *N* is the number of onshore grid-side converters), *j=1* to *M* (*M* is the number of intermediate nodes).

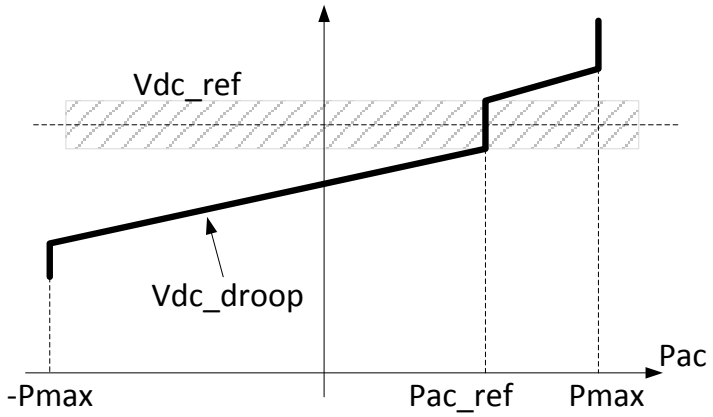

Figure 5-8 Active power DC voltage droop characteristic

The system was tested in steady-state operating conditions, and also shows the power management and performance when one of the converters is disconnected due to a fault or maintenance. This simulates either a fault in the converter or DC cable connected between buses B4-B6. Introducing the DC voltage droop characteristic into the control system of VSC4 and VSC5 will allow control of the power share between the VSC3-VSC5 converters.

Figure 5-9 (a) shows power sharing between the onshore grid-side converters, where the DC voltage droop control has been introduced. Figure 5-9 (b) shows the DC voltage in the DC network. As shown in Figure 5-9 (a) the power is dispatched to all of the converter stations equally from time t=0 to time t=1.5s. At time t=1.5s the droop control has been activated in VSC4 and VSC5, it and injects 180MW of additional power to the VSC3 slack/master converter where there is no droop control. VSC4 provides 75MW of power and VSC5 provides 105MW of power to VSC5, it is achieved by increasing the DC voltage at this station. The DC voltage is kept constant at all times by the converter VSC3.

At t=3s, the power command has been changed and required the additional power to be injected into VSC4 and VSC5. At t=4.5s, the droop control has been deactivated and each converter shares power equally around 255MW. At t=6s, the droop control is activated to increase the power flow in the VSC4 and VSC5 by decreasing the DC voltage, as shown in Figure 5-9 (b). This also results in a decreased power flow in VSC3 (master converter). At t=7.5s the droop control results in an increasing power flow inVSC4 and VSC5. The power injected into the system by VSC1 and VSC2 remains constant at 400MW each during the simulation period.

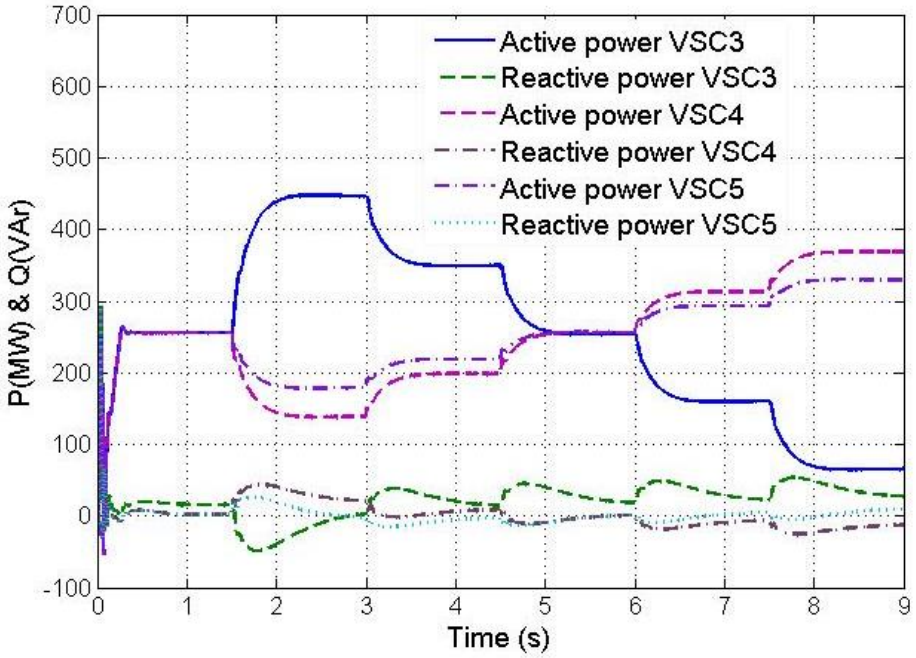

(a) Active and reactive power at buses B5-B7

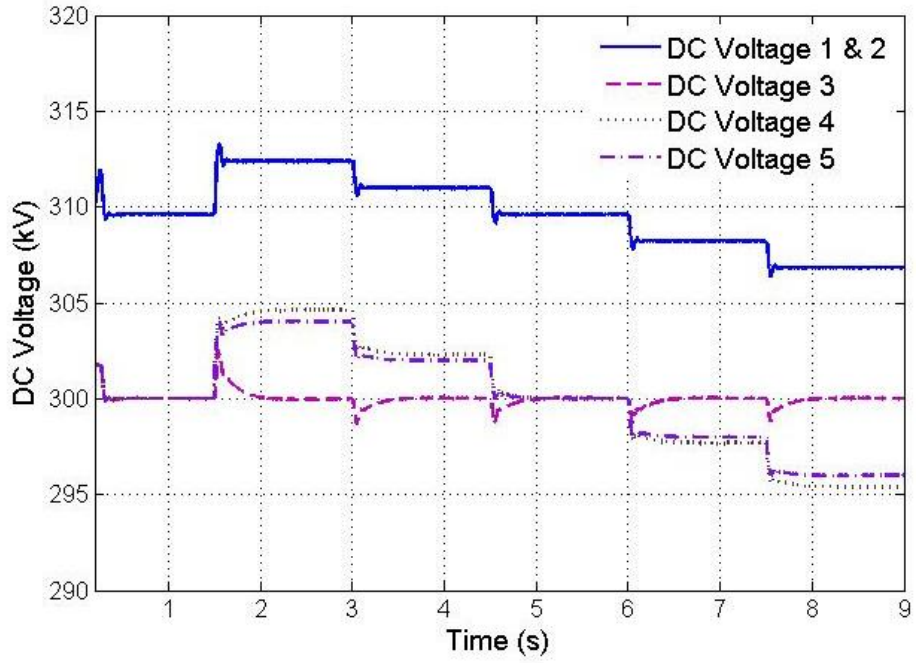

(b) DC voltage at the converters

Figure 5-9 Simulations for power management in multi-terminal HVDC with use of droop control

5.4.1 Multi-terminal connection during loss of converter – DC fault

Figure 5-10 shows the behaviour of the multi-terminal VSC-HVDC when one of the converters is lost due to a fault or maintenance work. Figure 5-10(a) shows the DC voltage in converters VSC1-VSC5. Figure 5-10(b) shows the active power during a sudden loss of VSC4 in VSC3-VSC5. At time t=0s to t=1.5s the power is shared equally in each of the

converter stations. The DC link cable between B4 and B6 is suddenly disconnected at t=3s and remains out of order for the rest of the simulation to mimic a fault in the DC cable.

At t= 1.5s the power is shared in the ratio of 2:1:1. As mentioned previously, at t=3s, the VSC4 converter is disconnected. It can be observed that, with the use of the droop control, the power from the lost converter can be easily controlled and delivered in the required proportions to the healthy converters. It is very important to ensure that the rating of the DC cables is sufficient to transfer additional power during a failure of one of the converters or DC links. This also increases the initial investment costs.

The power from the lost converter is split equally to the VSC3 and VSC5. At t=4.5s, power from both wind farms VSC1 and VSC2 is shared in a ratio of 1:1, which means that power from the VSC4 converter is transferred to the VSC5 converter. At t= 6s, the power from the lost converter goes to the master converter. See Table 5-1for details of these simulation events.

Table 5-1 Event sequence when converter VSC4 is lost

Time	Action	VSC3	VSC4	VSC5
0.0-1.5	Share power equally	33.3%	33.3%	33.3%
1.5-3.0	Droop control employed	50%	25%	25%
3.0-4.5	Droop control employed loss of VSC4	62.5%	0	37.5%
4.5-6.0	Droop control employed loss of VSC4	50%	0	50%
6.0-7.5	Droop control employed loss of VSC4	75%	0	25%

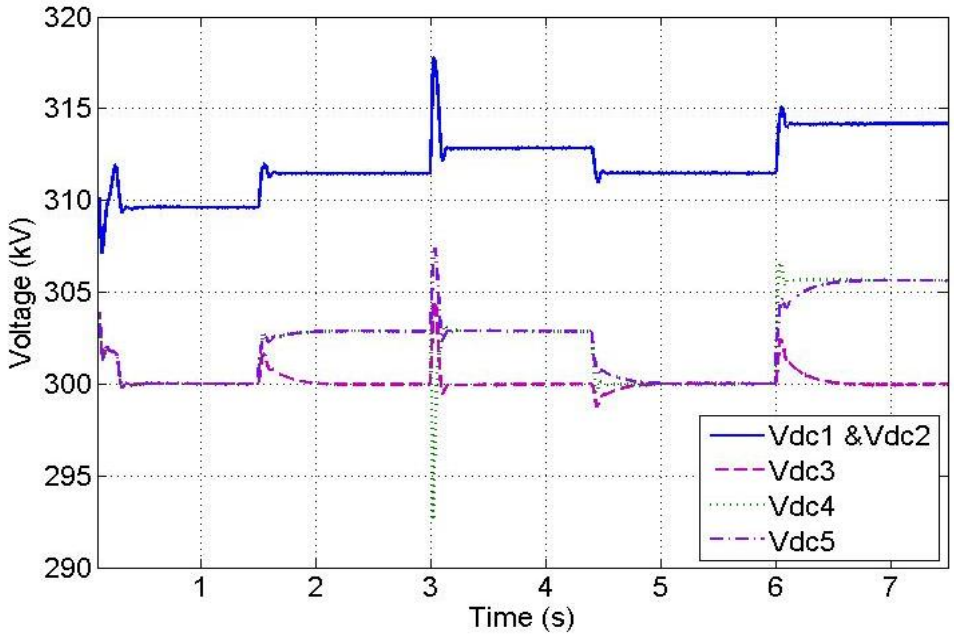

(a) DC voltage at the converters after loss of VSC4

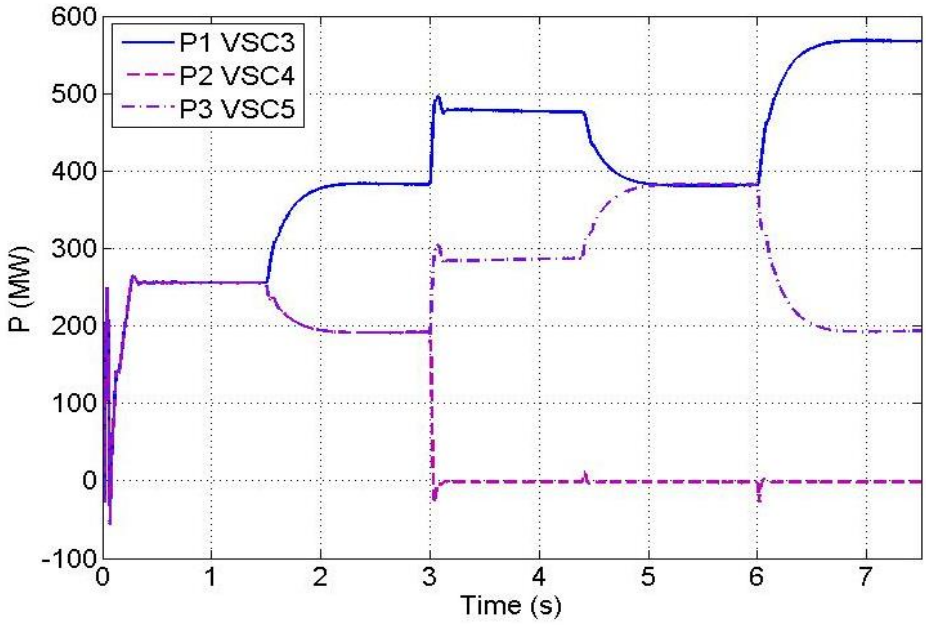

(b) Active power at busses B5-B7 after loss of VSC4

Figure 5-10 Simulations for power management in multi-terminal HVDC during loss of VSC4

5.5 Power exchange in a multi-terminal VSC-HVDC

A four multi–terminal VSC-HVDC is shown in Figure 5-11. This connection uses neutral point clamped converters with two DC link capacitors, each rated at 300mF, and it is controlled by using PWM at a frequency of 2kHz. The 400MW wind farm is connected to the DC network via VSC1. All converters in the network control active power between system terminals, excluding VSC3 which maintains DC voltage at 300kV[20]. In this case, VSC3 is a slack-bus, which supports power balancing and is used to export or import power, as shown in Figure 5-11. The converter which acts as a slack bus and is balancing power in the network should have high reserve of storage and high-power generation capabilities.

To show the steady-state power flow during changing loads, the multi-terminal model has been designed and simulated in Matlab/Simulink. During any change in power schedule, VSC3 will adapt to the new situation and will import or export power. The power delivered to, or drawn from, the slack bus converter, to keep the network balanced is calculated as follows:

$$P_{VSC3/\,slack} = P_{VSC1} + P_{VSC2} + P_{VSC4} + P_{Losses} \tag{5.5}$$

Where P_{VSCx} is the active power of the x converter and P_{Losses} are the overall losses of the converters and HVDC cables of the network.

The local controllers at each station are responsible for controlling DC and AC voltages, as well as active and reactive power [10, 21].

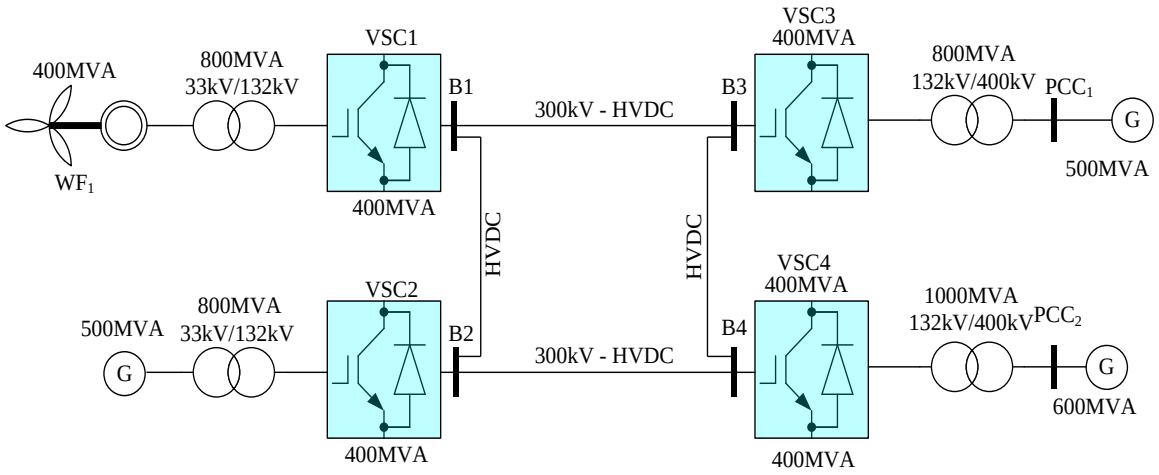

Figure 5-11 Multi-terminal VSC-HVDC for power exchange analysis

To demonstrate the practicality of using a VSC-HVDC for power exchange between AC grids, and to accommodate large amounts of wind power, the network is adapted to include one offshore wind farm and three onshore AC networks.

Initially, wind farm converter VSC1 and AC network converter VSC2 are injecting 300MW and 200MW in to the network at t=1s to t=2s, respectively, as shown in the Figure 12 (a). During that time, converters VSC3 and VSC4 are importing 300MW and 200MW from the network, as shown in Figure 12 (b). At t=2s, the power output of the wind farm is increased to 400MW and converter VSC2 is reducing power injection to 200MW, where converters VSC3 and VSC4 are drawing 200MW and 300MW each. At t=4.5s the power injected from the wind farm is reduced to 200MW and VSC2 is importing 100MW of power from the grid. At the same time, VSC4 is importing 200MW of power from the grid, and the VSC3 converter which works as a slack converter is providing the required 100MW of power to the grid. At t=6s, VSC4 requested an additional 100MW of power, and again this is fulfilled by the VSC3 converter.

Table 5-2 shows the results obtained from this simulation event of power sharing between converters.

Table 5-2 Power shearing between converters

Time (sec)	0.0-2.0	2.0-4.5	4.5-6.0	6.0-8.0
VSC1 (WF)	+300 MW	+400 MW	+200 MW	+200 MW
VSC2	+200 MW	+100 MW	-100 MW	-100 MW

VSC3	-300 MW	-200 MW	+100 MW	+200 MW
VSC4	-200 MW	-300 MW	-200 MW	-300 MW

Figure 5-12 (c) shows the variation of DC voltage during changes in the power exchange between regional AC networks. The VSC3 converter is a slack bus and it is also responsible for maintaining the DC voltage at 300kV during power exchange in the multi-terminal network.

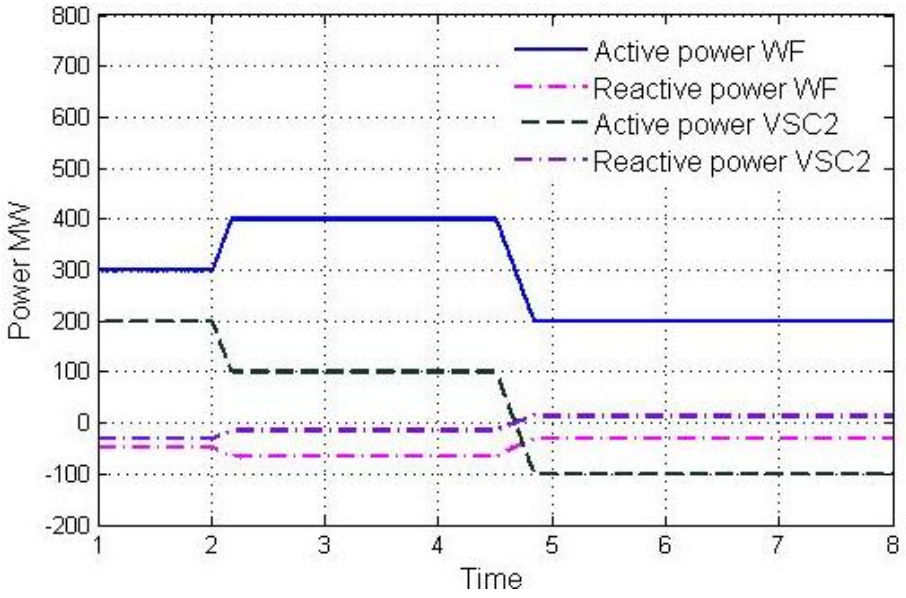

(a) Active and reactive power at WT and VSC2

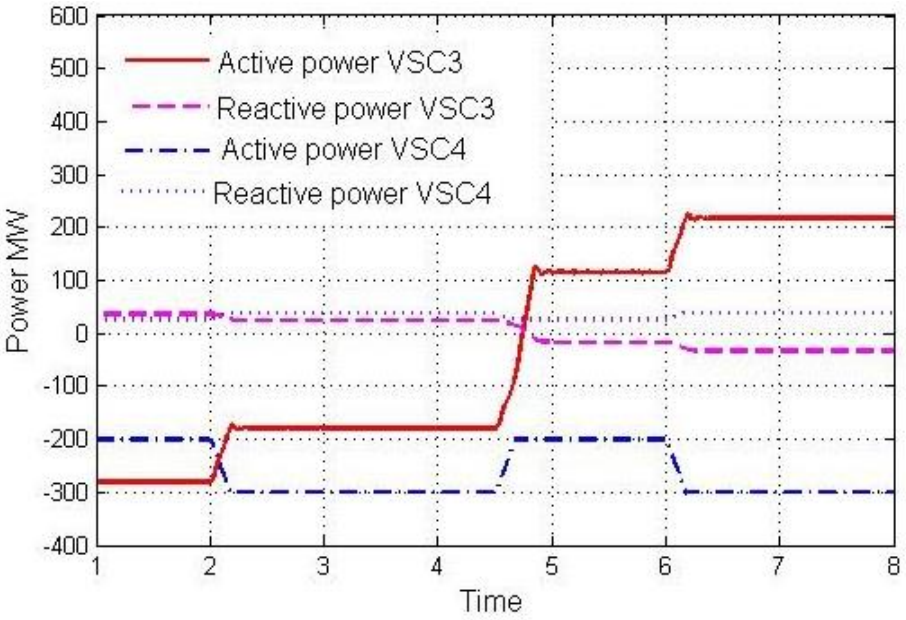

(b) Active and reactive power at VSC3 and VSC4

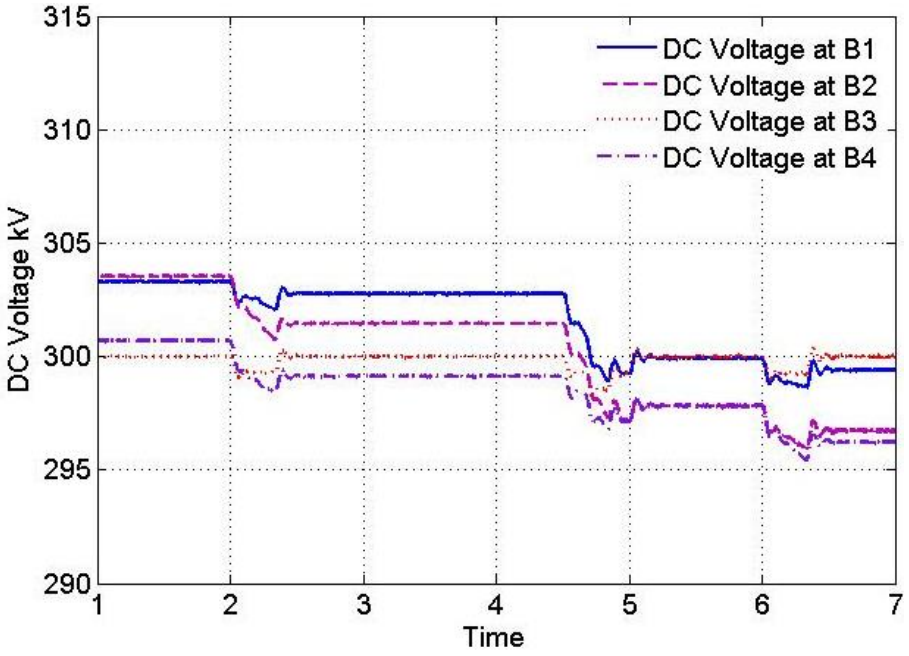

(c) DC link voltage.

Figure 5-12 Simulation results from multi-terminal power exchange network.

5.6 Multi-terminal connection during loss of converter – AC fault

The multi-terminal VSC-HVDC network connecting two wind farms to two onshore grids is shown in Figure 5-13. This section investigates system behaviour in the event of an AC fault, and also during a sudden loss of the converter/DC link cable. The four-terminal VSC-HVDC comprises two offshore wind farms (WF1 & WF2) connected to two onshore AC networks with an auxiliary DC cable connected offshore, near to the wind farms' converters. WF1 and WF2 inject 1200 MW into the DC network, while AC network 1 and AC network 2 withdraw 1200 MW each.

Wind farm converters are responsible for maintaining AC voltage and ensuring that all power produced by wind farms is transmitted to the DC grid. The system is 300kV bipolar connection, the converters VSC3 and VSC4 regulate DC voltages (±150kV pole-to-pole) and AC voltages. The power generation is controlled at wind turbine level and described in more detail in Chapter 4.

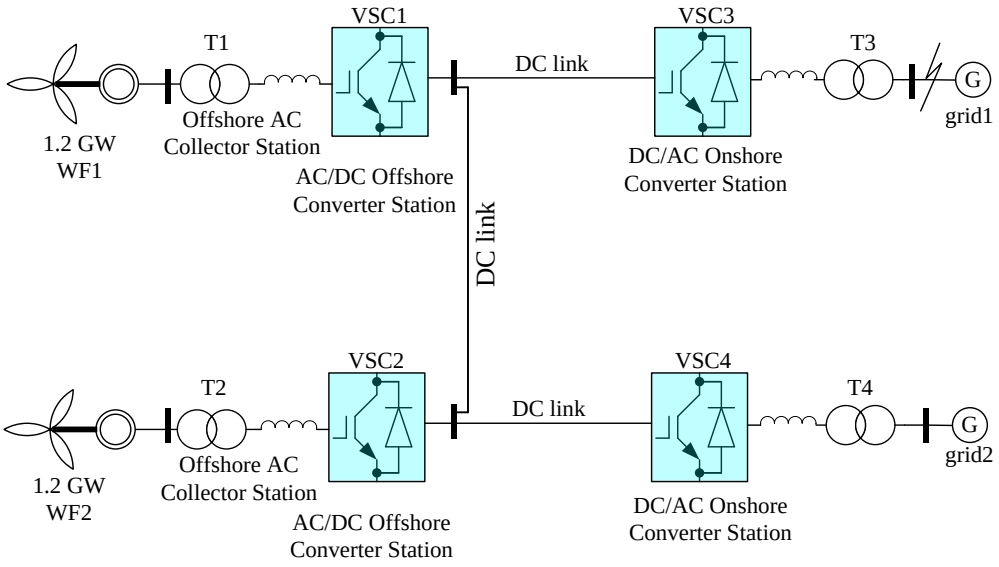

Figure 5-13 Simplified four-terminal VSC-HVDC transmission system.

AC Grid 1 has been subjected to a three-phase fault at t=1s, with a duration of 100ms to highlight the transient behaviour of the multi-terminal VSC-HVDC network during major system disturbances. In order to transfer the whole generated power during AC fault in the AC grid, the power rating of onshore converters VSC3 and VSC4 is twice the rating of offshore converters VSC1 and VSC2. This increases system reliability, but comes with extra cost. Figure 5-14(a) shows the AC voltage during fault - the voltage at the onshore converter at Grid 1 reduces to 0. The AC voltage at Grid 2 is less sensitive than the AC fault in Grid 1. This improves the AC fault ride-through capabilities by enabling decoupled operation, and the wind farm is isolated from the grids. Also noticeable is that the loss of AC Grid 1 has no significant effect on the transient stability of the whole system as the converters allow decoupled operation.

Active power mismatch during a fault, as shown in Figure 5-14(b), is handled by the slack-bus AC Grid 2. The regional network should have enough reserve capacity to take additional power into account for any mismatches in the DC network, as shown in the figures below. Figure 5-4 (b) shows active power being transferred to the AC Grid 2 where there is no fault, via the auxiliary DC cable.

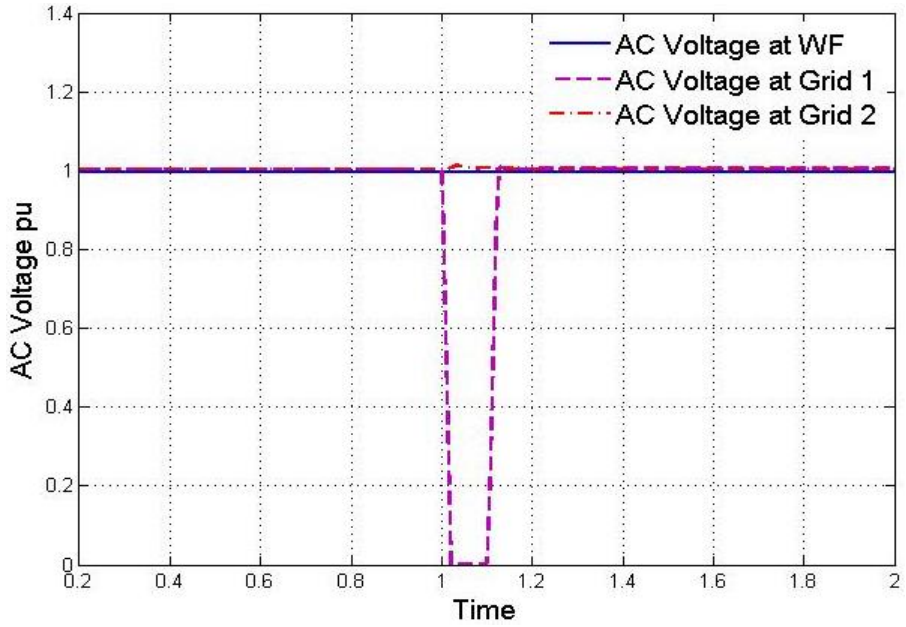

(a) AC voltages at wind farms side and Grid1,Grid2 sites

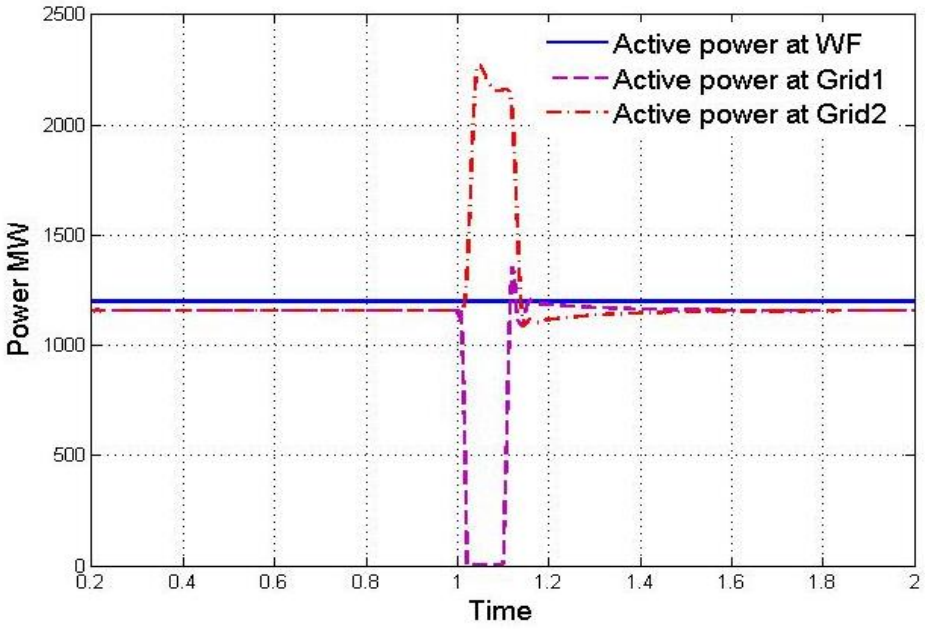

(b) AC voltages at wind farms side and Grid1,Grid2 sites

Figure 5-14(c) illustrates that the DC voltage at the converter VSC3 and auxiliary cable is increasing the most. However, the converter and DC cables are not going to be damaged, as the voltage is still at a safe level.

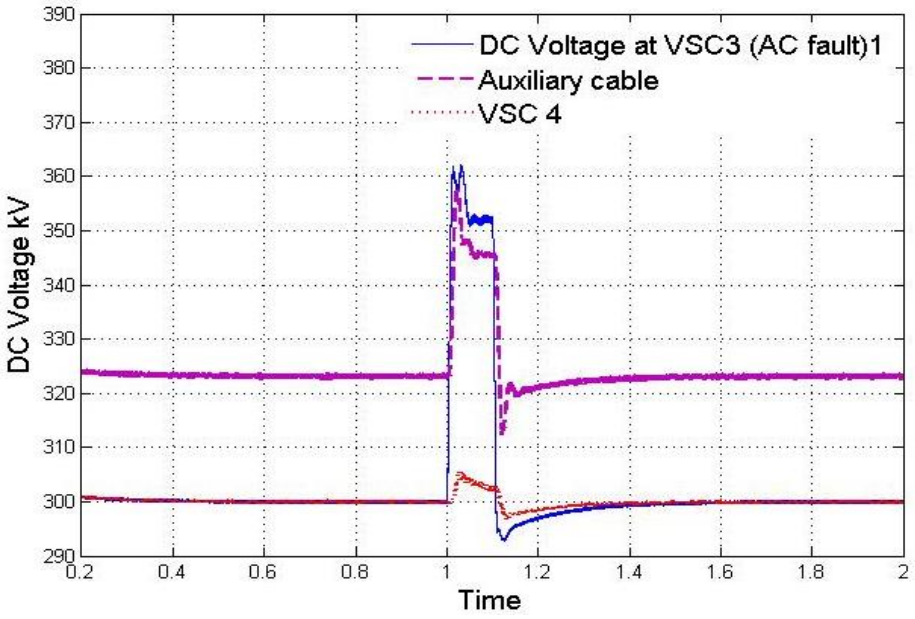

(c) DC link voltages at VSC3 (fault) VSC4 and auxilary cable.

Figure 5-14 Simulation results of the multi-terminal HVDC during AC fault.

5.6.1 Protection system – HVDC circuit breakers

System protection in a multi-terminal network is crucial, especially in a DC grid. In the point-to-point connection, in the event of a fault, the VSCs become uncontrollable diode bridges, which allow current flow towards the DC fault from the AC system. To prevent current flowing in to the DC network and from damaging converters, the AC side protection system is used. However, this solution leads to a temporary shut-down of the entire system, which is unacceptable in the case of large multi-terminal network. To avoid voltage collapse in the entire multi-terminal VSC-HVDC network, a fast protection system is required. It is expected that in multi-terminal network, DCCBs are going to be implemented, and the breaking time is expected to be less than 2ms [16].

Breaking the AC current is much easier than breaking the DC current. The AC current has a natural zero crossing sequence which enables breaking the current flow with switches. This type of protection on the AC side can be used in multi-terminal meshed system; however, it becomes problematic offshore where distances on the AC side are large, and additional equipment is needed to support the AC system. To break current in low to medium voltage DC lines, the DCCBs are limiting the current even more by additional resistive components to a sufficient level for arc extinction. Nevertheless they have never been scaled up and used in a HVDC system, which means they are insufficient [22, 23]. Figure 5-15 illustrates a typical configuration of HVDC circuit breaker with a low loss switch, communication path and energy absorption path.

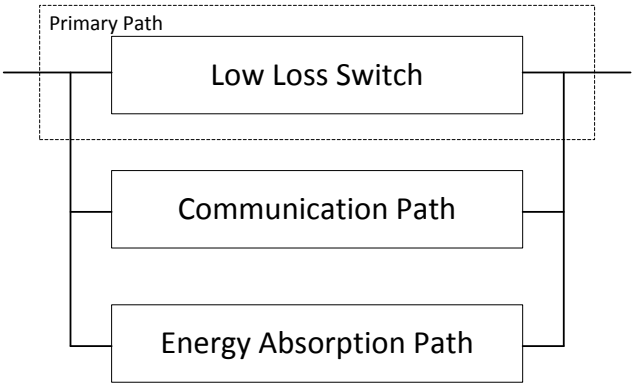

Figure 5-15 Typical topology of HVDC circuit breaker (adapted from [22])

The circuit breakers needs to fulfil the following requirements [22]:

- Create a current zero crossing to disturb the current
- Dissipate the energy stored in the system inductance.
- Withstand the high voltages

Currently they are three main topologies proposed for DCCB:

- Resonant circuit breaker
- Solid-State breaker
- Hybrid solid-state breaker

5.7 Summary

In this chapter, a multi-terminal DC (MTDC) network was investigated and simulated results were discussed. At first, different proposed configuration for multi-terminal HVDC network connections are discussed with alternative protection systems. The first MTDC model investigates the operation and power flow of 5 terminals, with assistance of a droop control. The droop control is suitable for more than three terminals for offshore wind farms integration and also to supply power to isolated areas. The generated power is delivered according to requirements of a grid however it also should have a huge storage system and generation reserve. Simulations show the behaviour of the MTDC network when one of the receiving-end converters is lost. In the second arrangement, the system reliability is increased, due to additional DC link between onshore converters that also improves power exchange between regional areas. This chapter shows that power can still be transferred in the case of a fault in the AC system. As proven by the simulation carried out, the multi-terminal VSC-HVDC increases system reliability; however, the main limitation is lack of appropriate DC protection for HVDC grids.

The future trends for large wind farm developments are offshore. VSC-HVDC is an ideal solution for offshore development since it increases system reliability, and a fault at any point of an AC system is not propagating to the DC network; power mismatch is delivered to the converter which acts as a slack bus. However, the vulnerability comes when the slack bus terminal is lost, since this also controls the DC link voltage. The main challenge is to handle a DC fault, as DC circuit breakers are currently unavailable or in early stages of commercialization, so up until now, during a DC fault there is no other option but to shut down the entire DC grid.

5.8 References

[1] W. Leterme, P. Tielens, S. D. Boeck, and D. V. Hertem, "Overview of Grounding and Configuration Options for Meshed HVDC Grids," *IEEE Transactions on Power Delivery,* vol. 29, pp. 2467-2475, 2014.

[2] Global Wind Energy Council, "Global Wind Energy Report: Annual Market Update 2016," ed, 2017.

[3] The North Seas Countries' Offshore Grid Initiative, "NSCOGI 2013/2014 progress report," 2014.

[4] W. F. Long, J. Reeve, J. R. McNichol, M. S. Holland, J. P. Taisne, J. LeMay, *et al.*, "Application aspects of multiterminal DC power transmission," *IEEE Transactions on Power Delivery,* vol. 5, pp. 2084-2098, 1990.

[5] Dragan Jovcic and K. Ahmed, *High Voltage Direct Current Transmission: Converters, Systems and DC Grids*, 2015.

[6] ABB. (2016). *Québec - New England*.

[7] G. Shi, Z. Chen, and X. Cai, "Overview of multi-terminal VSC HVDC transmission for large offshore wind farms," in *2011 International Conference on Advanced Power System Automation and Protection*, 2011, pp. 1324-1329.

[8] J. M. Guerrero, J. C. Vasquez, J. Matas, L. G. d. Vicuna, and M. Castilla, "Hierarchical Control of Droop-Controlled AC and DC Microgrids—A General Approach Toward Standardization," *IEEE Transactions on Industrial Electronics,* vol. 58, pp. 158-172, 2011.

[9] H. Li, C. Liu, G. Li, and R. Iravani, "An Enhanced DC Voltage Droop-Control for the VSC-HVDC Grid," *IEEE Transactions on Power Systems,* vol. PP, pp. 1-1, 2016.

[10] J. Beerten, S. Cole, and R. Belmans, "Modeling of Multi-Terminal VSC HVDC Systems With Distributed DC Voltage Control," *IEEE Transactions on Power Systems,* vol. 29, pp. 34-42, 2014.

[11] National Grid, "Round 3 Offshore Wind Farm Connection Study," 2011.

[12] K. Nieradzinska, C. MacIver, S. Gill, G. A. Agnew, O. Anaya-Lara, and K. R. W. Bell, "Optioneering analysis for connecting Dogger Bank offshore wind farms to the GB electricity network," *Renewable Energy,* vol. 91, pp. 120-129, 6// 2016.

[13] J. Machado, M. Ventim Neves, and P. J. Santos, "Economic limitations of the HVAC transmission system when applied to offshore wind farms," in *Compatibility and Power Electronics (CPE), 2015 9th International Conference on*, 2015, pp. 69-75.

[14] National Grid, "Electricity Ten Year Statement 2015, Appendix E," 2015.
[15] R. Derakhshanfar, T.U. Jonsson, U. Steiger, and M. Habert, "Hybrid HVDC breaker—A solution for future HVDC system," *presented at the CIGRÉ Paris Session, Paris, France,* , 2014.
[16] Cigré Working Group B4-52, "HVDC Grid Feasibility Study," 2013.
[17] Giddani Osman Addalan, "Control design and stability assessment of vsc-hvdc networks for large-scale offshore wind integration," PhD, Electrical & electronic engineering, University of Strathclyde, 2011.
[18] G. P. Adam, S. J. Finney, B. W. Williams, K. Bell, and G. M. Burt, "Control of multi-terminal DC transmission system based on voltage source converters," in *AC and DC Power Transmission, 2010. ACDC. 9th IET International Conference on*, 2010, pp. 1-5.
[19] G. O. Kalcon, "Control Design and Stability Assessment of VSC-HVDC network for Large-Scale Offshore Wind Integration," PhD Thesis, Electronic and Electrical Engineering, University of Strathclyde, 2011

2011.
[20] J. Beerten, S. Cole, and R. Belmans, "A sequential AC/DC power flow algorithm for networks containing Multi-terminal VSC HVDC systems," in *Power and Energy Society General Meeting, 2010 IEEE*, 2010, pp. 1-7.
[21] K. Nieradzinska, J. C. Nambo, G. P. Adam, G. Kalcon, R. Peña-Gallardo, O. Anaya-Lara, *et al.*, "North Sea Offshore Modelling Schemes with VSC-HVDC Technology: Control and Dynamic Performance Assessment," *Energy Procedia*, vol. 35, pp. 91-101, 2013/01/01 2013.
[22] C. M. Franck, "HVDC Circuit Breakers: A Review Identifying Future Research Needs," *IEEE Transactions on Power Delivery*, vol. 26, pp. 998-1007, 2011.
[23] Y. Wang and R. Marquardt, "Future HVDC-grids employing modular multilevel converters and hybrid DC-breakers," in *Power Electronics and Applications (EPE), 2013 15th European Conference on*, 2013, pp. 1-8.

Chapter 6:

Optioneering analysis for connecting Dogger Bank offshore wind farm to the GB electric network

The increasing demand for wind power production and reduced visual impact is driving the development of offshore wind farms. The UK Government has issued plans to install more than 40 GW of renewable power generation by 2020, with most of the energy being delivered from new offshore wind farms around the coast of Great Britain [1-3]. The Dogger Bank Round 3 offshore site in the North Sea is expected to be the largest, with an initial planned output of 7.2GW [3, 4].

In this chapter investigation of three VSC-HVDC connections schemes designed to transfer 2.4GW of power from two separate Dogger Bank wind farms to the UK grid is presented. Three options based on HVDC with Voltage Source Converters (VSC HVDC) are investigated [5]:

1. two separate point-to-point connections,
2. a four-terminal multi-terminal network and
3. a four-terminal network with the addition of an AC auxiliary cable between the two wind farms.

Each option is investigated in terms of investment cost, controllability and reliability against expected fault scenarios.

6.1 Introduction

This chapter seeks to investigate the merits of different connection options for far offshore wind farm installations including the possibility of introducing interconnection between two wind farms in relatively close proximity. It does this by exploring three VSC-HVDC connection schemes designed to transfer 2.4 GW of power from two separate Dogger Bank wind farms to the GB transmission system in Great Britain (GB). The study is based on option 1 from the National Grid "Round 3 Offshore Wind Farm Connection Study" shown in Figure 6-1 [6]. The studies focus on connecting wind farm 1 and wind farm 2 to the onshore grid with each farm sized at 1.2GW. The magnitude of power flows into the GB network suggests the use of two onshore connection points [6], and the scenarios presented in this study are based on this assumption.

The options considered are as follows:

- two separate point-to-point connections;
- a multi-terminal VSC-HVDC network; and
- point-to-point connections with an additional AC cable linking the two wind farms

Figure 6-1 Dogger Bank connection overview based on [6].

Each option is described in detail together with the advantages that each provides. A thorough cost analysis of the electrical connection infrastructure is carried out for each option using estimates for component costs that are validated by industry experts. A cost-benefit analysis is then carried out by estimating the level and value of undelivered energy

due to expected fault conditions over the project lifetime and comparing against the capital cost analysis.

The next section describes the three possible options for connecting 2.4GW of offshore wind power.

6.2 Dogger Bank Connection Case Study

A project to build and connect wind generation in Dogger Bank to the GB mainland grid can be split into two systems: the wind farm system and the transmission systems. In this thesis the wind farm system is assumed to consist of two separate 1.2GW wind farms within the Dogger Bank area as shown in Figure 6-1. The internal structure of the wind farms from the turbines to the AC to DC conversion is the same for all cases. Each wind farm consists of 240 5MW turbines connected at 33kV by HVAC inter-array cabling in strings of no greater than 9 wind turbines connected to the AC collector station. The turbines were consulted and selected from the several available on the market show in Table 6-1. Two AC offshore collector stations and a single offshore converter station are constructed at each wind farm. The collector and converter stations are connected at 275kV. The converter station houses the VSC-HVDC technology, gas insulated switchgear, advanced control and protection systems.

Table 6-1 Current and future offshore large turbine design

Turbine	Rated power (MW)	Blade (m)	Availability
Multibrid M5000	5	116	Available
REpower 5M	5	126	Available
REpower 6M	6	126	Available
Siemens SWT-6.0	6	154	Available
Gamesa G128	5	128	Available
Siemens SWT-7.0	7	154	Prototyping
Vestas V164	8	164	Prototyping

The converter station represents the point-of-connection of the wind farm system to the transmission system, and is itself assumed to be part of the transmission system. The converter station links to either the point-to-point or multi-terminal HVDC networks and in option 3, on the AC side, to the AC-auxiliary cable linking the converter stations of the two wind farms at 275kV.

Costs are estimated through consultation with a UK-based Engineering Design firm besides industry experts with significant offshore wind farm experience and therefore represent

industry estimates. Installation costs for the turbines have been verified with 3 wind turbine manufacturers that produce turbines of the desired specification. All cabling costs for the project are shown in Table 6-2. Cables cost between £1M per kilometre (33 kV Offshore AC Cable) and £2.5M per kilometre (275 kV HVAC Offshore Cable). Wind farm internal costs are shown in Table 2. Transportation includes one-off costs for installation of accommodation, daily costs for transportation of employees from accommodation to site and monthly costs for changes in working groups.

Table 6-2 Cables costs breakdown in £M

Cables	Price £M
VSC-HVDC Offshore Cable +/- 320kV	1.1/km
HVAC Offshore Cable 33kV Inter-array to collector	1/km
HVAC Offshore Cable 275kV Collector to Converter	2.5/km
HVAC Onshore Cable 275kV to transformer and 400kV to grid	2.5/km

Costs presented for the converter stations and wind turbines are the installed costs which include all civil works. Additional civil works are also included as separate items in the cost analysis where they are not directly related to individual items.

The costs associated with the internal wind farm infrastructure are the same for all three options. These fixed costs include: the wind turbines, 33kV inter-array cables, AC collector platforms, and 275kV cable between collector and converter stations, the civil/construction works and transport. The cost of the converter station is assumed to be part of the costs of the transmission system.

At the point of connection to the onshore grid, all options must deliver power at 400kV AC and much of the shore infrastructure will be the same for the three options investigated. The costs associated with these aspects of the project are included in the cost estimates for each option.

Table 6-3 Costs associated with the internal wind farm infrastructure in £M [7].

Item	Unit Price	Quantity	Total Cost
5 MW Offshore WT	6.6	480	3168
33kV inter-array cable (£M/km)	1	538	538
275kV AC cable (£M/km)	2.5	15	37.5
AC collector Station	100	4	400
Added Civil/Construction Works			5.25
Transport			2.9
Accommodation			6
Total			4171

6.3 Point-to-point connection study

This case, which represents the base-case, investigates a point-to-point connection which involves connecting each of the two wind farms separately with point-to-point VSC-HVDC links via +/-300kV symmetrical monopole configuration. The two wind farms and their related electrical infrastructure operate as separate systems up to the point of connection with the GB National Grid as shown in Figure 6-2.

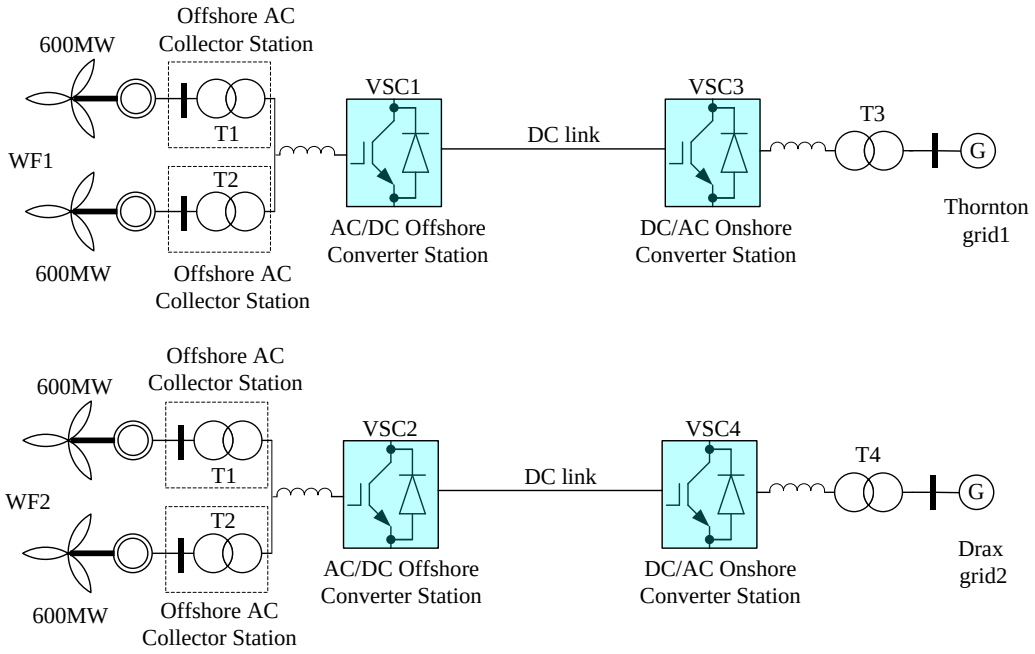

Figure 6-2 Simplified schematic of two point-to-point connections, based on National Grid connection study [6].

The transmission system for each wind farm includes a fully-sized VSC-HVDC converter capable of converting the full output of that wind farm. After the conversion to DC at +/-300kV, power will flow through an HVDC subsea cable to the GB coastline. Crossing structures will be necessary where cables cross existing subsea installations. Underground onshore DC cables will be laid between the foreshore and the onshore DC/AC converter station which will require up to 3 hectares of land and may be up to 30m in height. AC underground cables will then export power from the inverter to National Grid 400kV substations at Thornton and Drax after which point control lies with National Grid. As shown in

Figure 6-1, the grid connections points are a significant distance from the shore, with Drax situated 73km inland and Thornton 51km this topology and point of connections are based on option 1connection overview from National Grid [6]. The onshore converter stations will be located near the grid connection point.

The VSC-HVDC connection as shown in Figure 6-2, has been previously used in onshore and offshore applications, furthermore many different projects this kind are under development or planned [8-11]. There is a growing interest in this technology as a means of integrating offshore wind power plant to onshore grid.

The main advantages of using VSC-HVDC point to point connection compared with the classical LCC-HVDC connections are as follows [4, 12-15]:

- A point-to-point connection with a VSC-HVDC system as opposed to classical LCC-HVDC connection provides the ability to expand the network later to greater capacities, for example if further wind farm development occurs close to the existing wind farms. This creates increased system flexibility which will be crucial for meeting future energy demands and Grid Codes.
- There is no need to change voltage polarity for power reversal, which in multi-terminal arrangement it is essential.
- Unlike an LCC-HVDC system, a VSC-HVDC converter is capable of providing reactive power control, frequency control and oscillation damping. There is therefore, no need to implement costly reactive compensation on the offshore platforms.
- VSC-HVDC connections eliminate the requirement for a start-up generator in the offshore wind farm network as power flow can be reversed to provide start up power from the mainland, which also cut the costs of offshore installation and provides robust solution. LCC-HVDC systems are unable to provide this inherent black start capability.
- A VSC-HVDC system involves a lower investment cost and smaller space requirements compared to traditional LCC HVDC.
- As the use of VSC-HVDC eliminates the need for AC and DC filters and reactive power compensation there is a smaller footprint per station.

6.3.1 Cost estimations for point-to-point connection

The cost of the VSC-HVDC point-to-point transmission system consists of: the two offshore converters stations; the HVDC subsea cables linking the wind farm converter stations to the shore; the onshore converter station which assumed to be located close to the shore, the HVAC underground cables; the on-shore civil structures; and the associated construction costs. The estimated total cost of transmission system based on two VSC-HVDC point-to-point systems is £1.88 Billion. This compares with the £4.16 Billion cost of the wind farms themselves. As such the point-to-point connection option represents 31% of the total cost of

the project to build and connect the 2.4GW wind generation on Dogger Bank. Figure 6-3 shows the breakdown of the costs associated with the point-to-point connection in millions of pounds.

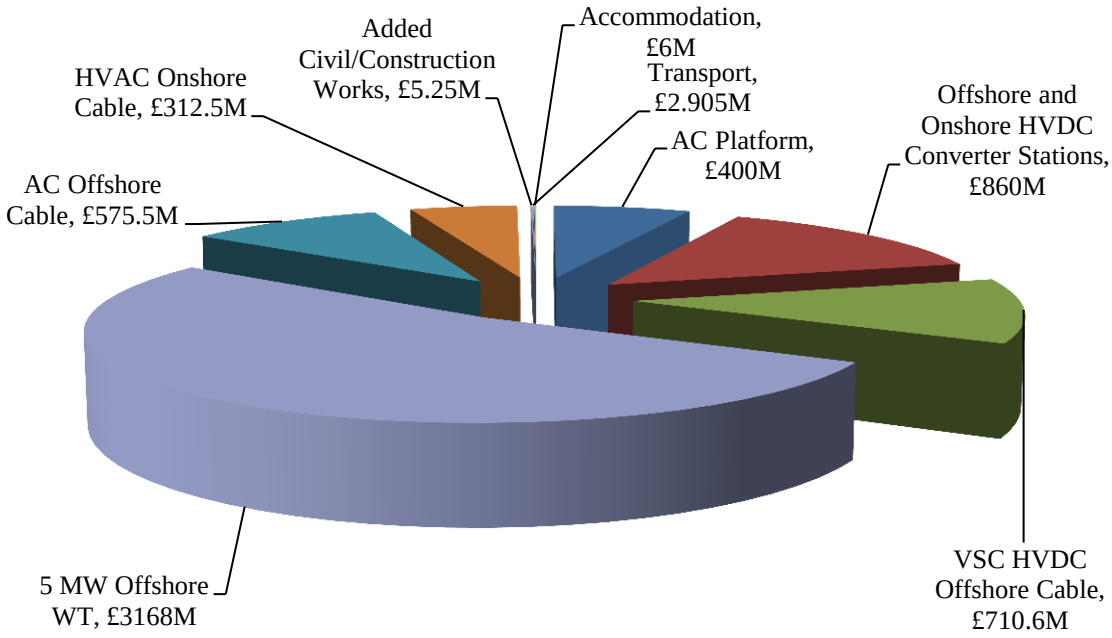

Figure 6-3 Total cost of construction of 2.4 offshore wind farm and point to point VSC-HVDC transmission connection to mainland GB in £M.

The greatest cost in the complete project comes from the installation of the wind turbines which constitute around 52.4% of the total cost of the works as shown in Table 6-4. The price of offshore wind turbine is assumed to be £1,320 per kW according to [16] and [7], the offshore wind turbines are still very expensive as the market is limited to a number of manufacturers specialising in this area. The total cost of four converter stations (2 onshore, 2 offshore) and offshore AC platform comes to nearly 21%. AC and DC cables are another large expense and together represent 26.5% of total costs including array cables within the wind farm and transmission cables onshore and offshore. After defining installation costs of the plant, additional costs such as transportation and accommodation are added. There is a requirement for onshore substation network reinforcements such as: substation extensions and reconfiguration, new connection protection and land purchase. These additional costs are the same for all three options and are explained further in [6]. The latter costs have been verified through consultation with leading GB companies with experience in such work. The cost presented does not include inflation, commissioning costs, design costs, financial risk,

or legal costs. The cost for offshore accommodation, transport, operations and maintenance infrastructure has been considered in each option.

Table 6-4 Cost weighting of each item as a percentage of total cost in £M

Item	Percentage of Total Cost
AC Platform	6.6%
Offshore and Onshore HVDC Converter Stations	14.2%
VSC HVDC Offshore Cable	11.8%
5 MW Offshore WT	52.4%
HVAC Offshore Cable	9.5%
HVAC Onshore Cable	5.2%
Added Civil/Construction Works	0.09%
Transport	0.10%
Accommodation	0.10%

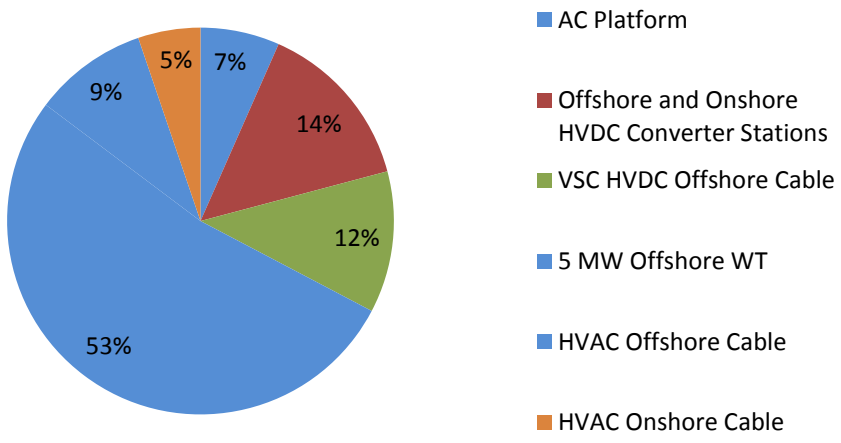

Figure 6-4 Percentage of total of installation 2.4GW of wind power visualised in chart

To visualise percentage, the costs are shown in the Figure 6-4. The two main structures of the wind farm system and the transmission systems represent 69% and 31% respectively.

6.4 Multi-terminal VSC-HVDC Connection

The multi-terminal VSC option involves adding an additional HVDC cable linking the two point-to-point connections of the base case scenario as shown in Figure 6-5. In such a topology it often assumed that direct current circuit breakers (DC-CBs) are required to protect the network. It would be possible to protect the full system using AC side protection only so long as the converters have appropriately sized anti-parallel diodes to handle the high fault currents that would flow during the period of up to 100ms that it would take the AC protection to isolate the DC system from the onshore grid. However, such a method of protection would require the temporary shutdown of the whole DC grid which for the 2.4GW system being investigated could potentially mean an unacceptable breach of the maximum

infrequent loss of load limit for the GB which is currently set at 1800MW [17], so it is considered inappropriate. Alternative protection strategies involving converter topologies that have reverse current blocking capability or that use a reduced number of DC-CBs have also been explored, for example in [18], this studies assumes the DC-CBs are used. The cost of DC-CBs remains relatively uncertain as they are yet to be put into production. The cost of the HVDC circuit breakers is estimated at 1/6 of the full cost of VSC-HVDC converter station in line with other work in this field [19].

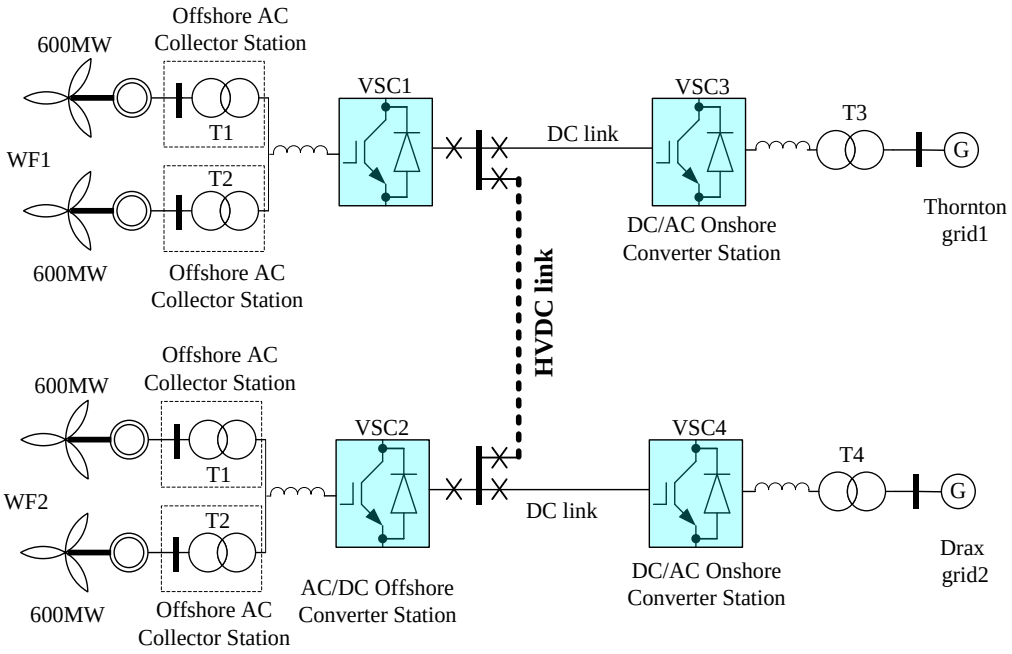

Figure 6-5 Multi-terminal VSC-HVDC connection with DC-CBs

The multi-terminal VSC-HVDC option presented here provides all the benefits of the point-to-point connection and has additional advantages in terms of reliability and controllability [20]. It is expected that a large number of wind farms will be developed on Dogger Bank, dispersed over a wide area. Multi-terminal VSC-HVDC provides a potential solution to the issue of collection and transmission of large amounts of wind power from geographically dispersed wind farms as opposed to the traditional option of using many point-to-point VSC-HVDC links. The main advantages of multi-terminal connections compared to point-to-point connections are [20, 21]:

- Improved system reliability and stability during loss of a single DC link.
- The ability to maintain electrical connection to both wind farms during the loss of a single DC link ensuring the ability to continue transferring some power from both wind farms to the GB grid.

- Multi-terminal VSC-HVDC connection increases the power flow controllability between different desired routes.
- Provides the ability to link offshore wind to multiple national AC power networks as part of a 'Supergrid'.

6.4.1 Cost of Multi-terminal VSC-HVDC Case

The multi-terminal VSC-HVDC option involves two major additional costs: the DC circuit breakers and the additional HVDC cabling linking the converter stations at the two wind farms. Additional cable costs for the 75km connection between the DC platforms equates to £165million. The DC circuit breakers are assumed to cost £342 million for 12 DC circuit breakers in total, that is 1/6 of the cost of the HVDC offshore converter station [19]. Therefore, the total cost of the multi-terminal VSC-HVDC option is £6.55Billion, an increase of £0.50 billion or 8.4%, over the simple point-to-point connection.

6.5 Point-to-point connection with auxiliary AC cables

This option reverts to the point-to-point HVDC connection of option 1, and adds an AC link between the two wind farms shown in Figure 6-6. The auxiliary AC cable provides a link between the two offshore converter stations and provides many of the benefits of multi-terminal VSC-HVDC option without the need for DC circuit breakers.

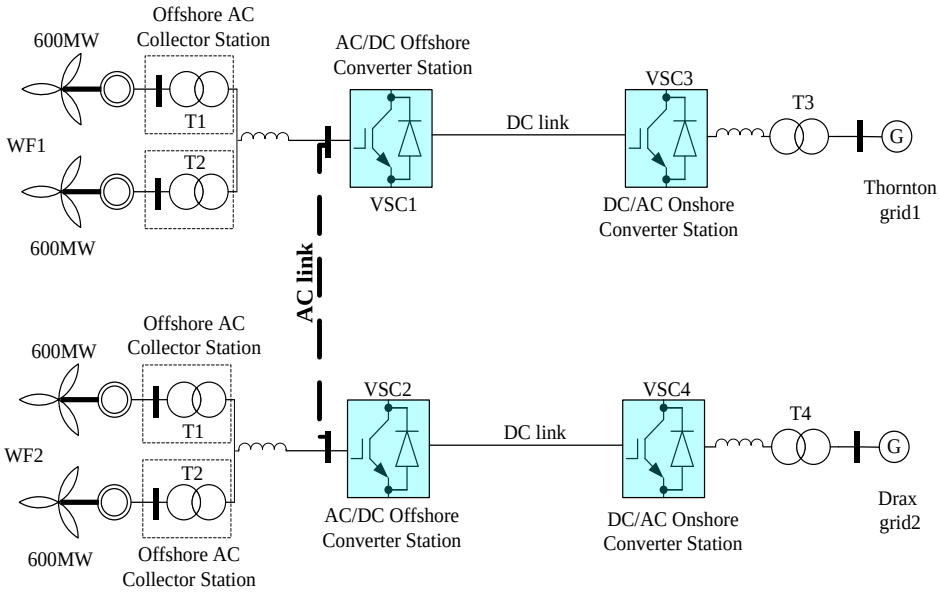

Figure 6-6 Point to point connection with auxiliary cable

The advantages of the auxiliary AC cable option are:

- During emergency conditions such as maintenance of one of the transformers, one of the 2 offshore HVDC converter stations or sudden loss of DC cables, an additional route is available to transfer some power to the GB grid
- There is no need for DC circuit breakers and this option could be delivered using relatively cheap and proven technologies.
- Additional benefits in terms of security of the system; power can still be transferred in the event of the loss of an offshore converter unlike the multi-terminal HVDC option.

6.5.1 Costs of Auxiliary AC Cable Option

The initial investment costs are higher compared to the point-to-point connection due to the cost of additional AC cable (75 km) and additional AC breakers. The cost of the additional AC cable is assumed to be £187.5 million. The estimated cost of this option is £6.22 Billion, an increase of £187.5 million compared with the base-case but £319 million less than the multi-terminal VSC-HVDC option.

6.6 Summary of option cost

Table 6-5 shows a cost summary of the three connection options. Two separate point-to-point connections is the cheapest with a total cost of £6.04 Billion. This option is therefore both technically viable and economically attractive in terms of capital cost.

The multi-terminal connection is the most expensive option at £6.55 billion, an increase of 8.3%. This option provides the possibility of future expansion of the HVDC grid, and has at the same time high security and reliability performance. Whilst DC-CBs are not currently commercially available, they are expected to become available in the near future so this option should be technically viable in coming years although a greater level of capital expenditure will be required.

The point-to-point connection with AC auxiliary cable comes to £6.22 billion, which is an increase of 3.1% compared with the point-to-point connection option. It represents very promising connection architecture if distance between wind-farm substations is small enough. This option is also technically viable using existing commercially available technology and requires a smaller capital expenditure than the multi-terminal HVDC option. It also has the added benefit of securing power transmission even during maintenance or a fault at one of the converter substations.

Table 6-5 Additional costs relative to the base case* in £billion

Option	Multi-terminal connection	AC auxiliary cable
HVDC cable	£0.165	0
HVDC breakers	£0.342	0
HVAC offshore cable	0	£0.187
Total Cost	£6.55	£6.22
Percentage increase	8.3%	3.1%

*Base case scenario £6.04 billions

6.7 Reliability Input Assumptions

The reliability analysis considers the potential for faults on all major components associated with the HVDC network. Faults are not applied to the internal wind farm network and so available energy is assumed to be 100% up to the point of connection with the HVDC network. The exception to this is Case 3 which makes use of an auxiliary AC connection between the two wind farms which has been included within the fault analysis. Table 6-6 gives a breakdown of the input mean time to fail (MTTF) values used as input to the reliability study along with the required time to repair (RTTR) values, which relate to the number of working hours required to carry out the repair or the size of the required weather window if a single continuous repair is required, and the fixed delay associated with each fault type. The reliability inputs used are a central case estimate derived from consideration of the range of published projections for component failure and repair rates given in [22-25] and through discussion with industry experts. For lack of more informed data it is assumed that both AC and DC circuit breakers have the same reliability characteristics. In this study only a central reliability case scenario is examined although it must be noted that a more thorough analysis might consider a range of input scenarios for comparison.

Table 6-6 Reliability input assumptions for HVDC network components

Component	MTTF (Hrs*) *Transmissin Branch – Hrs/100km	Repair Time (Hrs)	
		Fixed delay	RTTR
Onshore Converter	7200	-	6
Offshore Converter	7200	-	6
Onshore Transformer	438300	2160	72
Offshore Transformer	350640	2880	120
Transmission Branch	219150	2160	144
AC and DC Circuit Breakers	219150	-	6

6.7.1 Results

Table 6-7 shows the results of the reliability analysis using a 100000-year sequential Monte Carlo simulation with the reliability input assumptions outlined in Table 6-6. The results show that use of an alternative transmission path gives significant benefits in terms of deliverable energy. It is found that the Method using the AC link has the best reliability performance followed by the Multi-Terminal VSC-HVDC option. The expected level of undelivered energy each year is significantly higher under the base case scenario with no inherent redundancy or alternative transmission paths for re-routing power in the event of faults on the HVDC network. To fully appreciate the financial implications of these findings an estimate can be made as to the cost of this undelivered energy assuming that the value of offshore wind electricity is £120/MWh which is in line with the guaranteed strike price agreed for the largest UK offshore wind farm currently in development. The results are shown in Table 6-7.

Table 6-7 Annual average available energy not delivered due to faults on HVDC network

	Base case	MT HVDC	Auxiliary AC link
Undelivered Energy	3.94%	2.90%	2.14%
Annual Cost of Undelivered Energy	£42.06m	£30.96m	£22.89m

To understand how the cost of reliability impacts the overall finances of an offshore wind project the Net Present Value (NPV) of the undelivered energy can be calculated over the expected lifetime of the project. This has been done for a 25-year period using a standard discount rate of 6%. The value of energy delivered from each grid can then be calculated by subtracting the NPV of undelivered energy from the NPV of total expected generated energy over the 25-year period with a calculated capacity factor of 42.3%. Subtracting the total project costs from this value then gives a figure for the NPV of the project as a whole. The results of this analysis are shown in Figure 6-7.

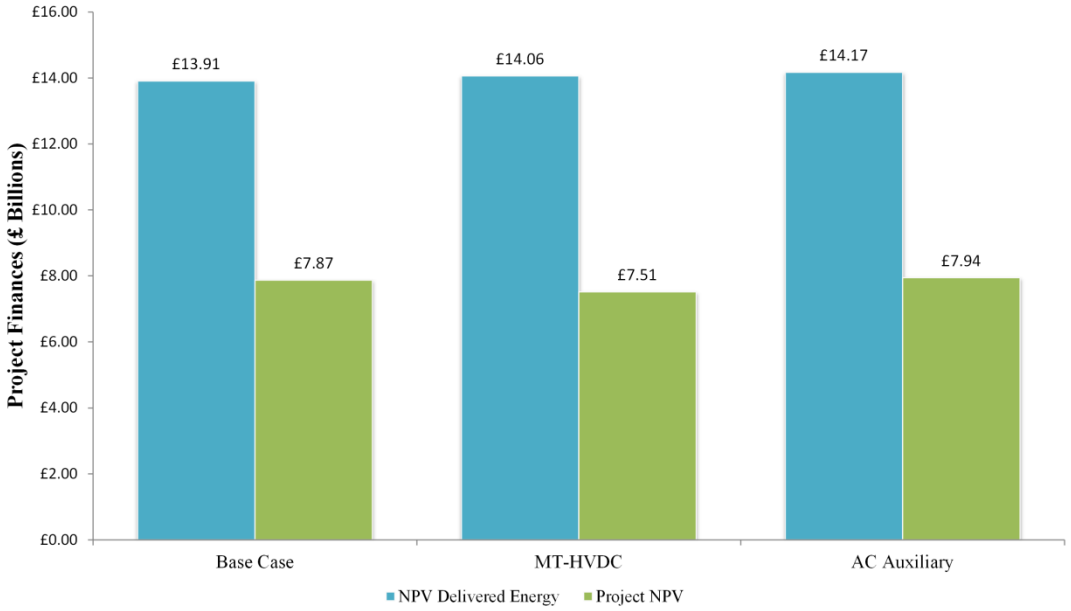

Figure 6-7 Cost analysis for a central case reliability evaluation

This reliability analysis shows that the base case network incurs the highest level of energy curtailment and therefore has the lowest NPV of expected delivered energy over the assumed 25-year project lifetime. The multi-terminal VSC-HVDC makes significant savings in terms of curtailed energy when compared with the base case scenario so the NPV of expected delivered energy is around £150 million higher over the project lifetime. This is not however enough to balance out the extra £507 million capital cost of the project so the multi-terminal VSC-HVDC option has the lowest overall project NPV and is therefore the least value for money option overall. The AC Auxiliary option has the lowest level of curtailed energy and so the highest value of delivered energy worth around £260 million more than the base case option. The option also has lower capital cost than the multi-terminal VSC-HVDC grid with additional costs over the base case of £187 million. It therefore has the highest total project NPV by a margin of over £70 million and so is the best value for money option of those considered. For the reliability scenario investigated it is found that there is high value in having an additional redundant transmission path however it has been shown that the overall cost effectiveness of this depends on the capital expenditure needed to implement the redundancy.

It must be noted that the results of this study are heavily dependent on the input assumptions used and a different set of assumptions could easily lead to different headline results. For example, if a more optimistic set of reliability inputs were used which assumed that failure and repair rates could be reduced then the importance of undelivered energy to the overall cost could be significantly lower. This could, for example, mean that the base case, point to

point network would remain the best value for money due to its significantly lower capital costs. The opposite is also true in that worse reliability performance of network components would emphasise the benefits of the systems incorporating redundant transmission paths. Further to this if the cost of DC breakers could be reduced to a more manageable level then the value for money of the MT-HVDC option could potentially be brought in line with the auxiliary AC cable option. Another variable which could alter the final results is the distance of the additional transmission path which in this case study is towards the upper limit of AC capability. It is conceivable that connections could be significantly shorter than this in clustered wind farm scenarios and this would reduce the capital cost of building in the redundancy using either method. This would further improve the overall cost effectiveness of the schemes incorporating redundancy. A full sensitivity analysis to failure and repair rates, component costs, transmission distances and cost of energy would be required to fully inform on which network options are likely to provide the most cost-effective solutions, however results are likely to be specific to each offshore network case study examined.

To further inform the investigation a number of additional factors could be considered further in future work. These include: the impact of electrical network losses on the overall delivered energy; the possibility of using more complex transmission methods, for example, bi-pole connection of VSC converters; the use of alternative protection strategies such as the use of DC breakers in a limited number of selected locations, perhaps in conjunction with reverse current blocking converters [18]; the possibility of incorporating a spares program to reduce repair delays; and the possibility of making anticipatory investment in offshore infrastructure to allow for future connection of additional offshore wind farm developments. The issue of anticipatory investment would itself raise further questions relating to the need to oversize particular components, how that process would be optimised and how the risk of stranded assets are accounted for. Such issues are yet to be fully addressed in the literature but have been discussed in more detail in [26].

6.8 Summary

The importance of HVDC technology is emphasised by the continued growth of renewable energy generation and in particular the potential for large far-offshore wind farm developments. VSC-HVDC is one solution to the challenge of integrating offshore wind power for Dogger Bank in the North Sea, and one that provides the opportunity to develop offshore-network topologies that support reliability of operation in order to minimise the impact of faults. This chapter identifies three network topologies for which VSC is suitable: point-to-point connection, Multi-terminal VSC-HVDC and a four terminal VSC-HVDC system with the use of AC axillary cable between offshore wind farms.

Point-to-Point systems are well understood and already used in connecting offshore wind power to the onshore grid in Germany. This option is shown to have the lowest capital cost of the options investigated in this study but does not provide the contingency to make it a highly reliable source of generation. Should one of the terminals experience an outage or if the DC transmission link were to fail then transmission to the onshore AC regional systems would be lost completely. This has also cost implications in that over the course of an expected project lifetime the level of undelivered energy will rise and therefore lost revenue will be high.

Multi-terminal VSC-HVDC arrangements provide valuable flexibility to developments like Dogger Bank as it can provide contingency against certain faults. Thess studies have shown the costs of multi-terminal-HVDC are very high and do not outweigh the benefits of additional revenue through continued operation under certain fault conditions. One of the key reasons for this, is the high projected cost of DC breakers, however if DC breaker costs came down then it could be a more competitive option.

In the multi-terminal HVDC option, power can be delivered to the onshore grid when one of the onshore converters station is not in operation or one of the transmission line fails, however both offshore station need to be in operation. This has been shown to significantly reduce the level of undelivered energy compared with the Point to Point grid option. Although there is still a need for larger size HVDC cables and HVDC circuit breakers which are not commercially available yet and are likely to come at a high capital cost. The use of a multi-terminal connection topology includes the potential for future interconnection of Dogger Bank with other offshore wind installations or even onshore connection to other countries, which would allow for power trading between regions, hence could have additional economic benefits.

Option 3, where there is an auxiliary cable on the AC side, shows that an economic advantage when the additional costs are compared against the additional revenues from the ability to continue operating the wind farms whilst faults are being repaired. The AC auxiliary cable can redirect power to the other converter station during a fault. Using an auxiliary cable on the AC side is advantageous as it means any of the (onshore or offshore) converter stations or one of the transmission line can be under maintenance or out of order while power can still be delivered to the onshore grid. Hence this option is the most reliable of those investigated and due to the use of established technology the capital costs are also relatively low. However, the use of this option is limited by distance, as losses in AC cables can become prohibitively high at distances beyond those investigated in this study. This

option also has the potential to oversize the whole system to allow additional power from other wind farms.

6.9 References

[1] EWEA, "The European Wind Initiative (2013) Wind power research and development to 2020," January 2013.

[2] European Environment Agency, "Europe's onshore and offshore wind energy potential," 2009.

[3] D. N. Fichaux and J. Wilkes, "Oceans of Opportunity. Harnessing Europe's largest domestic energy resource," European Wind Energy Association 2009.

[4] National Grid, "Offshore Electricity Transmission: Possible Options for the Future " 2011.

[5] K. Nieradzinska, C. MacIver, S. Gill, G. A. Agnew, O. Anaya-Lara, and K. R. W. Bell, "Optioneering analysis for connecting Dogger Bank offshore wind farms to the GB electricity network," *Renewable Energy*, vol. 91, pp. 120-129, 6// 2016.

[6] National Grid, "Round 3 Offshore Wind Farm Connection Study," 2011.

[7] EWEA, "The Economics of Wind Energy. A report by the European Wind Energy Association," 2010.

[8] N. Flourentzou, V. G. Agelidis, and G. D. Demetriades, "VSC-Based HVDC Power Transmission Systems: An Overview," *Power Electronics, IEEE Transactions on*, vol. 24, pp. 592-602, 2009.

[9] Siemens. (2011). *Ready for the future: Siemens erects power converter stations for HVDC link between France and Spain as part of the Trans-European Network* Available: http://www.energy.siemens.com/us/pool/hq/power-transmission/HVDC/HVDC-PLUS/pm-pdf/INELFE_en.pdf

[10] Statnett. (2015). *€1.5 billion contracts awarded to build the world's longest interconnector*. Available: http://www.statnett.no/en/News/News-archives/News-archive-2015/15-billion-contracts-awarded-to-build-the-worlds-longest-interconnector/

[11] Siemens. (2015). *Siemens receives major order for BorWin3 North Sea grid connection from TenneT*. Available: http://www.siemens.com/press/en/pressrelease/?press=/en/pressrelease/2014/energy/power-transmission/et201404036.htm

[12] G. Reed, R. Pape, and M. Takeda, "Advantages of voltage sourced converter (VSC) based design concepts for FACTS and HVDC-link applications," in *Power Engineering Society General Meeting, 2003, IEEE*, 2003, p. 1821 Vol. 3.

[13] G. P. Adam, O. Anaya-Lara, and G. Burt, "Multi-terminal DC transmission system based on modular multilevel converter," in *Universities Power Engineering Conference (UPEC), 2009 Proceedings of the 44th International*, 2009, pp. 1-5.

[14] F. Schettler, H. Huang, and N. Christl, "HVDC transmission systems using voltage sourced converters design and applications," in *Power Engineering Society Summer Meeting, 2000. IEEE*, 2000, pp. 715-720 vol. 2.

[15] M. Barnes and A. Beddard, "Voltage Source Converter HVDC Links – The State of the Art and Issues Going Forward," *Deep Sea Offshore Wind R&D Conference, Trondheim, Norway, 19-20 January 2012*, 2012.

[16] Kaj Lindvig, "The installation and servicing of offshore wind farms of offshore wind farms," 2010.

[17] ofgem. (2011). *National Electricity Transmission System Security and Quality of Supply Standard (NETS SQSS): Review of Infeed Losses (GSR007 as revised by GSR007-1)*. Available: https://www.ofgem.gov.uk/ofgem-publications/52793/gsr007-decision-letter-final.pdf

[18] C. D. Barker, R. S. Whitehouse, A. G. Adamczyk, and M. Boden, "Designing fault tolerant HVDC networks with a limited need for HVDC circuit breaker operation " *Cigré Paris Session, paper B4-112* Paris 2014.

[19] Cigré Working Group B4-52, "HVDC Grid Feasibility Study," 2013.

[20] J. Beerten and R. Belmans, "Modeling and Control of Multi-Terminal VSC HVDC Systems," *Energy Procedia*, vol. 24, pp. 123-130, // 2012.

[21] Siemems. (2011). *The Smart Way HVDC PLUS – One Step Ahead*. Available: http://www.energy.siemens.com/fi/pool/hq/power-transmission/HVDC/HVDC_PLUS_The%20Smart%20Way.pdf

[22] K. Linden, B. Jacobson, M.H.J. Bollen, and J. Lundquist, "Reliability study methodology for HVDC grids,," in *CIGRE Sessions*, Paris, 2012.

[23] ofgem. (2012). *Calculating Target Availability. Figures for HVDC Interconnectors*. Available: https://www.ofgem.gov.uk/ofgem-publications/59247/skm-report-calculating-target-availability-figures-hvdc-interconnectors.pdf

[24] R. Hodges and R. Bryans., "Reliability Analysis of Electrical Systems for Offshore Wind," in *42nd ESReDA Seminar on Risk and Reliability for Wind Energy and other Renewable Sources*, Glasgow, 2012.

[25] ISLES (The Scottish Government. Irish-Scottish Links on Energy Study), "Technology Roadmap Report," ed, 2012.

[26] K. Bell, L. Xu, and T. Houghton, "Considerations in design of an offshore network," presented at the Paper presented at CIGRE Session 2014, Paris, France, 2014.

Chapter 7:

Conclusions and Future Work

The thesis investigated the use of VSC-HVDC transmission system for large scale offshore wind farm integration and multi-terminal offshore grid connections. Moreover, the low voltage ride-through capabilities of a hybrid wind plant were explored in detail.

This chapter summarizes the work that has been carried out in this research work. Furthermore all the major conclusions and evidence for the contribution can be drawn from this research are described and used to define the future research work on the topic.

7.1 Conclusion and key findings.

The first part of this thesis (chapter 2) focused on reviewing the state-of-the-art of wind turbine and HVDC technologies. It described the current status of technology and highlighted the options available for future offshore wind power. It also described the current challenges faced by wind industry and National Grids in terms of grid code compliance and fault-ride-through. The general conclusion of this review is that DFIG wind turbines cannot comply with the grid code requirement unless additional fault ride through devices and external reactive power compensation units are provided. Furthermore, it is also concluded that using crowbar protection as a fault ride through mechanism for DFIGs conveys a violation of the grid codes concerning the reactive power provision requirements for wind turbines.

Chapter 3 of this thesis presented detail models of DFIG-based and FRC-based wind turbines and its performance in a hybrid wind farm model in Simulink. The design of control system for DFIG and FRC wind turbines was conducted to ensure robust dynamic performance. The addition of a voltage control loop to the rotor side converter of a fully rated converter wind

turbine allowed the provision of reactive power support to the DFIG wind turbine. The conclusion drawn in this chapter, after analysing the provided simulation results, is that IG-based wind farm can be supported by fully-rated converter wind turbines during low grid-voltage conditions. This is mainly because in the fully rated converter turbine the controller on the grid side converter has the ability to operate as an 'STATCOM'. For example, a 2MW FRC wind turbine can temporarily increase the wind farm voltage from 0.60pu to 0.75pu, in case of a voltage dip of 0.35 pu (which is ~15% voltage support). This support is proven enough to prevent a 1.5 MW DFIG-based wind farm from being disconnected from the grid. Thanks to the support provided by the fully rated converter wind turbines, the period of time in which DFIG-based wind turbines can remain connected to the grid during LV can be extended. This feature is highly beneficial for grid code compliance. Voltage support could be further increased if the FRC wind turbines had the possibility to curtail their active power production during fault periods and allow most of the power rating of the FRC converter being used as a STATCOM. The curtailment of the FRC active power production requires a synchronized action of converter and pitch angle controller of the turbine. This, however, requires further studies and research.

Additionally, the results and the analysis provided in chapter 3 demonstrated that hybrid wind farm can improve the grid-code compliance of existing IG-based wind farms in situations where the IG-Based wind farms need to be uprated and comply with the FRT requirements. The conclusion here is that by using a hybrid wind farm approach, there would be no need for decommissioning old wind farms on the basis that they no longer comply with grid code requirements.

In Chapter 4 of this thesis, a comprehensive model of a point-to-point connection of VSC-HVDC with neutral-point clamped converters was designed and developed to conduct research studies. Different control schemes for the system were designed to ensure robust dynamic performance and to demonstrate the effectiveness of the controllers during disturbances. The results obtained in the chapter demonstrated that the proposed VSC-HVDC transmission system addresses most of the shortcomings of conventional HVDC and HVAC systems; it also presented alternatives for connecting large amount of offshore wind power, and in order to allow multi-terminal and multi-technology operation. Notwithstanding, a major challenge for the massive implementation of multi-terminal VSC-HVDC grids is the lack of protection mechanisms in case of a DC fault. In this regard, the new MMC technologies presented a promising future scenario where DC faults can be dealt with. However, given the capacitive nature of the cable system in offshore systems, there is

still the risk of high transient fault currents that have little attenuation and have the real potential of damaging a power converter structure in very short periods of time (<5ms).

Chapter 5 investigated possible scenarios of the multi-terminal HVDC connections with alternative protection scenarios on the AC or DC side. Moreover, it analysed auxiliary path solutions for power delivery during a failure of one of the converters. The dynamic performance of five multi-terminal VSC-HVDC connections was explored using the controllers presented in Chapter 4 but with the inclusion of an additional active power DC droop control. The additional active power DC droop controller was added to the VSC-HVDC station working as inverter in the multi-terminal HVDC network. Thanks to this, the inverter VSC-HVDC station was able to dynamically change its DC voltage reference to provide/absorb additional active power in the HVDC network. This allowed the dynamic assessment of power flow in the event of power change and dispatch between different AC grids. The behaviour of the system was explored during the loss of one of the converters in the multi-terminal array. This thesis also showed the power management in multi-terminal VSC-HVDC network for the development of a transnational grid. Here, it was concluded that the VSC-HVDC is able to exchange power with synchronous generators, asynchronous generators, RLC loads and constant power loads. This is due to the great flexibility and fast control of the magnitude, angle and frequency of the voltage VSC-HVDC terminals. Hence any type of wind generator (from Type1 to Type4) can be seamlessly connected to the VSC-HVDC system.

Chapter 6 looked at multi-technology operation and optioneering analysis for connection of 2.4 GW of two separate offshore wind farms from the Dogger Bank development site to the GB grid. The studies showed three possible connection scenarios based on VSC-HVDC technology. All of the options had two windfarms each at 1.2GW, 2 AC collection stations, 4 VSC stations (two offshore and two onshore) and AC and DC cables. Furthermore, Chapter 6 investigated which option had better capital investment cost against fault condition to each scenario. Here it was concluded that the VSC-HVDC makes significant savings in terms of curtailed energy compared to point-to-point connection. However, the AC Auxiliary option had the lowest level of curtailed energy and makes it best value for money option of those considered for long-distance power transmission. Additionally, the reliability scenarios investigated found that there is high value in having an additional redundant transmission path on the HVDC site or AC site if the distance is suitable for such a solution.

7.2 Recommendations for offshore energy integration strategies.

The based in the research work and the key findings of this thesis the following recommendations are provided:

The DFIG wind turbines are compatible with future deployment of multi-terminal HVDC systems and its use is not discouraged for this type of systems. This is mainly because the VSC-HVDC system is able to provide the voltage reference needed for the proper functioning of the DFIG system without the need of additional controller effort in the VSC-HVDC station nor in the DFIG system. Additionally, the usual dq-based control of the DFIG variables is compatible with AC systems created by a VSC-HVDC interface. Since a DC fault in a multi-terminal system necessarily needs to be cleared in a specific time in order to avoid a collapse of the multi-terminal network (<= 150 ms), the Fault ride-through capabilities of a DFIG wind turbine are sufficient to withstand a fault of this nature as long as the DFIG controllers are able to synchronize with the VSC-HVDC AC voltage after the fault in the DC network is cleared.

The use of hybrid wind farm, consisting of DFIGs and FRCs, is better recommended for its use in onshore systems where there is no separation of the wind farm network and the main grid by DC links. This is because the benefit that the FRCs provide for better grid code compliance of the hybrid wind farm are much more attractive in onshore grids. In the case of HVDC-interfaced wind farms, a fault in the DC network would necessarily mean an interruption of the AC voltage reference at the converter terminals and a total loss of the electrical torque of the DFIG, under this situation an extra provision of reactive power from the FRC produces little effect in the dynamic response of the DFIG variables.

Even though a fast restoration of the DC voltage in a multi-terminal HVDC system is desirable after a DC fault, it is not recommended to increase the control constants of the DC voltage control in the HVDC systems because this may lead to instability in the control loop. This is because the controllers of the HVDC system assume the DC plant to be a minimum phase system, however more recent detailed models of the DC plant in an HVDC have proven that the dynamics of the DC voltage are governed by a non-minimum phase system which has the potential to destabilize the control loop if the controller bandwidth is increased excessively.

7.3 Future Work

The work presented in this thesis has explored potential future technologies that could be used in the offshore wind energy sector, hybrid wind farm and VSC-HVDC multi-technology systems. As mentioned earlier, there are many drawbacks of the future wind

farms and VSC-HVDC multi-technology grids and further research is needed, therefore suggestions for areas where this work can be expanded are listed below:

- Investigation of asymetrical faults in the hybrid wind farm and detail examination of how much FRC wind turbine can contribute to compansate thr asymetrical faults in the wind plant.
- The immediate action of VSC-HVDC converters during DC faults is to inmediatly protect its swtiching devices by stopping their commutation. As such, future work should focus on detailed investigation of the consequences of a DFIG-based offshore wind farm (and associated systems such as converters, PLLs, controllers) connected to the onshore grid via VSC-HVDC when its voltage reference is interrupted because of a DC fault.
- Investigate the possibility of including an "AC hub" in offshore networks comprising windfarms, oil ring platforms and converters where power is interchanged locally via AC current and transmitted remotely onshore via DC current.
- Investigate possible scenrios of hybrid converter topologies for HVDC network, the hybrid network would consist of LCC and VSC technology. Those types of topologies might significantly reduce capital costs.
- Investigate the effects of a DC fault in a hybrid DC network based on LCC and VSC technology.
- Investigate low frequency systems for transfer of offshore power, and analyze losses, cable limitations and reactive power compensation. In addition, compare investment costs for offshore windfarm with different transmission technologies.
- Investigation of converter topologies in order to protect multi-terminal HVDC transmission system during fault.
- Investigation of alternative protection strategies that avoid the use of DCCBs.
- Investigate multinational connection scenarios such as the Global Energy Interconnection project proposed by China, where a global grid would transmit solar, wind and hydroelectric-generated power from places on earth where they are abundant to major population centres, rely on HVDC transmission systems and converter-interfaced energy generation. As such, the research outcomes of this thesis can be used to analyse the scenario where power electronics, HVDC transmission and renewable energies synchronize to create a functional, multi-technology system where the advantages of power electronics are used to comply with Grid Codes and increase the overall robustness of the system in case of AC or DC. This system could

also take into account the individual requirements of grids in different countries in terms of grid strength.